frontiers | Research Topics

A fossil view of insect evolution: Integrating paleontological evidence to explore the origins of insect biodiversity

Edited by
Chenyang Cai, Taiping Gao, Phil Barden
and Dagmara Zyla

Published in
Frontiers in Ecology and Evolution
Frontiers in Earth Science

ISSN 1664-8714
ISBN 978-2-8325-3383-3
DOI 10.3389/978-2-8325-3383-3

About Frontiers

Frontiers is more than just an open access publisher of scholarly articles: it is a pioneering approach to the world of academia, radically improving the way scholarly research is managed. The grand vision of Frontiers is a world where all people have an equal opportunity to seek, share and generate knowledge. Frontiers provides immediate and permanent online open access to all its publications, but this alone is not enough to realize our grand goals.

Frontiers journal series

The Frontiers journal series is a multi-tier and interdisciplinary set of open-access, online journals, promising a paradigm shift from the current review, selection and dissemination processes in academic publishing. All Frontiers journals are driven by researchers for researchers; therefore, they constitute a service to the scholarly community. At the same time, the *Frontiers journal series* operates on a revolutionary invention, the tiered publishing system, initially addressing specific communities of scholars, and gradually climbing up to broader public understanding, thus serving the interests of the lay society, too.

Dedication to quality

Each Frontiers article is a landmark of the highest quality, thanks to genuinely collaborative interactions between authors and review editors, who include some of the world's best academicians. Research must be certified by peers before entering a stream of knowledge that may eventually reach the public - and shape society; therefore, Frontiers only applies the most rigorous and unbiased reviews. Frontiers revolutionizes research publishing by freely delivering the most outstanding research, evaluated with no bias from both the academic and social point of view. By applying the most advanced information technologies, Frontiers is catapulting scholarly publishing into a new generation.

What are Frontiers Research Topics?

Frontiers Research Topics are very popular trademarks of the *Frontiers journals series*: they are collections of at least ten articles, all centered on a particular subject. With their unique mix of varied contributions from Original Research to Review Articles, Frontiers Research Topics unify the most influential researchers, the latest key findings and historical advances in a hot research area.

Find out more on how to host your own Frontiers Research Topic or contribute to one as an author by contacting the Frontiers editorial office: frontiersin.org/about/contact

A fossil view of insect evolution: Integrating paleontological evidence to explore the origins of insect biodiversity

Topic editors
Chenyang Cai — Nanjing Institute of Geology and Paleontology, Chinese Academy of Sciences (CAS), China
Taiping Gao — Capital Normal University, China
Phil Barden — New Jersey Institute of Technology, United States
Dagmara Zyla — Leibniz Institute of the Analysis of Biodiversity Change, Zoological Museum Hamburg, Germany

Citation
Cai, C., Gao, T., Barden, P., Zyla, D., eds. (2023). *A fossil view of insect evolution: Integrating paleontological evidence to explore the origins of insect biodiversity*. Lausanne: Frontiers Media SA. doi: 10.3389/978-2-8325-3383-3

Table of contents

TYPE Editorial
PUBLISHED 15 August 2023
DOI 10.3389/feart.2023.1270883

OPEN ACCESS

EDITED AND REVIEWED BY
Bruce S. Lieberman,
University of Kansas, United States

*CORRESPONDENCE
Chenyang Cai,
cycai@nigpas.ac.cn

RECEIVED 01 August 2023
ACCEPTED 07 August 2023
PUBLISHED 15 August 2023

CITATION
Tihelka E and Cai C (2023), Editorial: A fossil view of insect evolution: integrating paleontological evidence to explore the origins of insect biodiversity.
Front. Earth Sci. 11:1270883.
doi: 10.3389/feart.2023.1270883

Editorial: A fossil view of insect evolution: integrating paleontological evidence to explore the origins of insect biodiversity

Erik Tihelka[1] and Chenyang Cai[2]*

[1]School of Earth Sciences, University of Bristol, Bristol, United Kingdom, [2]State Key Laboratory of Palaeobiology and Stratigraphy, Nanjing Institute of Geology and Palaeontology and Centre for Excellence in Life and Paleoenvironment, Chinese Academy of Sciences, Nanjing, China

KEYWORDS

insect evolution, insect phylogeny, timescale of evolution, paleobiology, Hexapoda, biodiversity

Editorial on the Research Topic
A fossil view of insect evolution: integrating paleontological evidence to explore the origins of insect biodiversity

Introduction

In 2025, 180 years will have elapsed since the publication of the first treatise on fossil insects, the *History of the Fossil Insects in the Secondary Rocks of England* published by the English rector Peter Bellinger Brodie in 1845. To celebrate the rich history of palaeoentomological research—from its accidental and unexpected beginnings to the present era—*Frontiers in Earth Science* and *Frontiers in Ecology and Evolution* are inviting a collection of contributions to capture the state of the art of fossil insect research today.

Reverend Brodie belonged to a defunct intellectual milieu. During the height of the Industrial Revolution, before the consolidation of modern academia, an extraordinary proportion of the breakthroughs in our understanding of Nature have been elaborated by members of the English clergy and affluent amateurs—men spared of debilitating manual labour, with a comfortable house and a steady supply of tea. The freedom to tinker and pursue the unlikely are what initially lead to the foundation of palaeoentomology. Along with an earthquake, a mass extinction 201 million years before that, and a good measure of luck.

Rumours were circulating along the course of the River Severn in western England regarding the presence of strange creatures embedded in rocks. On 27th May 1773, a powerful earthquake followed by a landslide occurred between Buildwas and Coalbrookdale in Shropshire. The river spilled out of its banks and eighteen acres of land were carried down the valley, opening up large chasms and exposing rocky slopes. John Fletcher, Vicar of Madeley, travelled to the scene of destruction and later recalled: "A great many fossils were found bearing the impression of a flying insect, not unlike the butterfly into which silkworms are changed" (Fletcher, 1833). At this time, palaeontology as a discipline did not yet exist–it would take half a century for that term to be coined and 70 years for the first dinosaurs to be recognised. For then, not much could be said about the strange insects engulfed in rocks.

Reverend Brodies' fascination with fossils dated back to his childhood spent in London and his later theological studies in Cambridge. Upon his first professional appointment in the parish of Wylye in Wiltshire, Brodie set out to investigate the claims. Over the succeeding 53 years, Brodie would discover and study some of the most famous classical localities yielding Triassic and Jurassic insects in England—including Aust Cliff, Dumbleton, Wainlode Cliff and Westbury in Gloucestershire—and amass a collection of some 25 thousand specimens, principally from the Rhaetian and Hettangian.

Anyone admiring insects in flight, visiting flowers, or pacing along footpaths in a forest would be excused to doubt how these fragile creatures could possibly preserve in the geological record. Brodie's key insight was that the fossilisation of insects was not just possible; under certain condition, fossil insects were abundant. He recognised that many of the fragmentary specimens he excavated in the Vale of Gloucestershire were not seeds or plant leaves but the disarticulated remains of ancient insects. Much of Brodie's fossils came from what he called the "Insect limestone," an unassuming about 30 cm thick blue-grey rock found at various exposures along southern-western England. A large part is associated with the so-called "Cotham marble," a massive stromatolite that sprawled over much of present-day England in waters vacated in the aftermath of the end-Triassic mass extinction that probably provided suitable conditions for the preservation of fragile insects. Unbeknown to Brodie. stromatolites indeed provide one widespread mechanism by which insects can become preserved in the fossil record and formed the perfect preconditions for him to make his discoveries, over 200 million years later.

Indeed, Brodie was not the first to describe fossil insects; Ernst Friedrich Germar, a German entomologist, had described fossil insects from the Solnhofen Limestone before him. However, Brodie's significant contribution came through his 1845 monograph and over a hundred shorter papers published during his lifetime, which provided the first coherent treatments of palaeoentomology, establishing the foundation for the discipline for decades to come. Among them were the then oldest record of mosquitos, dragonflies, and abundant beetles that inspired the imagination of his contemporaries of what ancient ecosystems must have looked like.

Palaeoentomology has come a long way since Brodie's initial exploratory work in Triassic and Jurassic of England. In the words of the mathematician Stanislaw Ulam, the hallmark of a *bona fide* scientific discipline is that it not only yields results that are correct and verifiable, but also non-trivial. In other words, for every right answer there should also be a surprise, a bang, a *something extra* that we had no idea about at all—that which has the potential to shock, fascinate and excite. This collection of papers is about that *something extra*. For palaeoentomology is no longer merely a cataloguing of the millions of insects that have been extirpated over the past 400 million years, but also has the power to bring insights into what we would have had no way of knowing otherwise, had it not been for the fossils.

Perspectives

In this Research Topic, Zhang et al., Du et al., and Zhang et al. present morphological data for Cretaceous velvety shore bugs, burrowing bugs, and assassin bugs, respectively. These studies contribute to our understanding of the evolution of key morphological characters and specialized behaviors in these insect groups. Li et al. describe rare tiny aquatic sphaeriusid beetles preserved in mid-Cretaceous Burmese amber, showcasing the effectiveness of confocal microscopy in studying dark bioinclusions within amber. Li et al. focus on psocid fossils and the insights they offer into insect phylogeny, particularly with respect to missing fossil links. Li et al. and Li et al. utilize advanced photography and phylogenetic analytical methods to shed light on the systematic positions of Cretaceous beetles in the Coleoptera Tree of Life. Additionally, they demonstrate how fossils bridge the morphological gaps between extinct and extant forms. Fossil insects play a crucial role in reconstructing the biogeography of ancient ecosystems, as Ma et al. illustrate through their visually captivating study of stream lacewings. Lastly, Li et al. show how detailed studies of both compression fossils and amber bioinclusions can enhance our understanding of the relationships among living taxa.

We look forward to welcoming many more contributions on new, fascinating aspects of palaeoentomology.

Author contributions

ET: Conceptualization, Writing–original draft, Writing–review and editing, Data–curation, Funding–acquisition, Project–administration, Resources, Validation. CC: Writing–original draft, Writing–review and editing, Project–administration, Validation.

Funding

The author(s) declare financial support was received for the research, authorship, and/or publication of this article. This study was supported by the National Natural Science Foundation of China (42222201 and 42288201) and the Second Tibetan Plateau Scientific Expedition and Research project (2019QZKK0706).

Acknowledgments

We deeply thank all the authors and reviewers who have participated in this Research Topic.

Conflict of interest

The authors declare that the research was conducted in the absence of any commercial or financial relationships that could be construed as a potential conflict of interest.

The author(s) declared that they were an editorial board member of Frontiers, at the time of submission. This had no impact on the peer review process and the final decision

References

Fletcher, J. (1833). *The works of the reverend john fletcher*. Carlton and Porter.

Publisher's note

All claims expressed in this article are solely those of the authors and do not necessarily represent those of their affiliated organizations, or those of the publisher, the editors and the reviewers. Any product that may be evaluated in this article, or claim that may be made by its manufacturer, is not guaranteed or endorsed by the publisher.

frontiers | Frontiers in Ecology and Evolution

ORIGINAL RESEARCH
published: 23 May 2022
doi: 10.3389/fevo.2022.908044

Morphological Phylogeny of New Cretaceous Fossils Elucidates the Early History of Soil Dwelling Among Bugs

Sile Du[1,2], *Lei Gu*[1], *Michael S. Engel*[3], *Dong Ren*[1] *and Yunzhi Yao*[1]*

[1] *College of Life Sciences and Academy for Multidisciplinary Studies, Capital Normal University, Beijing, China,* [2] *Science and Technology Research Center of China Customs, Animal Quarantine Intitute, Beijing, China,* [3] *Division of Entomology, Natural History Museum and Department of Ecology and Evolutionary Biology, University of Kansas, Lawrence, KS, United States*

Burrowing bugs are distinctive, beetle-like insects of the pentatomoid family Cydnidae, noteworthy for their morphological specializations for digging and a hemiedaphic life history. However, less is known about their biological significance and the early origin of soil dwelling. Direct fossil evidence illuminating the evolutionary history of soil dwelling in cydnids is extremely rare. In this study, we report four new species of the burrowing bug subfamily Amnestinae from mid-Cretaceous Burmese amber, including two exhibiting specialized bulldozing and digging morphological traits on the anterior of the head and forelegs. Associated morphological features and phylogenetic placement indicate that *Acanthamnestus* represents the earliest unequivocal soil-dwelling cydnids and pushes back the geological record of hemiedaphic true bugs to 99 Ma. Environmental evidence, the distribution of host plants, and the fossils provide a new window for understanding the early origin of soil habits in Amnestinae and may be linked to the appearance of Moraceae.

Keywords: fossorial insect, Pentatomomorpha, *Ficus*, Moraceae, angiosperm, modification of head and fore legs

OPEN ACCESS

Edited by:
Chenyang Cai,
Nanjing Institute of Geology and Paleontology (CAS), China

Reviewed by:
Dany Azar,
Lebanese University, Lebanon
Jacek Szwedo,
University of Gdansk, Poland

***Correspondence:**
Yunzhi Yao
yaoyz100@126.com

Specialty section:
This article was submitted to Paleontology, a section of the journal Frontiers in Ecology and Evolution

Received: *30 March 2022*
Accepted: *19 April 2022*
Published: *23 May 2022*

Citation:
Du S, Gu L, Engel MS, Ren D and Yao Y (2022) Morphological Phylogeny of New Cretaceous Fossils Elucidates the Early History of Soil Dwelling Among Bugs. Front. Ecol. Evol. 10:908044. doi: 10.3389/fevo.2022.908044

INTRODUCTION

Soils are dynamic and rich environments that play a dramatic role in shaping the terrestrial biota we observe above their surfaces. To no small extent, soil-dwelling insects play an integral role in edaphic ecosystems, and any number of specializations are associated with living within, even partially so, the ground. Iconic soil-dwelling insects include scarab beetles (Coleoptera: Scarabaeidae), mole crickets (Orthoptera: Gryllotalpidae), some termites (Isoptera), and nymphal cicadas (Hemiptera: Cicadidae), among many others (Frost, 1959; Snodgrass, 1967; Richards and Davies, 1977; Gullan and Cranston, 2000). Often, such species have modified morphological structures unique to particular environments that permit them to invade and thrive within the soil ecosystem. The true bugs (Heteroptera) are principally phytophagous insects that include some of the most prolific agricultural pests. Among these, the most noticeable soil-dwelling bugs are those of the family Cydnidae, often dubbed as burrower bugs (Schuh and Slater, 1995). The hemiedaphic species of Cydnidae typically burrow into the soil using anatomical specializations of the head and forelegs, where they lay eggs and often spend much of their life cycle, before emerging to mate. Some species can become pestiferous, such as those feeding on crops ranging from peanuts to spinach. Not all cydnids are strictly soil dwelling, with some living fully above the soil layer and either on or in close association with their host plants. Those species not living as burrowers lack the phenotypic specializations otherwise found in the hemiedaphic lineage. The following characters are known specializations among Cydnidae for digging and living hemiedaphically: head flattened with circular crown setae (especially peg-like setae) on anterior margin; protibiae broadened apically with several strong spines at apical and lateral margins; protibiae cultrate and metatibiae clavate; and tarsi reduced or absent (Dolling, 1981; Schwertner and Nardi, 2015).

Cydnidae have a long geological history, with fossil species ranging from the Early Cretaceous to Early Miocene (Shcherbakov and Popov, 2002; Grimaldi and Engel, 2005; Yao et al., 2007; Lis et al., 2018). Nonetheless, evidence of their transition and evolution to hemiedaphic life histories is lacking owing to an absence of definitive fossil species with digging traits, presumably because of a taphonomic bias away from taxa whose lives are spent mostly below the soil surface. Accordingly, understanding the early evolution of soil habits in this major lineage of insects has been severely hindered. To date, the only attempt at reconstructing the early biology of Cydnidae has been that of Lis et al. (2018) who explored their association with several plant syninclusions in mid-Cretaceous amber from Myanmar. In this study, we reported four new species and three new genera of the subfamily Amnestinae (Cydnidae) and combined the morphological and phylogenetic evidence to demonstrate that the mid-Cretaceous cydnids had already evolved specialized characters for subterranean life. Additionally, climatic history and vegetative distribution patterns also provide clues that amnestine burrowing bugs may have had a lengthy association with the plant family Moraceae (mulberry and figs) and their early stem group.

MATERIALS AND METHODS

Materials and Photography

The Burmese amber specimens investigated in this study were collected from the Hukawng Valley in Tanaing Township, Myitkyina District of Kachin State, Myanmar, and were acquired prior to June 2017. The Burmese amber deposits contain a diversity of fossil insects, such as termites (Zhao et al., 2020), hymenopterans (Cao et al., 2020), winged stick insects (Yang et al., 2020), and mecopterans (Lin et al., 2019). The age of this deposit has been dated radiometrically to a maximum of ca. 98.8 ± 0.6 Ma, using 206Pb/238U isotopes in magmatically derived zircon crystals taken from the volcaniclastic matrix of the amber (Shi et al., 2012). All specimens are housed in the Key Lab of Insect Evolution and Environmental Changes, College of Life Sciences, Capital Normal University, Beijing, China (CNUB; Yunzhi Yao, Curator).

The amber samples were examined and photographed using a Nikon SMZ25 dissecting microscope and a Nikon ECLIPSE Ni microscope, both of them with a Nikon DS-Ri 2 digital camera system (Nikon, Japan), and illustrated with the aid of a camera attached to the microscope. The figures were drawn using Sai, Adobe Illustrator CC, and Photoshop CC graphics software packages. Morphological terminology mainly follows Schuh and Slater (1995). Body length was measured from the apex of the head to the apex of the abdomen. Body width was measured at the maximal width of the body. The lengths of the pronotum and scutellum were measured at the midline. The length of the forewings was measured from the base of the hemelytron to its apex. The length of the corium was measured from the base of the hemelytron to the apex. The missing dimensions were marked "?".

Taxon Sampling, Morphological Characters

We carried out phylogenetic analyses for Amnestinae to clarify and confirm the position of our new taxa. Due to the phylogenetic relationships at the superfamily level in the superfamily Pentatomoidea, a lot of controversies about the monophyly of the Cydnidae and phylogenetic relationships with other pentatomoid families are still there (Schwertner and Nardi, 2015). Lis et al. (2017) indicated the non-monophyly of the "cydnoid" complex within Pentatomoidea. At the same time, 18 ingroup terminal taxa include 12 fossil taxa and 6 extant taxa. The earliest known Amnestinae were from the Early Cretaceous (Yao et al., 2007). All fossil species are from the Cretaceous (**Supplementary Table S1**). In addition, in the family Cydnidae, only Amnestinae are monophyletic groups, which can be confirmed by the presence of claval commissure, and have two genera. Hence, we used a hypothetical "all-zero" taxon as outgroup to polarize the individual characters. A complete list of the taxa used in the phylogenetic analyses is shown in **Table 1**. A total of 43 morphological characters were used in the analyses (characters 0–42), of which 26 are binary and 17 are multistate. All the characters are unordered and with equal weight, and the missing data were scored as unknown. The character matrix is provided in **Table 1**, and the description of morphological characters used in the phylogenetic analysis is provided in **Supplementary Material**.

Phylogenetic Analysis

Analysis of the character matrix (characters 0–41) was performed using the NONA version 2.0 (Goloboff, 1999) and the WinClada version 1.00.08 interface (Nixon, 2002). Runs were conducted using the following commands: multiple TBR+TBR search strategy, maximum trees to keep (hold) = 10,000; number of replications (mult*N) = 1,000; starting trees per rep (hold/) = 100. Bremer support values were obtained using TNT (Goloboff and Catalano, 2016). Ancestral character state reconstruction of soil-dwelling characteristics was conducted using equally weighted parsimony methods in Mesquite 2.75 (Maddison and Maddison, 2011). We coded the data for head and protibiae of terminal taxa based on morphological data from the corresponding species (**Table 1**, characters 42 and 43).

RESULTS AND DISCUSSION

Systematic Paleontology

Order: Hemiptera Linnaeus, 1758

Suborder: Heteroptera Latreille, 1810

Superfamily: Pentatomoidea Leach, 1815

Family: Cydnidae Billberg, 1820

TABLE 1 | Character matrix for phylogenetic analyses, including 43 morphological characters for 19 taxa.

Characters	0	1	2	3	4	5	6	7	8	9	10	11	12	13	14	15	16	17	18	19	20	21	22	23	24	25	26	27	28	29	30	31	32	33	34	35	36	37	38	39	40	41	42	43
Outgroup	0	0	0	0	0	0	0	0	0	0	0	0	0	0	0	0	0	0	0	0	0	0	0	0	0	0	0	0	0	0	0	0	0	0	0	0	0	0	0	0	0	0	0	0
Amnestus spinifrons	0	2	1	3	1	1	1	1	1	0	1	0	2	0	0	1	0	1	2	2	1	0	1	0	0	0	0	0	1	0	1	1	2	1	1	1	1	1	1	0	1	1	2	2
Amnestus ficus	0	2	0	3	1	1	1	1	1	0	1	0	2	0	2	1	0	1	1	1	1	0	1	1	0	0	0	0	0	0	1	1	2	1	2	1	1	1	1	0	1	1	2	2
Amnestus obscurus	0	2	1	0	1	0	1	1	1	0	1	0	2	?	?	1	0	1	2	1	1	0	1	0	0	0	0	0	1	0	1	1	2	1	2	1	1	1	1	0	1	1	2	2
Lattinestus andersoni	1	2	0	3	1	1	1	1	0	0	?	1	1	1	0	1	0	1	1	2	1	1	1	1	0	0	0	1	0	0	2	1	1	0	2	1	0	0	1	0	1	1	2	2
Lattinestus branstetteri	1	2	1	3	1	1	1	1	1	0	?	1	2	0	0	1	1	1	1	2	1	1	1	0	0	2	0	1	0	0	4	1	2	0	2	1	1	1	1	0	1	1	2	2
Lattinestus egeri	1	2	1	0	0	0	1	1	1	0	?	1	2	0	0	1	1	1	1	2	1	1	0	0	0	1	0	1	0	0	1	1	0	0	2	1	1	1	1	0	1	1	2	2
*****_Orienicydnus hongi_	1	0	1	0	1	1	1	1	0	1	0	1	0	1	2	0	2	?	0	0	1	0	?	?	0	?	?	?	?	?	?	?	?	0	?	1	0	0	0	0	1	2	2	1
*****_Cilicydnus robustispinus_	1	0	1	0	1	1	0	0	-	1	0	1	0	0	1	0	2	?	0	0	1	0	1	2	1	1	?	?	0	?	0	1	2	0	?	1	0	0	0	0	1	2	0	1
*****_Clavicoris cretaceus_	1	0	1	1	1	?	0	0	-	0	0	?	2	?	?	0	?	0	0	0	1	0	1	?	0	1	?	0	0	0	?	0	2	1	0	0	?	?	1	0	0	0	0	0
*****_Latiscutella santosi_	1	0	1	0	1	1	0	0	-	0	0	0	?	?	?	0	?	?	0	1	1	0	0	2	1	1	1	2	1	0	0	1	2	0	?	?	0	0	?	?	?	?	0	0
*****_Pricecoris beckerae_	1	2	1	0	1	1	0	0	-	0	0	0	?	?	?	0	?	?	0	0	1	0	1	2	0	1	1	0	1	0	0	1	2	0	0	0	0	0	0	?	0	0	0	0
*****_Chilamnestocoris mixtus_	1	2	1	3	1	1	1	1	2	0	1	0	1	?	?	1	1	1	1	1	1	0	1	1	0	0	0	0	1	0	2	1	2	0	1	?	0	0	0	0	1	1	2	1
*****_Punctacorona triplosticha_	1	2	1	3	1	1	1	1	2	0	1	0	?	?	?	1	0	1	2	1	1	0	1	1	0	0	0	0	1	0	1	1	2	0	2	1	0	0	1	0	1	1	2	2
*****_Pullneyocoris dentatus_	0	2	0	2	1	1	0	0	-	0	0	0	1	?	?	1	1	1	1	1	1	0	1	2	0	0	0	0	0	0	1	1	2	0	1	1	?	?	1	1	1	1	1	1
*****_Acanthamnestus tridorsus_	0	2	1	3	1	1	1	1	1	0	1	0	1	0	1	1	1	1	1	1	1	0	0	0	0	0	0	0	1	0	1	1	2	1	2	1	0	0	1	1	1	1	2	2
*****_Acanthamnestus ovoideus_	0	2	1	3	1	1	1	1	1	0	1	0	1	1	0	1	0	1	1	1	1	0	1	0	0	0	0	0	1	0	1	1	2	1	2	1	0	0	1	1	1	1	2	2
*****_Laevigemma lisorum_	1	1	0	2	1	1	0	0	-	1	0	0	2	0	0	1	1	1	1	1	1	0	1	2	0	0	1	0	0	1	2	1	2	0	1	1	0	0	1	0	1	1	1	1
*****_Quinalveus hui_	0	2	0	2	1	1	0	0	-	1	0	?	?	?	?	?	?	?	2	1	1	0	1	2	0	0	0	0	0	1	3	1	2	0	1	1	?	0	0	0	1	1	1	1

**Denotes fossil species.*

Subfamily: Amnestinae Hart, 1919

Genus: *Acanthamnestus* Du, Yao, and Engel, gen. nov.

http://zoobank.org/urn:lsid:zoobank.org:act:661DEEDE-6906-420F-BCA7-531749C09A1A

Type species: *Acanthamnestus atridorsus* Du, Yao, and Engel, sp. nov.

Included species: *Acanthamnestus atridorsus* Du, Yao, and Engel, sp. nov.; *Acanthamnestus ovoideus* Du, Yao, and Engel, sp. nov.

Etymology: The generic name is a combination of the Greek word *akanthos* (meaning, "similar") and the extant genus *Amnestus* of the subfamily Amnestinae. The gender is masculine.

Diagnosis: Body black with dense coarse punctures; clypeus with four peg-like setae, paraclypei with five peg-like setae marginally; rostrum not reaching metacoxae; fourth rostral segment shortest. Claval commissure nearly 1/2 length of scutellum; clavus with three rows of coarse punctures; end of corium curved; membrane almost translucent without veins. Meso- and metacoxae closer to each other than to procoxae; protibia flattened and broadened apically with a row of strong spines at the apical margin.

Remarks: The new genus shares with *Amnestus* a clypeus with four peg-like setae, the presence of ocelli, and a well-developed membrane. It is easy to distinguish from *Amnestus* in the following characteristics: membrane nearly 1/2 length of forewing, membranal suture distally curved near the edge of forewing (vs. membrane as long as 1/3 of forewing, base of membranal suture curved near claval suture or straight); profemur without a long, bifid spine on the posterior mesial region of ventral surface (vs. profemur usually with a long, bifid spine). *Acanthamnestus* gen. nov. is distinguished from *Chilamnestocoris* (Lis et al., 2018) by the following characteristics: three rows of coarse punctures in clavus and apex of protibia broadened with a row of strong spines along the apical margin with each marginal spine arising from its own well-developed tubercle (vs. with four rows of coarse punctures and simple spines); clypeus slightly longer than paraclypei (vs. clypeus as long as paraclypei); apex of clypeus with four long sharpened peg-like setae (vs. apex of clypeus with four short peg-like setae). It can also be excluded from *Punctacorona* (Wang et al., 2019) mainly by: paraclypei each with a row of five sharp peg-like setae and four to five hair-like setae (vs. paraclypei with six peg-like setae and one hair-like seta); pronotum with small, indistinct punctures, and posterior margin of calli without a distinct transverse cicatrice (vs. pronotum with large, coarse punctures and posterior margin of calli developed with a distinct transverse cicatrice), base of protibia slender, of even width (vs. protibia conspicuously thickened).

Acanthamnestus atridorsus Du, Yao, and Engel, sp. nov. (**Figures 1**, **2**, **9A–C**).

http://zoobank.org/urn:lsid:zoobank.org:act:43EF19B4-6558-4F3A-A67B-E2E7BFEAC819

Etymology: The specific epithet is a combination of the Latin words *ater* (meaning, "black") and *dorsum* (meaning, "back").

Material: *Holotype*: CNU-HET-MA2019002 (male), housed in the Key Lab of Insect Evolution and Environmental Changes, College of Life Sciences, Capital Normal University, Beijing, China.

Horizon and Locality: Hukawng Valley, Kachin State, northern Myanmar; mid-Cretaceous, lowermost Cenomanian.

Diagnosis: Body elongate. Evaporatorium with mycoid microsculpture, with elongate and strongly recurved peritreme. Apex of scutellum tapering. Forewing with C + Sc and R + M diverging in proximal fifth of corium. Tibial comb present.

Description: Completely preserved male specimen. Body flattened and elongate, length about 3× as long as maximum pronotal width, almost unicolorous, dorsal surface slightly polished; head, antennae, pronotum, scutellum, corium, femora, tibiae, tibial spines, and ventral body surface black, rostrum and membrane pale brown; dorsal surfaces of head, pronotum, scutellum, corium, and clavus with dense coarse punctures.

Head: Nearly semicircular, dorsally with clearly visible punctures, and with slightly developed oblique striae in posterior part of paraclypei; clypeus slightly longer than paraclypei, apex of clypeus broad, with four blackish brown, long, sharp, peg-like setae; paraclypei each with a submarginal row of five more or less sharpened, peg-like setae, and five hair-like setae; each marginal setigerous puncture arising from its own well-developed tubercle; compound eyes large and reniform, contiguous with anterior margin of pronotum, each with a short apical seta and a long hair-like seta on inner margin of compound eyes; ocelli present, interocellar distance about 3× greater than distance between ocellus and compound eye; antennae with five antennomeres, each with short, thick setae; first antennomere short, stout, barrel-shaped; second antennomere shortest and hardly visible; fifth antennomere fusiform, longer than third or fourth antennomeres; rostrum four-segmented, surpassing mesocoxae, not reaching metacoxae, first segment stout and shortest, second segment longest, third segment subequal to fourth segment.

Thorax: Pronotum nearly rectangular, almost parallel-sided, with dense setigerous punctures, without collar; anterior margin concave medially, anterior angles bulging forward, forming a distinct arc, posterior margin slightly convex medially, almost parallel with anterior margin, with 10–11 hair-like setae on the left side and nine hair-like setae on the right side, two long and inflexible hair-like setae on both sides of anterior margin; calli large, half of the protonal surface, without punctures, posterior margin of calli with dense large punctures; anterior margin of pronotum with midsized punctures, posterior margin of pronotum with small-sized punctures and about three rows of larger punctures on both sides. Mesopleuron and metapleuron with evaporatorium, covering most of the metapleuron, large, with mycoid microsculpture, with elongate and strongly recurved peritreme. Scutellum triangular, large, one-third length of hemelytron, lateral margin of scutellum with large coarse punctures; apex of scutellum tapering. *Hemelytron:* macropterous, clavus broad, with three rows of coarse punctures parallel to the lateral margin of scutellum; claval commissure present, nearly one-half length of scutellum; corium with a single row of large punctures close to clavus and anterior margin of forewing, with few punctures in between two rows; corium elongate, junction with membrane angled, base of corium with

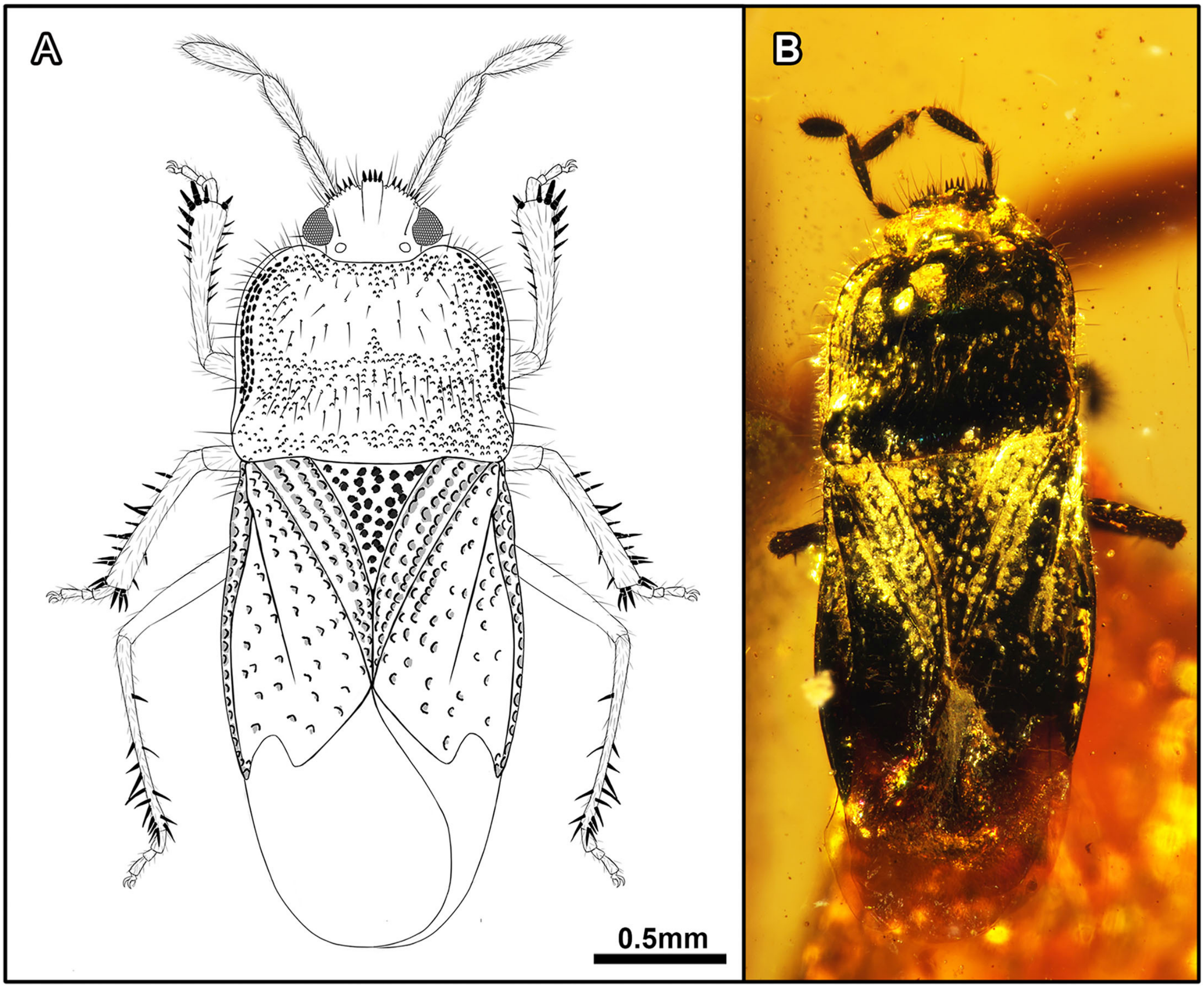

FIGURE 1 | *Acanthamnestus atridorsus* gen. et sp. nov., in mid-Cretaceous amber from Myanmar, Holotype CNU-HET-MA2019002 (male). **(A)** Line drawing habitus in dorsal view. **(B)** Photograph habitus in dorsal view. Scale bars: A = B = 0.5 mm.

four short setae; anterior margin of forewing angulate, C + Sc and R + M diverging in one-fifth length of corium, R + M in forewing raised and keel-like, extending to apex of corium; membrane almost translucent, faintly infumate, distinctly surpassing tip of the abdomen. *Legs*: meso- and metacoxae closer to each other than to procoxae; femora stout and robust with short setae; protibia flattened, broadened apically, and stouter than meso- and metatibiae, with row of nine stout spines along apical margin, each marginal spine arising from its own well-developed tubercle, protibial comb present (visible on right protibia), consisting of a row of eight setae (**Figure 9C**); apex of mesotibia as thick basally, with five spines along the apical margin, lateral margin with about 19 stout, relatively short spines, internal margin with scarcely any spines; metatibia slender, with four to five spines along apical margin, lateral margin with about 16 long, relatively slender spines; tarsi trimerous, tarsomeres equal in thickness, second tarsomere shortest, first tarsomere almost as long as the third tarsomere; pretarsal claws elongate, pulvilli narrowed, capitate apically, as long as claws.

Abdomen: Abdomen of equivalent width with thorax; sterna dark brown, third to eight sterna with numerous distinct small punctures and shiny semierect setae.

Dimensions (in mm): Body length: 2.93, maximal width of body: 1.10; length of head: 0.24, width 0.53; length of compound eyes: 0.14, width 0.08; distance of ocelli: 0.24; length of antennomeres I–V: 0.15, 0.05, 0.23, 0.25, 0.33; length of rostral segments I–IV: 0.18, 0.37, 0.27, 0.29; length of pronotum: 0.80, width: 0.97; length of scutellum: 0.46, width: 0.48; length of anterior margin of corium: 1.08; length of hemelytron: 1.84, width: 0.65; length of claval commissure: 0.40; length of clavus: 0.89; length of fore leg: profemur: 0.59, protibia: 0.55, protarsomeres I–III: 0.09, 0.03, 0.08; length of mid leg:

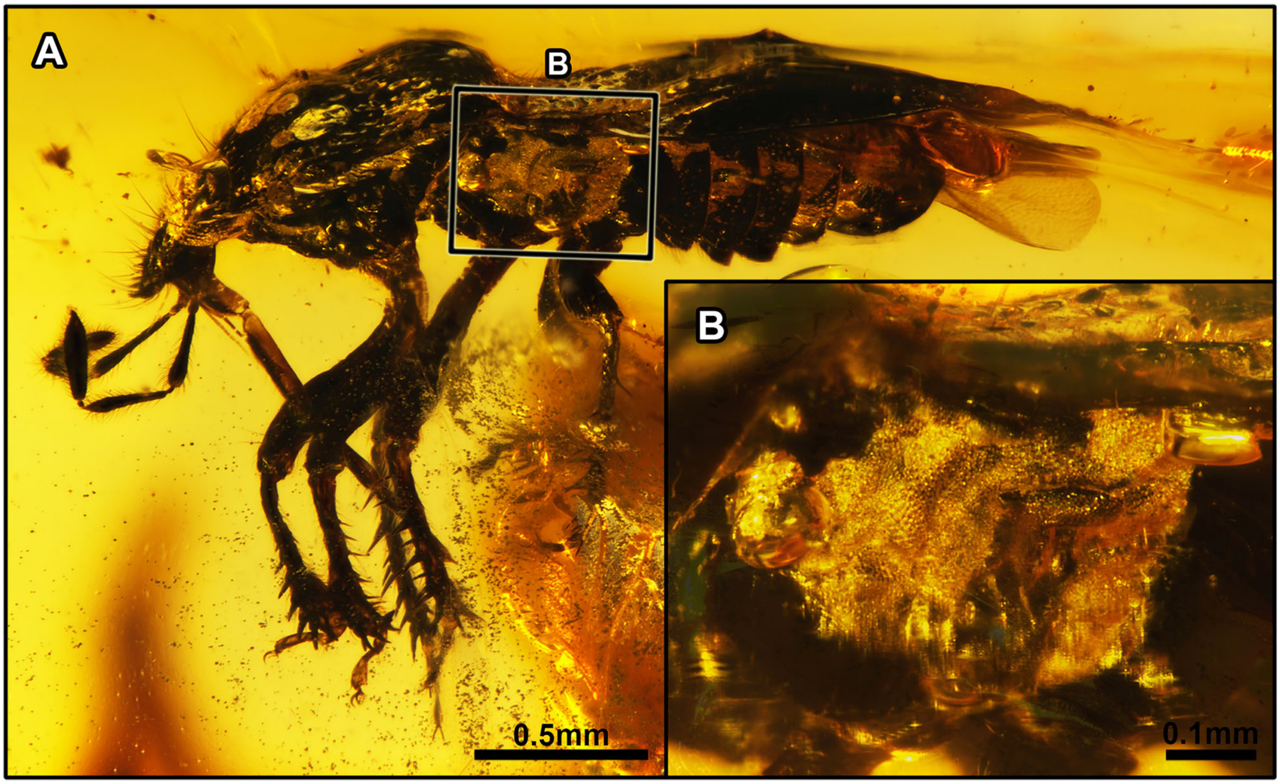

FIGURE 2 | *Acanthamnestus atridorsus* gen. et sp. nov., in Burmese amber. Holotype, CNU-HET-MA2019002 (male). **(A)** Habitus in left lateral view. **(B)** Detail of metathoracic scent gland, as located on **(A)**. Scale bars: A = 0.5 mm; B = 0.1 mm.

mesofemur: 0.50, mesotibia: 0.59, mesotarsomeres I–III: 0.09, 0.05, 0.08; length of hind leg: metafemur: ?, metatibia: 0.69, metatarsomeres I–III: 0.07; 0.03; 0.08.

Acanthamnestus ovoideus Du, Yao, and Engel, sp. nov. (**Figures 3**, **4**).

http://zoobank.org/urn:lsid:zoobank.org:act:60753144-B0EB-4475-B2C6-CFCBCCCD8D7D

Etymology: The specific epithet is taken from the Latin word *ovoideus* (meaning "egg-shaped" or "ovoid").

Material: *Holotype*: CNU-HET-MA2019003 (female), housed in the Key Lab of Insect Evolution and Environmental Changes, College of Life Sciences, Capital Normal University, Beijing, China (CNUB; Yunzhi Yao, Curator).

Horizon and Locality: Hukawng Valley, Kachin State, northern Myanmar; mid-Cretaceous, lowermost Cenomanian.

Diagnosis: Body oval. Evaporatorium lacking mycoid microsculpture. Apex of scutellum blunt. Forewing with C + Sc and R + M diverging in the proximal sixth of corium. Tibial comb absent.

Description: Completely preserved female specimen. Body flattened and oval, almost parallel-sided, length more than 2× as long as maximum pronotal width, overall blackish brown, rostrum brown, membrane castaneous, dorsum slightly polished; dorsal surfaces of head, pronotum, scutellum, clavus, and corium with dense small setae.

Head: Nearly semicircular, dorsally with small punctures; clypeus slightly longer than paraclypei and raised, apex of clypeus broad with four black, short, sharpened, peg-like setae; paraclypei each with a submarginal row of five short, stout, peg-like setae, and four hair-like setae; each marginal setigerous puncture arising from its own well-developed tubercle; compound eyes large and semicircular, contiguous with anterior margin of pronotum, each with a short apical seta on the surface of the compound eyes; ocelli present, round, interocellar distance more than 3× than distance between ocellus and compound eye; antenna with antennomeres, with dense short, thick setae, first antennomere short, stout, barrel-shaped; second antennomere shortest and clavate; third antennomere subequal to fifth antennomere, longer than fourth antennomere, fourth and fifth antennomeres fusiform; rostrum four-segmented, surpassing mesocoxae but not reaching to metacoxae, first segment stout and subequal to second segment, longer than fourth segment, third segment longest, apex of fourth segment tapering.

Thorax: Pronotum nearly rectangular, almost parallel-sided, with dense punctures bearing hair-like setae tigerous, without collar; anterior margin concave medially, anterior angles bulging forward, forming a distinct arc, posterior margin slightly convex medially, almost parallel with anterior margin, with seven hair-like setae on the left side and six hair-like setae on the right side; calli not visible; lateral view of pronotum with

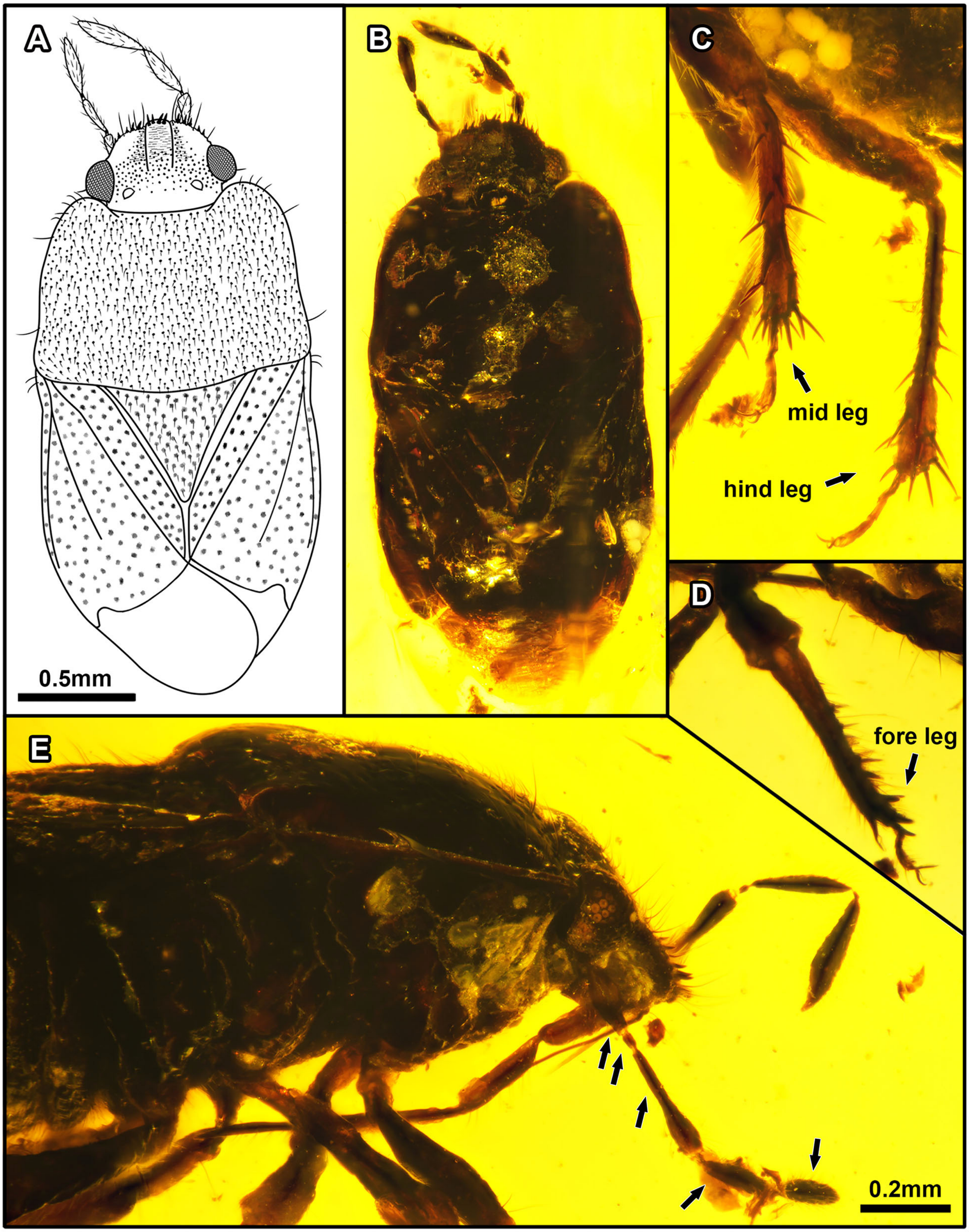

FIGURE 3 | *Acanthamnestus ovoideus* gen. et sp. nov., in Burmese amber. Holotype, CNU-HET-MA2019003 (female). **(A)** Line drawing in dorsal view. **(B)** Habitus in dorsal view. **(C)** Meso- and metatibiae. **(D)** Protibiae. **(E)** Habitus in right lateral view of head, arrows indicate five antennomeres. Scale bars: A = B = 0.5 mm; C = D = E = 0.2 mm.

FIGURE 4 | *Acanthamnestus ovoideus* gen. et sp. nov., in Burmese amber. Holotype, CNU-HET-MA2019003 (female). **(A)** Habitus in left lateral view. **(B)** Habitus in right lateral view. Scale bars: A = B = 0.5 mm.

dense small punctures. Mesopleuron and metapleuron with evaporatorium covering most of the metapleuron, peritreme not visible. Scutellum triangular, large, about one-third length of hemelytron, with large, indistinct coarse punctures; apex of scutellum blunt. **Hemelytron:** macropterous, clavus broad, with three rows of coarse punctures parallel to lateral margin of scutellum; claval commissure present, nearly one-half length of scutellum; corium elongate with same size punctures as those of clavus, junction with membrane angled, base of corium with two short setae; anterior margin of forewing angulate, C + Sc and R + M diverging at one-sixth length of corium, R + M in forewing raised and keel-like; membrane almost translucent, faintly infumate, distinctly surpassing tip of the abdomen. *Legs*: meso- and metacoxae closer to each other than to procoxae; femora stout and robust with short setae; protibia flattened and stout, broadened apically, with about five long spines along the apical margin, each marginal spine arising from its own well-developed tubercle, lateral margin with about six stout, relatively short spines; mesotibia as thick basally, with about eight long spines along the apical margin, lateral margin with about 12 stout, relatively short spines, internal margin with scarcely any spines; metafemur and metatibia more slender than other segments, metatibia with about 10 spines along the apical margin, lateral margin with about eight long, relatively slender spines; tarsi trimerous, tarsomeres equal in thickness, second tarsomere shortest, first tarsomere almost as long as the third tarsomere; pretarsal claws elongate, pulvilli narrowed, capitate apically, as long as claws.

Abdomen: Equivalent width with thorax; sterna dark brown, third to eight sterna with numerous distinct small punctures and shiny semierect setae; ovipositor platelike.

Dimensions (in mm): Body length: 2.53; maximal width of body: 1.21; length of head: ?, width: 0.68; length of compound eyes: 0.17, width: 0.14; distance of ocelli: 0.33; length of antennomeres I–V: 0.13, 0.04, 0.28, 0.23, 0.30; length of rostral segments I–IV: 0.23, 0.23, 0.36, 0.21; length of pronotum: 0.85, width: 1.19; length of scutellum: 0.49, width: 0.65; length of anterior margin of corium: 1.10; length of hemelytron: 1.69, width: 058; length of claval commissure: 0.28; length of clavus: 1.03; length of foreleg: profemur: 0.55, protibia: 0.46, protarsomeres I–III: 0.05, 0.03, 0.11; length of midleg: mesofemur: 0.67, mesotibia: 0.83, mesotarsomeres I–III: 0.05, 0.04, 0.06; length of hind leg: metafemur: 0.64, metatibia: 0.85, metatarsomeres I–III: 0.07, 0.04, 0.16.

Genus: *Laevigemma* Du, Yao, and Engel, gen. nov. (**Figures 5**, **6**, **9D,E**).

http://zoobank.org/urn:lsid:zoobank.org:act:B91285D6-13B7-4468-88E8-D9B0A126F5DB

Type species: *Laevigemma lisorum* Du, Yao, and Engel, sp. nov.

Included species: Type species only.

Etymology: The generic name is a combination of the Latin words *laevis* (meaning "smooth") and *gemma* (meaning "gemstone"), referencing the nearly smooth pronotum that differs from the large and coarse punctures of most Amnestinae. The gender of the name is masculine.

Diagnosis: Body relatively smooth dorsally. Clypeus and paraclypei without peg-like setae apically; rostrum reaching metacoxae. Clavus broad, with four rows of coarse punctures parallel to the lateral margin of scutellum; end of corium curved; claval commissure shorter than half of scutellar length; R+M separated from C+Sc at base of corium, membrane with four simple veins. Coxae of all three pairs of legs equally distant from each other; protibia with only longer weak spines at the apical margin.

Remarks: The new genus can be classified within the subfamily Amnestinae owing to the presence of a distinct claval commissure. It is excluded from the other genera of Amnestinae by the following combination of characters: clypeus and paraclypei without peg-like setae; membrane with four simple veins; protibiae not broadened apically; postiolar peritreme branching laterally, with anterior and lateral projections. This species is quite special as it does not have the typical coarse punctures or dark body of typical Amnestinae, and is instead relatively smooth dorsally. When the light hits its dorsum, the pronotum and forewings are shiny. The new genus is more like *Quinalveus* gen. nov.; however, the two genera have many differences, such as the relatively smooth body dorsally (vs. body with distinct large punctures); clavus with four rows of coarse punctures parallel to lateral margin of scutellum (vs. clavus with five rows of coarse punctures); end of corium curved (vs. end of corium straight); claval commissure shorter than half of scutellar length (vs. length of claval commissure subequal to half of scutellar length); membrane with four simple veins (vs. membrane with three simple veins).

Laevigemma lisorum Du, Yao, and Engel, sp. nov. (**Figures 5**, **6**, **9D,E**).

http://zoobank.org/urn:lsid:zoobank.org:act:79EA6BC3-242B-49CD-85B8-631233C09E65

Etymology: The specific epithet honors Prof. Jerzy A. Lis and his wife Barbara Lis for their considerable contributions to our knowledge of Cydnidae.

Material: *Holotype*: CNU-HET-MA2019004 (male), housed in the Key Lab of Insect Evolution and Environmental Changes, College of Life Sciences, Capital Normal University, Beijing, China.

Horizon and Locality: Hukawng Valley, Kachin State, northern Myanmar; mid-Cretaceous, lowermost Cenomanian.

Diagnosis: Same as generic diagnosis.

Description: Completely preserved male specimen. Body oval, almost unicolorous, relatively smooth dorsally, length about 2× as long as maximum body width. Head, pronotum, and scutellum whitish shiny; antennae, rostrum, and corium castaneous; legs and membrane yellowish brown. Venter of body black.

Head: Flattened, 2× as long as wide, with small punctures on posterior margin of head; clypeus slightly longer than paraclypei, apex blunt, not obviously broadened, without peg-like setae apically, with a pair of hair-like setae subapically; each paraclypei with three hair-like setae apically; compound eyes large, contiguous with anterior margin of pronotum, each with a short apical seta on inner margin of compound eyes; ocelli

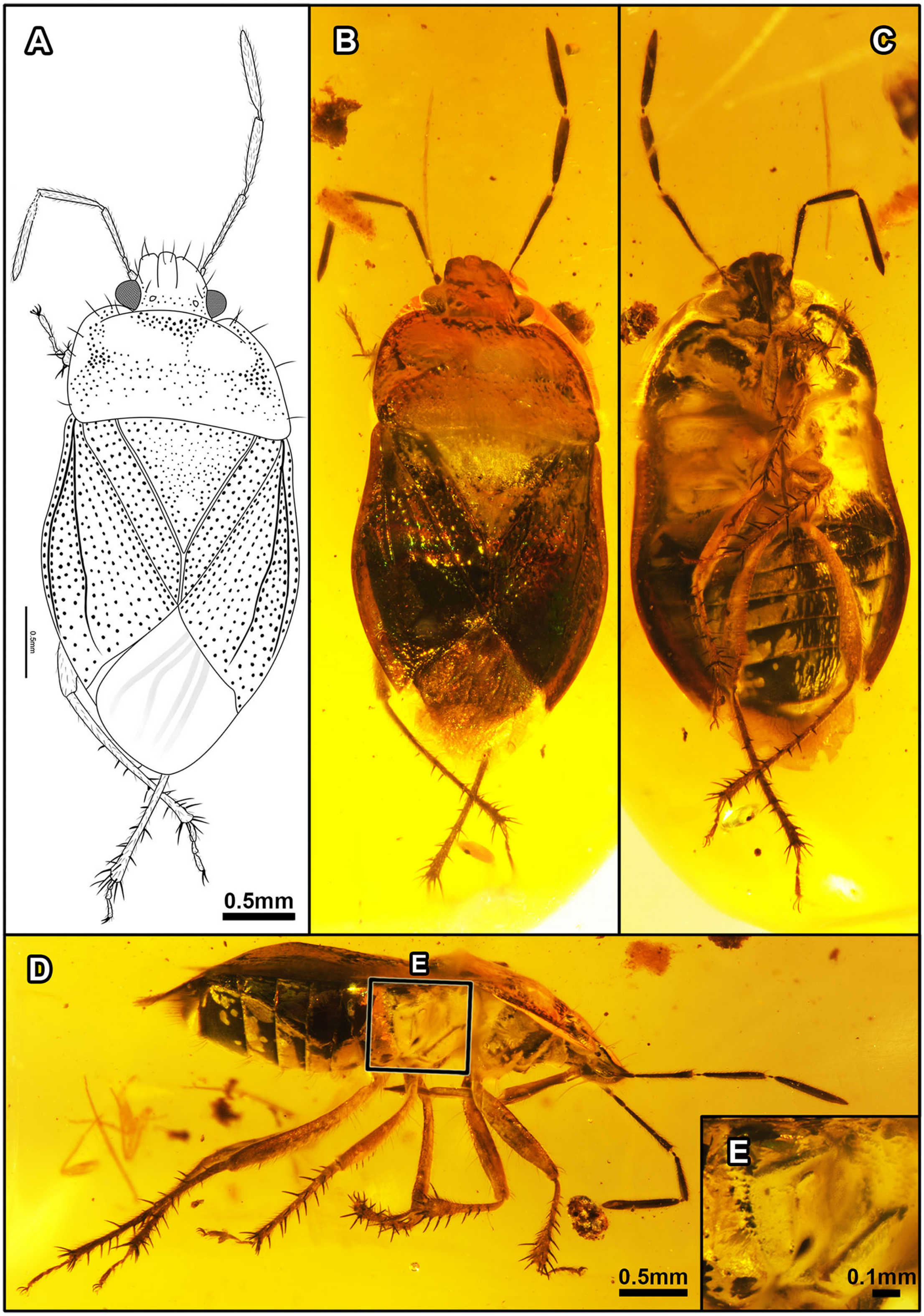

FIGURE 5 | *Laevigemma lisorum* gen. et sp. nov., in Burmese amber. Related to **Figure 2**. Holotype, CNU-HET-MA2019004 (male). **(A)** Line drawing in dorsal view. **(B)** Habitus in dorsal view. **(C)** Habitus in ventral view. **(D)** Habitus in right lateral view. **(E)** Detail of metathoracic scent gland, as located on **(D)**. Scale bars: A = B = C = 0.5 mm; D = 0.5 mm; E = 0.1 mm.

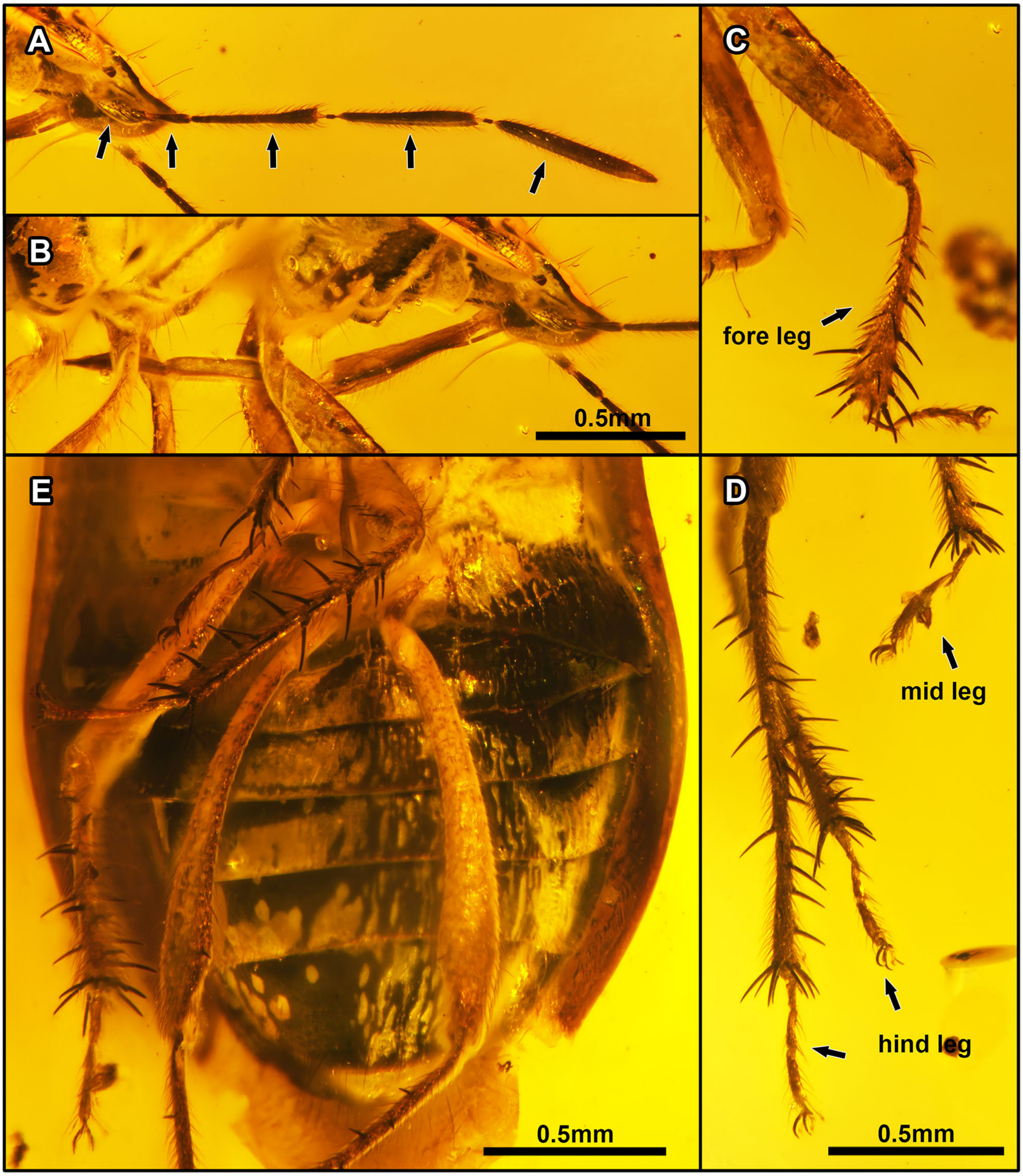

FIGURE 6 | *Laevigemma lisorum* gen. et sp. nov., in Burmese amber. Related to **Figure 2**. Holotype, CNU-HET-MA2019004 (male). **(A)** Habitus in right lateral view of head, arrows indicate five antennomeres. **(B)** Rostrum in right lateral view. **(C)** Right foreleg. **(D)** Mesotarsi and right metatarsus. **(E)** Abdomen in ventral view. Scale bars: A = B = 0.5 mm; C = D = 0.5 mm; E = 0.5 mm.

present, interocellar distance about 3× greater than the distance between ocellus and compound eye; five antennomeres with dense setae, second antennomere shortest, fifth antennomere longest, third antennomere subequal with fourth antennomere; rostrum with four segments, extending to metacoxae, first segment shortest, subequal with fourth segment, second segment longest, subequal with third segment.

Thorax: Pronotum nearly rectangular, almost parallel-sided without collar; anterior margin upward in middle with coarse punctures, anterior angles bulging forward, forming a distinct arc with a hair-like seta and several coarse punctures, posterior margin slightly swollen and concave medially without punctures, pronotum with four hair-like setae on both sides of edge; calli large, smooth, posterior margin of calli with dense small punctures. Metathoracic scent gland grooves present on metapleuron, metapleuron with large evaporatory area and peritreme, postiolar peritreme branching laterally, with anterior and lateral projections. Scutellum large, triangular, sides of more-or-less equal length, depressed basomedially, basal and lateral of margin of scutellum with large and coarse punctures, small punctures in middle of scutellum, scutellar tip narrow, slightly elongate. Hemelytron: macropterous, clavus broad, with four rows of coarse punctures parallel to lateral margin of scutellum; claval commissure present, shorter than half length of scutellum; corium large, two-thirds length of hemelytron, with a single row of distinct punctures close to clavus and anterior margin of forewing, with dense punctures in between two rows; corium elongate, junction with membrane curvilinear, base of corium without seta; anterior margin of forewing angulate, R+M separating from C+Sc at base of corium, R + M in forewing raised and keel-like; membrane almost translucent, faintly infumate, with four simple veins, not branching, distinctly surpassing tip of the abdomen. *Legs*: coxae of all three pairs of legs equally distant from each other; profemur stout and robust with dense long setae, stouter than meso- and metafemora, and a short spine apically on profemur; protibia slightly broadened apically, shorter than meso- and metatibiae, with about seven long spines along apical margin, each marginal spine arising from its own well-developed tubercle, lateral margin with about 12 stout and relatively short spines; mesofemur straight with four short spines on lateral margin apically; mesotibia as thick basally, with about nine long spines along apical margin, lateral margin with about 17 stout, relatively short spines, internal margin with scarcely any spines; meta-femur slender with a short spine at a distance from distal end, metatibia slender, with about 10 spines along apical margin, lateral margin with about 16 long, relatively slender spines; tarsi trimerous, tarsomeres equal in thickness, third tarsomere longest, first tarsomere almost as long as second tarsomere; pretarsal claws elongate, pulvilli narrowed, capitate apically, as long as claws.

Abdomen: Equivalent width with thorax; sterna black, third to eight sterna with numerous distinct small punctures and shiny semierect setae and distinctive longer setae medially.

Dimensions (in mm): Body length: 3.79, maximal width of body: 1.88; length of head: 0.46, width: 0.89; length of compound eyes: 0.21, width: 0.20; distance of ocelli: 0.43; length of antennomeres I–V: 0.27, 0.13, 0.40, 0.46, 0.62; length of rostral segments I–IV: 0.37, 0.54, 0.51, 0.39; length of pronotum: 0.76, width: 1.64; length of scutellum: 0.89, width: 1.10; length of anterior margin of corium: 1.50; length of hemelytron: 2.46, width: 0.87; length of claval commissure: 0.39; length of clavus: 1.36; length of fore leg: profemur: 1.06, protibia: 0.77, protarsomeres I–III: 0.16, 0.06, 0.14; length of mid leg: mesofemur: 0.93, mesotibia: 0.88, mesotarsomeres I–III: 0.15, 0.06, 0.19; length of hind leg: metafemur: 1.29, metatibia: 1.41, metatarsomeres I–III: 0.13, 0.08, 0.14.

Genus: *Quinalveus* Du, Yao, and Engel, gen. nov. (**Figures 7**, **8**).

http://zoobank.org/urn:lsid:zoobank.org:act:2F245C37-D6D0-4D53-A639-A53DF7B692C1

Type species: *Quinalveus hui* Du, Yao, and Engel, sp. nov.

Included species: Type species only.

Etymology: The generic name is a combination of the Latin words *quini* (meaning, "five") and *alveus* (meaning, "hollow" or "pit"), referring to the five rows of coarse punctures on the clavus. The gender is masculine.

Diagnosis: Body with large distinct punctures. Clypeus and paraclypei without peg-like setae apically. Clavus broad, with five rows of coarse punctures parallel to lateral margin of scutellum; end of corium straight; length of claval commissure subequal to half of scutellar length; R +M separated from C + Sc at basal fifth of corium, membrane with three simple veins. Protibia with only longer weak spines at the apical margin.

Remarks: The new genus is similar to the extinct genus *Pullneyocoris* (Lis et al., 2020). However, it also has two autapomorphies: clavus broad and clavus with five rows of coarse punctures; this is the first time it appears in fossil species. Meanwhile, the membrane has three simple veins.

Quinalveus hui Du, Yao, and Engel, sp. nov. (**Figures 7**, **8**).

http://zoobank.org/urn:lsid:zoobank.org:act:62E65192-ED0F-4F4B-B5B4-D372D38EC9D5

Etymology: The specific epithet honors Mr. Zhengkun Hu for his assistance and contribution in collecting Burmese amber.

Material: *Holotype*: CNU-HET-MA2019005 (male), housed in the Key Lab of Insect Evolution and Environmental Changes, College of Life Sciences, Capital Normal University, Beijing, China (CNUB; Yunzhi Yao, Curator).

Horizon and Locality: Hukawng Valley, Kachin State, northern Myanmar; mid-Cretaceous, lowermost Cenomanian.

Diagnosis: Same as generic diagnosis.

Description: Nearly complete preserved male specimen. Body flattened and elongate with large coarse punctures. Length about 2× as long as maximum pronotal width, overall brown, ventral view of thorax broken, not visible.

Head: Flattened and broad, nearly quadrate not 2× wider than long, with large punctures on posterior margin of head and clypeus; clypeus slightly longer than paraclypei, apex blunt, not obviously broadened, without peg-like setae apically, with a pair of hair-like setae subapically; each paraclypei with a hair-like seta apically; compound eyes large, contiguous with anterior margin of pronotum, each with a short apical seta on inner margin of compound eyes; ocelli not visible; base of antenna not visible, last three antennomeres subequal with each other; rostrum incompletely preserved.

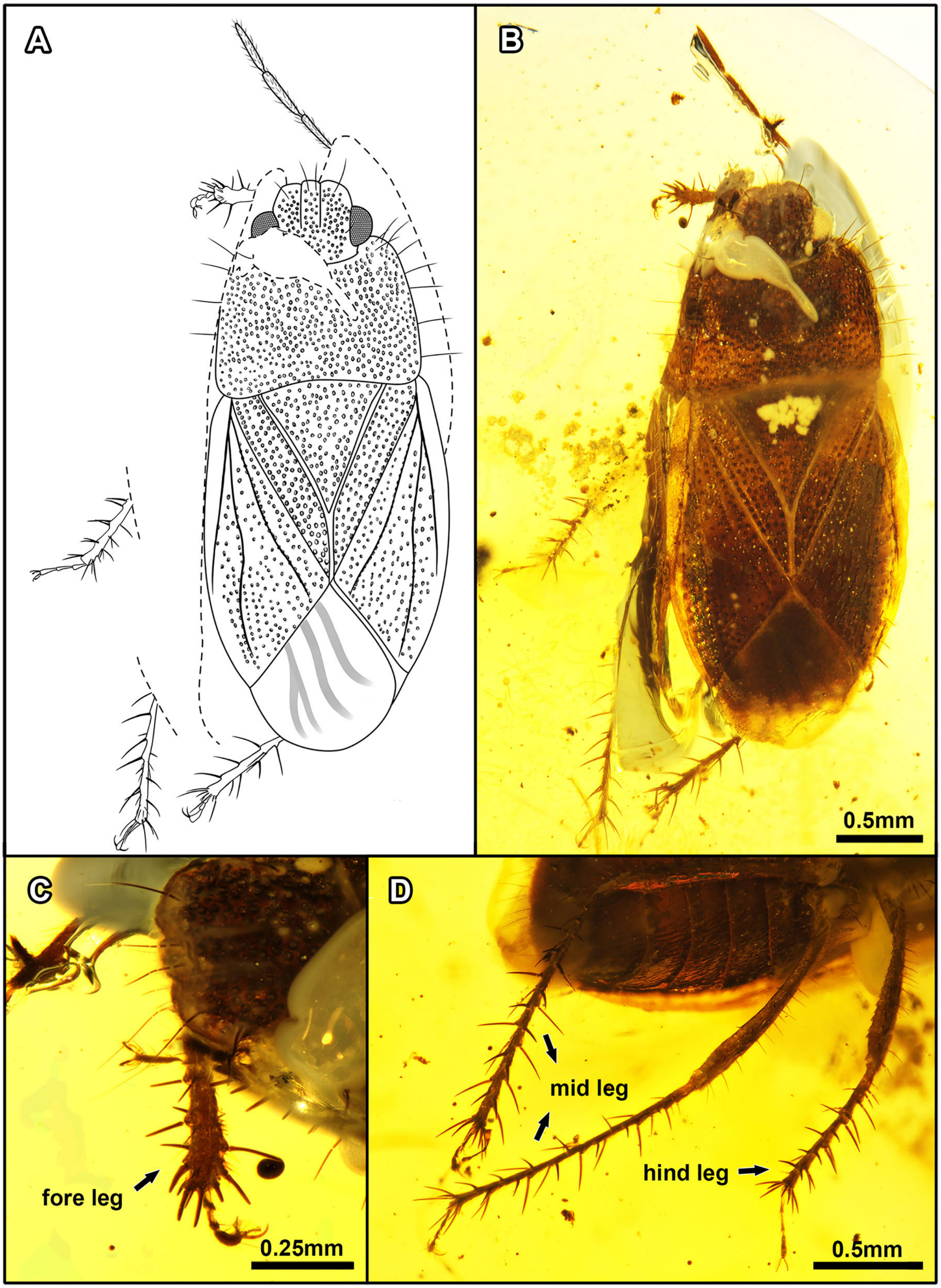

FIGURE 7 | *Quinalveus hui* gen. et sp. nov., in Burmese amber. Holotype, CNU-HET-MA2019005 (male). **(A)** Line drawing in dorsal view. **(B)** Habitus in dorsal view. **(C)** Protibia. **(D)** Meso- and metatibiae. Scale bars: A = B = 0.5 mm; C = 0.25 mm; D = 0.5 mm.

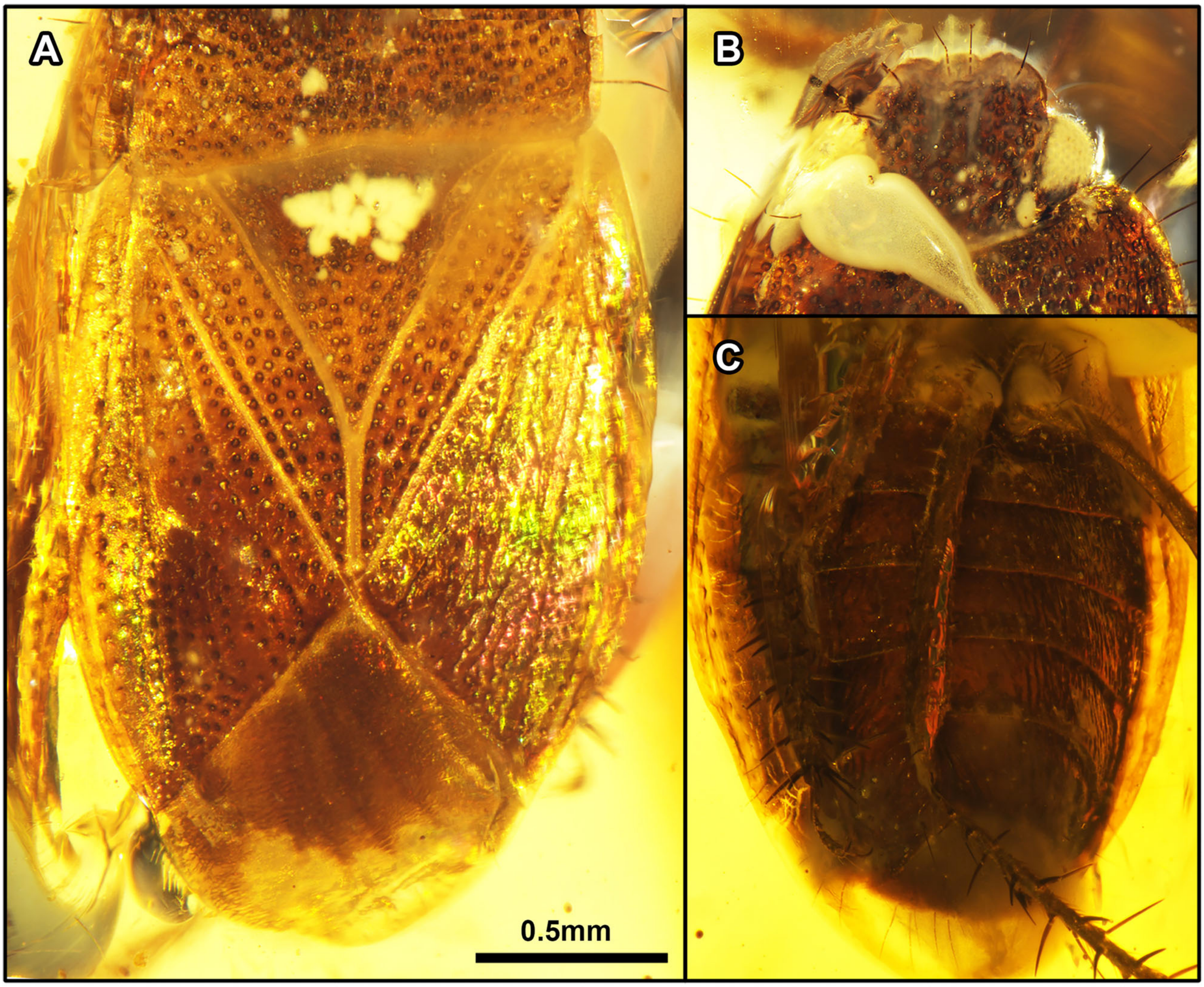

FIGURE 8 | *Quinalveus hui* gen. et sp. nov., in Burmese amber. Holotype, CNU-HET-MA2019005 (male). **(A)** Scutellum and forewings in dorsal view. **(B)** Head in dorsal view. **(C)** Abdomen in ventral view. Scale bars: A = B = C = 0.5 mm.

Thorax: Pronotum nearly trapezoidal with dense coarse punctures, collar absent; anterior margin raised upward medially, anterior angles bulging forward, forming a distinct arc with a hair-like seta, posterior margin slightly swollen and concave medially, pronotum with seven hair-like setae on both sides of edge at least; calli large in the middle of pronotum. Metathoracic scent gland not visible. Scutellum large, triangular, width subequal to length, depressed basomedially, margin of scutellum with relatively large and coarse punctures, fewer punctures medially on scutellum, apex of scutellum tapering. Hemelytron: macropterous, clavus broad, with five rows of coarse punctures parallel to lateral margin of scutellum; claval commissure present, length subequal to half of scutellar length; corium large, about two-thirds length of hemelytron, with a single row of distinct punctures close to clavus and anterior margin of forewing; corium elongate, junction with membrane straight, base of corium without seta; C entirely fused with Sc, R + M separated from C + Sc at about one-fifth length of corium, R + M in forewing raised and keel-like; Cu basally close to R + M, apex of Cu widely separated from the apex of R + M; membrane almost translucent, faintly infumate, with three simple veins, last vein branching at apex; forewing distinctly surpassing tip of the abdomen. *Legs*: meso- and metacoxae closer to each other than procoxae, meso- and metacoxae each with four long spines; femora thicker than tibiae with long setae; protibia flattened, broadened apically, shorter than meso- and metatibiae, with about eight long spines along apical margin, lateral margin with about 12 slender and relatively shorter spines; mesotibia as thick basally, with about seven long spines along apical margin, lateral margin with about 17 dense, slender, long spines; metatibia slender, with about seven long spines along the apical margin, lateral margin with more than 20 long, relatively slender spines; tarsi trimerous, tarsomeres equal in thickness, third tarsomere longest, first tarsomere almost as long as the second tarsomere;

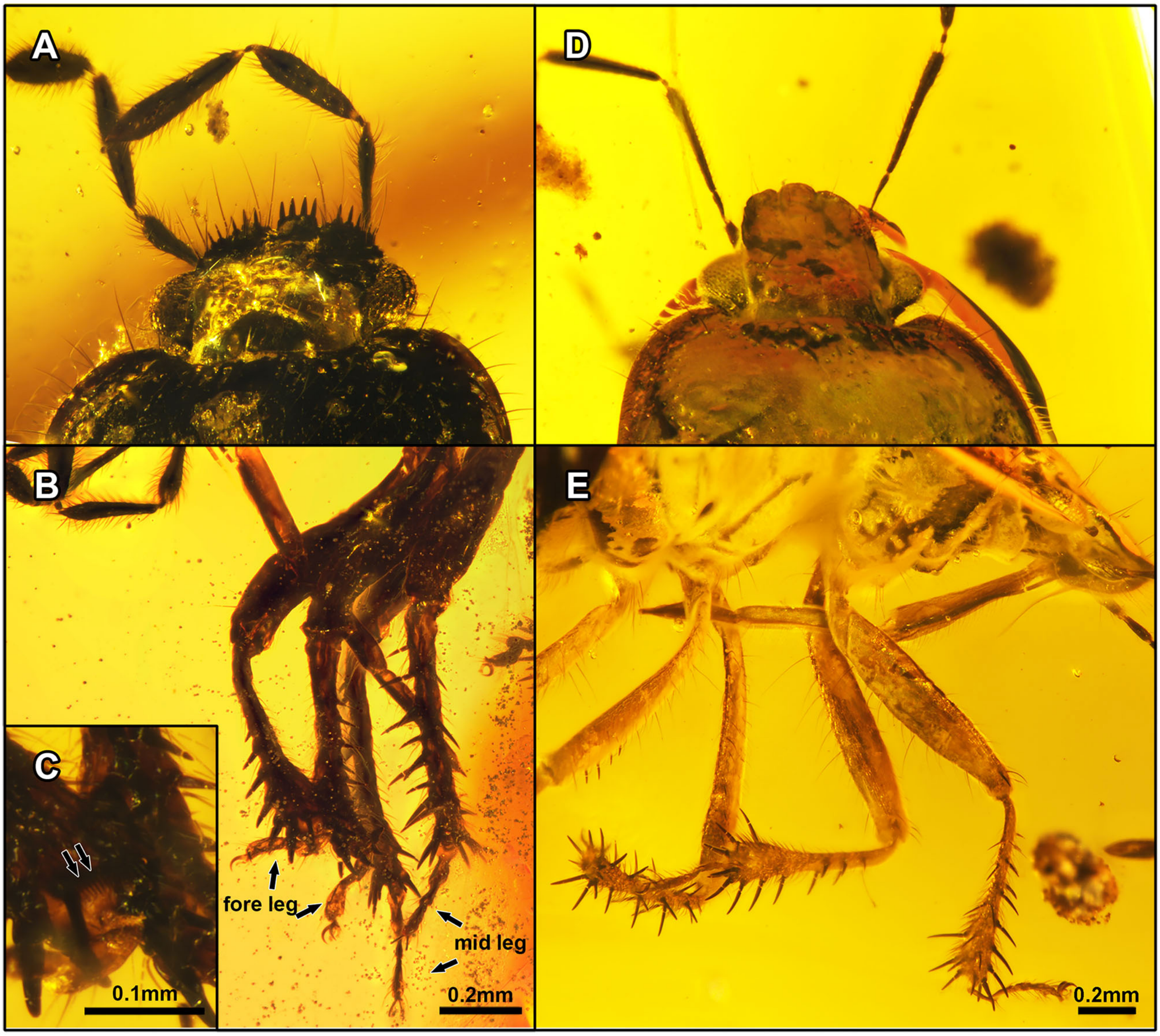

FIGURE 9 | Two different morphotypes in Burmese amber. Photograph of *Acanthamnestus ovoideus* gen. et sp. nov. in **(A–C)**. **(A)** Head in dorsal view. **(B)** Protibiae in left lateral view. **(C)** Detail of protibial comb. Photograph of *Laevigemma lisorum* gen. et sp. nov. in **(D,E)**. **(D)** Head in dorsal view. **(E)** Protibiae in left lateral view. Scale bars: A = B = 0.2 mm; C = 0.1 mm; D = E = 0.2 mm.

pretarsal claws elongate, pulvilli narrowed, capitate apically, as long as claws.

Abdomen: Abdomen of equivalent width with thorax; sterna brown, third to eight sterna with numerous distinct small punctures and shiny semierect setae and distinctive longer, dense setae medially.

Dimensions (in mm): Body length: 3.30; maximal width of body: 1.44; length of head: 0.49, width: 0.77; length of compound eyes: 0.17, width: 0.23; distance of ocelli: ?; length of antennomeres I–V: ?, ?, ?, 0.27, 0.24; length of rostral segments I–IV: ?, ?, 0.24, 0.28; length of pronotum: 0.82, width: 1.23; length of scutellum: 0.75, width: 0.77; length of anterior margin of corium: 1.49; length of hemelytron: 2.02, width: 0.81; length of claval commissure: 0.38; length of clavus: 1.18; length of fore leg: profemur: 0.69, protibia: 0.60, protarsomeres I–III: 0.13, 0.04, 0.11; length of mid leg: mesofemur: 0.82, mesotibia: 0.68, mesotarsomeres I–III: 0.11, 0.09, 0.13; length of hind leg: metafemur: 1.03, metatibia: 1.30, metatarsomeres I–III: 0.12, 0.07, 0.10.

Phylogenetic Analysis

Analyses of the character matrix yielded only one most parsimonious tree [tree length = 115, consistency index (CI) = 0.52, retention index (RI) = 0.66] as shown in **Supplementary Figure S1**. Pertinent results of the phylogenetic analysis include subfamily Amnestinae as monophyletic; the

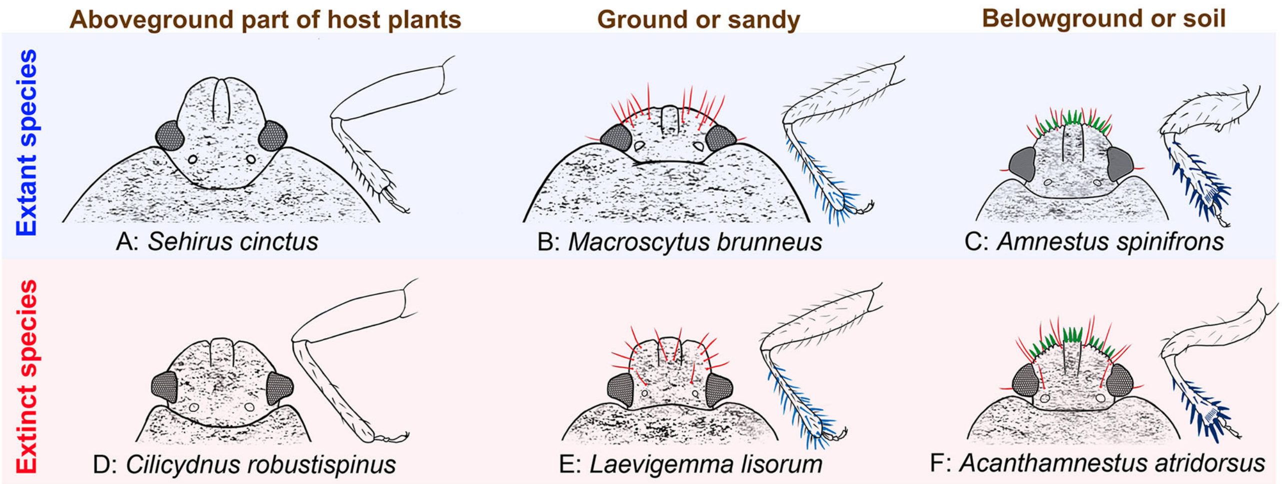

FIGURE 10 | Three morphotypes corresponding to three different habits in extant and extinct cydnids.

extant genus *Amnestus* with new genus *Acanthamnestus* being the sister group.

Monophyly of Amnestinae

The phylogenetic analyses are the first cladistic test of Amnestinae including fossil and extant taxa. Among all of the subfamilies of Cydnidae, the Amnestinae are easily recognized based on the claval commissure present, and this character state only appears in Amnestinae. Therefore, we regard Amnestinae as monophyletic.

Amnestus + Acanthamnestus

The results of our analysis show that the new genus *Acanthamnestus* and extant genus *Amnestus* have a sister-group relationship, with two character states supporting this clade: Body elongate, length more than 2× but <4× as long as maximum body width (character 0, state 0); forewing much longer than abdomen (character 33, state 1). Within this clade, the monophyly of *Amnestus* was supported by the following characteristics: Labium very long, reaching to metacoxae or abdomen (character 12, state 2); profemur and metafemur with a bifid spine on the ventral surface (character 36, state 1; character 37, state 1). The supporting character for the monophyly of *Acanthamnestus* is mesotibia broadened apically (character 39, state 1).

The Early Evolution of Soil Habits Among Amnestinae

The results of ancestral state reconstructions of soil-dwelling characters (**Figure 11**) indicated that soil-associated traits evolved once among Amnestinae. The lack of peg-like setae and strong protibial spines are considered plesiomorphies, and these features appear at different times independently on the tree. The appearance of peg-like setae on the head evolved later than the spines on the tibiae.

DISCUSSION

Among modern Heteroptera, two structures are closely linked to soil habits, situated on the head and foreleg, respectively: the anterior margins of the head with a circular crown consisting of hair- and peg-like setae; protibiae flattened and swollen, with thick spines or toe-like structures for pushing and digging. Lis and Pluot-Sigwalt (2002) noted that the rounded and flattened head with a circular crown of setae in Cydnidae suggested that such species are well suited for pushing and digging soil and are therefore bulldozers or diggers. They usually feed on roots, fallen fruits, or seeds, such as *Amnestus ficus* (Mayorga and Cervantes, 2001) (Amnestinae), *Schiodtella secundus* (Lis, 1991) (Cephalocteinae), and *Chilocoris heissi* (Lis, 1994) (Cydninae). Those lineages lacking peg-like setae on the head, such as the tribe Sehirini (Sehirinae), are commonly collected from the host-plant leaves above ground (Schwertner and Nardi, 2015), feeding on the fluids of plant stems and leaves, such as *Sehirus cinctus albonotatus* (Dallas, 1851) and *Canthophorus dubius* (Say, 1825; Hertzel and Scharmann, 1973). It is interesting that in Ochteridae such structures and behaviors are ontogenetically separated, with nymphs and adults differing. In this family, the fossorial nymphs possess the crown of setae and construct cavities in the soil in which they rest or molt (Dufour, 1833; Bobb, 1951; Boulard and Coffin, 1991; Lis and Pluot-Sigwalt, 2002), while the adults lack such structures and live aboveground and do not burrow. In addition, the flattened and swollen legs with stout thick spines or toe-like structures on the apical and lateral margins are similarly indicative of soil-dwelling insects, and similar burrowing/digging structures are found across numerous unrelated lineages, such as scarab beetles, mole crickets, and nymphal cicadas (Frost, 1959; Snodgrass, 1967; Richards and Davies, 1977; Gullan and Cranston, 2000).

Based on fossil records of Cretaceous Cydnidae (**Supplementary Table S1**), we can recognize three distinct morphotypes. In the first morphotype, the head lacks broad

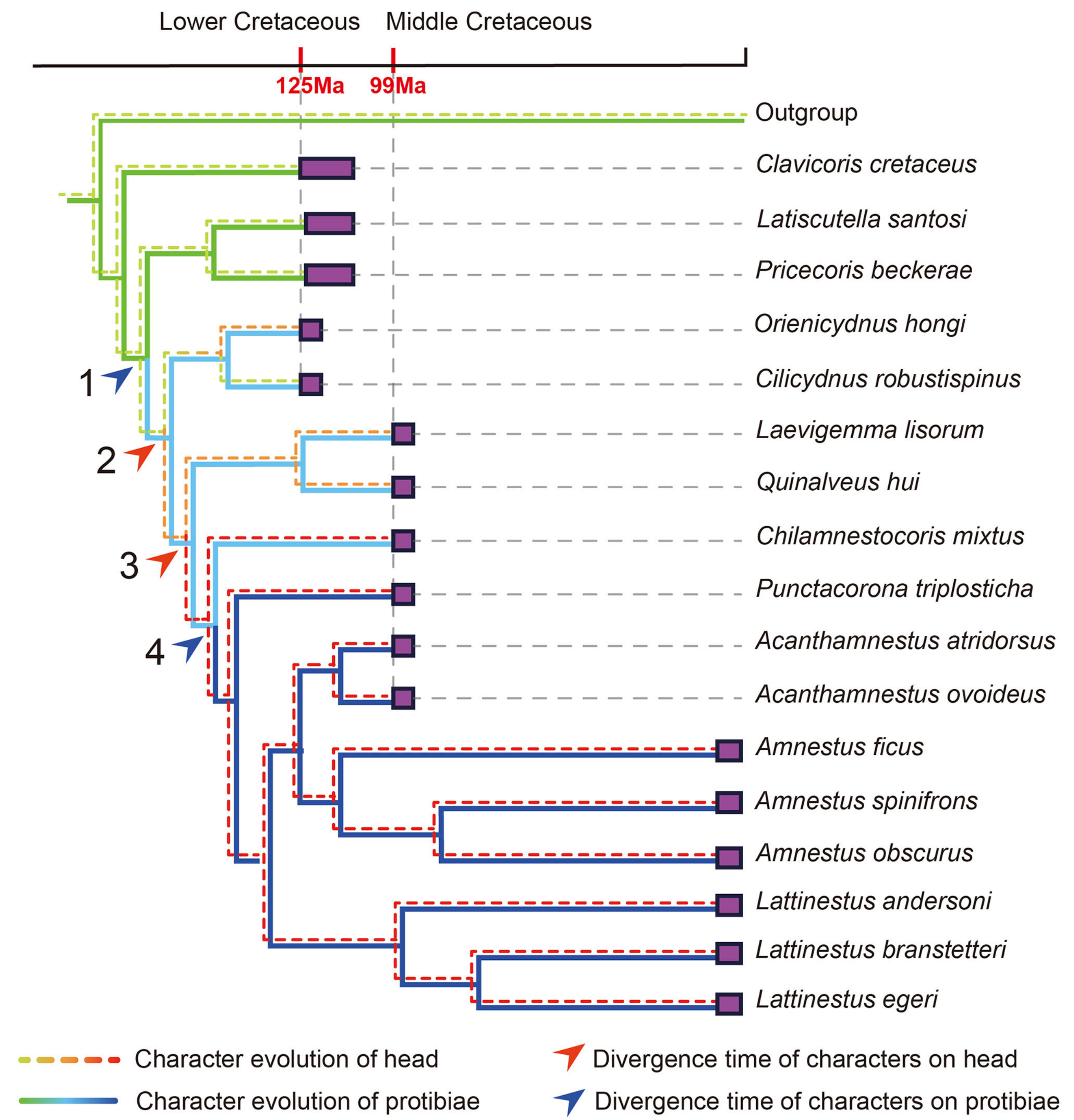

FIGURE 11 | Phylogeny of subfamily Amnestinae, including fossil species and two extant genera. Reconstructions of character evolution derived from phylogenetic analysis. At the top are geological periods calibrated to a time scale; arrows indicate the divergence time of characters on head and protibiae; purple blocks represent the occurrence time of species. Branches are color coded to represent the evolution of different head and protibial characters (see legend; see also **Supplementary Figure S1**).

and flattened clypeus and paraclypei, peg-like setae are absent (**Figure 10D**), and the protibiae are relatively slender and not broadened apically, lacking stout spines on the apical and lateral margins. Such a type can be found in *Clavicoris cretaceus* (Popov, 1986), *Pricecoris beckerae* (Pinto and Ornellas, 1974), and *Latiscutella santosi* (Pinto and Ornellas, 1974), among many others. Species of the second morphotype have the surface of the body relatively smooth, with tiny and distinct

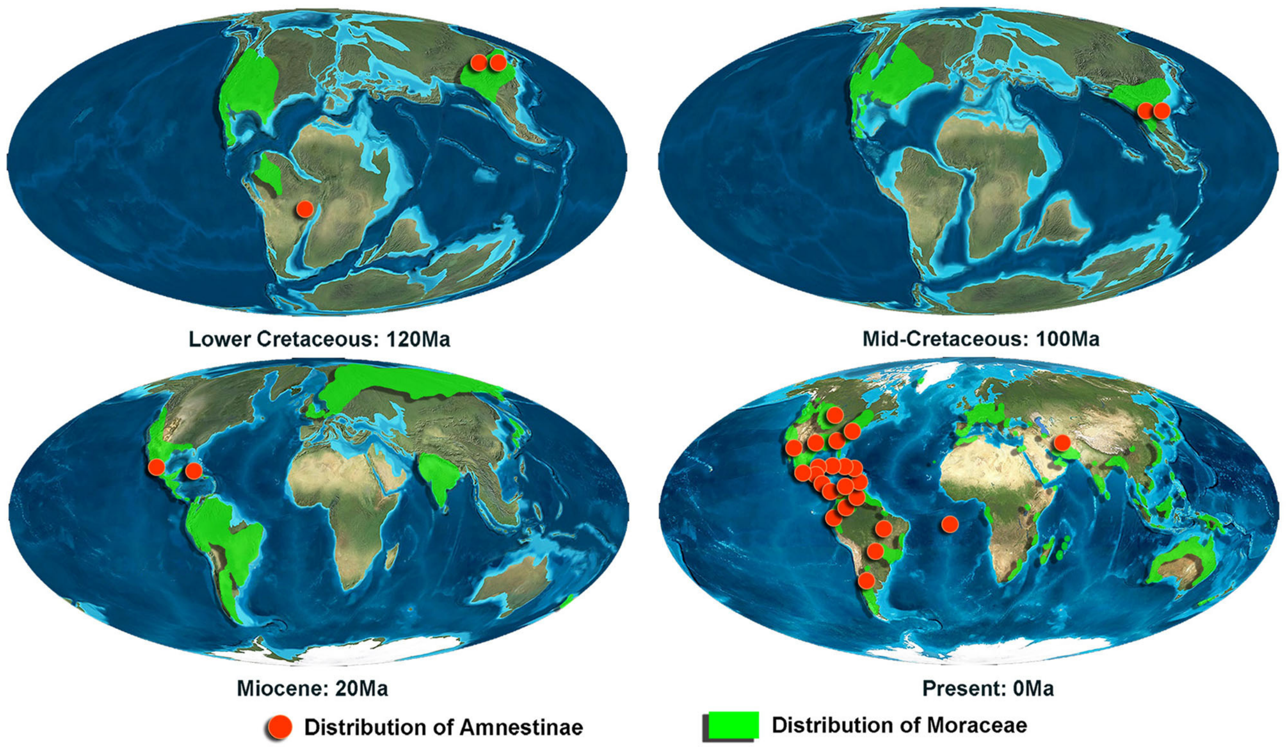

FIGURE 12 | Distribution of Amnestinae and Moraceae in different geological ages. Red dots represent the distribution of Amnestinae; green outlines represent the distribution of Moraceae.

punctures, the clypeus and paraclypei broad and flattened without peg-like setae, instead with only 4–6 hair-like setae (**Figures 9D,E**, **10E**), and the femora and tibiae bearing some slender, weakspines on the outer margin, and with the protibial apex slightly enlarged—as may be observed for *Pullneyocoris dentatus* (Lis et al., 2020), *Laevigemma lisorum* gen. et sp. nov. and *Quinalveus hui* gen. et sp. nov. In the last morphotype (**Figures 9A–C**, **10F**), the clypeus has four long, stout, sharp peg-like setae; and the paraclypei each bears a submarginal row of five more or less sharp-ended peg-like setae and five hair-like setae, with each marginal setigerous puncture arising from its own well-developed tubercle, and collectively, these form a circular crown; the profemur is relatively stout; the apex of the protibia is flattened and broadened, with distinct multiple short and stout spines in a longitudinal series from about mid-length of the lateral margin to the apex; and the apices of the meso- and metatibiae are slightly broadened, with many strong spines (**Figure 9B**). This third morphotype is found in *Acanthamnestus* gen. nov. It is interesting to note that the three morphotypes correspond to three different habitat preferences among modern cydnids (**Figure 10**).

Representatives of the first morphotype ("surface dwellers") are found from the outgroup and the earliest fossil cydnids. All of the known cydnid fossils in the Early Cretaceous belong to this type (**Figure 10D**), and they are generally similar to the extant subfamily Sehirinae (**Figure 10A**), which typically live on the aboveground portions of their host plants (Mcdonald, 1968; Rider, 2012; Schwertner and Nardi, 2015), and lack corresponding structures suitable for soil-dwelling habits. Fossils of the second and third morphotypes are both found in Burmese amber (**Figure 9**). The second morphotype (**Figures 9D,E**, **10E**) resembles the extant genus *Macroscytus* (Fieber, 1860) (**Figure 10B**) in characters of the head and protibia, suggesting that these taxa already had some ability to burrow and therefore represent the first of the hemiedaphic cydnids, albeit still living the majority of their life on the surface ("minor burrowers"). The final morphotype (**Figures 9A,B**, **10F**) is most consistent with the majority of extant cydnids which dig in and spend much of their life cycle in the soil ("true burrowers"), such as *Amnestus spinifrons* (Say, 1825) and *Cyrtomenus teter* (Spinola, 1837; Schwertner and Nardi, 2015). Within this lineage, there is often found a comb of setae at the protibial apex, a structure used to clean dust or soil from the antennae and/or labium. Referred to as a "grooming" or "cleaning" comb, such a structure is also present in *Acanthamnestus atridorsus* gen. et sp. nov (**Figure 9C**). Such grooming structures are particularly indicative of taxa spending much of their life within the soil, and its presence in *A. atridorsus* gen. et sp. nov. further supports the indication that this species lived a considerable part of its life in the soil, perhaps emerging as an adult only to mate and lay eggs, much like many modern cydnids (García and Bellotti, 1980; Riis et al., 2005; Nardi et al., 2008; Schwertner and Nardi, 2015). It further emphasizes that the

FIGURE 13 | Three-dimensional ecological reconstruction of *Acanthamnestus atridorsus* gen. et sp. nov.

origin of such soil-dwelling specializations among cydnids dates from at least the mid-Cretaceous. Reconstruction of character transitions across the phylogeny implies that soil-dwelling habits evolved once in Amnestinae and likely independently from other such occurrences elsewhere in Cydnidae as the basalmost amnestines lack such structures (**Figure 11**). Characters relating to soil habits first appeared during the Early Cretaceous, but only of the "minor burrowers" morphotype and were therefore not yet truly subterranean. *Orienicydnus hongi* (Yao et al., 2007) and *Cilicydnus robustispinus* (Yao et al., 2007) were found in the Early Cretaceous Yixian Formation in northeastern China, and both possessed characters for some limited burrowing but living principally on the soil surface. The true burrowers first appear in the record in the mid-Cretaceous. The time of appearance of different elements of the overall hemiedaphic suite of features is interesting, with the origin of peg-like setae on the head arising subsequent to the protibial spines. This pattern of transition is intuitive as the protibial structures are certainly necessary for digging a burrow and are present in many taxa that burrow into the soil, but do not necessarily live and feed within the soil substrate. The characters of the head, however, permit some degree of forward movement through the soil matrix for taxa not only burrowing into the soil but also simultaneously bulldozing their way through the substrate. Basically, the former one is simply removing soil and then moving into this space, while the latter one is digging but also penetrating forward into the matrix.

Acanthamnestus gen. nov. was recovered as a sister to the extant genus *Amnestus* (Dallas, 1851) (**Figure 11**), suggesting that they may perhaps share further biological similarities. Modern Amnestinae are found in the Western Hemisphere, living in warm, tropical or subtropical, moist deciduous forests. Perhaps not surprisingly, when looking at the paleoenvironments where fossil Amnestinae have been discovered (**Supplementary Table S1**), these same conditions are repeated in different geological periods—all were warm and humid, with rich tropical and subtropical vegetation. Species of the subfamily have preferred these same environmental conditions over a vast expanse of geological time. Myanmar in the mid-Cretaceous was also a warm, humid tropical forest and hosted a rich diversity of arthropods (Grimaldi et al., 2002; Grimaldi and Ross, 2017). This particular niche restriction suggests that, at least to some degree, the subfamily could be an indicator insect for the paleoenvironment. Some extant species of Amnestinae live in the soil near and feed on plants of the family Moraceae, such as *Amnestus ficus* (Mayorga and Cervantes, 2001), *Amnestus obscurus* (Mayorga and Cervantes, 2005), and *Amnestus calakmulensis* (Mayorga and Cervantes, 2005). Mayorga and Cervantes (2001) have reported that species of *Ficus* (Moraceae) were the primary food of *A. ficus*, especially when the fruits were mature. When large numbers of fruits and seeds fall to the ground, individuals of *A. ficus* would feed on these and females sometimes laid individual eggs inside the fruits of *Ficus*. Interestingly, fossil and modern occurrences of Amnestinae are consistently found within the historical range of Moraceae, or, during the Early and mid-Cretaceous, stem groups to Moraceae (Zerega et al., 2005; Zhang et al., 2018; **Figure 12**; **Supplementary Table S2**). Such a correlation suggests that the emergence of soil habits in Amnestinae may be related to the appearance of Moraceae, and there seems to have been a lengthy association between them. This would seem to suggest that early ancestors of Moraceae may have already been present by the mid-Cretaceous.

The discovery of *Acanthamnestus* from the mid-Cretaceous represents the earliest unequivocal soil-dwelling cydnids and pushes back the geological record of hemiedaphic true bugs to 99 Ma. The morphology and phylogenetic position of *A. atridorsus* indicate that it used its protibiae and crown of setae to dig and shovel through the soil as it lived beneath the surface. Environmental evidence, the pattern of distribution for host plants, and the present fossils provide new insight into the early origin of soil habits and that their emergence may be linked to the appearance of Moraceae, with a subsequent lengthy association between these plants and Amnestinae (**Figure 13**).

DATA AVAILABILITY STATEMENT

The datasets presented in this study can be found in online repositories. The names of the repository/repositories and accession number(s) can be found below: ZooBank (urn:lsid:zoobank.org:pub:383D9EDF-02C3-4565-BED1-8C72E13E6FB9).

AUTHOR CONTRIBUTIONS

SD and YY: conceptualization. YY: methodology and project administration. SD: software, formal analysis, investigation, data curation, writing—original draft preparation, and visualization. YY and ME: validation. YY and DR: resources, supervision, and funding acquisition. ME, YY, and LG: writing—review and editing. All authors have read and agreed to the published version of the manuscript.

FUNDING

This project was supported by the National Natural Science Foundation of China (Nos. 31970436, 31730087, 32101239, and 32020103006), Joint Fund of the Beijing Municipal Natural Science Foundation, and Beijing Municipal Education Commission (KZ201810028046).

ACKNOWLEDGMENTS

We are grateful to Xiao Zhang, Yijia Wang, and Mao Zhang for their comments on the manuscript and Mr. Zhengkun Hu for his assistance and contribution in collecting Burmese amber. We also thank Xiaoran Zuo for assistance with reconstruction.

SUPPLEMENTARY MATERIAL

The Supplementary Material for this article can be found online at: https://www.frontiersin.org/articles/10.3389/fevo.2022.908044/full#supplementary-material

REFERENCES

Bobb, M. L. (1951). Life history of *Ochterus banksi* Barber (Hemiptera: Ochteridae). *Bull. Brookl. Entomol. Soc*. 46, 92–100.

Boulard, M., and Coffin, J. (1991). Sur la biologie juvénile d'*Ochterus marginatus* (Latreille, 1804). Camouflage et construction (Hemiptera: Ochteridae). *Travaux Lab. Biol. Evol. Insectes EPHE*. 4, 57–68.

Cao, H. J., Boudinot, B. E., Shih, C. K., Ren, D., and Gao, T. P. (2020). Cretaceous ants shed new light on the origins of worker polymorphism. *Sci. China Life Sci*. 63, 1085–1088. doi: 10.1007/s11427-019-1617-4

Dallas, W. S. (1851). List of the specimens of hemipterous insects in the collection of the British Museum. *J. British Astron. Assoc*. 2, 1368.

Dolling, W. R. (1981). A rationalized classifi cation of the burrower bugs (Cydnidae). *Syst. Entomol*. 6, 61–67 doi: 10.1111/j.1365-3113.1981.tb00016.x

Dufour, L. (1833). Recherches anatomiques et physiologiques sur les Hémiptères accompagnées de considérations relatives à l'histoire naturelle et à la classification de ces insectes. *Mém. Savants Etrang. Acad. Sci. Paris*. 4, 123–432. doi: 10.5962/bhl.title.12418

Fieber, F. X. (1860). *Die europäischen Hemiptera, Halbflüger (Rhynchota, Heteroptera), I-II*. Wien: Gerold's Sohn Press, 1–112.

Frost, S. W. (1959). *Insect Life and Insect Natural History, 2nd Edn*. New York, NY: Dover Publications.

García, C. A., and Bellotti, A. C. (1980). Estudio preliminar de la biología y morfología de *Cyrtomenus bergi* F. Nueva plaga de la yuca. *Rev. Colombiana de Ento*. 6, 55–61.

Goloboff, P. A. (1999). *NoName (NONA), Version 2.0. Program and Documentation*. Tucumán: Fundación Instituto Miguel Lillo.

Goloboff, P. A., and Catalano, S. A. (2016). TNT version 1.5, including a full implementation of phylogenetic morphometrics. *Cladistics*. 32, 221–238. doi: 10.1111/cla.12160

Grimaldi, D., and Engel, M. S. (2005). *Evolution of the Insects*. Cambridge: Cambridge University Press.

Grimaldi, D. A., Engel, M. S., and Nascimbene, P. C. (2002). Fossiliferous Cretaceous amber from Myanmar (Burma): its rediscovery, biotic diversity, and paleontological significance. *Am. Mus. Nov*. 3361, 1–71. doi: 10.1206/0003-0082(2002)3612.0.CO;2

Grimaldi, D. A., and Ross, A. J. (2017). "Extraordinary Lagerstätten in amber, with particular reference to the Cretaceous of Burma," in *Terrestrial Conservation Lagerstätten: Windows into the Evolution of Life on Land*, eds N.C. Fraser, H-D. Sues (Edinburgh: Dunedin Academic Press), 287–342.

Gullan, P. J., and Cranston, P. S. (2000). *The Insects: An Outline of Entomology*. Oxford: Wiley-Blackwell, Press.

Hertzel, G., and Scharmann, K. H. (1973). Beitrag zur Kenntnis der Biologie und Verbreitung von *Canthophorus dubius* (Scopoli, 1765) (Het.: Cydnidae). *Entomol. Ber*. 33–39.

Lin, X. D., Labanderira, C. C., Shih, C. K., Hotton, C. L., and Ren, D. (2019). Life habits and evolutionary biology of new two-winged long-proboscid scorpionflies from mid-Cretaceous Myanmar amber. *Nat. Commun*. 10, 1235. doi: 10.1038/s41467-019-09236-4

Lis, J. A. (1991). Studies on Oriental Cydnidae. IV. New species, new synonyms and new records (Heteroptera: Pentatomoidea). *Ann. Upper Silesian Mus. Entomol.* 2, 165–190.

Lis, J. A. (1994). *A Revision of Oriental Burrower Bugs (Heteroptera: Cydnidae)*. Bytom: Upper Silesian Museum, Department of Natural History, 349.

Lis, J. A., Lis, B., and Ernest, H. (2018). Chilamnestocoris mixtus gen. et spec. nov., the first burrower bug (Hemiptera: Pentatomoidea: Cydnidae) in Upper Cretaceous Burmese amber. *Cretaceous Res*. 91, 257–262. doi: 10.1016/j.cretres.2018.06.017

Lis, J. A., and Pluot-Sigwalt, D. (2002). Nymphal and adult cephalic chaetotaxy of the Cydnidae (Hemiptera: Heteroptera), and its adaptive, taxonomic and phylogenetic significance. *Eur. J. Entomol*. 99, 99–109. doi: 10.14411/eje.2002.017

Lis, J. A., Roca-Cusachs, M., Lis, B., and Jung, S. H. (2020). Pullneyocoris dentatus gen. et sp. nov. (Hemiptera: Pentatomoidea: Cydnidae), the third representative of the subfamily Amnestinae from mid-Cretaceous amber of northern Myanmar. *Cretaceous Res*. 115, 104562. doi: 10.1016/j.cretres.2020.104562

Lis, J. A., Ziaja, D. J., Lis, B., and Gradowska, P. (2017). Non-monophyly of the "cydnoid" complex within Pentatomoidea (Hemiptera: Heteroptera) revealed by Bayesian phylogenetic analysis of nuclear rDNA sequences. *Arthropod Syst. Phylo*. 75, 481–496.

Maddison, W. P., and Maddison, D. R. (2011). *Mesquite: A Modular System for Evolutionary Analysis Version 2.75*. Available online at: http://mesquiteproject.org

Mayorga, C. M., and Cervantes, L. P. (2005). Description of six new species of *Amnestus* Dallas (Hemiptera: Heteroptera: Cydnidae) from Mexico. *J N Y Entomol. Soc*. 113, 159–173. doi: 10.1664/0028-7199(2005)113[0159:DOSNSO]2.0.CO;2

Mayorga, M. C., and Cervantes, P. L. (2001). Life cycle and description of a new species of *Amnestus* Dallas (Hemiptera-Heteroptera: Cydnidae) associated with the fruit of several species of *Ficus* (Moraceae) in Mexico. *J N Y Entomol. Soc*. 109, 392–402. doi: 10.1664/0028-7199(2001)109[0392:LCADOA]2.0.CO;2

Mcdonald, F. J. D. (1968). Some observations on *Sehirus cinctus* (Palisot de Beauvois) (Heteroptera: Cydnidae). *Can. J. Zool*. 46, 855–858. doi: 10.1139/z68-122

Nardi, C., Fernandes, P. M., and Bento, J. M. S. (2008). Wing polymorphism and dispersal of *Scaptocoris carvalhoi* (Hemiptera: Cydnidae). *Ann. Entomol. Soc. Am*. 101, 551–557. doi: 10.1603/0013-8746(2008)101[551:WPADOS]2.0.CO;2

Nixon, K. C. (2002). *WinClada ver. 1.00.08. Published by the author, Ithaca, New York, Renner and Weerasooriya, USA*. Available online at: http://www.cladistics.com/ (accessed August 6, 2019).

Pinto, I. D., and Ornellas, L. P. (1974). "New Cretaceous Hemiptera (Insecta) from Codó Formation—Northern Brazil," in *Anais 28th Congresso Brasileiro de Geologia* (Brazil), 289–304.

Popov, Y. A. (1986). "Peloridiina (=Coleorrhyncha) et Cimicina (=Heteroptera)," in *Insects in Early Cretaceous Ecosystems of Western Mongolia,* ed A. P. Rasnitsyn, Vol. 28, Transactions of the Joint Soviet-Mongolian Paleontological Expedition, 47–84.

Richards, O. W., and Davies, R. G. (1977). *Imms' General Textbook of Entomology, vol. I: Structure, Physiology and Development, 10th Edn*. London: Chapman and Hall.

Rider, D. A. (2012). The heteroptera (Hemiptera) of North Dakota I: pentatomomorpha: pentatomoidea. *Gr. Lakes. Entomol*. 45, 312–380.

Riis, L., Esbjerg, P., and Bellotti, A. C. (2005). Influence of temperature and soil moisture on some population growth parameters of *Cyrtomenus bergi* (Hemiptera: Cydnidae). *Fla. Entomol*. 88, 11–22. doi: 10.1653/0015-4040(2005)088[0011:IOTASM]2.0.CO;2

Say, T. (1825). Description of new hemipterous (and orthopterous) insects collected in the expedition to the Rocky Mountains, performed by order of Mr. Calhoun, Secretary of War, under command of Major Long. *Journ. Acad. Nat. Sci*. 4, 307–345.

Schuh, R. T., and Slater, J. A. (1995). *True Bugs of the World (Hemiptera: Heteroptera): Classification and Natural History*. New York, NY: Cornell University Press, 336.

Schwertner, C. F., and Nardi, C. (2015). "Chapter 21. Burrower bugs (cydnidae)," in *True Bugs (Heteroptera) of the Neotropics*, eds A. R. Panizzi, and J. Grazia (Dordrecht-Heidelberg-New York-London: Springer Netherland), XXII + 901.

Shcherbakov, D. E., and Popov, Y. A. (2002). "Superorder Cimicidea Laicharting, 1781. Order Hemiptera Linne, 1758. The bugs, cicadas, plant lice, scale insects, etc," in *History of Insects*, eds A. P. Rasnitsyn, and D. L. J. Quicke (Dordrecht: Kluwer), 143–157.

Shi, G. H., Grimaldi, D. A., Harlow, G. E., Wang, J., Wang, J., Yang, M. C., et al. (2012). Age constraint on Burmese amber based on U-Pb dating of zircons. *Cretaceous Res*. 37, 155–163. doi: 10.1016/j.cretres.2012.03.014

Snodgrass, R. E. (1967). *Insects: Their Ways and Means of Living*. New York, NY: Dover Publications.

Spinola, M. (1837). *Essai sur les genres d'insectes appartenants à l'ordre des Hémiptéres, Lin. ou Rhyngotes, Fab. et à la section des Hètèroptères, Dufour*. Genoa: Yves Graviers, p. 383.

Wang, Y. J., Du, S. L., Yao, Y. Z., and Ren, D. (2019). A new genus and species of burrower bugs (Heteroptera: Cydnidae) from the mid-Cretaceous Burmese amber. *Zootaxa*. 4585, 351–359. doi: 10.11646/zootaxa.4585.2.8

Yang, H. R., Shi, C. F., Engel, M., Zhao, Z. P., Ren, D., and Gao, T. P. (2020). Early specializations for mimicry and defense in a Jurassic stick insect. *Natl. Sci. Rev*. 8, nwaa056. doi: 10.1093/nsr/nwaa056

Yao, Y. Z., Cai, W. Z., and Ren, D. (2007). The first fossil Cydnidae (Hemiptera: Pentatomoidea) from the Late Mesozoic of China. *Zootaxa*. 1388, 59–68. doi: 10.11646/zootaxa.1388.1.5

Zerega, N. J. C., Clement, W. L., Datwyler, S. L., and Weiblen, G. D. (2005). Biogeography and divergence times in the mulberry family (Moraceae). *Mol. Phylogenet. Evol*. 37, 402–416. doi: 10.1016/j.ympev.2005.07.004

Zhang, Q., Onstein, R. E., Little, S. A., and Sauquet, H. (2018). Estimating divergence times and ancestral breeding systems in *Ficus* and Moraceae. *Ann. Botany*. 20, 1–14. doi: 10.1093/aob/mcy159

Zhao, Z. P., Yin, X. C., Shih, C. K., Gao, T. P., and Ren, D. (2020). Termite colonies from mid-Cretaceous Myanmar demonstrate their early eusocial lifestyle in damp wood. *Natl. Sci. Rev*. 7, 381–390. doi: 10.1093/nsr/nwz141

Conflict of Interest: The authors declare that the research was conducted in the absence of any commercial or financial relationships that could be construed as a potential conflict of interest.

Publisher's Note: All claims expressed in this article are solely those of the authors and do not necessarily represent those of their affiliated organizations, or those of the publisher, the editors and the reviewers. Any product that may be evaluated in this article, or claim that may be made by its manufacturer, is not guaranteed or endorsed by the publisher.

frontiers | Frontiers in Ecology and Evolution

ORIGINAL RESEARCH
published: 03 June 2022
doi: 10.3389/fevo.2022.920255

A New Jurassic Kempynine Species With Notes on Historical Distributions of Kempyninae Integrated Both Fossil and Extant Taxa (Neuroptera: Osmylidae)

*Yiming Ma[1,2], Chungkun Shih[1,3], Dong Ren[1] and Yongjie Wang[4]**

[1] College of Life Sciences and Academy for Multidisciplinary Studies, Capital Normal University, Beijing, China, [2] Beijing No. 50 Middle School, Beijing, China, [3] Department of Paleobiology, National Museum of Natural History, Smithsonian Institution, Washington, DC, United States, [4] Guangdong Key Laboratory of Animal Conservation and Resource Utilization, Guangdong Public Laboratory of Wild Animal Conservation and Utilization, Institute of Zoology, Guangdong Academy of Sciences, Guangzhou, China

OPEN ACCESS

Edited by:
Phil Barden, New Jersey Institute of Technology, United States

Reviewed by:
Alexander Khramov, Russian Academy of Sciences (RAS), Russia
Yuyu Wang, Agricultural University of Hebei, China

***Correspondence:**
Yongjie Wang
wangyjosmy@foxmail.com

Specialty section:
This article was submitted to Paleontology, a section of the journal Frontiers in Ecology and Evolution

Received: 14 April 2022
Accepted: 09 May 2022
Published: 03 June 2022

Citation:
Ma Y, Shih C, Ren D and Wang Y (2022) A New Jurassic Kempynine Species With Notes on Historical Distributions of Kempyninae Integrated Both Fossil and Extant Taxa (Neuroptera: Osmylidae). Front. Ecol. Evol. 10:920255. doi: 10.3389/fevo.2022.920255

The extant kempynines, a strict "southern group," are confined to South America and Australia, while their most fossil relatives are abundantly recorded in the Northern Hemisphere. This pattern of the biogeographic distribution implies the complicated evolutionary scenario of Kempyninae. Herein, a new northern species *Arbusella platyptera* Ma *et* Wang, sp. nov. is described from the Jiulongshan Formation in Daohugou, Inner Mongolia, China. Additionally, a key to the extinct species and extant genera of Kempyninae is provided. Integrating all extant and most fossil genera of Kempyninae, we conducted phylogenetic analyses to explore the inner relationships of Kempyninae for the first time. The results corroborate the monophyly of Kempyninae and retrieve three clades within the subfamily, namely, two northern fossil genera (†*Arbusellla* + †*Jurakempynus*), constituting the basalmost clade and three other northern fossil genera (†*Sauktangida* + †*Mirokempynus* + †*Ponomarenkius*), forming a monophylic clade, which is sister to the third clade that includes all extant southern genera and the southern fossil genus of †*Euporismites*. Also, the extant kempynines were hypothesized to evolve independently from their northern Mesozoic relatives. The Dispersal-vicariance (DIVA) analysis revealed a northern and prepangean origin of Kempyninae, and the northern ancestral kempynines first colonized the Southern Hemisphere before the split of Pangea. Our results expose a more complicated evolutionary scenario of the insects with a long evolutionary history and provide new insights into the formation of distribution patterns in current relictual insects.

Keywords: new species, phylogeny, evolution, fossil, biogeography, DIVA

INTRODUCTION

Kempyninae, a subfamily of Osmylidae, currently comprises 11 genera, including three extant genera, namely, *Kempynus* Navás, 1912; *Australysmus* Kimmins, 1940; and *Euosmylus* Krüger, 1913, and eight fossil genera, namely, †*Euporismites* Tillyard, 1916; †*Cretosmylus* Makarkin, 1990; †*Jurakempynus* Wang et al., 2011b; †*Kempynosmylus* Makarkin, 2014; †*Sauktangida*

Khramov, 2014a; †*Arbusella* Khramov, 2014b; †*Ponomarenkius* Khramov et al., 2017; and †*Mirokempynus* Ma et al., 2020a (Winterton et al., 2019; Ma et al., 2020a). The extant Kempyninae, as an absolute "southern group," is restricted to Australia, New Zealand, Argentina, and Chile in South America (Kimmins, 1940; New, 1983; Martins et al., 2016), of which most genera are confined to a single area except for the genus *Kempynus*, occurring in all areas. Contradictory to the extant lineages, the fossil kempynines were almost entirely documented from the Northern Hemisphere in the Mesozoic, with the exception of one Cenozoic fossil species *Euporismites balli* from Queensland, which appears to be more closely related to the extant species in distribution (Lambkin, 1987; Makarkin, 1990, 2014; Wang et al., 2011a; Khramov, 2014a,b; Khramov et al., 2017; Ma et al., 2020a). The distribution pattern of fossil and extant lineages indicates the evolutionary process, and the historical biogeographic dynamics of Kempyninae may be more complicated (Wang et al., 2011b). Furthermore, the recent phylogenetic study of Osmylidae proposed the northern subfamily Osmylinae be sister to the other four southern subfamilies, i.e., Kempyninae, Eidoporisminae, Porisminae, and Stenosmylinae, instead of the current northern distributed groups, i.e., Protosmylinae and Spilosmylinae (Winterton et al., 2017). These results implied an earlier pre-Pangaea origin of Osmylidae and introduced a more complicated evolutionary scenario, and as a result, the current distributions of extant Kempyninae should not be simply attributed to the Gondwanan biogeographic events. To address the issues regarding the historical vicariance biogeographic distributions of Kempyninae, it is essential to study the phylogeny of Kempyninae by combining all fossil and extant lineages.

Herein, we describe a new species, *Arbusella platyptera* Ma *et* Wang, sp. nov., from the Middle Jurassic Jiulongshan Formation in Daohugou, Inner Mongolia, China. This new species can be assigned to Kempyninae based on the following apomorphic characters: The M space in the hind wing is extremely broad and sinuate cross-veins are arranged in the intramedial area to produce two rows of irregular cells, which are regarded as an apomorphy of Kempyninae (Winterton et al., 2019; Ma et al., 2020a). To investigate the inner relationships of Kempyninae, we conducted a phylogenetic analysis including all extant and most fossil genera. The phylogenetic results corroborated the monophyly of the subfamily, and the historical biogeography of Kempyninae was outlined by using the DIVA analysis. This study first investigated the historical biogeography of Kempyninae under the phylogenetic framework, and then promoted our understanding of this particular insect group.

MATERIALS AND METHODS

Material

The type specimen was collected from the Jiulongshan Formation of the Middle Jurassic at Daohugou Village, Shantou Township, Ningcheng County, Inner Mongolia, China, and deposited in the Key Laboratory of Insect Evolution and Environmental Changes, College of Life Sciences and Academy for Multidisciplinary Studies, Capital Normal University, Beijing (CNUB; Dong Ren, Curator). The specimen was observed and photographed by using a stereoscopic microscope, Nikon SMZ25 with an attached Nikon DS-Ri2 digital camera system. The line drawing was produced using the Adobe Photoshop CC and Adobe Illustrator CC software. The terminology for wing venation and genitalia follows Breitkreuz et al. (2017) and Winterton et al. (2019).

Wing vein abbreviations are as follows: C, costa; Sc, subcosta; RA, anterior branch of radius; RP, posterior branch of radius; MA, anterior branch of media; MP, posterior branch of media; CuA, anterior cubitus; CuP, posterior cubitus; A, anal veins. Other abbreviations involved are as follows: J_1, Early Jurassic; J_2, Middle Jurassic; J_3, Late Jurassic; O_1, late Paleocene-early Eocene; AUS, Australia; CHN, China; KG, Kyrgyzstan; KZ, Kazakhstan; MGL, Mongolia; NZL, New Zealand; SA, South America.

Phylogenetic Analyses

Taxa Sampling

Nine genera of Kempyninae were sampled in the phylogenetic analyses, including three extant genera, namely, *Kempynus*, *Euosmylus*, and *Australysmus*, and six extinct genera, namely, †*Arbusella*, †*Euporismites*, †*Jurakempynus*, †*Mirokempynus*, †*Ponomarenkius*, and †*Sauktangida* (refer to **Table 1** for more details). Three genera are selected as outgroups, including †*Vetosmylus* (a fossil genus of Osmylinae), *Osmylus* (the type genus of Osmylinae), and *Heterosmylus* (an extant genus of Protosmylinae). Two nominal kempynine genera, *Cretosmylus* Makarkin, 1990, and *Kempynosmylus* Makarkin, 2014, from the Baissa of Lower Cretaceous were not included in the analysis due to the absence of the key features (Makarkin, 1990, 2014), and their kempynine affinity requires further investigation.

Phylogenetic Analyses

As most fossil taxa of Kempyninae were established based on the characters of wings, we primarily adopted the wing characters in the phylogenetic analysis, including ten characters for the

TABLE 1 | Species examined in the phylogenetic analysis.

Taxa	Fossil/extant	Distributions
Outgroups		
Heterosmylus wolonganus Yang, 1992	Extant	China
Osmylus fulvicephalus Scopoli, 1763	Extant	Europe
Vetosmylus tentus Ma et al., 2020b	Fossil	China
Ingroups		
Sauktangida aenigmatica Khramov, 2014a	Fossil	Kyrgyzstan
Jurakempynus sinensis Wang et al., 2011b	Fossil	China
Jurakempynus loculosus Ma et al., 2020a	Fossil	China
Mirokempynus profundobifurcus Ma et al., 2020a	Fossil	China
Ponomarenkius excellens Khramov et al., 2017	Fossil	China
Arbusella bella Khramov, 2014a	Fossil	Kazakhstan
Arbusella platyptera sp. nov.	Fossil	China
Euporismites balli Tillyard, 1916	Fossil	Australia
Australysmus lacustris Kimmins, 1940	Extant	Australia
Euosmylus stellae McLachlan, 1899	Extant	New Zealand
Kempynus incisus McLachlan, 1863	Extant	New Zealand, Australia

forewing and seven characters for the hind wing. The list of characters and character states for the phylogenetic analyses of Kempyninae are outlined as follows. The data matrix of characters used in the phylogenetic analyses is shown in **Table 2**. The missing data were coded as "?" The character matrix was edited using NDE 0.5.0 (Page, 2001). The parsimony analyses were performed with Nona/WinClada using a heuristic search that employed a TBR + TBR search strategy, holding 10,000 trees and 1,000 replicates of random additions (Nixon, 2002).

Biogeographic Analysis

To trace the historical biogeographic distributions, the ancestral distribution reconstruction of Kempyninae was conducted with RASP 4.0 using the dispersal-vicariance optimization model, which is generally used in the analyses of ancestral reconstruction (Yu et al., 2010, 2015; Liu et al., 2012). Based on the current phylogenetic analysis and the previous study (Winterton et al., 2017), the sampled tree was compiled to declare a fully resolved topology of kempynine genera. The DIVA analysis was performed with default settings except for the maximum number of areas in ancestral ranges being constrained to three, considering the widest kempynine genus *Kempynus* distributed in three areas, i.e., South America, Australia, and New Zealand.

List of Characters and Character States for the Phylogenetic Analyses

Morphological character states are scored 0–2 and ? (0 = plesiomorphic state; 1–2 = apomorphic state; ? = state unknown). As the phylogenetic analysis was conducted for fossil and extant kempynine genera, the sampled characters were primarily selected from the wings that were most shared by fossil and extant taxa.

Characters of Forewing

1. An outline of the apical margin. 0, normal or slightly convex; 1, distinctly concave. The normal outer margin occurs in the most sampled genera. State 1 exists as an apomorphy in two extant genera: *Kempynus* and *Euosmylus*, whose shape of forewings is evidently modified into the falcate shape.
2. Position of M forking. 0, proximally branched, before (or corresponding to) the RP1 point from RP; 1, distinctly beyond the RP1 point from RP, and often present in-between RP1 and RP2 from RP. The position of M fork stably occurs before RP1 among Protosmylinae, Spilosmylinae, and most fossil kempynines. Although the sampled Osmylinae outgroups *Osmylus fulvicephalus* and *Vetosmylus tentus* have the proximally branched M, state 1 is also common in some extant species, implying the distinct variation in the position of the M fork within the subfamily. Among Kemypinae, M fork commonly located at the in-between of RP1 and RP2 from RP.
3. Subcostal veinlets. 0, simple, no distal forks; 1, many distal forks present. Simple subcostal veinlets are present in six subfamilies of Osmylidae. State 1 occurs in some genera of the subfamilies Kempyninae and Osmylinae.
4. The number of RP branches. 0, lesser, not more than 10; 1, numerous, more than 10. Number of RP branches is variable in Osmylidae, but state 0 is common in most families of Neuroptera. State 1 occurs in Kempyninae (except *Euosmylus* and *Australysmus*) and Osmylinae.
5. Arrangement of RP cross-veins. 0, two or more gradate series are present; 1, one gradate series is present; 2, irregular, gradate series is absent. State 0 occurs in the outgroups, *Heterosmylus* and *Osmylus*. In *Vetosmylus* and most extant kempynines, RP cross-veins generally form a row of gradate series. The irregularly arranged cross-veins in the radial sector are common in the fossil kempynine species.
6. Forewing MP. 0, branched pectinately distally; 1, branched dichotomously near the middle of the wing; 2, branched proximally (near the wing base). State 0 is common in most species of Osmylidae. State 1 occurs in a few extant species of *Kempynus*. State 2 only occurs in *Ponomarenkius*.
7. Length of CuP. 0, more than three-quarters the length of CuA, approximating equal length with CuA; 1, about half the length of CuA, and less than three-quarters the

TABLE 2 | Data matrix of characters used in the phylogenetic analyses.

Taxa	Characters																
	01	02	03	04	05	06	07	08	09	10	11	12	13	14	15	16	17
Heterosmylus wolonganus	0	0	0	0	0	0	1	0	0	0	0	0	0	0	0	1	0
Osmylus fulvicephalus	0	0	1	1	0	0	0	0	0	0	0	0	0	1	0	0	1
Vetosmylus tentus	0	0	1	1	1	0	0	2	0	0	0	0	0	1	0	0	?
Sauktangida aenigmatica	?	?	?	?	?	?	?	?	?	?	0	0	2	2	1	1	2
Jurakempynus sinensis	0	0	1	1	2	0	1	2	2	0	0	0	0	1	1	1	?
Jurakempynus loculosus	?	1	1	1	2	0	1	2	2	0	0	?	0	1	1	0	1
Mirokempynus profundobifurcus	?	?	?	?	?	?	?	?	?	?	0	0	1	2	1	0	2
Ponomarenkius excellens	0	1	1	1	1	2	0	0	0	2	0	0	1	2	1	0	?
Arbusella bella	0	1	1	1	2	0	0	0	0	0	1	0	0	1	1	?	?
Arbusella platyptera sp. nov.	?	?	?	?	?	?	?	?	?	?	1	0	0	1	1	?	?
Euporismites balli	0	?	?	1	?	?	?	?	?	0	0	0	2	2	2	0	?
Australysmus lacustris	0	1	1	0	1	0	0	1	1	0	0	0	2	2	2	0	1
Kempynus incisus	1	1	1	1	1	1	0	1	1	1	0	1	2	2	2	0	1
Euosmylus stellae	1	1	0	0	1	0	0	1	1	0	0	1	2	2	0	0	1

length of CuA. State 0 commonly occurs in Kempyninae and Osmylinae. State 1 occurs in *Jurakempynus* and *Heterosmylus*.

8. Forewing CuA. 0, branched pectinately distally; 1, branched dichotomously distally; 2, branched complicatedly near the middle of the wing. The pectinately branched CuA is common in Osmylidae and is considered as a synapomorphy of the family (Winterton et al., 2019; Ma et al., 2020a). State 1 only occurs in extant species of Kempyninae. State 2 only occurs in *Jurakempynus*.
9. Length of A1. 0, approximately half the length of CuP, and less than three quarters; 1, less than or approximately half the length of CuP; 2, more than three-quarters the length of CuP. The moderate length of A1 (approximately half the length of CuP) occurs in most extant Osmylidae. In the Kempyninae, Al is distinctly beyond half the length of CuP, of which two states are detected, i.e., approximately three-quarters the length of CuP and approximately equal length of CuP. State 1 only occurs in extant species of Kempyninae. State 2 commonly occurs in most fossil kempynines.
10. Space between M branches. 0, normal or slightly dilated, with a single row of cells; 1, obviously broadened, with a single row of cells; 2, strongly broadened, with multiple rows of cells. State 0 occurs commonly in all subfamilies except Kempyninae. State 1 is distinct in some species of *Kempynus* that are apomorphies of the genus. State 2 only occurs in *Ponomarenkius*.

Characters of Hind Wing

11. The interlinked cross-veins between costal veinlets. 0, absent; 1, present. State 0 is common in Osmylidae, and state 2 only occurs in *Arbusella* within Kempyninae.
12. RP branches. 0, branched regularly, straight or slightly bent near wing margin; 1, strongly curved in distal half of RP, and slightly sinuous in distal part. State 0 occurs commonly in five subfamilies: Osmylinae, Protosmylinae, Gumillinae Porisminae and Spilosmylinae. State 1 is distinct in *Kempynus* and *Euosmylus*.
13. Pattern of MP branches. 0, branched pectinately in distal; 1, branched proximally near the wing base; 2, branched dichotomously in distal. State 0 is common in outgroups and most species of Osmylidae. State 1 only occurs in two fossil genera *Mirokempynus* and *Ponomarenkius*. State 2 generally presents in other kempynine genera.
14. Space between M branches. 0, both branches parallel, obviously un-broadened; 1, distinctly broadened from the middle; 2, gradually widened from the base to the distal. State 0 occurs in most subfamilies of Osmylidae except Kempyninae and Osmyninae. State 1 occurs in Osmylinae and some fossil genera of Kempyninae. State 2 is common in Kempyninae, which is regarded as an apomorphy of the subfamily.
15. Arrangement of cells between M branches. 0, a single row of cells present; 1, multiple rows of cells occupying the entire area; 2, multiple rows of cells present in distal half of MP. Multiple rows of cells only occur in Kempyninae, which is an apomorphy of this subfamily. State 1 occurs in almost all fossil species of Kempyninae. State 2 only occurs to *Kempynus*, *Euosmylus* and *Euporismites*.
16. Length of A1. 0, about equal to or less than half the length of CuP; 1, more than half the length of CuP. State 0 occurs in most species of Osmylidae. State 1 only occurs to *Sauktangidas*, *Jurakempynus* and *Heterosmylus*.
17. Pattern of A3. 0, A3 simple, directly reaching the margin; 1, A3 fused with the first branch of A2 and forming a small loop; 2, A3 well-development, with some pectinated branches. State 0 occurs in the outgroup of Heterosmylus and also occurs in a few genera of Gumilinae. State 1 is present in Osmylinae and Kempyninae (e.g., *Euosmylus*). State 2 is common within the fossil osmylids.

RESULTS AND DISCUSSION

Systematic Paleontology

Order NEUROPTERA Linnaeus, 1758
Family OSMYLIDAE Leach, 1815
Subfamily KEMPYNINAE Carpenter, 1943
Genus ARBUSELLA Khramov, 2014b
Type species. *Arbusella bella* Khramov, 2014b
Included species. *Arbusella bella* Khramov, 2014b; *Arbusella magna* Khramov et al., 2017; Arbusella platyptera Ma *et* Wang, sp. nov.

Keys to the Extinct Species and Extant Genera of Kempyninae

1. HW: MP proximally branched and forming deep forking............2
- HW: MP forked at the middle or in distal half of wing...............3
2. HW: MA and MP forming the similar deep branches, three rows of regular cells present in medial region............ †*Ponomarenkius* Khramov et al., 2017 (CHN, J2)
- HW: The branches of MA and MP are different: MA branched distally, and MP proximally forked.................... †*Mirokempynus* Ma et al., 2020a (CHN, J2)
3. HW: cross-veins between MA and MP sinuous, and forming multiple rows of cells before branching of MP...........................4
- HW: cross-veins between MA and MP relatively straight, only forming a single row of cells before branching of MP....................13
4. HW: MP forked close to the middle, each branch of MP with pectinated or dichotomous branches.....................†*Sauktangida* Khramov, 2014a (KG, J1)
- HW: MP only forming the distal branches.........................5
5. HW: the presence of an additional row of gradate series between the subcostal veinlets .... 6 (†*Arbusella* Khramov, 2014b)
- HW: the absence of the gradate series between the subcostal veinlets...................................... 8 (†*Jurakempynus* Wang et al., 2011b)
6. Presence of large eye spots in hind wing.................. 7

- Absence of large eye spots in the hind wing; the presence of three tint longitudinal stripes in the forewing....... †*Arbusella magna* Khramov et al., 2017 (CHN, J2)

7. HW: Presence of two large eye spots, CuA forming more pectinate branches (ca. 12)............ †*Arbusella bella* Khramov, 2014b (KZ, J3)
   - HW: Presence of three large eye spots, CuA with less pectinate branches (ca. 6)....... *Arbusella platyptera* Ma *et* Wang, sp. nov. (CHN, J2)
8. HW: M region with two relatively regular rows of quadrangular cells; CuP with deeply dichotomic branches................ †*Jurakempynus bellatulus* Wang et al., 2011b (CHN, J2)
   - HW: M region with 2–3 irregular rows of cells; CuP with many pectinated branches....... 9
9. HW: CuP with relatively few branches, only forming 4–5 branches.............. †*Jurakempynus sinensis* Wang et al., 2011b (CHN, J2)
   - HW: CuP with numerous branches, more than 9 branches............ 10
10. HW: M region relatively narrow with an additional short and narrow row of cells............ †*Jurakempynus sublimis* Khramov, 2014b (MGL, J3)
    - HW: M region without an additional short and narrow row of cells............ 11
11. HW multi-row cells appeared only in distal half of the M widened region............ †*Jurakempynus epunctatus* Wang et al., 2011b (CHN, J2)
    - HW multi-row cells occupied almost all the M widened regions before MP distal fork....... 12
12. FW: A2 with relatively few and short branches; A2 shorter than half of A1........................ †*Jurakempynus arcanus* Khramov, 2014b (KZ, J3)
    - FW: A2 with relatively numerous and long branches; A2 longer than half of A1.............. †*Jurakempynus loculosus* Ma et al., 2020a (CHN, J2)
13. HW: MP deeply forked at the mid-length of wing; gradate series absent from both wings.................. †*Euporismites* Tillyard, 1916 (AUS, P1)
    - HW: MP with dichotomous branched beyond the mid-length of wing; outer gradate series distinct on both wings................. 14
14. HW: M branches widely forked, cross-veins between them somewhat sinuous........................ *Kempynus* Navás, 1912 (AUS, NZL, and SA)
    - HW: M branches normally forked, cells between them relatively quadrate..................15
15. Forewings distinctly falcate, membrane strongly patterned; relative small insect (wingspan ca. 20–30 mm)...........*Euosmylus* Krüger, 1913 (NZL)
    - Forewings not or slightly falcate, membrane-less patterned and scattered with sporadic spots; relatively large insect (wingspan > 40 mm).................. *Australysmus* Kimmins, 1940 (AUS)

Arbusella platyptera Ma and Wang, sp. nov. (**Figure 1**).

Diagnosis. Large hind wing with length exceeding 40 mm and width exceeding 15 mm; membrane with three large eye spots, one located at proximal one-third of wing, and the other two closely spaced and located at distal one-third of wing; numerous and sinuate cross-veins arranged in the two-third of radial region forming densely distributed cells with irregular sizes and shapes, and the outer well-defined gradate series; MP with irregularly arranged pectinated branches in the distal, and the first branch forming dichotomous branches; CuA with 6 pectinated branches.
Etymology. From the Greek combination of *platy-* and *-ptera*, referring to the broad wing.
Type material. Holotype CNU-NEU-NN2020005. Only the hind wing is preserved.
Type locality and age. Daohugou Village, Shantou Township, Ningcheng County, Inner Mongolia, China; Jiulongshan Formation, Aalenian/Bajocian boundary, Middle Jurassic.
Description. Hind wing *ca*. 43.8 mm in length, 16.6 mm in width. The proximal part of the hind wing is incompletely preserved.

Hind wing (**Figure 1**): membrane nearly transparent except for three distinct eye spots; trichosors well-developed along the margin; subcostal veinlets dichotomously forked from the pterostigma region to the apex; subcostal cross-veins regularly arranged and forming a row of gradate series in-between subcostal veinlets; RP with more than 25 branches, and each RP branch with irregular distal bifurcations; the region between MA and MP dilated visibly in the middle, with two rows of irregular cells in-between; MA only forming three simple primary branches in distal; CuP with 11 pectinated branches; A1 relatively straight and long, about one-half of CuP.
Remarks. The hind wing is significant to the generic taxonomy of Kempyninae, and many fossil genera were established based on the characters of the hind wing (Winterton et al., 2019). The genus *Arbusella* was first erected by Khramov based on a species from the Late Jurassic of Kazakhstan, which was most characterized by the presence of a row of gradate series in-between subcostal veinlets (Khramov, 2014a). In spite of the absence of forewing, the new specimen can be clearly assigned to the genus of *Arbusella* for sharing this character. It is noted that the hind wing length of the new specimen exceeds 40 mm long as preserved, which is the hitherto known largest fossil kempynine. Although the hind wings of two other *Arbusella* species are preserved partially, it can still be concluded that the two species are distinctly smaller than the new specimen according to the lengths of their forewings, i.e., 22.5 mm long in *A. bella* and *ca*. 37 mm long in *A. magna*. Comparing two *Arbusella* species, the new specimen can be easily distinguished from *A. bella* by three eye spots in the hind wing and CuA with 6–7 branches (*cf*. two large eye spots and 12 branches in *A. bella*). As only the partial hind wing of *A. magna* was preserved, the new specimen was just separated from the latter species by one apomorphic character, i.e., a large eye spot present in the middle of the hind wing vs. distinctly absent in *A. magna* (**Figure 1**, Khramov, 2017: figure 4B). Considering the significant differences between the new specimen and the known *Arbusella* species, we established a new species for it, and it is hoped

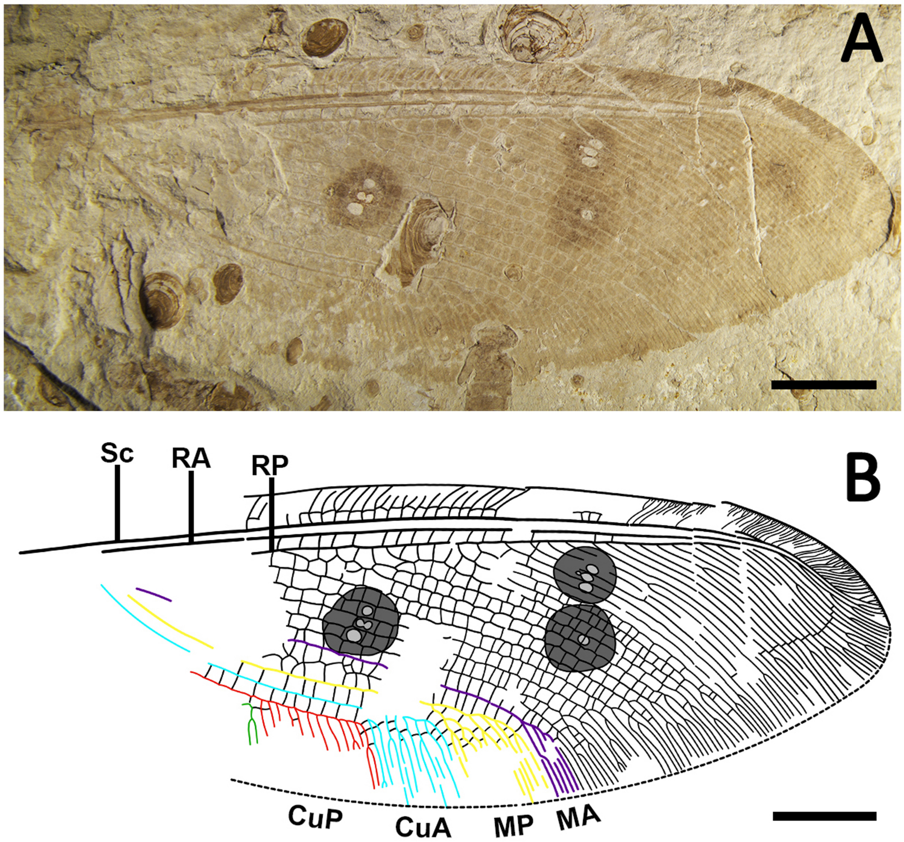

FIGURE 1 | Lance lacewing *Arbusella platyptera* Ma and Wang, sp. nov. (holotype, CNU-NEU-NN2020005) from the Middle Jurassic of Jiulongshan Formation in Daohugou, China. **(A)** Photograph of the hind wing. **(B)** Line drawing of the hind wing. Scale bars are 10 mm.

that more evidence could be found to further corroborate the taxonomic status of the new species.

Phylogenetic Results

The phylogenetic analyses resulted in one most parsimonious tree (tree length = 35; consistency index = 0.74; retention index = 0.76), which is shown in **Figure 2**. Based on the phylogenetic results, all fossil and extant kempynine genera were well grouped as a monophyly, which was supported by two synapomorphic characters: the distal branched M in the forewing (Cha. 2: 1) and multiple rows of cells between M branches in the hind wing (Cha. 15: 1). The latter character has been considered as a diagnostic feature of Kempyninae (Winterton et al., 2019; Ma et al., 2020b). The Kempyninae was divided into two primary clades, namely, clade A, consisting of two fossil genera *Arbusella* + *Jurakempynus*, and clade B + C, consisting of the other genera (**Figure 2**). The grouping of *Arbusella* and *Jurakempynus* was anticipated for their homologous venation, which was supported by one synapomorphy: the absence of gradate series in the forewing (Cha. 5: 2). The other kempynine genera were well grouped, which was supported by two apomorphic characters of the hind wing: distal branched MP (Cha. 13: 2) and the gradually divergent M branches (Cha. 14: 2). Two clades were identified in this grouping, namely, clade B, comprising three other Mesozoic fossil genera, *Sauktangida*, *Mirokempynus*, and *Ponomarenkius*, and clade C, comprising the only Cenozoic genus of *Eupoismites* and all extant genera (**Figure 2**). In clade B, the genus *Sauktangida* from the Early Jurassic is sister to *Mirokempynus* and *Ponomarenkius*, which is supported by one synapomorphy: well-developed A2 with several pectinated branches (Cha. 17:2). The grouping of two Middle Jurassic genera, *Mirokempynus* and *Ponomarenkius* was also anticipated for sharing the distinct pattern of MP branches in the hind wing (Cha. 13: 1). The four southern genera were well grouped (clade C), which was supported by three apomorphic characters: distally dichotomously branched CuA (Cha. 8: 1), A1 approximately the half the length of CuP (Cha. 9: 1); the multiple rows of cells present in the distal half of MP (Cha. 15: 2). However, the inner relationships of these southern genera were not well resolved except for the grouping of *Kempynus* and *Euosmylus* that were supported by two apomorphic characters: the modified outer margin of the forewing (Cha. 1: 1) and distinctly curved RP branches (Cha. 12: 1) (**Figure 2**).

Discussion

Considering the distribution pattern of extant lineages, Kempyninae unequivocally belongs to a typical Gondwanan group, especially for the occurrence of the Cenozoic genus

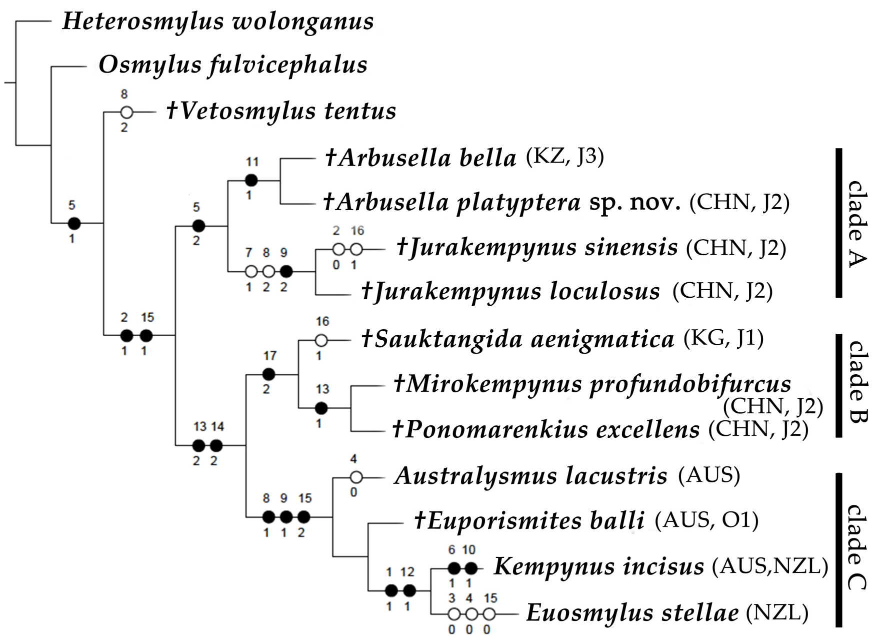

FIGURE 2 | Most parsimonious tree of Kempyninae from phylogenetic analyses (tree length = 35 steps; consistency index, CI = 0.74; retention index, RI = 0.76); ●, apomorphic characters; ○, parallelisms and reversals.

Euporismites, also from Australia. However, the occurrences of diverse fossil kempynines from the Northern Hemisphere imply that the evolution of this group should have a more complicated scenario. Based on the results of phylogenetic analyses (**Figure 2**), the northern Mesozoic kempynines occupied the earliest divergence of the group (**Figure 2**: Clades A, B), which strongly implies an earlier and northern origin of this subfamily. Two questions have arisen: how and when the northern ancestors migrated to the austral areas, and how the extant kempynines shaped the current distribution pattern.

It is noted that the ancestral distribution reconstruction from DIVA analysis acquired multiple ancestral distributions, in which Australia was consistently aligned with the Northern distributions (**Figure 3A**: node 17). The genus *Sauktangida*, as the earliest fossil record of Kempyninae, in the phylogenetic tree (**Figure 2**), is not the most basal clade of Kempyninae, and instead, along with two Middle Jurassic genera, constitutes a derived clade that is sister to the southern lineages. The results strongly implied an earlier and prepangean origin of Kempyninae, and the ancestors first migrated to the future Gondwana before the breakup of Pangea [no later than 174 Mya (Dietz and Holden, 1970; Cox, 2000)]. This point partly agrees with the results of molecular dating that concluded the divergence time of major clades of Osmylidae was before the breakup of Pangaea (Early to Mid-Triassic, 247 Mya) (Winterton et al., 2017). In this hypothesis, the northern and southern kempynines are considered to evolve independently after the separation of Laurasia and Gondwana. As Laurasia was an intact landmass (Dietz and Holden, 1970; Cox, 2000), the northern kempynine ancestors were able to achieve a widespread distribution by an early dispersal over land (**Figure 3A**: nodes 10, 12), resulting in the remarkable diversity of Kempyninae in North Hemisphere. Although we could not determine the origin place of Kempyninae, it is evident that the early colonization had been proceeding, considering the widespread distribution of Jurassic kempynines in the Northern Hemisphere. It is noteworthy that no convincing Cretaceous kempynines were reported except for several equivocal records (Makarkin, 1990, 2014). Also, it is still an enigma for the ultimate disappearance of these kempynine antiques in the Northern Hemisphere. Considering the stable Laurasia landmass, the extinction of kempynines in the Northern Hemisphere was possibly not related to the plate drift but more possibly to the subsequent climate changes.

It is bewildering that the absence of the Mesozoic fossil kempynines in the Southern Hemisphere (Khramov, 2017), which hindered our understanding to further trace the history of Kempyninae. It is noted that the youngest known kempynine fossil is from the Redbank Plains Formation of the late Paleocene-early Eocene in Australia [ca. 55 Mya (Tillyard, 1916; Rozefelds et al., 2016)], and it means that the ancestors of Kempyninae should have reached the southern destination no later than this time. Based on the current analyses, it is noted that all southern kempynines are grouped into a single clade (**Figure 2**), which shared a common ancestral distribution in DIVA analysis, i.e., Australia (**Figure 3A**: node 15). Considering the prepangean origin of Kempyninae, it is easy to conclude that the first southern colonizers could disperse southerly through South America or Africa to the southernmost destination (**Figure 3B**). It means that the extant kempynines should have no direct ancestor-descendent relationships with their northern Mesozoic relatives, but instead descended from the "first southern ancestors." It should be mentioned that the most

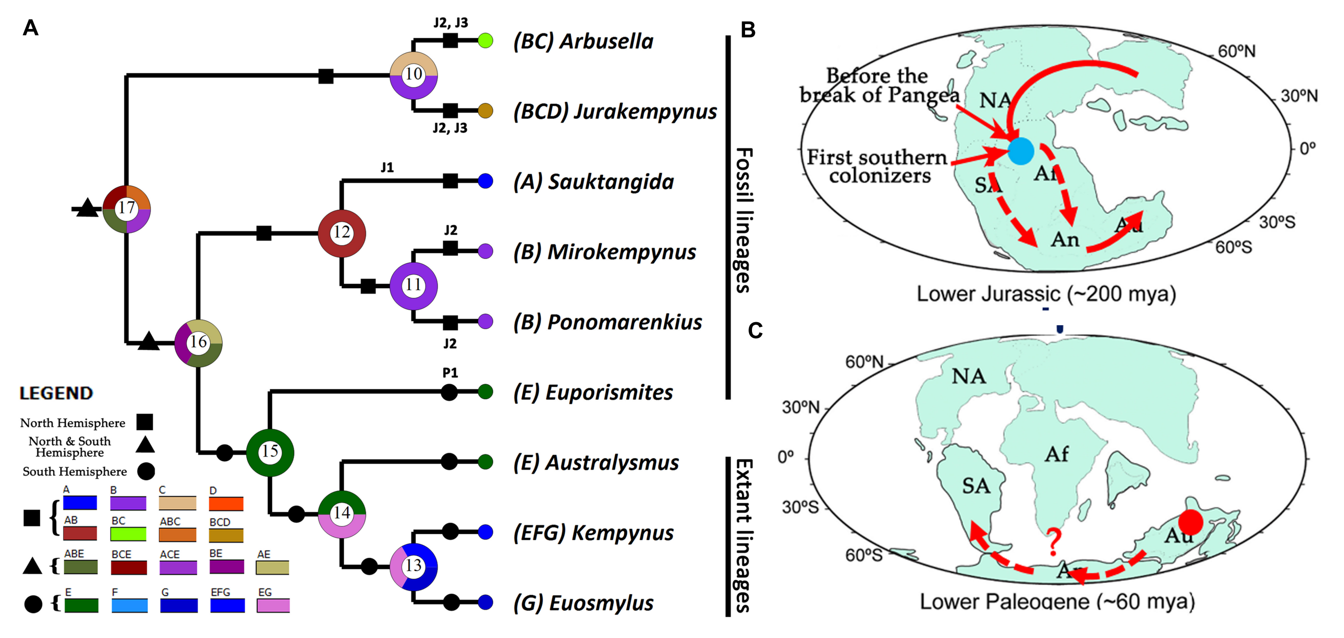

FIGURE 3 | Ancestral distribution reconstruction and putative dispersal routes of Kempyninae. **(A)** Ancestral distribution reconstruction of kempynine genera from DIVA analysis (A, Sauk-Tanga of early Jurassic, Kyrgyzstan; B, Daohugou of middle Jurassic, China; C, Karatau of later Jurassic, Kazakhstan; D, Shar-Teg of late Jurassic, Mongolia; E, Australia; F, South America; G, New Zealand). **(B,C)** Hypothesized historical dispersal routes of kempynine ancestors (NA, North America; SA, South America; Af, Africa; An, Antarctica; Au, Australia).

widespread genus *Kempynus* [occurs in Australia, New Zealand, and South America (Argentina and Chile)] and a New Zelanian endemic genus *Euosmylus* were placed in the most derived clade (**Figure 2**). If considering the northern origin of Kempyninae, it is easy to deduce that the northerly American lineages should represent the earlier divergence, and the Australian lineages should be a more derived clade. If so, the *Kempynus* should be the basalmost lineage of Kempyninae. Herein, an alternative hypothesis is proposed to explain this contradiction: the extant kempynines of Southern America should derive from Australia, which means that the extant kempynines possibly re-dispersed to South America following their Mesozoic ancestors' route, representing a recent Paleocene-Eocene dispersal event (**Figure 3C**). Nevertheless, this hypothesis is far from being supported just based on the current evidence. It is hoped that a future phylogeny of extant kempynines, especially for the inclusion of all *Kempynus* species, could provide a deep insight into this question.

As the relic of ancient lineages, it is vital to trace the history by combining both fossil and extant groups. Although it is far from eventually revealing the evolutionary history of Kempyninae due to the currently limited evidence, the results still exposed a more complicated scenario of Kempyninae, which could direct the future research to the insects.

CONCLUSION

In this study, we described a new species *Arbusella platyptera* Ma *et* Wang, sp. nov. from the Jiulongshan Formation in Daohugou, Inner Mongolia, China. A key to the extinct species and extant genera of Kempyninae is provided. Combining all extant and most fossil genera, we performed phylogenetic and dispersal-vicariance analyses to trace the history of Kempyninae for the first time. The results corroborated the monophyly of Kempyninae and revealed a northern and prepangean origin for the subfamily. Our results also indicated that the Mesozoic kempynine and the extant lineages had no direct ancestor-descendent relationships. The results expose a more complicated evolutionary scenario of the relic insects and provide new insight into understand the historical evolution of insects that have a long history.

DATA AVAILABILITY STATEMENT

The original contributions presented in the study are included in the article/supplementary material, further inquiries can be directed to the corresponding author.

AUTHOR CONTRIBUTIONS

YM contributed to conceptualization, formal analysis, and writing—original draft. CS contributed to writing—original draft. DR contributed to funding acquisition, investigation, resources, supervision, and writing—original draft. YW contributed to conceptualization, data curation, formal analysis, funding acquisition, investigation, methodology, project administration, resources, supervision, and writing—original draft. All authors contributed to the article and approved the submitted version.

FUNDING

This study was supported by grants from the National Natural Science Foundation of China, grant numbers: 31970383 and 31730087; the Beijing Natural Science Foundation, grant number: 5192002; the Academy for Multidisciplinary Studies of Capital Normal University; the Capacity Building for Sci-Tech Innovation–Fundamental Scientific Research Funds, grant number: 19530050144; the Program For Changjiang Scholars and Innovative Research Team in University, grant number: Irt-17r75, and the Support Project of High Level Teachers in Beijing Municipal Universities, grant number: IDHT20180518.

ACKNOWLEDGMENTS

We sincerely thank the two reviewers' critical comments to improve this study.

REFERENCES

Breitkreuz, L. C. V., Winterton, S. L., and Engel, M. S. (2017). Wing tracheation in Chrysopidae and other Neuroptera (Insecta): a resolution of the confusion about vein fusion. *Am. Mus. Novit.* 3890, 1–44. doi: 10.1206/3890.1

Cox, C. B. (2000). Plate tectonics, seaways and climate in the historical biogeography of mammals. *Mem. Inst. Oswaldo Cruz* 95, 509–516. doi: 10.1590/S0074-02762000000400012

Dietz, R. S., and Holden, J. C. (1970). Reconstruction of Pangaea: breakup and dispersion of continents, Permian to present. *J. Geophys. Res.* 75, 4939–4956. doi: 10.1029/JB075i026p04939

Khramov, A. V. (2014a). Early osmylids (Neuroptera: Osmylidae) from the lower–middle Jurassic of Kyrgyzstan. *Russ. Entomol. J.* 23, 53–60. doi: 10.15298/rusentj.23.1.07

Khramov, A. V. (2014b). Lacewings of the family Osmylidae (Insecta: Neuroptera) from the Upper Jurassic of Asia. *Paleontol. J.* 48, 300–309. doi: 10.1134/S0031030114030095

Khramov, A. V., Liu, Q., and Zhang, H. (2017). Mesozoic diversity of relict subfamily Kempyninae (Neuroptera: Osmylidae). *Hist. Biol.* 31, 938–946. doi: 10.1080/08912963.2017.1411351

Kimmins, D. E. (1940). A revision of the osmylid subfamilies Stenosmylinae and Kalosmylinae (Neuroptera). *Novit. Zool.* 42, 165–201.

Lambkin, K. J. (1987). A re-examination of *Euporismites balli* Tillyard from the Palaeocene of Queensland (Neuroptera: Osmylidae: Kempyninae). *Neuroptera Int.* 4, 295–300.

Liu, X., Wang, Y., Shih, C., Ren, D., and Yang, D. (2012). Early evolution and historical biogeography of fishflies (Megaloptera: Chauliodinae): implications from a phylogeny combining fossil and extant taxa. *PLoS One* 7:e40345. doi: 10.1371/journal.pone.0040345

Ma, Y. M., Shih, C. K., Ren, D., and And Wang, Y. J. (2020a). New lance lacewings (Osmylidae: Kempyninae) from the Middle Jurassic of Inner Mongolia, China. *Zootaxa* 4822, 94–100. doi: 10.11646/zootaxa.4822.1.4

Ma, Y. M., Shih, C. K., Ren, D., and Wang, Y. J. (2020b). A new genus of lance lacewings from the Middle Jurassic of Inner Mongolia, China. *Acta Palaeontol. Pol.* 65, 363–369. doi: 10.4202/app.00691.2019

Makarkin, V. N. (1990). A new fossil genus and species of Osmylidae from the Lower Cretaceous of East Siberia (Neuroptera). *Dtsch. Entomol. Z.* 37, 101–103. doi: 10.1002/mmnd.19900370121

Makarkin, V. N. (2014). A new fossil genus of Osmylidae (Neuroptera) from the Early Cretaceous of Baissa. *Transbaikalia* 278, 8–12.

Martins, C. C., Ardila-Camacho, A., and Aspöck, U. (2016). Neotropical osmylids (Neuroptera, Osmylidae): three new species of *Isostenosmylus* Krüger, 1913, new distributional records, redescriptions, checklist and key for the Neotropical species. *Zootaxa* 4149, 1–66. doi: 10.11646/zootaxa.4149.1.1

New, T. R. (1983). A revision of the Australian Osmylidae: Kempyninae (Insecta: Neuroptera). *Aust. J. Zool.* 31, 393–420. doi: 10.1071/ZO9830393

Nixon, K. C. (2002). *WinClada ver. 1.00.08*. Ithaca, NY: KC Nixon. doi: 10.1016/B978-0-08-050625-8.50005-5

Page, R. (2001). *NDE (NEXUS Data Editor for Windows): Version 0.5.0*. Glasgow: University of Glasgow.

Rozefelds, A. C., Dettmann, M. E., Clifford, H. T., and Lewis, D. (2016). Macrofossil evidence of early sporophyte stages of a new genus of water fern Tecaropteris (Ceratopteridoideae: Pteridaceae) from the Paleogene Redbank Plains Formation, southeast Queensland, Australia. *Alcheringa* 40, 1–11. doi: 10.1080/03115518.2015.1069460

Tillyard, R. J. (1916). Studies in Australian Neuroptera. No. II. Descriptions of new genera and species of the families Osmylidae, Myrmeleontidae, and Ascalaphidae. *Proc. Linn. Soc. N. S. W.* 41, 41–70. doi: 10.5962/bhl.part.15306

Wang, Y. J., Liu, Z. Q., Ren, D., and Shih, C. K. (2011b). New Middle Jurassic kempynin osmylid lacewings from China. *Acta Palaeontol. Pol.* 56, 865–869. doi: 10.4202/app.2010.0050

Wang, Y. J., Winterton, S. L., and Liu, Z. Q. (2011a). Phylogeny and biogeography of *Thyridosmylus* (Neuroptera: Osmylidae). *Syst. Entomol.* 36, 330–339. doi: 10.1111/j.1365-3113.2010.00565.x

Winterton, S. L., Martins, C. C., Makarkin, V., Ardila-Camacho, A., and And Wang, Y. J. (2019). Lance lacewings of the world (Neuroptera: Archeosmylidae, Osmylidae & Saucrosmylidae): a review of living and fossil genera. *Zootaxa* 4581, 1–99. doi: 10.11646/zootaxa.4581.1.1

Winterton, S. L., Zhao, J., Garzón-Orduña, I., Wang, Y. J., and Liu, Z. Q. (2017). Phylogeny of lance lacewings (Neuroptera: Osmylidae). *Syst. Entomol.* 42, 555–574. doi: 10.1111/syen.12231

Yu, Y., Harris, A. J., Blair, C., and He, X. J. (2015). RASP (Reconstruct Ancestral State in Phylogenies): a tool for historical biogeography. *Mol. Phylogenet. Evol.* 87, 46–49. doi: 10.1016/j.ympev.2015.03.008

Yu, Y., Harris, A. J., and He, X. J. (2010). S-DIVA (statistical dispersal-vicariance analysis): a tool for inferring biogeographic histories. *Mol. Phylogenet. Evol.* 56, 848–850. doi: 10.1016/j.ympev.2010.04.011

Conflict of Interest: The authors declare that the research was conducted in the absence of any commercial or financial relationships that could be construed as a potential conflict of interest.

frontiers | Frontiers in Ecology and Evolution

ORIGINAL RESEARCH
published: 09 June 2022
doi: 10.3389/fevo.2022.907903

New Genus and Species of Empheriidae (Insecta: Psocodea: Trogiomorpha) and Their Implication for the Phylogeny of Infraorder Atropetae

Sheng Li[1], Kazunori Yoshizawa[2], Qiuzhu Wang[3], Dong Ren[4], Ming Bai[1] and Yunzhi Yao[4]*

[1] Key Laboratory of Zoological Systematics and Evolution, Institute of Zoology, Chinese Academy of Sciences, Beijing, China, [2] Systematic Entomology, School of Agriculture, Hokkaido University, Sapporo, Japan, [3] Huilongguan Yuxin School Affiliated to Capital Normal University, Beijing, China, [4] College of Life Sciences and Academy for Multidisciplinary Studies, Capital Normal University, Beijing, China

OPEN ACCESS

Edited by:
Chenyang Cai,
Nanjing Institute of Geology and Paleontology (CAS), China

Reviewed by:
Dany Azar,
Lebanese University, Lebanon
Marina Hakim,
Nanjing Institute of Geology and Paleontology (CAS), China
Shuo Wang,
Qingdao University of Science and Technology, China

***Correspondence:**
Yunzhi Yao
yaoyz100@126.com

Specialty section:
This article was submitted to Paleontology, a section of the journal Frontiers in Ecology and Evolution

Received: 30 March 2022
Accepted: 04 May 2022
Published: 09 June 2022

Citation:
Li S, Yoshizawa K, Wang Q, Ren D, Bai M and Yao Y (2022) New Genus and Species of Empheriidae (Insecta: Psocodea: Trogiomorpha) and Their Implication for the Phylogeny of Infraorder Atropetae. Front. Ecol. Evol. 10:907903. doi: 10.3389/fevo.2022.907903

Two species of psocids discovered from the Mid-Cretaceous Burmese amber, *Latempheria kachinensis* Li, Yoshizawa, and Yao, gen. et sp. nov. and *Burmempheria curvatavena* Li, Yoshizawa, and Yao, sp. nov., are described and assigned to the Empheriidae (Trogiomorpha: Atropetae) family. A phylogenetic analysis of the infraorder Atropetae is conducted based on 38 morphological characters of three outgroups and fifteen ingroups, which supported the monophyly of Atropetae including fossil and extant taxa. In the phylogenetic result, all the genera of fossil families Empheriidae and Archaeatropidae form a monophyletic group, sister to the extant members of Atropetae. The two fossil families also share a lot of similarities in morphology, locality, and geological period. Recently discovered fossil species exhibited combined morphological characters of both families. Based on these observations and the results of the phylogenetic analysis, Archaeatropidae is treated here as a new junior synonym of Empheriidae.

Keywords: Archaeatropidae, new taxon, phylogeny, synonymy, Trogiomorpha, psocoptera

INTRODUCTION

The infraorder Atropetae Pearman, 1936 represents the largest group in the suborder Trogiomorpha, with more than 400 species mainly occurring in warm and humid regions (Lienhard and Smithers, 2002). These species are classified into two extinct families (Empheriidae and Archaeatropidae) (Smithers, 1972; Baz and Ortuño, 2000, 2001; Azar and Nel, 2004; Azar et al., 2010, 2014; Li et al., 2020) and three extant families (Psoquillidae, Lepidopsocidae, and Trogiidae) (Roesler, 1944; Badonnel, 1951). Fossil Psocodea have been studied for over 100 years; however, because of limitations in fossil specimens and incomplete preservation, and different interpretations of taxonomic characteristics, many species were classified into uncertain positions. For example, based on morphological characters, two families in Trogiomorpha, i.e., Empheriidae and Archaeatropidae, are hard to distinguish (Baz and Ortuño, 2000, 2001; Perrichot et al., 2003; Li et al., 2020).

Atropetae fossils are known in five families (including three extant families) and thirty-five genera. Their geological history ranged from Cretaceous to Paleogene, and they were distributed in Lebanon (Azar and Nel, 2004), Spain (Baz and Ortuño, 2000, 2001), Myanmar (Azar and Nel, 2004; Li et al., 2020; Liang et al., in press), France SW (Azar et al., 2014), New Jersey (Azar et al., 2010), France Oise (Nel et al., 2005), Siberia (Vishnyakova, 1975; Hakim et al., 2021), and Baltic region (Hagen, 1856; Enderlein, 1911). Most of the fossil species are placed in the extinct families Empheriidae and Archaeatropidae. Empheriidae was established by Kolbe (1884), with eight genera and eleven species (Hagen, 1856, 1882; Baz and Ortuño, 2001; Nel et al., 2005; Azar et al., 2010; Li et al., 2020; Hakim et al., 2021). Archaeatropidae was established by Baz and Ortuño (2000) based on amber specimens from Spain. The family is now composed of eight genera with twelve species recorded mainly from Lebanon, Myanmar, and France SW (Baz and Ortuño, 2000; Perrichot et al., 2003; Azar and Nel, 2004; Azar et al., 2014; Cumming and Le Tirant, 2021; Liang et al., in press). Li et al. (2020) mentioned that based on high similarity in morphological characters, living period, and fossil locality, Empheriidae and Archaeatropidae are likely to be synonyms. Previous phylogenetic analyses showed that Atropetae is a monophyletic group that comprises three extant families (Smithers, 1972; Yoshizawa et al., 2006; de Moya et al., 2021). However, these analyses did not include the extinct families of Atropetae, Empheriidae, and Archaeatropidae. Consequently, the phylogenetic placement of the two families remains unsolved to date.

In this study, all ambers were collected from the Hukawng Valley, Myitkyina District, Kachin State, Myanmar (Lin et al., 2019; Zhao et al., 2020). Herein, a new genus, *Latempheria* Li, Yoshizawa and Yao, gen. nov., distinguished by broad external valves and a new species of *Burmempheria* Li et al., 2020 in Empheriidae are described. Based on present observations and published information, 38 morphological characters for three outgroups and fifteen ingroups are coded. Using this data matrix, phylogenetic analyses were conducted to estimate the phylogenetic relationships among the families of Atropetae, including fossil taxa, for the first time. The result suggests that Empheriidae and Archaeatropidae, together form a monophyletic group, and their morphological differences are obscure. Therefore, we synonymize the latter family with Empheriidae.

MATERIALS AND METHODS

Materials

The amber specimens were collected from Kachin (Hukawng Valley) in Northern Myanmar. The specimens are housed in the Key Lab of Insect Evolution and Environmental Changes, College of Life Sciences, Capital Normal University, Beijing, China (CNU, Curator: Yunzhi Yao). The specimens were acquired before 2013 and then studied in 2019, with no conflict (Wang et al., 2016; Engel, 2020; Shi et al., 2021).

The specimens were examined and photographed under a Nikon SMZ25 microscope with an attached Nikon DS-Ri2 digital camera system. The morphological terminology mainly follows Yoshizawa (2005). Abbreviations: mx, maxillary palp; la, labium; Sc, subcostal vein; Sc', distal part of the subcostal vein; R, radius vein; Rs, radial sector; M, median vein; Cu, cubital vein; A, anal vein; ep, epiproct; p, paraproct; pa, parameres; s, subgenital plate; V3, external valve; mt: tarsus of mid leg; ht: tarsus of hind leg.

Taxon Sampling and Character Choice

The outgroups were selected from Prionoglarididae, Psyllipsocidae, and Cormopsocidae, and the ingroups from Atropetae (**Supplementary Table 1**). For coding the morphological data from the fossil taxa, we selected those that were widespread and that had extensive information available on morphology. Thirty-eight multistate characters were treated as non-additive (= unordered) and equally weighted. The data matrix used in this phylogenetic analysis is provided in **Supplementary Data Sheet 1**. Inapplicable states were assigned as a gap value ("—") and treated as equivalent to missing data ("?").

Phylogenetic Analysis

The character matrix (**Supplementary Datasheet**) was compiled using Nexus Data Editor v0.5.0 (Page, 2001). A phylogenetic analysis was conducted by maximum parsimony analysis in WINCLADA v1.00.08 (Nixon, 2002) with NONA script (Goloboff, 1997; Nixon, 2002) and TNT v1.5 (Goloboff and Catalano, 2016). The analysis conducted in WINCLADA was set to keep 10,000 maximum trees, 1,000 replications, and 100 starting trees per replication. A repeated analysis was run in TNT using "Traditional Search."

RESULTS

The maximum parsimony analyses using TNT and WINCLADA both yielded 6 most parsimonious trees (tree length of 86 steps, consistency index (CI) of.51, and retention index (RI) of.6), and a strict consensus tree with a tree length of 93 steps, consistency index (CI) of.47, and retention index (RI) of.54 (**Figure 1** and **Supplementary Figure 1**). Bremer Supports are shown in **Figure 1**. The result supported that Empheriidae + Archaeatropidae constitutes a monophyletic group, and that Lepidopsocidae + Psoquillidae + Trogiidae constitutes a monophyletic group. These two groups formed a monophyletic group, the infraorder Atropetae.

Infraorder Atropetae

The monophyly of Atropetae including fossil and extant taxa was demonstrated for the first time, with the following four character states supporting its monophyly: mx2 with sensillum (character 5, state 1); Areola Postica long (character13, state 1); M_{1+2} longer than the second section of M (character 22, state 2); long and thin female external valves (character 34, state 1).

Clade Lepidopsocidae + Psoquillidae + Trogiidae

In Atropetae, the families Lepidopsocidae, Psoquillidae, and Trogiidae, i.e., the extant members of the infraorder, formed a monophyletic group, with two character states

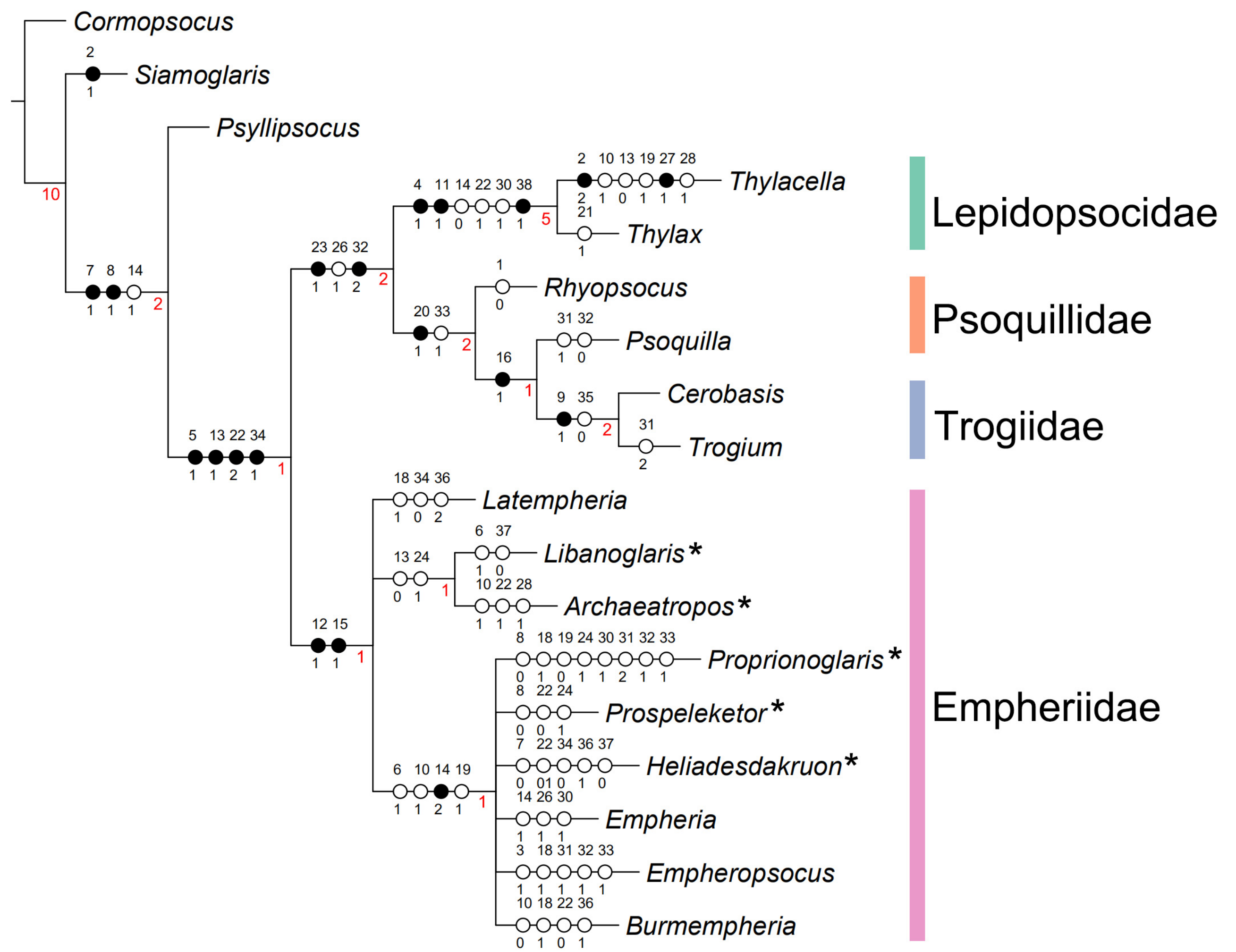

FIGURE 1 | Strict consensus tree of the most parsimonious tree. Phylogeny of Atropetae based on 18 species and 38 characters, with characters being non-additive, under equal weighting. Analyzed with WINCLADA v1.00.08 with NONA script (length = 93, CI = 0.47, RI = 0.54). * Represents the genus originally placed in Archaeatropidae.

supporting this clade: (1) Radial cell absent in forewing (character 23, state 1); (2) pulvillus broad (character 32, state 2). In this clade, Psoquillidae + Trogiidae formed a monophyletic group, the supporting character for this clade was: forewing Rs and R_1 not connected by a short crossvein (character 20, state 1). In the present analysis, the monophyly of Lepidopsocidae has been well-supported by three character states: (1) ocelli arranged far apart (character 4, state 1); (2) forewing pointed (character 11, state 1); (3) body covered by scales (character 38, state 1).

Clade Empheriidae + Archaeatropidae

Empheriidae and Archaeatropidae formed a monophyletic group (**Figure 1**), with two characters supporting this clade: (1) forewing membrane with setae (character 12, state 1); (2) forewing veins with setae (character 15, state 1). In this lineage, the relationship of each genus remained unclear.

Systematic Paleontology

Suborder Trogiomorpha Roesler, 1940.

Infraorder Atropetae Pearman, 1936.

Family Empheriidae Kolbe, 1884.

Empheriidae Kolbe, 1884: 37 [Type genus: *Empheria* Hagen, 1856: *Berliner Entomologische Zeitschrift.* 28, 35–38].

Archaeatropidae Baz and Ortuño, 2000: 369 [Type genus: *Archaeatropos* Baz and Ortuño, 2000: Annals of the Entomological Society of America. 93, 367–373]. New junior synonymy of Empheriidae.

Included genera (* represents this genus originally placed in Archaeatropidae): *Empheropsocus* Baz and Ortuño, 2001; *Preempheria* Baz and Ortuño, 2001; *Jerseyempheria* Azar et al., 2010; *Eoempheria* Nel et al., 2005; *Empheria* Hagen, 1856; *Trichempheria* Enderlein, 1911; *Burmempheria* Li et al., 2020; *Empherium* Hakim et al., 2021; **Archaeatropos* Baz and Ortuño, 2000; **Bcharreglaris* Azar and Nel, 2004; **Libanoglaris* Perrichot et al., 2003; **Proprionoglaris* Perrichot et al., 2003;

**Prospeleketor* Perrichot et al., 2003; **Setoglaris* Azar and Nel, 2004; **Heliadesdakruon* Cumming and Le Tirant, 2021; **Longiantennum* Liang et al., in press*; *Latempheria* Li, Yoshizawa, and Yao, gen. nov.

Genus: *Latempheria* Li, Yoshizawa and Yao, gen. nov.

Etymology: The generic name is a combination of Latin words "*lat*" (broad) and "*empheria*" (type genus of Empheriidae), referring to the broad external valves of the type species. The gender is feminine.

Type species: *Latempheria kachinensis* Li, Yoshizawa and Yao, gen. et sp. nov.

Diagnosis: Forewing Sc long, almost half length of forewing, ended in the middle of Radial cell; all tibiae with two apical spurs, and tibiae covered with two rows of obvious setae; external valves broad and elongate, lobate-liked.

Remarks: *Latempheria* shares a series of characters with Trogiomorpha: (1) antennae with more than 20 segments; (2) tarsi with three segments; (3) forewing pterostigma slightly opaque; (4) ventral and dorsal valves of gonapophyses strongly reduced (or absent), external valves well-developed and setose; (5) subgenital plate short, covering at most basal part of external valves (Yoshizawa et al., 2006). In addition, *Latempheria* can be classified into Atropetae by the following characters: (1) forewing basal segment of Sc well-developed; (2) hind wing A simple; (3) external valves of gonapophyses elongated and partially joined together on midline by membrane; (4) paraproct with anal spine (Yoshizawa et al., 2006). *Latempheria* can be assigned to Empheriidae according to (1) wings well-developed, rounded at apex; (2) forewing Sc bend to R; (3) venation covered with setae; (4) claws without preapical tooth (Baz and Ortuño, 2001).

In the family, *Latempheria* shares similar characteristics with *Burmempheria* Li et al., 2020 in forewing venation, legs, and antennae. The main difference between *Latempheria* and *Burmempheria* are: (1) *Latempheria* with broad and elongated external valves (vs. rod-like external valves in *Burmempheria*); (2) all tibiae with two rows of obvious spur in *Latempheria* (vs. *Burmempheria* with tibia bearing setae or bare).

Latempheria kachinensis Li, Yoshizawa and Yao, gen. et sp. nov. (**Figures 2**, **3**).

urn:lsid:zoobank.org:act:8500CE76-8F78-402B-AB7D-376B939FC0A9.

Etymology: "*Kachin*" indicates the type locality of the new species.

Material: Holotype, CNU-PSO-MA2015001 (female, head covered by impurities). Paratype, CNU-PSO-MA2015002 (female with head well preserved, gonapophyses distorted).

Locality and horizon: Hukawng Valley, Kachin State, Northern Myanmar; mid-Cretaceous, lowermost Cenomanian.

Diagnosis: All tibiae with two rows of obvious setae, with two apical spurs; external valves without setae; CuP and A_1 fused for long distance before wing margin; CuA_1 obviously curved, nearly 2 times longer than CuA_2.

Description: Female, body completely preserved, head with some impurities (**Figures 2A,B**), antennae broken (**Figure 2C**); mouthpart well-preserved; three ocelli present, arranged in inverted triangle. Body length 1.71 mm (measured from frons to terminalia). Forewing length 1.812 mm, width.809 mm; hind wing length 1.46 mm, width.509 mm. IO/d = 2.23. Mt = 307 mm; ht = 0.361 mm.

Head: head narrow, compound eyes small, diameter less than 1/2 the length of interorbital distance; antennae long, obviously broken, left 25 segments preserved, right 7 segments preserved, distal part of flagellum with soft and thin setae, secondary annulations absent (**Figures 3A,B**). Maxillary palps with four segments (**Figure 3C**), second segments longest, terminal article hatchet-shaped, with sensillum (**Figure 3D**). Labium palps with two articles, terminal augment rounded (**Figure 3E**).

Thorax: prothorax broad, mesothorax well-developed, and mesonotum triangular.

Legs: All legs covered with setae, all tibiae with two rows of obvious setae, with two apical spurs (**Figures 3F,G**); tarsus three segmented, claws without pulvillus and preapical tooth.

Forewings: Macropterous, forewing oval (**Figure 2D**), margin glabrous, veins with long setae except CuP, membrane glabrous except vannal region. Veins with Sc, M, Cu, and A with long setae arranged along both edges of veins; other veins with one row of long setae; Sc long, basally fused with R for short distance, distally curved strongly, ended at R_1 vein, short vein arises from top of curved Sc reaching to anterior margin; Sc' long, pterostigma quadrilateral, not thickened; Rs and M fused for short distance; Rs fork distal to M fork; M_{1+2} longer than second section of M, almost 2.5 times longer with it. CuA_1 and CuA_2 long, CuA_1 curved, nearly 2 times longer than CuA_2; CuP weaker than other veins; CuP and A_1 fused for long distance before reaching wing margin (**Figure 3H**).

Hind wing oval (**Figure 2E**). Hind wing margin and membrane glabrous (**Figure 2E**). Not preserved well. Distal part of R_1 curved; R_1 and Rs + M connected by a short crossvein; CuA unforked; A not visible.

Abdomen: Epiproct and paraproct covered with setae; epiproct with anal spine; dorsal valves degraded, external valves elongate, broad, lobate-liked, and partially joined together on midline by membrane (**Figures 3I,J**).

Genus: *Burmempheria* Li et al., 2020.

Type species: *Burmempheria densuschaetae* Li et al., 2020.

Burmempheria curvatavena Li, Yoshizawa and Yao, sp. nov. (**Figures 4**, **5**).

urn:lsid:zoobank.org:act:89231F37-E4CC-44BA-85F0-CCDE453FB3AA.

Etymology: A combination of Latin words "*curvata*" (bent) and "*vena*" (vein), indicating that CuA_1 is obviously curved.

Material: Holotype, CNU-PSO-MA2015003, male, well-preserved, with genitalia covered by impurities.

Locality and horizon: Hukawng Valley, Kachin State, Northern Myanmar; mid-Cretaceous, lowermost Cenomanian.

Diagnosis: All tibiae with two rows of sparse and short setae; tibia with three apical spurs; distal part of forewing CuA_1 obviously curved; M_{1+2} extremely long, almost 3 times longer than the distal section of M.

Description: Male, well -preserved, with folded distal left forewing. Body length 1.71 mm (measured from frons to terminalia). Forewing length 1.887 mm, width.762 mm; hind wing length 1.354 mm, width.453 mm. IO/d = 2.16. Mt = 0.375 mm; ht = 0.417 mm.

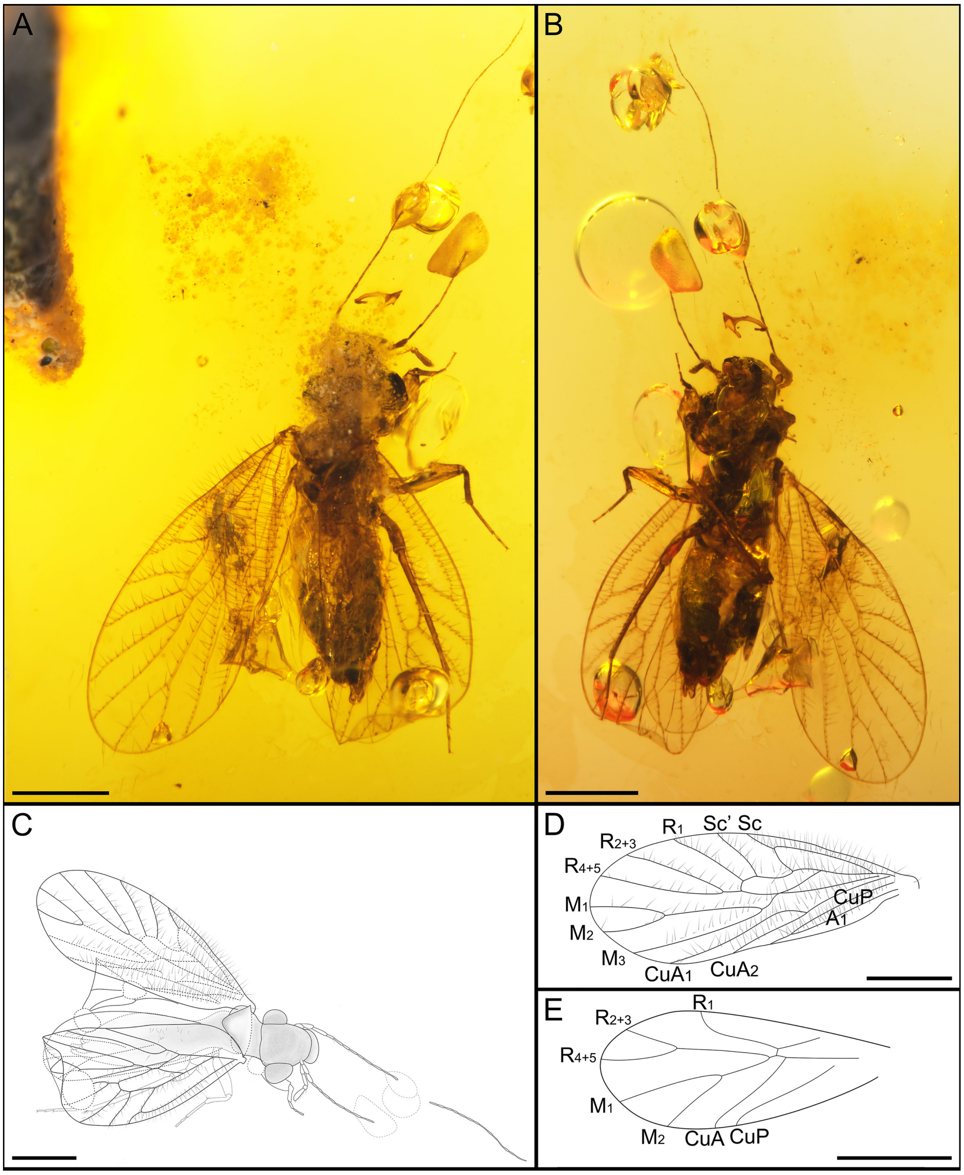

FIGURE 2 | Habitus of *Latempheria kachinensis* Li, Yoshizawa and Yao, gen. et sp. nov. CNU-PSO-2015001. **(A)** Photograph in dorsal view; **(B)** photograph in ventral view; **(C)** line drawing in dorsal view; **(D)** line drawing of forewing; **(E)** line drawing of hind wing. Scale bars:0.5 mm.

Head: vertex broad, covered with sparse and long setae (**Figures 4A,B**); compound eyes large, diameter longer than 1/2 the length of interorbital distance; three ocelli present, arranged in inverted triangle. Antennae long (**Figure 4C**), right flagellum with 30 segments, left with 32 flagellomeres, basal 10 segments covered with setae, secondary annulations absent (**Figures 5A,B**). Maxillary palps with four segments, covered with setae, terminal article hatchet-shaped, second article longest (**Figures 5C,D**).

Thorax: slight deformation, prothorax invisible, mesothorax well-developed, mesonotum triangular.

Legs. All legs long, all tibiae covered two rows of obvious setae, with three apical spurs (**Figures 5E,F**); tarsus three segmented, terminal segment with two claws, without pulvillus and preapical tooth.

Forewing: Macropterous, forewing oval (**Figure 4D**), margin glabrous, all veins with long setae except CuP, membrane glabrous except vannal region. Sc, R, M, and Cu with setae along both edges of veins, other veins with single row of setae; Sc long, basally fused with R for short distance and distally curved, short vein arises from top of curved Sc, reaching to the anterior margin; Sc' long, not curved; distal R_1 slightly curved; pterostigma quadrilateral, not thickened; M_{1+2} very long, almost 3 times longer than the second section of M; CuA with two branches, CuA_1 is twice as CuA_2, CuA_1 distinctly curved; CuP

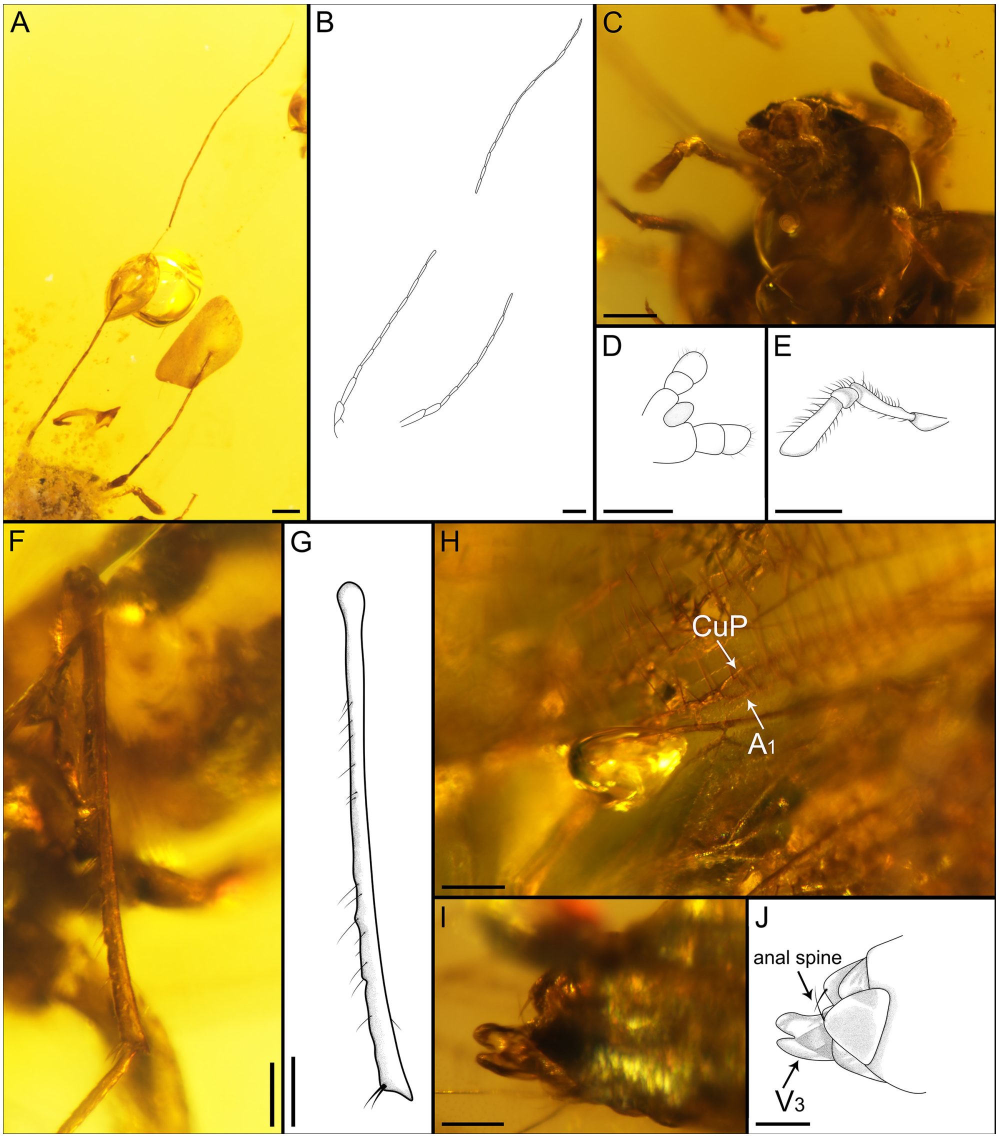

FIGURE 3 | Detailed photograph of *Latempheria kachinensis* Li, Yoshizawa and Yao, gen. et sp. nov. **(A)** Photograph of antennae; **(B)** line drawing of antennae; **(C)** photograph of mouthpart; **(D)** line drawing of right maxillary palps (dorsal view); **(E)** line drawing of labial palps; **(F)** photograph of left hind leg (dorsal view); **(G)** line drawing of left hind leg (dorsal view); **(H)** photograph of CuP and A1 in left forewing; **(I)** photograph of female terminalia; **(J)** line drawing of female terminalia. Scale bars:0.1 mm.

weaker than other veins, CuP and A1 merged for short distance before reaching wing margin (**Figure 5G**).

Hind wing oval (**Figure 4E**), hind wing margin and membrane glabrous, right hind wing folded; R1 slightly curved; M_1 and M_2 relatively long; CuA unforked; A not visible.

Abdomen: genitalia covered by impurities, not well-preserved.

Remarks: *Burmempheria curvatavena* can be assigned into *Burmempheria* based on: (1) flagellum more than 30 segments; (2) Sc long and reaching to the anterior margin; (3) lack of pulvillus. There are obvious differences between *B. curvatavena* and other species: (1) tibiae with three apical spurs (vs. two apical spurs in *B. densuschaetae* and *B. raruschaetae*); (2) M_{1+2} extremely long, almost thrice the distal section of M (vs. M_{1+2} nearly twice the distal section of M in *B. densuschaetae* and *B. raruschaetae*).

DISCUSSION

The monophyly of Atropetae, including the fossil taxa, is recovered in the current analysis for the first time. Based on the extant species, Smithers (1972) mentioned that the reduction of female genitalia to setose, lobar external valves is the main apomorphy of Atropetae. Previous molecular research also supported the monophyly of Atropetae (Yoshizawa et al., 2006; de Moya et al., 2021). Based on their result,

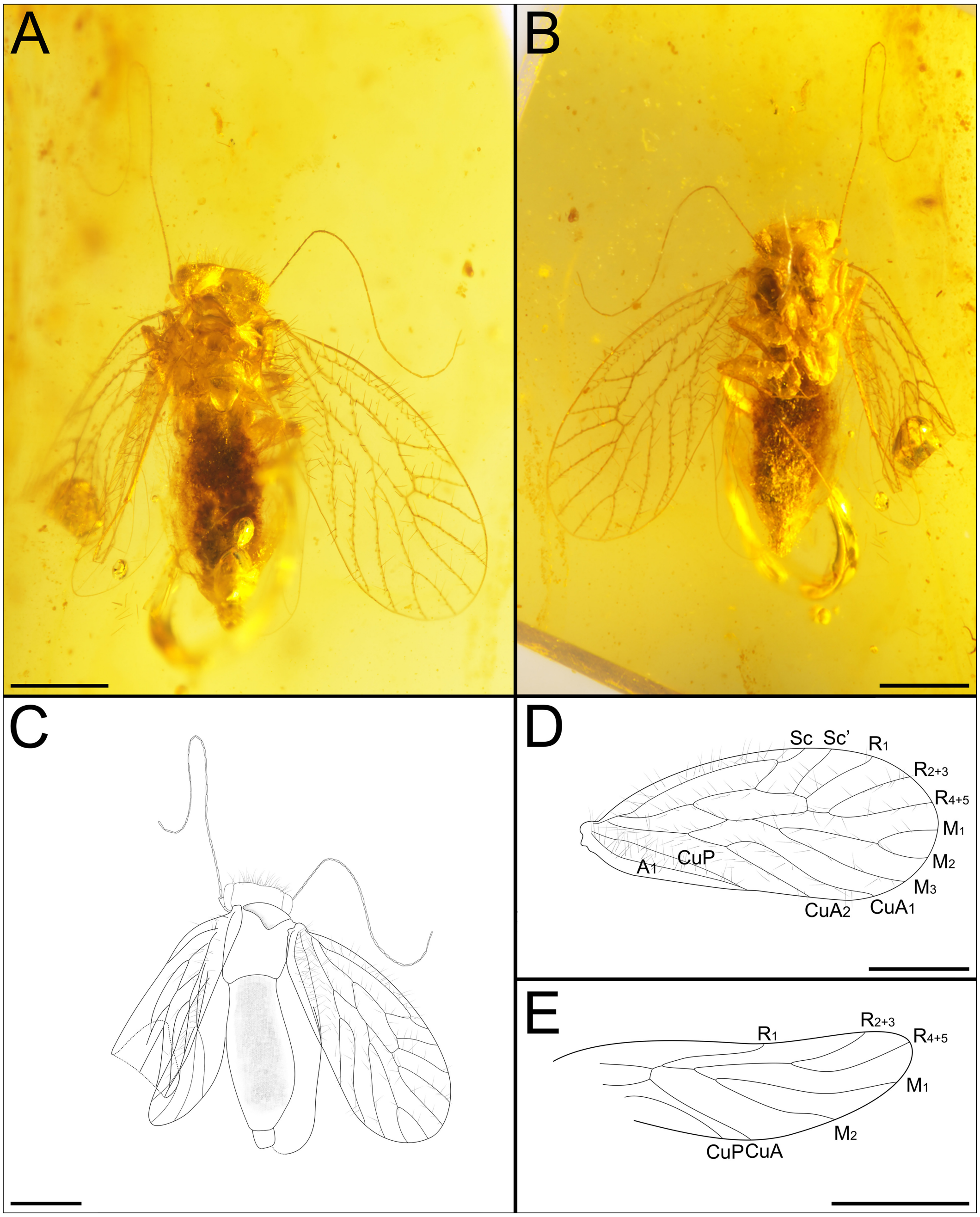

FIGURE 4 | Habitus of *Burmempheria curvatavena* Li, Yoshizawa and Yao, sp. nov. CNU-PSO-2015003. **(A)** Photograph in dorsal view; **(B)** photograph in ventral view; **(C)** line drawing in dorsal view; **(D)** line drawing of forewing; **(E)** line drawing of hind wing. Scale bars:0.5 mm.

Yoshizawa et al. (2006) proposed two autapomorphies of extant Atropetae: (1) external valves of gonapophyses elongated and partially joined together on midline by membrane, composing the ovipositor; (2) spermathecal sac with one or two glandular accessory bodies.

The present analyses recovered the monophyly of Lepidopsocidae + Psoquillidae + Trogiidae, extant members of Atropetae, as recovered by Smithers (1972) and Yoshizawa et al. (2006). The autapomorphies of this clade identified by the present analyses are: forewing Radial cell absent (character 23, state 1); pulvillus broad (character 32, state 2). In this clade, Psoquillidae + Trogiidae formed a monophyletic group. This relationship had already been discussed by Smithers (1972) based on the presence of spermathecal accessory bodies, but Mockford (1993) suggested that this character is an autapomorphy of Atropetae (Yoshizawa et al., 2006). Mockford (1993) and

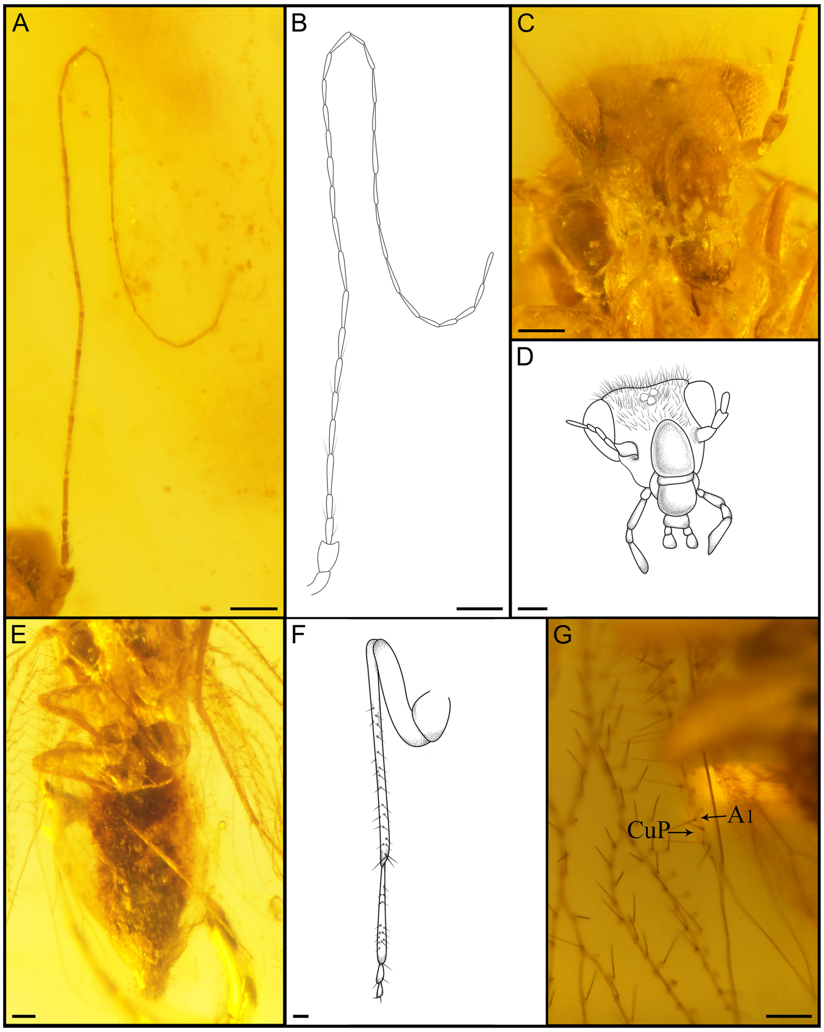

FIGURE 5 | Detailed photograph of *Burmempheria curvatavena* Li, Yoshizawa and Yao, sp. nov. **(A)** Photograph of right antenna; **(B)** line drawing of right antenna; **(C)** photograph of mouthpart; **(D)** line drawing of mouthpart; **(E)** photograph of right hind leg (dorsal view); **(F)** line drawing of right hind leg (dorsal view); **(G)** photograph of CuP and A1 in left forewing. Scale bars:0.1 mm.

Lienhard (1998) proposed two synapomorphies supporting the close relationship between Psoquillidae and Trogiidae: (1) pretarsal claw without preapical tooth; (2) pulvillus distinctly enlarged through its whole length. The autapomorphies of this clade identified by the present analyses are: R1 and Rs not connected by a short crossvein (character 20, state 1).

The current research suggested that Psoquillidae is paraphyletic, and Psoquilla Hagen, 1865 was placed to be the sister taxon of Trogiidae supported by reduced forewing veins (character 16, state 1). Based on Hagen (1856) and Smithers (1972), Psoquilla forewing veins are distinct but much simpler or more reduced than other genera. In Yoshizawa et al. (2006) and de Moya et al. (2021), both analyses are based on a single species of Psoquillidae. According to Yoshizawa et al. (2006), Psoquillidae and Trogiidae are treated as sister taxa, and in de Moya et al. (2021), Psoquillidae was placed as the sister group of Lepidopsocidae. The relationships among Psoquillidae, Lepidopsocidae, and Trogiidae remain unclear while the monophyly of Psoquillidae still requires further studies. The monophyly of Trogiidae is well-supported by an apparent apomorphic character, i.e., reduced forewing (character 9, state 1), as also suggested by a previous study (Mockford, 1993). Mockford (1993) and Yoshizawa et al. (2006) suggested the monophyly of Lepidopsocidae was supported by body covered by scales, which was also recovered by the present analyses.

Based on the differences in the forewing setae arrangement and nodulus condition, Empheriidae and Archaeatropidae have been treated as two different families. However, these families share a lot of similarities in amber deposit (Spain, France, Myanmar), living period, and morphological characters such as number of flagellomeres, shape of maxillary palps, wing shape and venation, and shape of external valves (Baz and Ortuño, 2001). The main differences between them are the rows of forewing veins setae (Empheriidae with two rows of

TABLE 1 | Genera and species of Empheriidae.

Taxa	Locality	Age
Archaeatropos randatae Azar and Nel, 2004 *	Lebanon	Lower Cretaceous
Bcharreglaris amunobi Azar and Nel, 2004 *		
Libanoglaris mouawadi Perrichot et al., 2003 *		
Libanoglaris chehabi Azar and Nel, 2004 *		
Setoglaris reemae Azar and Nel, 2004 *		
Empheropsocus arilloi Baz and Ortuño, 2001	Spain	Lower Cretaceous
Empheropsocus margineglabrus Baz and Ortuño, 2001		
Preempheria antiqua Baz and Ortuño, 2001		
Archaeatropos alavensis Baz and Ortuño, 2000 *		
Proprionoglaris axioperierga Azar et al., 2014 *	France SW	Lower Cretaceous
Proprionoglaris guyoti Perrichot et al., 2003 *		
Prospeleketor albianensis Perrichot et al., 2003 *		
Empherium rasnitsyni Hakim et al., 2021	Siberian	Lower Cretaceous
Burmempheria densuschaetae Li et al., 2020	Myanmar	Upper Cretaceous
Burmempheria raruschaetae Li et al., 2020		
Burmempheria curvatavena Li, Yoshizawa & Yao, sp. nov.		
Latempheria kachinensis Li, Yoshizawa & Yao, sp. nov.		
Archaeatropos perantiqua Cockerell, 1919 *		
Heliadesdakruon morganae Cumming and Le Tirant, 2021 *		
Longiantennum fashengi Liang et al., in press*		
Jerseyempheria grimaldii Azar et al., 2010	New Jersey	Upper Cretaceous
Eoempheria intermedia Nel et al., 2005	France Oise	Lower Eocene
Empheria (*Bebiosis*) *pertinens* Enderlein, 1911	Baltic	Eocene
Empheria (*Bebiosis*) *reticulata* Pictet-Baraban and Hagen, 1856		
Trichempheria villosa Hagen, 1882		

**Represent this genus originally placed in Archaeatropidae.*

setae vs. Archaeatropidae with one row of setae) and forewing nodulus (Empheriidae without nodulus vs. Archaeatropidae with nodulus) (Baz and Ortuño, 2000, 2001; Mockford et al., 2013). However, the forewing veins setae are not stable (Li et al., 2020). For example: *Prospeleketor albianensis* Perrichot et al., 2003 and *Proprionoglaris axioperierga* Azar et al., 2014 have been assigned to Archaeatropidae, but they have two rows of vein setae, and the Empheriidae species: *Preempheria antiqua* Baz and Ortuño, 2001 has one row of vein setae; *Burmempheria* has two rows of vein setae in Sc, A and Cu, but other veins have only one row; *Jerseyempheria grimaldii* Azar et al., 2010 with the setae covering the membrane of forewing. The forewing nodulus is also an unstable character (Wang et al., 2019) and cannot be used to distinguish these two families (Li et al., 2020). Li et al. (2020) mentioned that Empheriidae and Archaeatropidae are presumed to be closely related because of shared morphological conditions in the forewing veins setae and the setose anal area. The present phylogenetic analysis suggests for the first time that Empheriidae and Archaeatropidae form a monophyletic group supported by the membranous region of forewing with setae (character 12, state 1); forewing veins with setae (character 15, state 1). Based on these results, we conclude that Archaeatropidae Baz and Ortuño, 2000 should be treated as a junior synonymy of Empheriidae (Kolbe, 1884). As a result, Empheriidae now contains sixteen genera and twenty-five species in total (including this study) (**Table 1**).

This is the first study to explore the phylogenetics of the atropine families including the fossil taxa. To avoid reduction of tree resolution, we only selected well-preserved fossils and did not include highly autapomorphic genera (e.g., *Jerseyempheria* Azar et al., 2010 with the forewing membrane covered with setae). However, due to the limitations of fossil preservation, some important characters could not be observed from the fossils, and the phylogenetic placement of poorly preserved fossil taxa remains unknown. Further research is still needed to obtain more data using techniques, i.e., CT scanning, to obtain more information and to elucidate their relationship. Over the past 40 years, the phylogeny and taxonomy of Psocodea including their higher level of classification have been studied extensively based on the evidence of extant insects, including morphological and molecular systematics (Smithers, 1972; Yoshizawa, 2002; Perrichot et al., 2003; Yoshizawa and Johnson, 2003, 2006; Johnson et al., 2004, 2018; de Moya et al., 2021), but there are still some disagreement (Yoshizawa and Saigusa, 2001; Misof et al., 2014). The bias of sampling, the homogeneity of evidence, and the instability of taxonomic characteristics may be the important reasons for the above arguments. Therefore, it is important to integrate the fossil evidence and the modern insects to construct a phylogenetic tree in order to elucidate the morphological characteristics, origin, and evolutionary history of these insect groups.

The fossil records of Atropetae are mainly from Mesozoic, and twenty-four genera with twenty-nine species have been recorded during Cretaceous from Lebanon, Spain, France SW, Myanmar, New Jersey, and Siberia (Vishnyakova, 1975; Baz and Ortuño, 2000, 2001; Perrichot et al., 2003; Azar and Nel, 2004, 2011; Azar et al., 2010, 2014, 2017; Hakim et al., 2018, 2021; Wang et al., 2019; Li et al., 2020; Corentin et al., 2021; Cumming and Le Tirant, 2021; Liang and Liu, 2021). Only ten genera with thirteen species are known during Cenozoic from the Baltic region, France Oise, FuShun, and Tanzania (Hagen, 1856, 1865, 1866, 1882; Enderlein, 1911; Nel et al., 2005; Azar et al., 2018). The earliest fossil record was from Lebanon (Cretaceous, Lower Barremian). Most extant species of Atropetae live in tropical and subtropical regions (Smithers, 1972, 1999; New, 1975; Mockford, 1991; Lienhard, 2000). During the Cretaceous and Cenozoic, environment about the locality of the fossil record is mainly under a warm and humid tropical or subtropical climate (Scotese, 2002). Research showed that Myanmar had a tropical forest palaeoenvironment during the Cretaceous (Grimaldi et al., 2002; Shi et al., 2022), which also met their requirements for living environment. Over the 100 million years of evolution, the distributional range of Atropetae is probably mainly restricted to warm and humid areas. The Atropetae insects may be an indication of an ancient environment.

DATA AVAILABILITY STATEMENT

The datasets presented in this study can be found in online repositories. The names of the repository/repositories and accession number(s) can be found below: Zoobank, https://zoobank.org/52D5D725-1731-4855-86CB-4C2714781C65, https://zoobank.org/e490780d-ac0e-4bf7-a9f1-5ee8f0b01316, (urn:lsid:zoobank.org:act:8500CE76-8F78-402B-AB7D-376B939FC0A9) and (urn:lsid:zoobank.org:act:89231F37-E4CC-44BA-85F0-CCDE453FB3AA). Further enquires can be directed to the corresponding author(s).

AUTHOR CONTRIBUTIONS

SL, YY, and DR designed the research. SL conceived the study with support from KY, DR, and YY. DR and YY provided the materials. SL and QW took the photographs and prepared the line drawings. SL, KY, and QW performed the morphological analysis. SL and KY conducted the phylogenetic analyses. KY and MB revised the draft. All authors contributed to the article and approved the submitted version.

FUNDING

This study was supported by the National Natural Science Foundation of China (Nos: 31970436, 31730087, 32101239, and 32020103006), Joint Fund of the Beijing Municipal Natural Science Foundation and Beijing Municipal Education Commission (KZ201810028046), and Japan Society for the Promotion of Science (19H03278).

ACKNOWLEDGMENTS

We are grateful to Charles Lienhard, editor, and reviewers for constructive criticism and valuable comments on the manuscript. We thank Yongjie Wang, Ruiqian Wang, and Xiangbo Guo of Capital Normal University, Chaofan Shi of Sun Yat-sen University, Xiaodan Lin of Hainan University, Xinyu Li of China Agricultural University, Feiyang Liang of Hunan University of Science and Technology, and Josh Jenkins Shaw of Natural History Museum of Denmark for helping with data collection and phylogenetic analysis, and providing valuable comments and suggestions.

SUPPLEMENTARY MATERIAL

The Supplementary Material for this article can be found online at: https://www.frontiersin.org/articles/10.3389/fevo.2022.907903/full#supplementary-material

Supplementary Figure 1 | The most parsimonious tree obtained by TNT analysis. Phylogeny of Atropetae based on 18 species and 38 characters, with characters being nonadditive, under equal weighting. Analyzed with TNT v1.5. * Representsthe genus originally placed in Archaeatropidae.

REFERENCES

Azar, D. A., Nel, A., and Perrichot, V. (2014). Diverse barklice (Psocodea) from Late Cretaceous Vendean amber. *Paleontol. Contribut.* 10, 9–15.

Azar, D., and Nel, A. (2004). Four new Psocoptera from Lebanese amber (Insecta: Psocomorpha: Trogimorpha). *Ann. Soc. Entomol. Fr.* 40, 185–192. doi: 10.1080/00379271.2004.10697415

Azar, D., and Nel, A. (2011). The oldest psyllipsocid booklice, in Lower Cretaceous amber from Lebanon (Psocodea, Trogiomorpha, Psocathropetae, Psyllipsocidae). *Zookeys* 130, 153–165. doi: 10.3897/zookeys.130.1430

Azar, D., Huang, D. Y., El-Hajj, L., Cai, C. Y., Nel, A., and Maksoud, S. (2017). New Prionoglarididae from Burmese amber (Psocodea: Trogiomorpha: Prionoglaridetae). *Cretac. Res.* 75, 146–156. doi: 10.1016/j.cretres.2017.03.028

Azar, D., Maksoud, S., Nammour, C., Nel, A., and Wang, B. (2018). A new trogiid genus from lower Eocene Fushun amber (Insecta: Psocodea: Trogiomorpha). *Geobios* 51, 101–106. doi: 10.1016/j.geobios.2018.02.002

Azar, D., Nel, A., and Petrulevièius, V. (2010). First Psocodean (Psocadea, Empheriidae) from the Cretaceous Amber of New Jersey. *Acta Geol. Sin.-Engl. Ed.* 84, 762–767. doi: 10.1111/j.1755-6724.2010.00255.x

Badonnel, A. (1951). "Psocoptères," in *Traité de Zoologie*, ed. P. P. Grassé (Paris: Masson), 1301–1340.

Badonnel, A. (1986). Psocoptères de Colombie (Insecta, Psocoptera). Missions écologiques du Professeur Sturm (1956 à 1978). *Spixiana* 9, 179–223. doi: 10.5962/bhl.part.82381

Baz, A. (1993). Revision of the Cerobasis annulata group (Psocoptera: Trogiidae) from the Canary Islands. *Zoo. Med.* 67, 487–504.

Baz, A., and Ortuño, V. M. (2000). Archaeatropidae, a new family of Psocoptera from the Cretaceous amber of Alava, northern Spain. *Ann. Entomol. Soc. Am* 93, 367–373. doi: 10.1603/0013-87462000093[0367:AANFOP]2.0.CO;2

Baz, A., and Ortuño, V. M. (2001). New genera and species of empheriids (Psocoptera: Empheriidae) from the Cretaceous amber of Alava, northern Spain. *CretacRes* 22, 575–584. doi: 10.1006/cres.2001.0275

Casasola González, J. A. (2006). Phylogenetic relationships of the genera of Epipsocetae (Psocoptera: Psocomorpha). *Zootaxa* 1194, 1–32.

Cockerell, T. D. A. (1919). Insects in Burmese Amber. *Entomologist* 52, 241–243.

Corentin, J., Yoshizawa, K., Hakim, M., Huang, D. Y., and Nel, A. (2021). New psocids (Psocodea: Prionoglarididae, Psyllipsocidae) from Cretaceous Burmese amber deposits. *CretacRes* 126:104890. doi: 10.1016/j.cretres.2021.104890

Cumming, R. T., and Le Tirant, S. (2021). Review of the Cretaceous †Archaeatropidae and †Empheriidae and description of a new genus and species from Burmese amber (Psocoptera). *Faunitaxys* 9, 1–11.

de Moya, R. S., Yoshizawa, K., Kimberly, K. O. W., Andrew, D. S., Christipher, H. D., and Johnson, K. P. (2021). Phylogenomics of parasitic and non-parasitic lice (Insecta: Psocodea): Combining sequence data and Exploring compositional bias solutions in Next Generation Datasets. *Syst. Biol.* 70, 719–738, doi: 10.1093/sysbio/syaa075

Enderlein, G. (1911). Die Fossilen Copeognathen und ihre Phylogenie. *Palaeontographica* 58, 279–360.

Engel, M. S. (2020). Myanmar: palaeontologists must stop buying conflict amber. *Nature* 584, 525. doi: 10.1038/d41586-020-02432-z

Goloboff, P. A. (1997). *NoName (NONA), Version 2.0.* Fundación Instituto Miguel Lillo, Tucumán: Program and Documentation.

Goloboff, P. A., and Catalano, S. A. (2016). TNT version 1.5, including a full implementation of phylogenetic morphometrics. *Cladistics* 32, 221–238. doi: 10.1111/cla.12160

Grimaldi, D. A., and Engel, M. S. (2006). Fossil Liposcelididae and the lice ages (Insecta: Psocodea). *Proc. Royal Soc. B.* 273, 625–633. doi: 10.1098/rspb.2005.3337

Grimaldi, D. A., Engel, M. S., and Nascimbene, P. C. (2002). Fossiliferous Cretaceous Amber from Myanmar (Burma): Its Rediscovery, Biotic Diversity, and Paleontological Significance. *Am. Mus. Novit.* 3361, 1–71. doi: 10.1206/0003-008220023612.0.CO;2

Hagen, H. (1856). "Die im Bernstein befindlichen Neuropteren der Vorwelt," in *Die im Bernstein Befindlichen Organischen Reste der Vorwelt*, eds G. C. Berendt, F. J. Pictet de la Rive, and H. A. Hagen (Berlin: Gerhard), 1–122.

Hagen, H. (1865). On some aberrant genera of Psocina. *Entomol. Month. Magazine* 2, 148–152.

Hagen, H. (1866). On some aberrant genera of Psocina. *Entomol. Month. Magazine* 2, 170–172.

Hagen, H. (1876). Contributions to the natural history of Kerguelen Island, made in connection with the United States transit of Venus Expedition, 1874-75. II. *Bull. U. S. Natl. Museum* 2, 1–122.

Hagen, H. (1882). Beitrage zur Monographie der Psociden. über Psociden im Bernstein. *Stettin. Entomol. Zeitung* 43, 217–237.

Hakim, M., Azar, S., Maksoud, S., Huang, D. Y., and Azar, D. (2018). New polymorphic psyllipsocids from Burmese amber (Psocodea: Psyllipsocidae). *Cretac. Res.* 84, 389–400. doi: 10.1016/j.cretres.2017.11.027

Hakim, M., Huang, D. Y., and Azar, D. (2021). New fossil psocids from Cretaceous Siberian ambers (Psocodea: Trogiomorpha: Atropetae). *Palaeoentomology* 4, 186–198. doi: 10.11646/palaeoentomology.4.2.8

Huang, D. Y., Bechly, G., Nel, P., Engel, M. S., Prokop, J., Azar, D., et al. (2016). New fossil insect order Permopsocida elucidates major radiation and evolution of suction feeding in hemimetabolous insects (Hexapoda: Acercaria). *Sci. Rep.* 6:23004. doi: 10.1038/srep23004

Illiger, J. C. W. (1798). *Kugelann Verzeuchniss der Käfer Preussens, entworfen von J. G. Kugelann, ausgearbeitet von Illiger, mit einer Vorrede von Hellwig und dem angehängten Versuch einer natürlichen Ordnung und Gattungsfolge der Insecten*. Halle: Bei Johann Jacob Gebauer.

Johnson, K. P., Dietrich, C. H., Friedrich, F., Beutel, R. G., Wipfler, B., Peters, R. S., et al. (2018). Phylogenomics and the evolution of hemipteroid insects. *PANS* 115, 12775–12780. doi: 10.1073/pnas.1815820115

Johnson, K. P., Yoshizawa, K., and Smith, S. V. (2004). Multiple origins of parasitism in lice. *Proc. Royal Soc. B.* 271, 1771–1776. doi: 10.1098/rspb.2004.2798

Kolbe, H. J. (1882). Neue Psociden der paläarktischen Region. *Entomol. Nachrichten Berlin.* 8, 207–212.

Kolbe, H. J. (1884). Der Entwickelungsgang der Psociden im Individuum und in der Zeit. *Berlin. Entomol. Zeitschrift* 28, 35–38.

Kolbe, H. J. (1885). Zur Kenntniss der Psociden-Fauna Madagaskars. *Berlin. Entomol. Zeitschrift* 29, 183–192.

Li, F. S. (2002). *Psocoptera of China*. Beijing: National Natural Science Foundation of China, Science Press.

Li, S., Wang, Q. Z., Ren, D., and Yao, Y. Y. (2020). New genus and species of Empheriidae (Psocodea: Trogiomorpha) from mid-Cretaceous amber of northern Myanmar. *CretacRes* 110:104421. doi: 10.1016/j.cretres.2020.104421

Liang, F. Y., and Liu, X. Y. (2021). A new species of Psyllipsocus (Psocodea: Trogiomorpha: Psyllipsocidae) from the mid-Cretaceous amber of Myanmar. *Zootaxa* 5072, 081–087. doi: 10.11646/zootaxa.5072.1.9

Liang, F. Y., Li, S., Liu, X. Y., Bai, M., and Yao, Y. Z. (in press). A new genus and species of the family Archaeatropidae (Psocodea: Trogiomorpha) from mid-Cretaceous amber of Northern Myanmar. *CretacRes* 105233. doi: 10.1016/j.cretres.2022.105233

Lienhard, C. (1998). Psocoptères euro-méditerranéens. *Faune de France* 83:517.

Lienhard, C. (2000). A new desert psocid from Namibia (Insecta: Psocoptera: Trogiidae). *Rev. Suisse Zool.* 107, 277–281.

Lienhard, C. (2004). Siamoglaris zebrina gen. n., sp. n., the first representative of Prionoglarididae from the Oriental Region (Insecta: Psocoptera). *Rev. Suisse Zool.* 111, 865–875.

Lienhard, C. (2011). A new species of Siamoglaris from Thailand with complementary description of the type species (Psocodea: 'Psocoptera': Prionoglarididae). *Rev. Suisse Zool.* 118, 293–306.

Lienhard, C., and Smithers, C. N. (2002). *Psocoptera (insecta): World Catalogue and Bibliography*. Geneva: Muséum d'Histoire Naturelle de Genève.

Lin, X. D., Labandeira, C. C., Shih, C. K., Hotton, C. L., and Ren, D. (2019). Life habits and evolutionary biology of new two-winged long-proboscid scorpionflies from mid-Cretaceous Myanmar amber. *Nat. Commun.* 10:1235. doi: 10.1038/s41467-019-09236-4

Misof, B., Liu, S. L., Meusemann, K., Peters, R. S., Donath, A., Mayer, C., et al. (2014). Phylogenomics resolves the timing and pattern of insect evolution. *Science* 346, 763–767. doi: 10.1126/science.1257570

Mockford, E. L. (1991). New species and records of Psocoptera (Insecta) From Roraima State, Brazil. *Acta Amazon* 21, 211–318.

Mockford, E. L. (1993). *North American Psocoptera (Insecta). Flora and Fauna Handbook*. Gainesville, FL: Sandhill Crane Press.

Mockford, E. L. (2005). New Genus of Perientomine Psocids (Psocoptera: Lepidopsocidae) with a Review of the Perientomine Genera. *Trans. Am. Entomol. Soc.* 131, 201–215.

Mockford, E. L., and Garcia Aldrete, A. N. (2010). Psoquilla infuscata Badonnel (Psocoptera: Psoquillidae) in the Western Hemisphere with description of the male and brachypterous form. *Zootaxa* 2618, 61–68. doi: 10.11646/zootaxa.2618.1.4

Mockford, E. L., Charles, L., and Yoshizawa, K. (2013). Revised classification of "Psocoptera" from Cretaceous amber, a reassessment of published information. *Insect. Matsumurana N. S.* 69, 1–26.

Nel, A., Prokop, J., De Ploeg, G., and Millet, J. (2005). New Psocoptera (Insecta) from the lowermost Eocene amber of Oise, France. *J. Syst. Palaeontol.* 3, 371–391. doi: 10.1017/S1477201905001598

New, T. R. (1975). Lepidopsocidae and Aamphientomidae (Psocoptera) from Malaysia and Singapore. *Orient. Insects* 9, 177–194. doi: 10.1080/00305316.1975.10434490

Nixon, K. C. (2002). *WinClada, Version 1.00.08*. New York, NY: Program and Documentation. Cornell University Press.

Page, R. D. M. (2001). *NDE: NEXUS Data Editor 0.5.0*. Scotland, UK: University of Glasgow

Pearman, J. V. (1936). The taxonomy of the Psocoptera: preliminary sketch. *Proc. Royal Soc. B.* 5, 58–62. doi: 10.1111/j.1365-3113.1936.tb00596.x

Perrichot, V., Azar, D., Néraudeau, D., and Nel, A. (2003). New Psocoptera in the Early Cretaceous amber of SW France and Lebanon (Insecta: Psocoptera: Trogiomorpha). *Geol. Mag.* 140, 669–683. doi: 10.1017/S0016756803008355

Pictet-Baraban, F., and Hagen, H. (1856). "Die im Bernstein befindlichen Neuroptera der Vorwelt," in *Die im Bernstein Befindlichen Organischen Reste der Vorwelt*, ed. G. Berendt (Berlin: Nicholaische Buchhandlung), 57–64.

Roesler, R. (1940). Neue und wenig bekannte Copeognathengattungen. *I. Zool. Anz.* 129, 225–243.

Roesler, R. (1944). Die Gattungen der Copeognathen. *Stettiner Entomol. Zeitung* 105, 117–166.

Scotese, C. R. (2002). *Goal of the PALEOMAP Project.* Available online at: http://www.scotese.com (accessed October 20, 2020).

Selys-Longchamps, E. D. (1872). Note on two new genera of Psocidae. *Entomol. Month. Magazine* 9, 145–146.

Shi, C., Cai, H. H., Jiang, R. X., Wang, S., Engel, M. S., Yuan, J., et al. (2021). Balance scientific and ethical concerns to achieve a nuanced perspective on 'blood amber'. *Science* 351, 926–926.

Shi, C., Wang, S., Cai, H. H., Zhang, H. R., Long, X. X., Tihelka, E., et al. (2022). Fire-prone Rhamnaceae with South African affinities in Cretaceous Myanmar amber. *Nat. Plants* 8, 125–135. doi: 10.1038/s41477-021-01091-w

Smithers, C. N. (1972). The classification and phylogeny of the Psocoptera. *Memo. Aust. Museum* 14, 1–349.

Smithers, C. N. (1999). First records of Pteroxanium marrisi n.sp. and Haplophallus maculatus (Tillyard) for the Chatham Islands and list of Psocoptera from the subantarctic islands of New Zealand. *Nz. Entomol.* 22, 9–13. doi: 10.1080/00779962.1999.9722050

Vishnyakova, V. N. (1975). Psocoptera in Late Cretaceous insect-bearing resins from Taimyr. *Entomol. Obozrenie* 54, 94–96.

Wang, R. Q., Li, S., Ren, D., and Yao, Y. Z. (2019). New genus and species of the Psyllipsocidae (Psocodea: Trogiomorpha) from mid-Cretaceous Burmese amber. *Cretac. Res.* 104:104178. doi: 10.1016/j.cretres.2019.07.008

Wang, S., Shi, C., Zhang, Y. J., Hu, G. X., and Gao, L. Z. (2016). Trading away ancient amber's secrets. *Science* 351, 926–926. doi: 10.1126/science.351.6276.926-a

Yoshizawa, K. (2002). Phylogeny and higher classification of suborder Psocomorpha (Insecta: Psocodea: 'Psocoptera'). *Zool. J. Linn. Soc.* 136, 371–400. doi: 10.1046/j.1096-3642.2002.00036.x

Yoshizawa, K. (2005). Morphology of Psocomorpha (Psocodea: 'Psocoptera'). *Ins. matsum. N. S.* 62, 1–44.

Yoshizawa, K., and Johnson, K. P. (2003). Phylogenetic position of Phthiraptera (Insecta: Paraneoptera) and elevated rate of evolution in mitochondrial 12S and 16S rDNA. *Mol. Phylogenet. Evol.* 29, 102–114. doi: 10.1016/S1055-7903(03)00073-3

Yoshizawa, K., and Johnson, K. P. (2006). Morphology of male genitalia in lice and relatives and phylogenetic implications. *Syst. Entomol.* 31, 350–361. doi: 10.1111/j.1365-3113.2005.00323.x

Yoshizawa, K., and Lienhard, C. (2020). †Cormopsocidae: A new family of the suborder Trogiomorpha (Insecta: Psocodea) from Burmese amber. *Entomol. Sci.* 23, 208–215. doi: 10.1111/ens.12414

Yoshizawa, K., and Saigusa, T. (2001). Phylogenetic analysis of paraneopteran orders (Insecta: Neoptera) based on forewing base structure, with comments on monophyly of Auchenorrhyncha (Hemiptera). *Syst. Entomol.* 26, 1–13. doi: 10.1046/j.1365-3113.2001.00133.x

Yoshizawa, K., Lienhard, C., and Johnson, K. P. (2006). Molecular systematics of the suborder Trogiomorpha (Insecta: Psocodea: "Psocoptera"). *Zool. J. Linn. Soc.* 146, 287–299. doi: 10.1111/j.1096-3642.2006.00207.x

Zhao, Z. P., Yin, X. C., Shih, C. K., Gao, T. P., and Ren, D. (2020). Termite colonies from mid-Cretaceous Myanmar demonstrate their early eusocial lifestyle in damp/rotting wood. *Natl. Sci. Rev.* 7, 381–390. doi: 10.1093/nsr/nwz141

Conflict of Interest: The authors declare that the research was conducted in the absence of any commercial or financial relationships that could be construed as a potential conflict of interest.

Publisher's Note: All claims expressed in this article are solely those of the authors and do not necessarily represent those of their affiliated organizations, or those of the publisher, the editors and the reviewers. Any product that may be evaluated in this article, or claim that may be made by its manufacturer, is not guaranteed or endorsed by the publisher.

ORIGINAL RESEARCH
published: 16 June 2022
doi: 10.3389/fevo.2022.892530

Three New Species of Velvety Shore Bugs (Hemiptera: Heteroptera: Ochteroidea) From Mid-Cretaceous Kachin Amber Shed Light on the Evolution of Rostrum Length in Ochteroidea

Mao Zhang[1], Zhipeng Zhao[2], Dong Ren[1] and Yunzhi Yao[1]*

[1] Key Laboratory of Insect Evolution and Environmental Changes, College of Life Sciences and Academy for Multidisciplinary Studies, Capital Normal University, Beijing, China, [2] Fishery Resource and Environment Research Center, Chinese Academy of Fishery Sciences, Beijing, China

OPEN ACCESS

Edited by:
Chenyang Cai, Nanjing Institute of Geology and Paleontology (CAS), China

Reviewed by:
Tian Jiang, China University of Geosciences, China
Jiu-Yang Luo, Sun Yat-sen University, China

***Correspondence:**
Yunzhi Yao
yaoyz100@126.com

Specialty section:
This article was submitted to Paleontology, a section of the journal Frontiers in Ecology and Evolution

Received: *09 March 2022*
Accepted: *20 April 2022*
Published: *16 June 2022*

Citation:
Zhang M, Zhao Z, Ren D and Yao Y (2022) Three New Species of Velvety Shore Bugs (Hemiptera: Heteroptera: Ochteroidea) From Mid-Cretaceous Kachin Amber Shed Light on the Evolution of Rostrum Length in Ochteroidea. Front. Ecol. Evol. 10:892530. doi: 10.3389/fevo.2022.892530

Two new genera of velvety shore bugs, *Arcochterus* Zhang, Ren and Yao gen. nov. and *Parvochterus* Zhang, Ren and Yao gen. nov. are described, with three new species between them—*Arcochterus fuscus* Zhang, Ren and Yao sp. nov., *Parvochterus reticulatus* Ren and Yao sp. nov., and *P. lanceolarus* Zhang, Ren and Yao sp. nov. Based on the combination of fossil and extant taxa, a cladistic analysis is conducted to confirm the phylogenetic position of these species and allows reconstruction of the inter-genus relationships within the superfamily Ochteroidea. Major conclusions of the phylogenetic analysis: (1) these new species and *Grimaldinia pronotalis* belong to Ochteridae; (2) Ochteroidea is a monophyletic group, Ochteridae and Gelastocoridae are sister group and monophyletic, respectively. (3) The ancestral character state reconstruction (ACSR) shows that the length of the rostrum has occurred in at least three independent transitions during the evolution of the superfamily Ochteroidea.

Keywords: Ochteridae, Gelastocoridae, new species, morphological phylogenetics, ancestral character state reconstruction, independent evolution

INTRODUCTION

The family Ochteridae are commonly known as "velvety shore bugs", together with its sister group, Gelastocoridae (the toad bugs), jointly form the extent superfamily Ochteroidea, belonging to the infraorder Nepomorpha which is a small riparian group (Kment et al., 2020; Schuh and Weirauch, 2020). Ochteridae consist of three extant genera (*Ochterus* Latreille, 1807, *Megochterus* Jaczewski, 1934 and *Ocyochterus* Drake and Gómez-Menor, 1954) and 91 species (Kment et al., 2020; Polhemus, 2021). Gelastocoridae includes two subfamilies, Gelastocorinae Champion (1901) and Nerthrinae Kirkaldy (1906) with two extant genera (*Gelastocoris* Kirkaldy, 1897 and *Nerthra* Say, 1832) and 106 species (Estévez and Ruf, 2006; Poinar and Brown, 2016; Schuh and Weirauch, 2020).

Fossil Ochteroidea are scarce, including Ochteridae, Gelastocoridae, Propreocoridae, and Pseudonerthridae (Kment et al., 2020; Schuh and Weirauch, 2020). The fossil ochterids definitely contains four genera and five species (Kment et al., 2020), including the oldest on the fossil record—three genera and four species from the Early Cretaceous of China: *Pristinochterus zhangi* Yao et al., 2007, *P. ovatus* Yao et al., 2011, *Angulochterus quatrimaculatus* Yao et al., 2011, and *Floricaudus multilocellus* Yao et al., 2011, and one genus and species from Miocene Dominican amber: *Riegerochterus baehri* Popov and Heiss, 2014a. Fossil gelastocorids include three genera and five species, with two species from Early Cretaceous of Brazil (Ruf et al., 2005; Xie and Liu, 2018), two species from the mid-Cretaceous of Myanmar (Poinar and Brown, 2016) and one species from the late Holocene of Chile (Faúndez and Ashworth, 2015). Only one genus and species of Pseudonerthridae was reported: *Pseudonerthra gigantea* (Ruf et al., 2005), from the Early Cretaceous of Brazil. *Propreocoris maculatus* Popov et al., 1994, from the Early Jurassic of Britain, was considered the earliest fossil record of Ochteridae, nonetheless, Shcherbakov and Popov (2002) supposed it as the endemic subfamily Proprepocorinae, later Grimaldi and Engel (2005) and Yao et al. (2011) believed it should be as a common ancestor of the Ochteridae and Gelastocoridae; eventually, Kment et al. (2020) formally raised Proprepocorinae to family rank. *Grimaldinia pronotalis* Popov and Heiss, 2014b, from mid-Cretaceous Myanmar, was assigned to the Leptosaldinae (Leptopodomorpha: Leptopodidae) and regarded as a controversial species, was revised to Ochteroidea by Schuh and Weirauch (2020).

Recent phylogenetic analyses of Nepomorpha indicated superfamily Ochteroidea is a monophyletic group, Ochteridae and Gelastocoridae are sister group and monophyletic, respectively (Andersen and Weir, 2004; Hebsgaard et al., 2004; Yao et al., 2011; Ye et al., 2020). The main diagnostic characters of the family Ochteridae are as follows: eyes large, with inner margins emarginated; ocelli present; antennae 4-segmented, partially visible dorsally; rostrum long, segment III longest; legs adapted for walking, without swimming hairs, profemora not enlarged; tarsal formula 2-2-3; membrane of forewings with several closed cells (Chen et al., 2005; Schuh and Weirauch, 2020). Herein, we reported five Kachin amber ochterids with short rostrum from Hukawng Valley in northern Myanmar. These newly described taxa supplement Ochteridae and provided new evidence for clarifying the phylogeny of Ochteridae.

MATERIALS AND METHODS

Material Study and Terminology

The amber specimens are from the Hukawng Valley (Kachin State, Northern Myanmar), near Tanai Village (26°21′33.41″ N, 96°43′11.88″ E) (Zhang et al., 2018; Wang et al., 2019) approximately from the Turonian or Cenomanian, 98.79 ± 0.62 Ma (Du et al., 2019; Li et al., 2020). There are five specimens, in one of which the amber embeds two individuals at once, including a female and a male. All these specimens herein are deposited in the Key Laboratory of Insect Evolution and Environmental Changes from the College of Life of Science at Capital Normal University, Beijing, China (CNU; Yunzhi Yao, Curator).

Morphological terminology and taxonomy mainly follow Andersen and Weir (2004) and Schuh and Weirauch (2020). All measurements are in millimeters (mm).

Taxon Sampling and Character Choice

Two representatives from the family Belostomatidae (*Belostoma lutarium* Stål, 1856) and Naucoridae (*Idiocarus minor* La Rivers, 1971) are selected as the outgroup taxa (Hebsgaard et al., 2004; Yao et al., 2011; Ye et al., 2020; Wang et al., 2021), and 16 species of Ochteroidea are as the ingroup (nine extant taxa and three fossil taxa of Ochteridae; two extant taxa and two fossil taxa of Gelastocoridae). A total of 32 morphological characters from adults were used, most of the characters are from Hebsgaard et al. (2004) and Yao et al. (2011) (see **Appendix 1** for the definitions of characters) and all the characters are equal-weighted (**Table 1**).

Phylogenetic Analysis

The matrix (**Appendix 1**) was compiled using Nexus Data Editor (Version 0.5.0) (Page, 2001). Phylogenetic analysis based on the maximum parsimony was conducted in Winclada (Version 1.00.08) with NONA script and a repeated verification in TNT (Version 1.5) (Goloboff, 1999; Nixon, 2002; Goloboff and Catalano, 2016). Heuristic searches using Winclada were performed with a parameter of 10,000 maximum trees, 1,000 random-taxa-addition replicates, and 100 starting trees per replication. The repeated analysis in TNT was using "traditional search" and the Bremer Support values (BS) were calculated through the script "Bremer. Run."

Ancestral Character State Reconstruction

We reconstructed the ancestral state of rostrum length in Ochteroidea based on the phylogenetic analysis, using the Mesquite (Version 3.70) (Maddison and Maddison, 2021). The rostrum length of each of the 18 species of Ochteroidea is selected from character 21 in the matrix (**Table 1**). Three kinds of rostrum lengths were identified: (0) reaching procoxae, (1) reaching mesocoxae, and (2) reaching metacoxae.

RESULTS AND DISCUSSION

Phylogenetic Analyses

The phylogenetic analysis returned the two most parsimonious trees [tree length = 52, consistency index (CI) = 0.65, retention index (RI) = 0.83]. The strict consensus tree [tree length = 53, consistency index (CI) = 0.64, retention index (RI) = 0.83] is shown in **Figure 1**, with unambiguous characters and Bremer support values (BS) marked. The major results of our phylogenetic analysis are as follows: the superfamily Ochteroidea (BS = 7) is well supported as a monophyletic; the monophyly of Ochteridae (BS = 4) and Gelastocoridae (BS = 2) are strongly supported, they are the sister group, and the new fossils all belong to Ochteridae.

TABLE 1 | Character state matrix of 32 characters for the 18 taxa included in the phylogenetic study.

	1	2	3	4	5	6	7	8	9	10	11	12	13	14	15	16	17	18	19	20	21	22	23	24	25	26	27	28	29	30	31	32
Belostoma lutarium	0	0	0	0	0	0	0	0	0	0	0	1	0	0	0	0	1	0	0	0	0	0	1	0	0	0	1	1	0	0	0	0
Idiocarus minor	0	0	0	0	0	0	0	0	0	0	0	1	0	0	0	1	1	1	0	0	0	0	0	0	0	0	1	1	0	0	1	0
Nerthra fuscipes	1	0	0	0	0	1	1	1	1	0	0	1	1	0	0	1	1	1	1	0	2	0	0	1	1	1	0	1	1	0	1	0
Nerthra bichelata	1	0	0	0	0	1	1	1	1	0	0	1	1	0	0	1	1	1	1	?	0	0	0	1	1	1	0	1	?	?	1	1
Gelastocoris rotundatus	1	0	0	1	0	1	1	1	1	0	0	1	1	0	0	1	1	1	1	1	0	0	1	1	1	1	0	1	1	0	1	0
Gelastocoris curiosus	1	0	0	0	0	1	1	1	1	0	0	1	1	0	?	1	1	1	1	?	0	0	1	1	1	1	0	1	1	0	1	1
Ochterus marginatus	1	1	0	1	1	0	1	1	1	0	0	0	1	0	1	1	0	1	0	0	2	1	1	1	1	1	1	0	1	1	1	1
Ocyochterus victor	1	1	0	1	1	0	1	1	1	0	0	1	1	0	1	1	1	1	0	0	2	1	1	1	1	1	1	0	1	1	1	1
Megochterus nasutus	1	1	1	1	1	1	1	1	1	0	0	1	1	0	1	1	0	1	0	0	2	1	1	1	1	1	1	0	1	1	1	0
Pristinochterus zhangi	1	1	1	0	1	0	0	?	1	0	1	0	1	0	0	1	0	0	0	0	1	1	1	1	1	1	1	0	0	1	1	0
Pristinochterus ovatus	1	1	1	0	1	0	0	?	1	0	1	0	1	0	0	1	0	0	0	0	1	1	1	1	1	1	1	0	0	1	1	0
Floricaudus multilocellus	1	1	1	0	1	0	0	?	1	0	1	0	1	1	0	1	0	1	0	0	1	1	1	1	1	1	1	0	0	1	1	0
Angulochterus quatrimaculatus	1	1	1	1	1	0	0	?	1	0	1	0	1	0	0	1	0	0	0	0	1	1	1	1	1	1	1	0	0	1	1	0
Riegerochterus baehri	1	1	0	-	1	0	1	1	1	0	1	1	1	0	1	1	1	1	0	0	2	1	1	1	1	1	1	0	1	1	1	1
Grimaldinia pronotalis	1	1	0	-	1	0	2	1	1	1	1	0	1	0	0	1	1	1	0	0	0	1	1	1	1	1	1	0	?	?	1	1
Arcochterus fuscus gen. et sp. n.	1	1	0	0	1	0	2	1	1	1	1	1	1	0	0	1	0	1	0	0	0	1	1	1	1	1	1	0	1	1	1	1
Parvochterus reticulatus gen. et sp. n.	1	1	0	0	1	0	2	1	1	1	1	0	1	1	0	1	0	1	0	0	0	1	1	1	1	1	1	0	1	1	1	1
Parvochterus lanceolarus gen. et sp. n.	1	1	0	0	1	0	2	1	1	1	1	0	1	1	0	1	0	1	0	0	0	1	1	1	1	1	1	0	1	1	1	1

Unknown data were assigned as "?" and inapplicable data as "-."

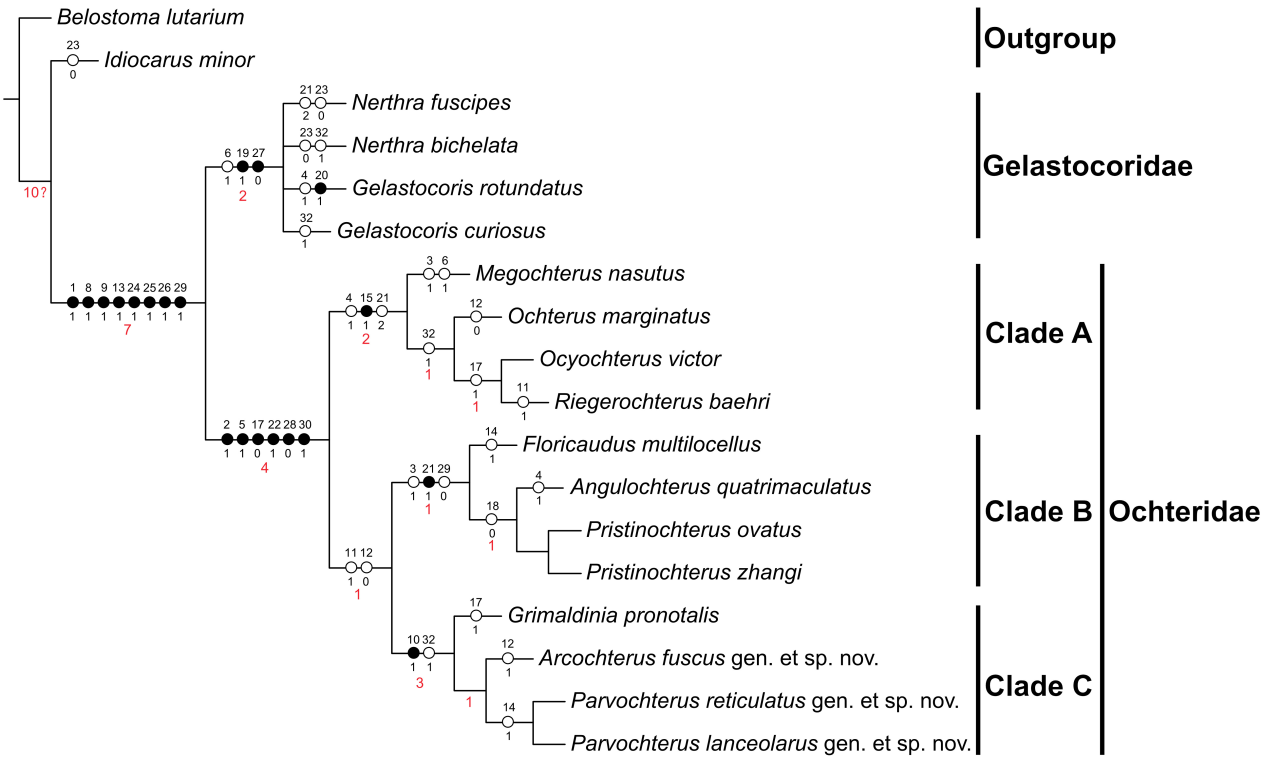

FIGURE 1 | The strict consensus tree for the analyzed Ochteridae: tree length = 53, consistency index (CI) = 0.64, retention index (RI) = 0.83. •, non-homoplastic changes; ∘, homoplastic changes. The red numbers below the branches are Bremer support values (BS).

The results reconfirm the monophyly of Ochteroidea, Ochteridae, and Gelastocoridae, consistent with most previous studies (Rieger, 1976; Mahner, 1993; Hebsgaard et al., 2004; Li et al., 2012, 2014; Ye et al., 2020). The monophyly of Ochteroidea is supported by eight synapomorphies: clypeus divided by a cross fold (character 1, state 1), ocelli present (character 8, state 1), head and prothorax discretely (character 9, state 1), propleuron undeveloped (character 13, state 1), metacoxae short (character 24, state 1), metatibia without swimming hairs (character 25, state 1), tarsal formula not 2:3:3 (character 26, state 1), distal of sternum VII in males asymmetrical (character 29, state 1). The monophyly of Gelastocoridae is supported by two synapomorphies: the surface of thorax and forewings with wartlike sculpturation (character 19, state 1), tarsal formula: 1:2:3 (character 27, state 0). Ochteridae has 6 synapomorphies: clypeus with a pattern of ridges (character 2, state 1), antennae short, but visible dorsally, projecting (character 5, state 1), forewing with spots (character 17, state 0), forelegs cursorial (character 22, state 1), tarsal formula 2:2:3 (character 28, state 0), abdominal sternum VIII in males divided into two lobes (character 30, state 1). The monophyly of Clade A is supported by one synapomorphic character and two homoplastic characters: clavus not broad (character 15, state 1) and clypeus distinctly transversely rugose (character 4, state 1), rostrum generally extended beyond metacoxae (character 21, state 2). Clade B and Clade C are the sister group. Clade B is supported by one synapomorphy and two homoplastic characters: rostrum extending beyond procoxae, but never extended beyond metacoxae (character 21, state 1) and frontal plate produced above the base of the rostrum strongly (character 3, state 1), distal of sternum VII in males symmetrical (character 29, state 0). Clade C is supported by one synapomorphy and one homoplastic character: eye outer margin exceeding pronotal costal margin distinct (character 10, state 1) and body length less than 7 mm (character 32, state 2). The taxonomic location of *Grimaldinia pronotalis* has long been controversial (Popov and Heiss, 2014b; Schuh and Weirauch, 2020), but as shown according to our phylogenetic results, this species has six synapomorphies of Ochteridae. *Grimaldinia* with *Arcochterus* gen. nov. and *Parvochterus* gen. nov. as a monophly form clade C.

Phylogenetic reconstruction indicates the length of the rostrum has occurred at least three times independent transitions from exceeding to procoxa to meso- and metacoxa during the evolution of Ochteroidea: twice transitions occurred during the evolution of Ochteridae, once transition in Gelastocoridae (**Figure 2**). We hence conclude the different evolutionary trends in the length of rostrum of two groups: in Ochteridae, it gradually evolved from short to long, and in Gelastocoridae, more representatives retain the ancestral form.

Systematic Paleontology

Suborder Heteroptera Latreille, 1810.

Infraorder Nepomorpha Popov, 1968.

Superfamily Ochteroidea Kirkaldy, 1906.

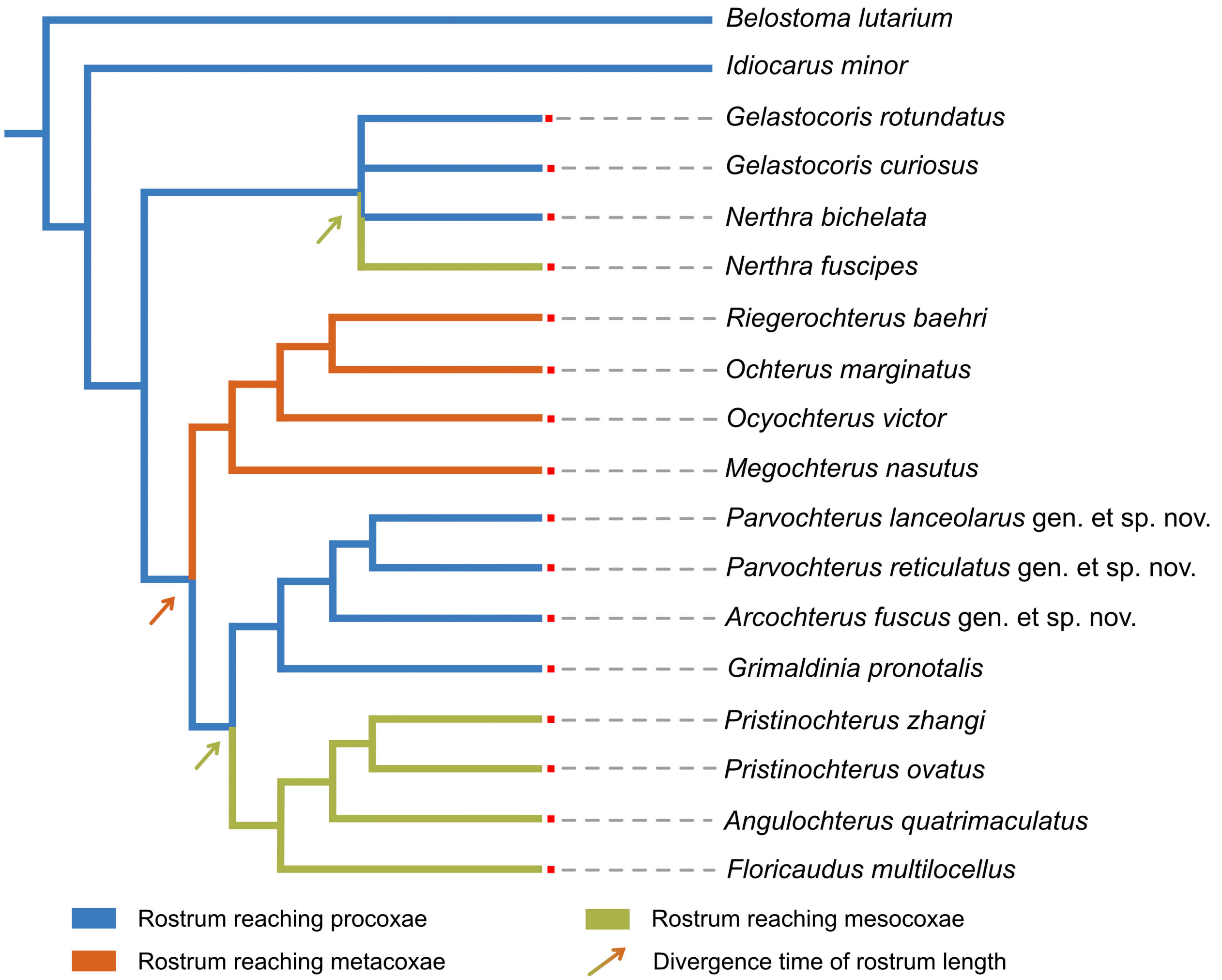

FIGURE 2 | Ancestral state reconstruction of the rostrum length of Ochteridae.

Family Ochteridae Kirkaldy, 1906.

Genus *Arcochterus* Zhang, Ren and Yao gen. nov.

Type species: *Arcochterus fuscus* Zhang, Ren and Yao sp. nov. (**Figure 3**).

Included species: *Arcochterus fuscus* Zhang, Ren and Yao sp. nov.

Etymology: The generic name is a combination of the Latin "*arcus*" (arch) and "*ochterus*" (type genera of Ochteridae) because the forewings costal margin with one-row arch cells. Gender: masculine.

Diagnosis: Eyes reniform. Two distal segments of antennae are longer than two basal segments (**Figures 3C,E**). Rostrum 4-segmented, short, reaching to procoxae, segment III in length subequal to segment IV (**Figures 3C,F**). Outer margins of the pronotum strongly explanate, the extended part wider than the eyes in width. Scutellum longer than pronotum at midline. Clavus broad, about two-thirds as long as forewing, with a long anal vein. Claval commissure is subequal to scutellum in length. Forewing with median fracture and deep costal fracture, costal fracture length about one-third of forewing width, rest of costal margins with over 20 cells (**Figures 3A,D**). SC curved, fused with C at one fifth basally, C reaching forewing apex. Tibia with dense, thin setae, and stout spines. Male abdominal sternum VI arched, sternum VII and VIII split into two large asymmetrical lobes (**Figures 3G,H**).

Remarks: The new genus is assigned to Ochteridae based on the following shared characters: body ovoid; eyes large, with inner margins emarginated; ocelli present; antennae 4-segmented, partially visible dorsally; tarsal formula 2-2-3; abdominal end of male asymmetrical.

Arcochterus gen. nov. can be distinguished from the same locality extinct genus *Grimaldinia* Popov and Heiss, 2014b, by the following characters: antennae distal three segments slender (vs. segment III larger than segments I and II); rostrum 4-segmented (vs. rostrum 3-segmented); pronotum anterior margins concave (vs. pronotum anterior margin convex); portion of mesoscutum invisible (vs. portion of mesoscutum visible); claval commissure subequal to scutellum length (vs. claval

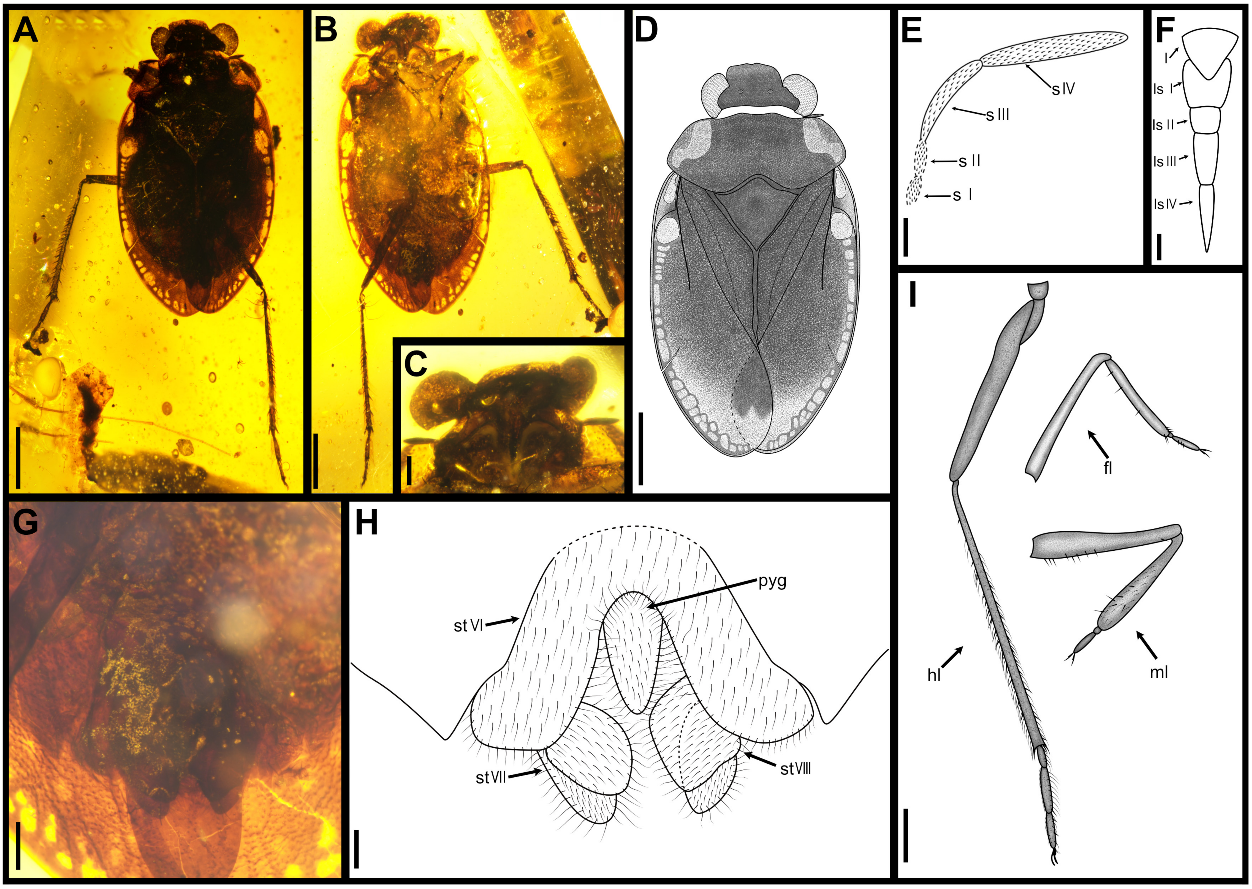

FIGURE 3 | *Arcochterus fuscus* gen. et sp. nov., holotype, CNU-HET-MA2015003, male. **(A)** photograph in dorsal view; **(B)** photograph in ventral view; **(C)** rostrum; **(D)** line drawing habitus in dorsal view; **(E)** antenna, outline; **(F)** rostrum, outline; **(G)** abdomen apex; **(H)** abdomen apex, outline; **(I)** legs, outline. fl, foreleg; hl, hindleg; l, labrum; ls I-IV, labial segment I to IV; ml, midleg; pyg, pygophore; s I-IV, segment I to IV; st VI-VIII, sternum of segments VI to VIII. Scale bars: panels **(A,B,D,I)** = 0.5 mm, panels **(C,F)** = 0.1 mm, panels **(E,G,H)** = 0.2 mm.

commissure insignificantly longer than scutellum length), clavus with a long anal vein (vs. clavus without vein); forewing with deep costal fracture (vs. costal fracture short), costal margin with two spots (vs. costal margin without spots); forewing with more than 20 serried cells (vs. forewing with 4 larger elongate and 2 smaller round cells).

Arcochterus fuscus Zhang, Ren and Yao sp. nov. (**Figure 3**).

Etymology: The new specific name is from a Latin "*fuscus*" (fuscous), referring to the particularly deep black presented by the dorsal view. Gender: masculine.

Material: Holotype, CNU-HET-MA2015001 (male), a well-persevered specimen.

Distribution: Hukawng Valley, Kachin State, Northern Myanmar (mid-Cretaceous amber: one species).

Diagnosis: Body length is about 5.50 mm, about 1.86 times as long as the width. Body dorsally very dark brown. Head width about half as long as body width. Antennae segment IV longest, subequal to segment III (**Figures 3C,E**). Rostrum segment I shortest, segment III subequal in length to segment IV (**Figures 3C,F**). Scutellum length and width almost equal. Clavus width 0.56 times as long as scutellum, with one anal vein. Costal fracture slender and straight. Medial fractures length about one-third of forewing. Basal of costal margins with two large and transparent spots. Profemur longer than mesofemur. Protibia longer than mesotibia. Pro- and mesotibia with few spurs; metatibia with two-row spurs and long setae dorsally, apex with a row of spines around (**Figures 3B,I**). Male abdomen apex covered by forewing. Sternum VI-VIII with densely and thin setae. The lobe in sternum VIII lager than sternum VII (**Figures 3G,H**).

Description: Body dorso-ventrally flattened with dense small points, without spines and setae. Surface except for head densely punctate.

Head broad, about 2.33 times as wide as long. Eyes large, smallest interocular distance 0.44 times of head width, prominent, with inner margins emarginated lightly and eyes stylate small. Ocelli separate, width of ocellus subequal to length of ocelli to eyes. Frontal plate declivent, not protruded anteriorly. Clypeus with pattern of ridges and divided by a cross fold and without distinct transverse wrinkles. Antennae 4-segmented, with dense setae, inserted below eyes, only segment IV partly visible in dorsal view; three distal segments of antennae slender, segment III twice as long as segment II, segment IV longest and subequal in length to segments II and III. Rostrum 4-segmented, short, reaching to procoxae, segment I shortest, segment III longest, segment III and segment IV almost equal length, segment III dark color.

Pronotum strongly transverse, 2.80 times as wide as long, moderately punctured. Anterior margin emarginate. Lateral margins attenuated, and widely rounded. Posterior margin strongly convex at the middle. Scutellum triangular, 1.15 times as wide as long, anterior margin slightly convex, elevated weakly baso-medially, tip pointed, punctured.

Forewings macropterous, in dark color, produced laterally and posteriorly over abdomen, with punctateed surface. Forewing 2.23 times as long as wide, nearly 0.72 times as long as body. Clavus wide and large, with claval suture distinct. Costal fracture extension line not reaching median fracture. Narrow membrane of right forewing overlapping left one.

Legs all walking legs and profemur strong. All legs surface densely setae. Tarsus with two curved claws, two setiform parempodium. Pro- and mesofemora with long setae, without spines; Pro- and mesotibia clavate, with some long spines and short spines mixed; tarsi two segments with some spines and long setae, segment I short. Metafemora thick and strong; tarsi three segments with long setae, segment I shortest, segment II subequal to segment III in length, tip of segment II with a row of spines.

Abdomen apex covered by forewing, abdominal segment VI bent, sternum VII and VIII divided into two independent plates, slightly stout, asymmetrical, with long setae. Sternum VII and VIII slightly smaller and subequal in length.

Dimensions (in mm): Body length 5.45, width 2.92; head length 0.66, width 1.54; antennae length 0.80 (I 0.07, II 0.11, III 0.26, IV 0.36); eye length 0.67, diameter of eye 0.31, interocular space 0.68; interocellar space 0.32; rostrum length 0.52, segment I 0.05, II 0.10, III 0.19, IV 0.18; pronotum length 0.83, width 2.32; scutellum length 1.00, width 1.15; hemelytron length 3.92, width 1.76; clavus length 2.62 width 0.56; abdomen width 1.83; length of foreleg: femur 1.52, tibia 0.91, tarsi 0.32 (I 0.06, II 0.26), claw 0.15; length of midleg: femur 1.36, tibia 1.12, tarsi 0.34 (I 0.05, II 0.29), claw 0.12; length of hindleg: femur 1.83, tibia 2.19, tarsi 0.82 (I 0.11, II 0.39, III 0.32), claw 0.15.

Genus *Parvochterus* Zhang, Ren and Yao gen. nov.

Type species: *Parvochterus reticulatus* Zhang, Ren and Yao sp. nov. (**Figures 4**, **5**).

Included species: *Parvochterus reticulatus* Zhang, Ren and Yao sp. nov., and *P. lanceolarus* Zhang, Ren and Yao sp. nov. (**Figure 6**).

Etymology: The generic name is a combination of the Latin "*parv-"*(small) and "*ochterus*" (type genera of Ochteridae) because the shape of scutellum is significantly smaller than the others. Gender: masculine.

Diagnosis: Head anterior margin emarginated. Eyes oblong, mesal margin emarginate lightly. Antennae segment IV length longer than segment III, segment III length subequal to segment I and segment II (**Figures 5D,G**). Rostrum 4-segmented, short, reaching to procoxae, segment III longer than segment IV (**Figures 5E,F**). Pronotum anterior margin depressed, outer margins explanate part in width narrower than width of an eye. Scutellum small, away from pronotum, shorter than pronotum in length at midline. Clavus broad, width subequal to scutellum length, length about 0.50 times as long as forewing. Claval commissure length longer than scutellum. Forewing SC arcuate, fused with C one fifth basally, with costal fracture and medial fracture. Membrane without cells. Pronotum, scutellum, and forewing with silvery-white spots. Tibia with stout spines and long setae. Femur apex with 1–2 spines. Profemur sturdy. Abdominal sterna VI sinuate; male abdominal sternum VII and VIII subdivided into two separate asymmetrical plates (**Figures 5A,H,J**).

Remarks: *Parvochterus* gen. nov. resembles *Arcochterus* gen. nov., for example the rostrum 4-segmented, short, reaching to procoxae; clavus broad; forewing SC arcuate, fused with C, with costal fracture and medial fracture; tibia with spines and setae. abdominal sterna VI sinuate; male abdominal sternum VII and VIII subdivided into two separate asymmetrical plates. The main differences between *Parvochterus* gen. nov. and *Arcochterus* gen. nov. are eyes oblong (vs. eyes reniform); rostrum segment length longer than segment IV (vs. rostrum segment III length subequal to segment IV); pronotum outer margins explanate part in width narrower than width of an eye (vs. pronotum extended part in width wider than width of an eye); scutellum small, shorter than pronotum in length at midline (vs. scutellum longer than pronotum at midline); forewings without cells (vs. forewings over 20 cells); Pronotum, scutellum, and forewing with silvery-white spots (vs. pronotum, scutellum, and forewing without spots); femur apex with 1–2 spines (vs. femur apex without spines).

Parvochterus reticulatus Zhang, Ren and Yao sp. nov. (**Figures 4**, **5**).

Etymology: The new specific name is from a Latin word "*reticulatus*" (reticular), referring to the surface of hemelytron with many reticular punctuations. Gender: masculine.

Material: Holotype, CNU-HET-MA2015002 (male); allotype, CNU-HET-MA2015003 (female); paratype, CNU-HET-MA2015005 (male); three well-persevered specimens, the holotype and allotype in the same amber.

Distribution: Hukawng Valley, Kachin State, Northern Myanmar (mid-Cretaceous amber: one species).

Diagnosis: Antennae apical two segments slender, segment II expanded apically. Rostrum segment II shortest, segment III longest (**Figure 5C–F**). Pronotum with seven spots in male, and four spots in female. Scutellum with two spots. Forewings with two larger and four smaller ellipse silvery-white spots, clavus with two round silvery-white spots on both sides of anal vein, costal margins with six transparent spots. Costal fracture arched. Medial fractures extension and costal fracture without connection. Fore wing costal margin with dense protrusion notches like tiny grids. Protibia with dense long hairs. Metatibia with two-row thorns and one row of long hairs on each side. Male abdominal segments VII and VIII exposed in dorsal view, sternum VII plates slightly thinner, sternum VIII slightly expanded, with dense long hairs. Female abdomen apex covered by forewings.

Description: Male. Body small-sized, ovoid, about 3.38 mm, 1.92 times as long as wide, dorso-ventrally flattened with dense points, without spines and setae.

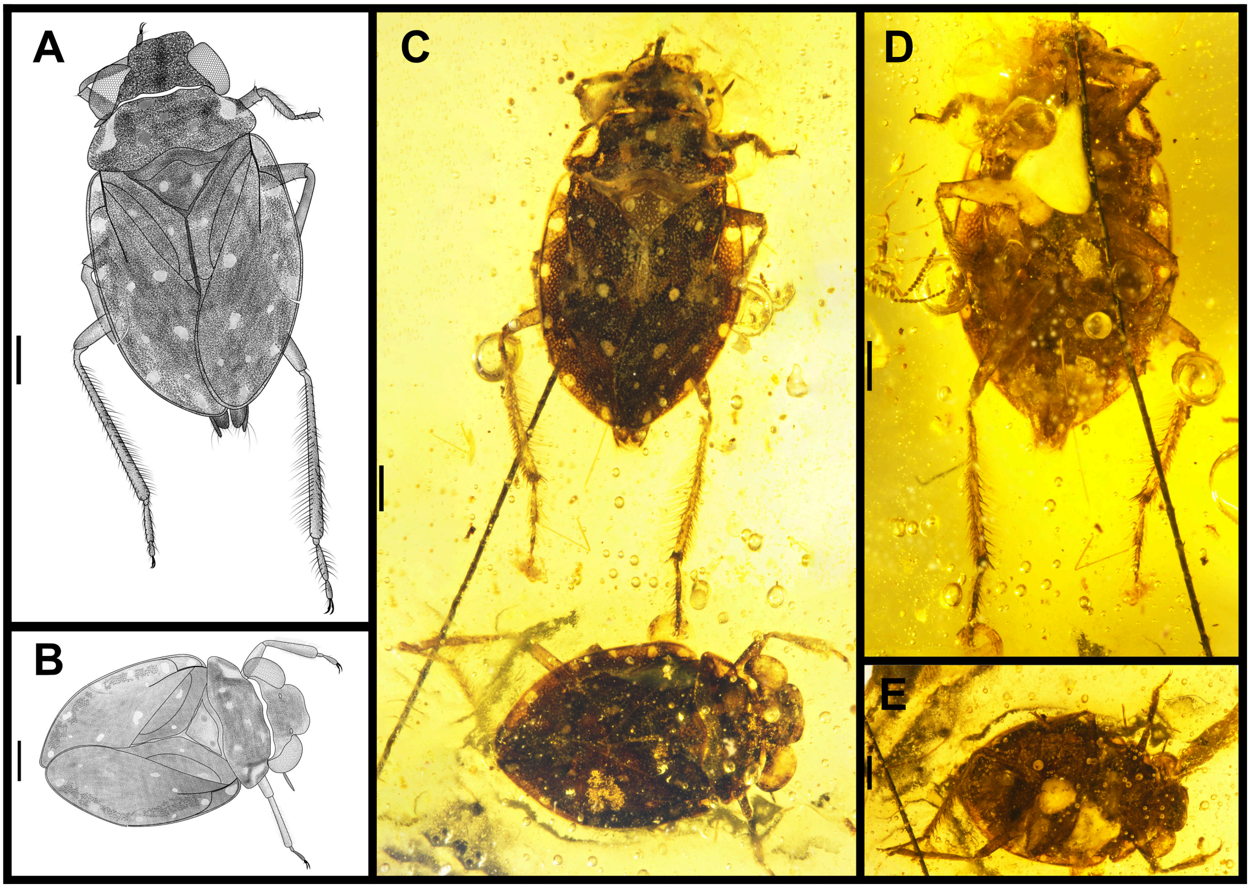

FIGURE 4 | *Parvochterus reticulatus* gen. et sp. nov. **(A)** holotype, CNU-HET-MA2015001, male, Line drawing habitus in dorsal view; **(B)** allotype, CNU-HET-MA2015002, female, Line drawing habitus in dorsal view; **(C)** holotype (upper), allotype (lower), photograph in dorsal view; **(D)** holotype, photograph in ventral view; **(E)** allotype, photograph in ventral view. Scale bars: 0.5 mm.

Head broad, about 3.08 times as wide as long. Eyes large, ellipse porrect, smallest interocular distance 0.47 times head width, with eyes stylate. Ocelli small, widely separated, close to eyes. Frontal plate declivent, not protruded anteriorly. Clypeus with a pattern of ridges and divided by a cross fold, anterior margin concave. Antennae 4-segmented, segment IV 1.33 times longer than segment III, apical two segments thicker than basal two segments, with dense setae, inserted below eyes, only segment IV partly visible in dorsal view. Labrum small triangle with dense setae, reaching to base of rostrum. Rostrum 4-segmented, short and stout, reaching to procoxae, segment I shortest, segment III 1.8 times longer than segment IV, segment IV dark color.

Pronotum strongly transverse, 3.33 times as wide as long at middle, moderately punctured, with 7 spots. Anterior margin emarginated lightly, posterior margin strongly convex at middle. Scutellum triangular, with two large and silvery-white spots, anterior margin convex, elevated weakly baso-medially, tip blunt, punctured.

Forewings macropterous or submacropterous, surface punctate. Forewing 2.06 times as long as wide, nearly 0.65 times as long as body. Clavus wide and large, with distinct vein penetration, with two spots on each side. Claval commissure, length longer than scutellum length. Costal fracture present, extension line reaching nearly to median fracture. Narrow membrane of right forewing overlapping left one.

Legs all walking legs. Procoxae close to mesocoxae, mesocoxae apart from metacoxae. Metafemora are longer than mesofemora and mesofemora longer than profemora. Tarsus with two curved claws and two setiform parempodium. Pro- and mesofemur stout. Protibia clavate with some rows of spines and dense short hairs. Pro- and mesotibia shorter than femur. Pro- and mesotarsi 2-segmented without spines and hair. Metatibia longer than others tibia, longer than metafemur, with some rows of short to long thin spines and long setae. Metatarsi 3-segmented, segment I shortest, other segments equal length, with hairs and short setae.

Male abdomen apex exceeding forewings submacropterous, not over macropterous, with seven visible segments, abdominal segments V-VI sinuate, segments VII and VIII divided into two long independent plates, asymmetrical, with dense long hairs. Pygophore with long hairs. Segment VII in length subequal to VIII.

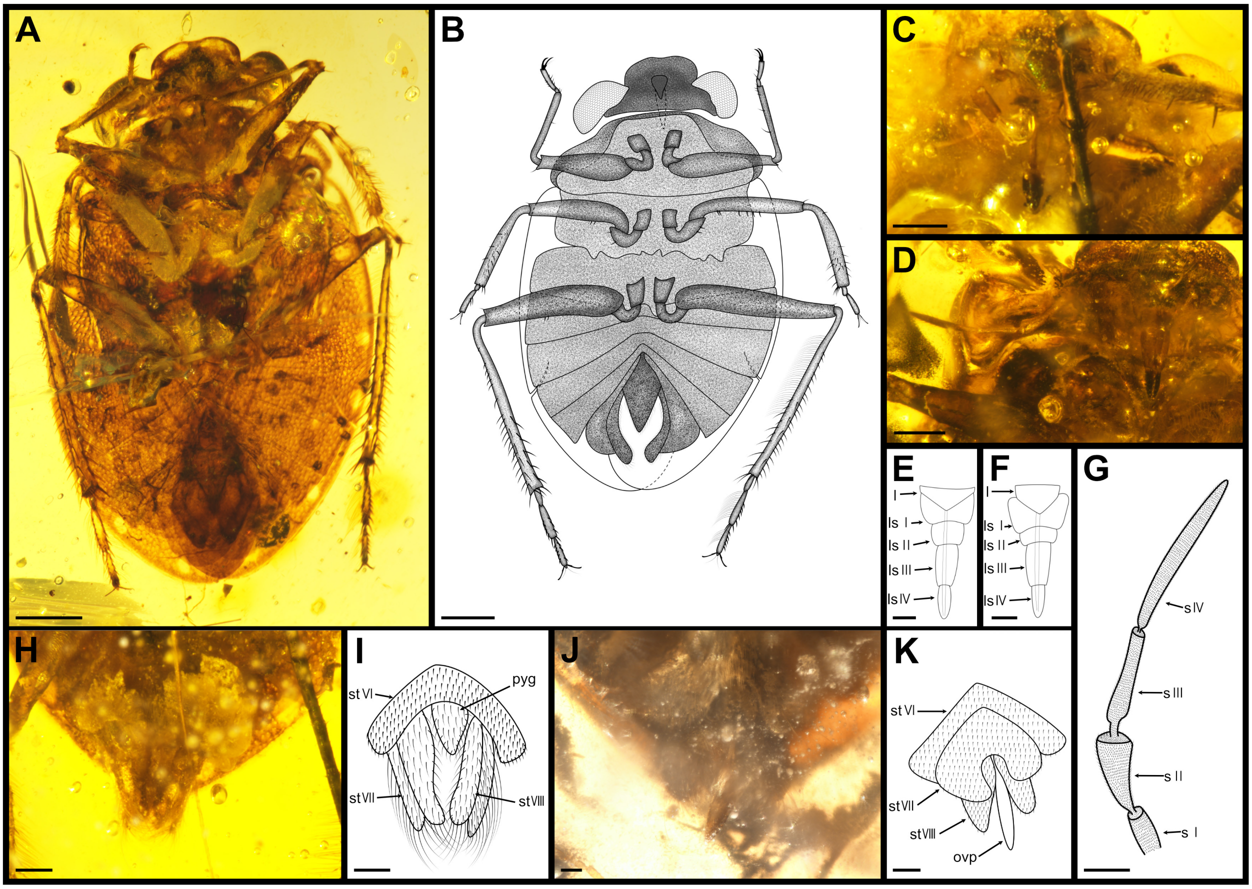

FIGURE 5 | *Parvochterus reticulatus* gen. et sp. nov. **(A)** paratype, CNU-HET-MA2015005, male, photograph in ventral view. **(B)** Line drawing habitus in ventral view. **(C)** holotype, rostrum; **(D)** allotype, rostrum, and antenna. **(E)** holotype, rostrum, outline. **(F)** allotype, rostrum, outline. **(G)** allotype, antenna, outline. **(H)** holotype, abdomen apex. **(I)** allotype, abdomen apex. **(J)** holotype, abdomen apex, outline. **(K)** allotype, abdomen apex, outline. fl, foreleg; hl, hindleg; l, labrum; ls I-IV, labial segment I to IV; ml, midleg; ovp, ovipositor; pyg, pygophore; s I-IV, segment I to IV; st VI-VIII, sternum of segments VI to VIII. Scale bars: panels **(A,B)** = 0.5 mm, panels **(C,D,G–K)** = 0.2 mm, panels **(E,F)** = 0.1 mm.

Female. The structure and color similar to male, differences: body size of male is larger than female, but female abdomen width is longer than male; male hind femora are longer than middle femora, and middle femora longer than profemora, however, female has three pairs of similar length femora. Abdomen covered by forewings, sternum VII posterior margin strongly hollow, with dense setae, and ovipositor long, exceeding to last abdominal segment.

Dimensions (in mm): Male: body length 4.16, width 2.16; head length 0.48, width 1.48; eye length 0.63, diameter of eye 0.29, interocular space 0.70; interocellar space 0.39; rostrum length 0.58 (I 0.15, II 0.10, III 0.18, IV 0.15); pronotum length 0.55, width 1.83; scutellum length 0.53, width 0.95; hemelytron length 2.72, width 1.32; clavus length 1.53, width 0.45; abdomen width 1.63; length of foreleg: femur 1.01, tibia 0.60, tarsi 0.28 (I 0.06, II 0.22),claw 0.15; length of midleg: femur 1.10, tibia 0.81, tarsi 0.36 (I 0.08, II 0.28), claw 0.13; length of hindleg: femur 1.45, tibia 1.71, tarsi 0.63 (I 0.10, II 0.31, III 0.23), claw 0.12. Female: body length 3.38, width 2.06; head length 0.43, width 1.52; eye length 0.54, diameter of eyes 0.27, interocular space 0.67; interocellar space 0.39; antennae length 0.60 (I 0.07, II 0.15, III 0.21, IV 0.38); rostrum length 0.51 (I 0.15, II 0.07, III 0.17, IV 0.12); pronotum length 0.55, width 1.70; scutellum length 0.40, width 0.78; hemelytron length 2.36, width 0.95; clavus length 1.24, width 0.41; abdomen width 1.76; length of foreleg: femur 0.90, tibia 0.64, tarsi 0.22 (I 0.08, II 0.14), claw 0.15; length of midleg: femur 0.95, tibia 0.72, tarsi 0.27 (I 0.05, II 0.22), claw 0.11; length of hindleg: femur 1.62, tibia 1.64, tarsi 0.64 (I 0.08, II 0.29, III 0.27), claw 0.12.

Parvochterus lanceolarus Zhang, Ren and Yao sp. nov. (**Figure 6**).

Etymology: The new specific name is from the Latin word "*lanceolarus*" (lanceolar) by forming two lanceolar bulges with anterior margin of the pronotum. Gender: masculine.

Material: Holotype, CNU-HET-MA-2015003 (male), a well-persevered specimen.

Distribution: Hukawng Valley, Kachin State, Northern Myanmar (mid-Cretaceous amber: one species).

Diagnosis: Rostrum segment I shortest, segment III and segment IV almost equal length (**Figures 6E,F**). Pronotum with

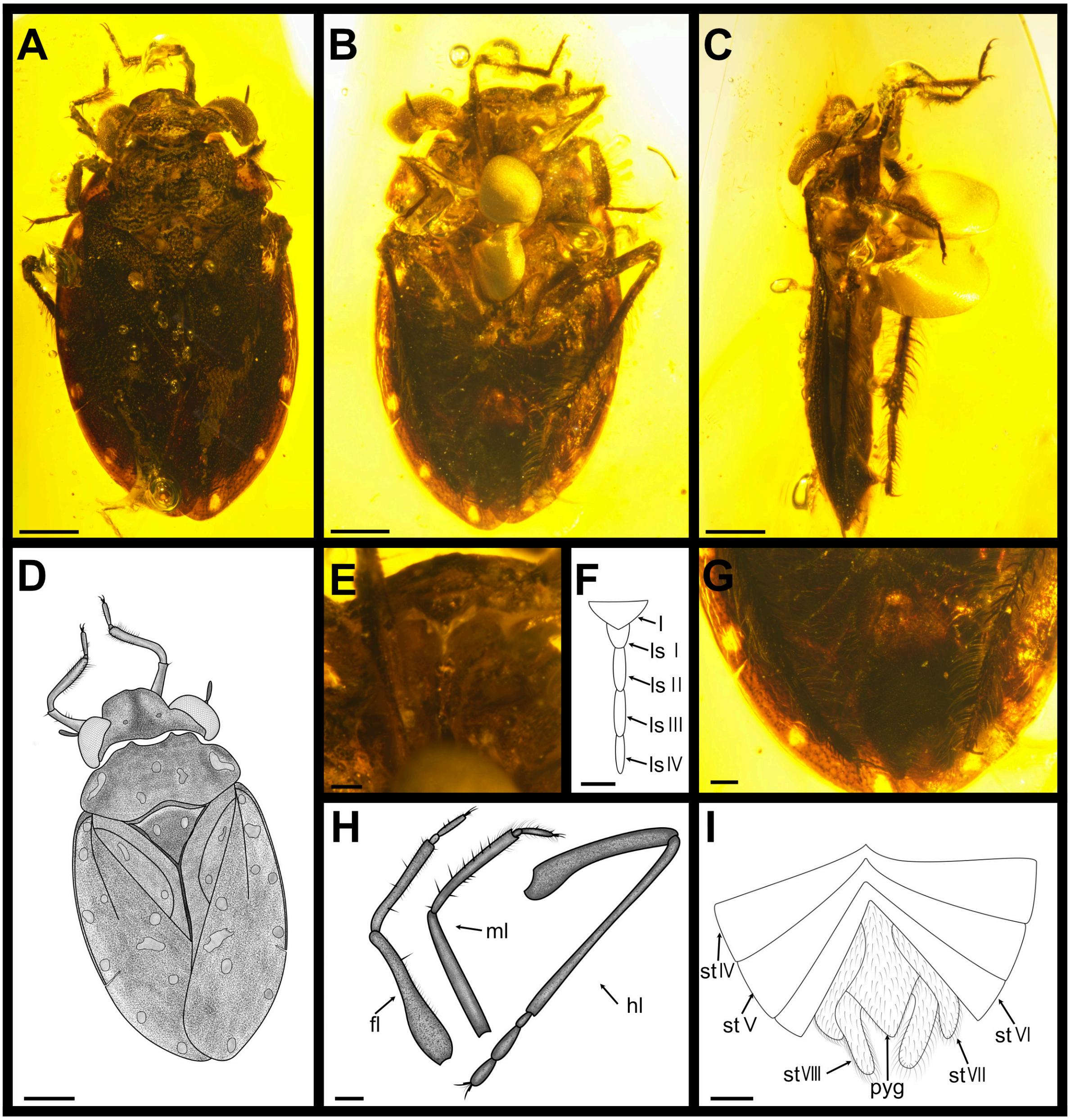

FIGURE 6 | *Parvochterus lanceolarus* gen. et sp. nov., Holotype, CNU-HET-MA2015004, ♂. **(A)** photograph in dorsal view; **(B)** photograph in ventral view; **(C)** photograph in lateral view; **(D)** line drawing habitus in dorsal view; **(E)** rostrum; **(F)** rostrum, outline; **(G)** abdomen; **(H)** legs, outline; **(I)** abdomen, outline. fl, foreleg; hl, hindleg; l, labrum; ls I-IV, labial segment I to IV; ml, midleg; pyg, pygophore; st VI-VIII, sternum of segments VI to VIII. Scale bars: panels **(A–D,I)** = 0.5 mm, panels **(E,F)** = 0.1 mm, panels **(G,H)** = 0.2 mm.

3 spots. Scutellum with 2 spots. Clavus wide, with 2 spots on anal vein side, claval commissure longer than scutellum. Forewing costal margin with 6 transparent spots, membrane without cells. Costal fracture short and straight, about one-fifth of forewing width, medial fractures long, about two-fifth of forewing length, far from costal fracture. Protibia with dense long hairs; mesotibia latter part gradually coarsens with long setae and apical spines; metabiba with long setae and long, bent and rigidity spines; mesotarsi with two straight claws; metatarsi with two curved claws, with long setae and a row of spines (**Figures 6B,C,H**). Abdomen apex covered by forewings, sternum IV-VI bent strongly, sternum VII and VIII significantly reduced and retracted into sternum VI, divided into two independent plates, slightly stout, asymmetrical, with long setae (**Figures 6G,I**).

Description: Small size, ovoid, about 3.82 mm, about 1.80 times as long as wide. Body dorso-ventrally flattened with dense points, without spines and setae.

Head broad, about 3.14 times as wide as long. Eyes large, inner margins emarginated lightly, stylate smaller, smallest interocular distance 0.43 times of head width. Ocelli small, widely separated, close to eyes. Frontal plate declivent, not protruded anteriorly. Clypeus with pattern of ridges and divided by a cross fold. Antennae 4-segmented, slender and short, surface densely setae, inserted below eyes, only segment IV partly visible in dorsal view, fusiformis. Rostrum 4-segmented, short, reaching to procoxae, segment I shortest, segment III segment III longest, and segment IV almost equal length, about 2 times longer than segment I, segment IV dark color.

Pronotum strongly transverse, 2.38 times as wide as long at middle, moderately punctured; Anterior margin concave with two lanceolar bulges, Lateral margins flimsy and widely rounded, Posterior margin strongly convex at middle. Scutellum triangular, with one large marking on each side, anterior margin slightly convex, elevated weakly baso-medially, tip blunt, punctured.

Forewings macropterous, dark color, produced laterally and posteriorly over abdomen, surface punctate. Forewing 2.05 times as long as wide, nearly 0.68 times as long as body. Clavus wide and large, with distinct anal vein and claval suture. Claval commissure not straight, longer than scutellum length. Costal fracture obvious, median fracture extension line without gear into Costal fracture. Narrow membrane of right forewing overlapping left one.

Legs all walking legs. All legs with dense setae. Tarsus with two claws, two setiform parempodium. Metafemur sturdy, with some thin spines and long setae; protibia clavate, with some rows of spines; protarsus 2-segmented, with some spines and long setae, and with two curved claws. Mesotibia latter part gradually coarsens with long setae. Mesotarsi with two straight claws. Metatarsi with two curved claws.

Abdomen apex covered by forewings, sternum VII and VIII significantly reduced and retracted into sternum VI, divided into two long independent plates, slightly stout, asymmetrical, with dense long setae. Sternum VII longer than VIII.

Dimensions (in mm): Male: body length 3.82, width 2.03; head length 0.43, width 1.35; eye length 0.50, diameter of eyes 0.25, interocular space 0.58; interocellar space 0.28; antennae length, segment I ?, II ?, III ?, IV 0.32; rostrum length 0.46, segment I 0.08, II 0.13, III 0.14, IV 0.11; pronotum length 0.70, width 1.65; scutellum length 0.58, width 0.77; hemelytron length 2.61, width 1.27; clavus length 1.45 width 0.38; abdomen width 1.76; length of foreleg: femur 0.61, tibia 0.52, tarsi 0.30 (I 0.09, II 0.21), claw 0.12; length of midleg: femur 0.94, tibia 0.70, tarsi 0.33 (I 0.08, II 0.25), claw 0.12; length of hindleg: femur 1.11, tibia 1.48, tarsi 0.82 (I 0.11, II 0.39, III 0.32), claw 0.15.

DATA AVAILABILITY STATEMENT

The datasets presented in this study can be found online at Zoobank.org [https://zoobank.org] with the below accession number(s). *Arcochterus* Zhang, Ren and Yao; 8D0187BE-8202-4320-89AF-35B312A67381; *Arcochterus fuscus* Zhang, Ren and Yao; 85E72289-7F18-4479-9620-1F3A18B1ED0A; *Parvochterus* Zhang, Ren and Yao; FE840D9F-2F7B-46B3-A1A6-2FC2084C5EB8; *Parvochterus lanceolarus* Zhang, Ren and Yao; 19E8C1CB-3C96-4BE7-9FBF-30EC7A945467; *Parvochterus reticulatus* Zhang, Ren and Yao; 4B8B8279-E101-4516-AEE8-E331BC3D75F5.

AUTHOR CONTRIBUTIONS

MZ conceived the study with support from DR and YY. DR and YY provided materials. MZ drew the figures and wrote the draft. ZZ, DR, and YY revised the draft many times. All authors contributed to the article and approved the submitted version.

FUNDING

This research was funded by the National Natural Science Foundation of China (Nos. 31970436, 31730087, 32101239, and 32020103006), Joint Fund of the Beijing Municipal Natural Science Foundation and Beijing Municipal Education Commission (KZ201810028046), and Central Public-interest Scientific Institution Basal Research Fund, CAFS (No. 2020TD11).

ACKNOWLEDGMENTS

We are grateful to the editor and reviewers for constructive criticism and valuable comments on the manuscript.

REFERENCES

Andersen, N. M., and Weir, T. A. (2004). *Australian water bugs. Their biology and identification (Hemiptera-Heteroptera, Gerromorpha & Nepomorpha).* Collingwood, CAN: Apollo Books, doi: 10.1163/187631204788920185

Champion, G. C. (1901). "*Insecta* Rhynchota. *Hemiptera-Heteroptera*, Vol II," in *Biologia Centrali-Americana: Zoology, Botany and Archaeology*, eds F. D. Godman and O. Salvin (London, UK: Taylor & Francis), 345–416.

Chen, P. P., Nieser, N., and Zettel, H. (2005). *The aquatic and semi-aquatic bugs (Heteroptera: Nepomorpha & Gerromorpha) of Malesia*. Leiden-Boston, NL: Brill Academic Publishers, doi: 10.1163/9789047416807

Drake, C. J., and Gómez-Menor, J. (1954). A new genus of American Ochteridae (*Hemiptera*). *Eos Rev. Española de Entomol.* 30, 157–159.

Du, S. L., Hu, Z. K., Yao, Y. Z., and Ren, D. (2019). New genus and species of the Yuripopovinidae (*Pentatomomorpha*: *Coreoidea*) from mid-Cretaceous Burmese amber. *Cretac. Res.* 94, 141–146. doi: 10.1016/j.cretres.2018.10.022

Estévez, A. L., and Ruf, M. (2006). Separación de subfamilias en la familia de chinches Gelastocoridae (*Hemiptera*). *Rev. Biol. Trop.* 54, 1319–1322. doi: 10.15517/rbt.v54i4.3107

Faúndez, E. I., and Ashworth, A. C. (2015). Notas sobre la familia Gelastocoridae (*Hemiptera*: *Heteroptera*) en el extremo sur de Chile, con descripción de un subgénero y especie nuevos. *An. Inst. Patagon.* 43, 69–74. doi: 10.4067/S0718-686X2015000200005

Goloboff, P. A. (1999). *NONA (No Name), Version 2.0. Program and Documentation*. Tucumán, Argentina: Fundación Instituto Miguel Lillo.

Goloboff, P. A., and Catalano, S. A. (2016). TNT version 1.5, including a full implementation of phylogenetic morphometrics. *Cladistics* 32, 221–238. doi: 10.1111/cla.12160

Grimaldi, D., and Engel, M. S. (2005). *Evolution of the Insects*. New York, USA: Cambridge University Press.

Hebsgaard, M. B., Andersen, N. M., and Damgaard, J. (2004). Phylogeny of the true water bugs (*Nepomorpha*: *Hemiptera-Heteroptera*) based on 16S and 28S rDNA and morphology. *Syst. Entomol.* 29, 488–508. doi: 10.1111/j.0307-6970.2004.00254.x

Henry, T. J. (1997). Phylogenetic analysis of family groups within the infraorder Pentatomomorpha (Hemiptera: Heteroptera), with emphasis on the Lygaeoidea. *Ann. Entomol. Soc. Am*. 90, 275–301.

Jaczewski, T. (1934). Notes on the Old World species of Ochteridae (*Heteroptera*). *Ann. Mag. Nat. Hist.* 10, 597–613. doi: 10.1080/00222933408654862

Kirkaldy, G. W. (1897). Synonymic notes on aquatic Rhynchota. *Entomologist* 30, 258–260.

Kirkaldy, G. W. (1906). List of the pagiopodous *Hemiptera-Heteroptera*, with their type species, from 1758 to 1904 (and also of the aquatic and semi-aquatic Trochalopoda). *Acta Ent. Mus. Nat. Pra.* 32, 117–156.

Kment, P., Carapezza, A., and Jindra, Z. (2020). Taxonomic catalogue of the family Ochteridae with description of *Ochterus papaceki* sp. nov. from Socotra Island and Tanzania (*Hemiptera*: *Heteroptera*). *Acta Ent. Mus. Nat. Pra.* 60, 23–64. doi: 10.37520/aemnp.2020.003

La Rivers, I. (1971). Studies of Naucoridae (*Hemiptera*). *Biol. Soc. Nevada Mem.* 2, 1–120.

Latreille, P. A. (1807). *Genera Crustaceorum Et Insectorum Secundem Ordinem Naturalem In Familias Disposita Iconibus Exemplisque Plurimis Explicata*. France: Apud Amand Kænig.

Latreille, P. A. (1810). *Considérations Générals sur I'ordre Naturel des Animaux. Composant les Classes des Crustacés, des Arachnides, et des Insectes*. Paris: F. Schoell.

Li, M., Wang, J., Tian, X. X., Xie, Q., Liu, H. X., and Bu, W. J. (2012). Phylogeny of the true water bugs (*Hemiptera-Heteroptera*: *Nepomorpha*) based on four Hox genes. *Entomotaxonomia* 34, 35–44.

Li, S., Wang, Q. Z., Ren, D., and Yao, Y. Z. (2020). New genus and species of Empheriidae (*Psocodea*: *Trogiomorpha*) from mid Cretaceous amber of northern Myanmar. *Cretac. Res.* 110:104421. doi: 10.1016/j.cretres.2020.104421

Li, T., Hua, J. M., Wright, A. M., Cui, Y., Xie, Q., Bu, W. J., et al. (2014). Long-branch attraction and the phylogeny of true water bugs (*Hemiptera*: *Nepomorpha*) as estimated from mitochondrial genomes. *BMC Evo. Biol.* 14:99. doi: 10.1186/1471-2148-14-99

Maddison, W. P., and Maddison, D. R. (2021). *Mesquite: a modular system for evolutionary analysis. Version 3.70*. Available Online at: http://www.mesquiteproject.org/ (accessed Aug 31, 2021).

Mahner, M. (1993). Systema cryptoceratorum phylogeneticum (*Insecta*, *Heteroptera*). *Zoologica* 143:302.

Nixon, K. C. (2002). *WinClada ver. 1.00.08*. Available Online at: http://www.cladistics.com/ (accessed Apr 11, 2009).

Page, R. D. M. (2001). *NDE: NEXUS Data Editor 0.5.0*. Scotland, UK: University of Glasgow.

Poinar, G. O. , and Brown, A. E. (2016). Toad bugs (*Hemiptera*: *Gelastocoridae*) in Myanmar amber. *Cretac. Res.* 63, 39–44. doi: 10.1016/j.cretres.2016.02.013

Polhemus, D. A. (2021). Two new species of *Ocyochterus* (*Heteroptera*: *Ochteridae*) from Ecuador and Panama. *Zootaxa* 4958, 34–44. doi: 10.11646/zootaxa.4958.1.5

Popov, Y. A. (1968). "Origin and main evolutionary trends of Nepomorpha bugs," in *Proceedings of the 13th international Congress of Entomology, Moscow*, Vol. 1. (Leningrad: Nauka), 282–283.

Popov, Y. A., Dolling, W. R., and Whalley, P. E. S. (1994). British Upper Triassic and Lower Jurassic *Heteroptera* and *Coleorrhyncha* (*Insecta*: *Hemiptera*). *Genus* 5, 307–347.

Popov, Y. A., and Heiss, E. (2014a). *Riegerochterus baehri* gen. nov. and spec. nov., the first fossil velvety bug (*Hemiptera*: *Heteroptera*, *Ochteridae*) from Dominican Amber. *Andrias* 20, 185–190.

Popov, Y. A., and Heiss, E. (2014b). *Grimaldinia pronotalis* n. gen., n. sp. from Mid-Cretaceous Burmese Amber (*Hemiptera*: *Heteroptera*, *Leptopodidae*, *Leptosaldinae*). *Zootaxa* 3878, 444–450. doi: 10.11646/zootaxa.3878.5.2

Rieger, C. (1976). Skelett und Muskulatur des Kopfes und Prothorax von *Ochterus marginatus* Latreille. *Zoomorphologie* 83, 109–191. doi: 10.1007/BF00993483

Ruf, M. L., Goodwyn, P. P., and Martins-Neto, R. G. (2005). New *Heteroptera* (*Insecta*) from the Santana Formation, Lower Cretaceous (Northeastern Brazil), with description of a new family and new taxa of *Naucoridae* and *Gelastocoridae*. *Gaea* 1, 68–74.

Say, T. (1832). *Descriptions of new species of Heteropterous Hemiptera of North America Dec. 1831:(Annual report of New-York state agricultural society)*. New Harmony, Ind: Erscheinungsort nicht ermittelbar.

Schuh, R. T., and Weirauch, C. (2020). *True bugs of the World (Hemiptera: Heteroptera) Classification and Natural history*, 2nd Edn. Manchester, UK: Siri Scientific Press.

Shcherbakov, D. E., and Popov, Y. A. (2002). "Superorder Cimicidea Laicharting, 1781. Order *Hemiptera* Linné, 1758. The bugs, cicadas, plantlice, scale insects, etc," in *History of Insects*, eds A. P. Rasnitsyn and D. L. J. Quicke (Dordrecht, NL: Kluwer Academic Publishers), 143–157.

Stål, C. (1856). *Hemiptera* från Kafferlandet. *Ofversigt af Kongliga Svenska Vetenskaps-Akademiens Förhandlingar* 12, 89–100.

Wang, Y., Moreira, F. F. F., Rédei, D., Chen, P. P., Kuechler, S. M., Luo, J. Y., et al. (2021). Diversification of true water bugs reveled by transcriptome-based phylogenomics. *Syst. Entomol.* 46, 339–356. doi: 10.1111/syen.12465

Wang, Y. J., Du, S. L., Yao, Y. Z., and Ren, D. (2019). A new genus and species of burrower bugs (*Heteroptera*: *Cydnidae*) from the mid-Cretaceous Burmese amber. *Zootaxa* 4585, 351–359. doi: 10.11646/zootaxa.4585.2.8

Xie, T. Y., and Liu, G. Q. (2018). Notes on some toad bugs from china (*Hemiptera*, *Heteroptera*, *Gelastocoridae*). *Zookeys* 759, 137–147. doi: 10.3897/zookeys.759.21627

Yao, Y. Z., Cai, W. Z., and Ren, D. (2007). *Pristinochterus* gen. n. (*Hemiptera*: *Ochteridae*) from the Upper Mesozoic of northeastern China. *Eur. J. Entomol.* 104, 827–835. doi: 10.14411/eje.2007.103

Yao, Y. Z., Zhang, W. T., Ren, D., and Shih, C. K. (2011). New fossil Ochteridae (*Hemiptera*: *Heteroptera*: *Ochteroidea*) from the Upper Mesozoic of northeastern China, with phylogeny of the family. *Syst. Entomol.* 36, 589–600. doi: 10.1111/j.1365-3113.2011.00578.x

Ye, Z., Damgaard, J., Yang, H. H., Hebsgaard, M. B., Weir, T., and Bu, W. J. (2020). Phylogeny and diversification of the true water bugs (*Insecta*: *Hemiptera*: *Heteroptera*: *Nepomorpha*). *Cladistics* 36, 72–87. doi: 10.1111/cla.12383

Zhang, X., Ren, D., and Yao, Y. Z. (2018). A new genus and species of Mimarachnidae (*Hemiptera*: *Fulgoromorpha*: *Fulgoroidea*) from mid-Cretaceous Burmese amber. *Cretac. Res.* 90, 168–173. doi: 10.1016/j.cretres.2018.04.012

Conflict of Interest: The authors declare that the research was conducted in the absence of any commercial or financial relationships that could be construed as a potential conflict of interest.

APPENDIX

Appendix 1 Character states.

A description of the 32 morphological characters compiled from literature sources.

1. Clypeus: (0) not so modified; (1) divided by a cross fold (Hebsgaard et al., 2004). State 1 occurs only in Ochteridae and Gelastocoridae.
2. Clypeus: (0) without such pattern; (1) with pattern of ridges (Hebsgaard et al., 2004). State 1 occurs only in Ochteridae.
3. Frontal plate produced above base of rostrum: (0) slightly; (1) strongly (Yao et al., 2011). All of the Mesozoic fossils with broad frontal plate, sides subparallel.
4. Clypeus: (0) not transversely rugose; (1) distinctly transversely rugose (Yao et al., 2011). The transversely rugose clypeus is relatively common in all extant Ochteridae. In all fossil taxa and outgroup, this trait only occurs in *Angulochterus*.
5. Antennae: (0) short, not visible from above; (1) short, visible dorsally, projecting; (2) long (Hebsgaard et al., 2004; Yao et al., 2011). Antennal apex visible in dorsal is only found in Ochteridae.
6. Antennal segment IV: (0) normal; (1) broad (Hebsgaard et al., 2004). Antennal segment IV broad occurs only in Gelastocoridae.
7. Eye: (0) without eyestalk; (1) reniform, with distinct eyestalk; (2) ellipse, with small eyestalk (Henry, 1997). Eye without eyestalk occurs only in the Early Cretaceous species, the remaining Ochteridae with eyestalk, but the mid-Cretaceous Ochteridae with small eyestalk and eye ellipse, the extent Ochteridae and *Riegerochterus baehri* with distinct eyestalk.
8. Ocelli: (0) absent; (1) present (Hebsgaard et al., 2004). Ocelli absence occurs in the outgroup and the Early Cretaceous Ochteridae.
9. Head and prothorax: (0) tight junction; (1) discretely (Hebsgaard et al., 2004). Head and prothorax tight junction occur only in the outgroup.
10. Eye outer margin exceeding pronotal costal margin: (0) not obvious; (1) distinct. Eye outer margin exceeding pronotal costal margin is only found in the mid-Cretaceous Ochteridae.
11. Pronotum: (0) with transverse sulcus; (1) without transverse sulcus (Yao et al., 2011). The pronotum with transverse sulcus is the common condition in the outgroup and is also found in all extant Ochteridae. Whereas transverse sulci are absent in all fossil taxa.
12. Pronotum: (0) with spots; (1) without spots (Yao et al., 2011). In the extent and the mid-Cretaceous Ochteridae, spots on the Pronotum can be treated as being different between species.
13. Propleuron: (0) developed; (1) simple (Hebsgaard et al., 2004). Propleuron undeveloped occurs in the Ochteridae and Gelastocoridae.
14. Scutellum: (0) without spots; (1) with spots (Yao et al., 2011). Only *Floricaudus multilocellus*, *Parvochterus reticulatus* gen. et sp. nov., and *P. lanceolarus* gen. et sp. nov., spots on the Scutellum can be treated as being different from other species.
15. Clavus: (0) broad; (1) normal. The broad clavus occurs only in the mid-Cretaceous Ochteridae.
16. Forewing: (0) with thorny fields (“Dornfelder”); (1) without thorny fields (Hebsgaard et al., 2004). Forewing with thorny fields occurs only in the Belostomatidae.
17. Forewing: (0) with spots; (1) without spots (Yao et al., 2011). Forewing without spots is usually found in the outgroup, *Ocyochterus victor*, *Riegerochterus baehri*, *Grimaldinia pronotalis* and *Parvochterus* gen. nov. have some different pattern spots on the forewings.
18. Costal fracture: (0) absent; (1) present (Yao et al., 2011). Forewing with distinct costal fracture is a very stable character in extant velvety shore bugs.
19. Surface of thorax and forewings: (0) smooth; (1) with wartlike sculpturation (Hebsgaard et al., 2004). Surface of thorax and fore wings with wartlike sculpturation occurs only in the Gelastocoridae.
20. Rostrum: (0) inserted distally on head; (1) inserted posteriorly on head (Hebsgaard et al., 2004). Rostrum inserted distally on head occurs only in the *Gelastocoris*.
21. Rostrum: (0) short, only reaching beyond procoxae; (1) extending beyond procoxae, but never extended beyond metacoxae; (2) generally extended beyond metacoxae (Yao et al., 2011). The short rostrum occurs in the mid-Cretaceous Ochterids and outgroup, which is assigned as a plesiomorphy. State 1 occurs only in Early Cretaceous fossils. State 2 occurs in all extant Ochteridae and *Riegerochterus*.
22. Forelegs: (0) raptorial; (1) cursorial (Hebsgaard et al., 2004; Yao et al., 2011). Raptorial forelegs are only found in the outgroup and Gelastocoridae.
23. Protarsus and protibia: (0) fused; (1) normal (Schuh and Weirauch, 2020: ha 24). Foretarsus and foretibia fused are found in the Naucoridae and *Nerthra*.
24. Metacoxae: (0) conical, firmly united with metapleuron; (1) short, free (Hebsgaard et al., 2004). Metacoxae conical and firmly united with metapleuron occur in the Belostomatidae.
25. Metatibia: (0) flattened, with swimming hairs; (1) simple (Hebsgaard et al., 2004). Hind tibiae flattened with swimming hairs occurs in the Belostomatidae.

26. Tarsal formula: (0) 2:3:3; (1) different (Yao et al., 2011). Naucoridae and Belostomatidae with 2-3-3 tarsal formula.
27. Tarsal formula: (0) 1:2:3; (1) different (Yao et al., 2011). Gelastocoridae with 1-2-3 tarsal formula.
28. Tarsal formula: (0) 2:2:3; (1) different (Yao et al., 2011). Ochteridae with 2-2-3 tarsal formula.
29. Distal sternum VII in males: (0) symmetrical; (1) asymmetrical (Yao et al., 2011). Asymmetry of distal segment VII in males is found in all extant Ochteridae and Gelastocoridae. In our fossils, we found mid-Cretaceous Ochteridae with this character.
30. Sternum VIII in males: (0) undivided; (1) split into two lobes (Yao et al., 2011). Sternum VIII undivided in males is only found in the outgroup.
31. Respiratory siphon: (0) present; (1) absent (Hebsgaard et al., 2004; Yao et al., 2011). The respiratory siphon only occurs in Belostoma.
32. Body length: (0) over 7 mm; (1) less than 7 mm (Yao et al., 2011). The body length over 7 mm is only found in all extinct Ochteridae from Early Cretaceous and extant *Megochterus*. The longer bodies in the Early Cretaceous are the same as the outgroup taxa, as a plesiomorphy in Ochteri dae.

frontiers | Frontiers in Ecology and Evolution

ORIGINAL RESEARCH
published: 22 June 2022
doi: 10.3389/fevo.2022.911512

The First Fossil of Nossidiinae From Mid-Cretaceous Amber of Northern Myanmar (Coleoptera: Ptiliidae)

*Yan-Da Li[1,2], Alfred F. Newton[3], Di-Ying Huang[1] and Chen-Yang Cai[1,2]**

[1] State Key Laboratory of Palaeobiology and Stratigraphy, Center for Excellence in Life and Paleoenvironment, Nanjing Institute of Geology and Palaeontology, Chinese Academy of Sciences, Nanjing, China, [2] School of Earth Sciences, University of Bristol, Bristol, United Kingdom, [3] Negaunee Integrative Research Center, Field Museum of Natural History, Chicago, IL, United States

Ptiliidae is a group of distinctly miniaturized staphylinoid beetles with a scarce fossil record. Here, we report a new ptiliid genus and species, *Crenossidium slipinskii* Li, Newton and Cai **gen. et sp. nov.**, from mid-Cretaceous amber from northern Myanmar. *Crenossidium* can be attributed to the subfamily Nossidiinae based on the hind wing morphology, which has also been confirmed through phylogenetic analyses. *Crenossidium* differs from other extant nossidiine genera in the combination of the wide apical maxillary palpomeres, posteriorly widest pronotal disk, (almost) contiguous procoxae, fewer setae along wing margin, and multidentate pygidium.

urn:lsid:zoobank.org:pub:8038D763-6856-4AC5-972C-E20D636137EE.

Keywords: Ptiliidae, fossil, Burmese amber, Mesozoic, phylogeny

OPEN ACCESS

Edited by:
Li Tian,
China University of Geosciences
Wuhan, China

Reviewed by:
Alexey Polilov,
Lomonosov Moscow State University, Russia
Michael Darby,
Natural History Museum, United Kingdom
Andrei Legalov,
Institute of Systematics and Ecology of Animals (RAS), Russia

****Correspondence:***
Chen-Yang Cai
cycai@nigpas.ac.cn

Specialty section:
This article was submitted to Paleontology, a section of the journal Frontiers in Ecology and Evolution

Received: *02 April 2022*
Accepted: *09 May 2022*
Published: *22 June 2022*

Citation:
Li Y-D, Newton AF, Huang D-Y and Cai C-Y (2022) The First Fossil of Nossidiinae From Mid-Cretaceous Amber of Northern Myanmar (Coleoptera: Ptiliidae). Front. Ecol. Evol. 10:911512. doi: 10.3389/fevo.2022.911512

INTRODUCTION

The family Ptiliidae is a cosmopolitan beetle group in Staphylinoidea. The number of described ptiliid species increased fast in the past several years (e.g., 77 new species of *Cissidium* Motschulsky in a single article: Darby, 2020). Currently, there are 1,015 valid species known (Newton, 2019, updated by A.F. Newton through March 2022). Ptiliidae is well-known for their minute body size. The smallest member of this family, which is also the smallest beetle and the smallest free-living insect, *Scydosella musawasensis* Hall, has an adult body length of 325 μm (Polilov, 2015). Even the largest members do not exceed 3 mm in length (Polilov, 2016). The adults of Ptiliidae are distinctively characterized by their feather-like hind wings (Polilov et al., 2019a; Petrov et al., 2020), which are effectively adapted for flight under miniaturization (Farisenkov et al., 2022).

The sister relationship between Ptiliidae and Hydraenidae has long been recognized, supported by multiple lines of morphological and molecular evidence (e.g., Beutel and Leschen, 2005; Lawrence et al., 2011; Mckenna et al., 2015). Their relationship with other staphylinoids has also become rather certain based on several recent phylogenomic studies (Zhang et al., 2018; McKenna et al., 2019; Cai et al., 2022). However, the internal relationships within Ptiliidae are much less clear. The subfamily Nossidiinae, now considered as the deepest branch in Ptiliidae, was formally established only in 2019, based initially on larval characters (Sörensson and Delgado, 2019) and quickly confirmed by adult characters plus molecular data (Polilov et al., 2019b). In the most recent version of the Handbook of Zoology (Hall, 2016), three subfamilies were recognized (Acrotrichinae, Cephaloplectinae, and Ptiliinae). However, based on new phylogenetic analyses, Polilov et al. (2019b) placed all the groups except Nossidiinae (originally in Ptiliinae) in the subfamily Ptiliinae. Seven tribes were recognized within Ptiliinae by Polilov et al. (2019b), although

Ptiliini and Discheramocephalini were still likely to be paraphyletic, and the inclusion of Ptenidiini in Ptiliinae was not fully confirmed (Polilov et al., 2019b: Figure 8).

The fossil record of Ptiliidae is very scarce. A few members have been reported from various Cenozoic deposits, although all of them were either placed in extant genera or not determined to the generic level (e.g., Polilov and Perkovsky, 2004; Shockley and Greenwalt, 2013). The only described Mesozoic fossil (*Kekveus jason* Yamamoto et al.) comes from the mid-Cretaceous Burmese amber (Yamamoto et al., 2018). Kirejtshuk and Azar (2013) additionally mentioned three undescribed specimens from the Early Cretaceous Lebanese amber. In this study, we describe the second member of Ptiliidae from Burmese amber, which also represents the first fossil of the subfamily Nossidiinae.

MATERIALS AND METHODS

Materials

The Burmese amber specimen studied herein (**Figures 1–4**) originated from amber mines near Noije Bum (26°20' N, 96°36' E), Hukawng Valley, Kachin State, northern Myanmar. Zircon U-Pb dating has suggested an age of ∼99 Ma for the amber-producing strata (Shi et al., 2012), although Mao et al. (2018) suggested that it might be slightly younger than the actual age. Based on the biota of Burmese amber, the Burma Terrane, where the amber mines are located, has been suggested to have a Gondwanan origin (Poinar, 2019). During the mid-Cretaceous, the Burma Terrane was probably an isolated island at near-equatorial latitude based on paleomagnetic evidence (Westerweel et al., 2019).

The specimen is deposited in the Nanjing Institute of Geology and Paleontology (NIGP), Chinese Academy of Sciences, Nanjing, China. The amber piece was trimmed with a small table saw, ground with emery papers of different grit sizes, and finally polished with polishing powder.

Fossil Imaging

Brightfield images were taken with a Zeiss Discovery V20 stereomicroscope. Confocal images were obtained with a Zeiss LSM710 confocal laser scanning microscope, using the 488 nm Argon laser excitation line (Fu et al., 2021). Brightfield images were stacked with Helicon Focus 7.0.2 and Adobe Photoshop CC. Confocal images were stacked with color-coding for depth in ZEN 3.4 (Blue Edition), or semi-manually stacked in Helicon Focus 7.0.2 and Adobe Photoshop CC. Microtomographic data were obtained with a Zeiss Xradia 520 Versa 3D X-ray microscope at the micro-CT laboratory of NIGP and analyzed in VGStudio MAX 3.0. Scanning parameters were as follows: isotropic voxel size, 1.7807 μm; power, 3 W; acceleration voltage, 40 kV; exposure time, 6 s; projections, 3001. Images were further processed in Adobe Photoshop CC to adjust brightness and contrast.

Phylogenetic Analyses

To evaluate the systematic placement of the new species, constrained morphological phylogenetic analyses were performed under Bayesian inference and weighted parsimony. The data matrix (**Supplementary Data 1**, **2**) was mainly derived from a previously published dataset (Polilov et al., 2019b). The vein CuA (character 54) was originally coded as absent for *Nossidium* Erichson, *Motschulskium* Matthews and *Sindosium* Johnson by Polilov et al. (2019b), but according to Polilov et al. (2019a), the posterior vein in the petiole of these species was interpreted as CuA. Thus, the coding of this character was amended accordingly in our analyses. The Bayesian molecular tree (their Figures 8 and S9) by Polilov et al. (2019b) was used as the constraining backbone tree. For taxa with both morphological and molecular data, their interrelationships were fixed according to the molecular tree. The fossil and other extant taxa without molecular data were allowed to move freely across the reference tree (e.g., Fikáček et al., 2020).

The Bayesian analysis was performed using MrBayes 3.2.6 (Ronquist et al., 2012). Two Markov chain Monte Carlo (MCMC) analyses were run simultaneously, each with one cold chain and three heated chains. Trees were sampled every 1,000 generations. Analyses were stopped when the average standard deviation (SD) of split frequencies remained below 0.01. The first 25% of sampled trees were discarded as burn-in, and the remains were used to build a majority-rule consensus tree.

The parsimony analysis was performed under implied weights with R 4.1.0 (R Core Team, 2021) and the R package TreeSearch 1.0.1 (Smith, 2021). Parsimony analyses achieve the highest accuracy under a moderate weighting scheme (i.e., when concavity constants, *K*, are between 5 and 20) (Goloboff et al., 2018; Smith, 2019). Therefore, the concavity constant was set to 12 here, as suggested by Goloboff et al. (2018).

The trees were drawn with the online tool iTOL 6.5.2 (Letunic and Bork, 2021) and graphically edited with Adobe Illustrator CC 2017.

SYSTEMATIC PALEONTOLOGY

Order Coleoptera Linnaeus, 1758
Suborder Polyphaga Emery, 1886
Superfamily Staphylinoidea Latreille, 1802
Family Ptiliidae Erichson, 1845
Subfamily Nossidiinae Sörensson and Delgado, 2019

Genus *Crenossidium* Li, Newton and Cai gen. nov.

Type-Species

Crenossidium slipinskii **sp. nov.**

Etymology

The generic name is a combination of "Cretaceous" and "*Nossidium*", the type genus of Nossidiinae. The name is neuter in gender.

Diagnosis

Hind wings with comparatively wide wing blade; petiole with two veins; wing margin with fewer than 130 setae; anterior edge of petiole almost without setae; posterior edge of petiole with setae (**Figures 1C,D**). Maxillary palpomere 4 more than half as wide at base as palpomere 3 (**Figure 3C**). Pronotum

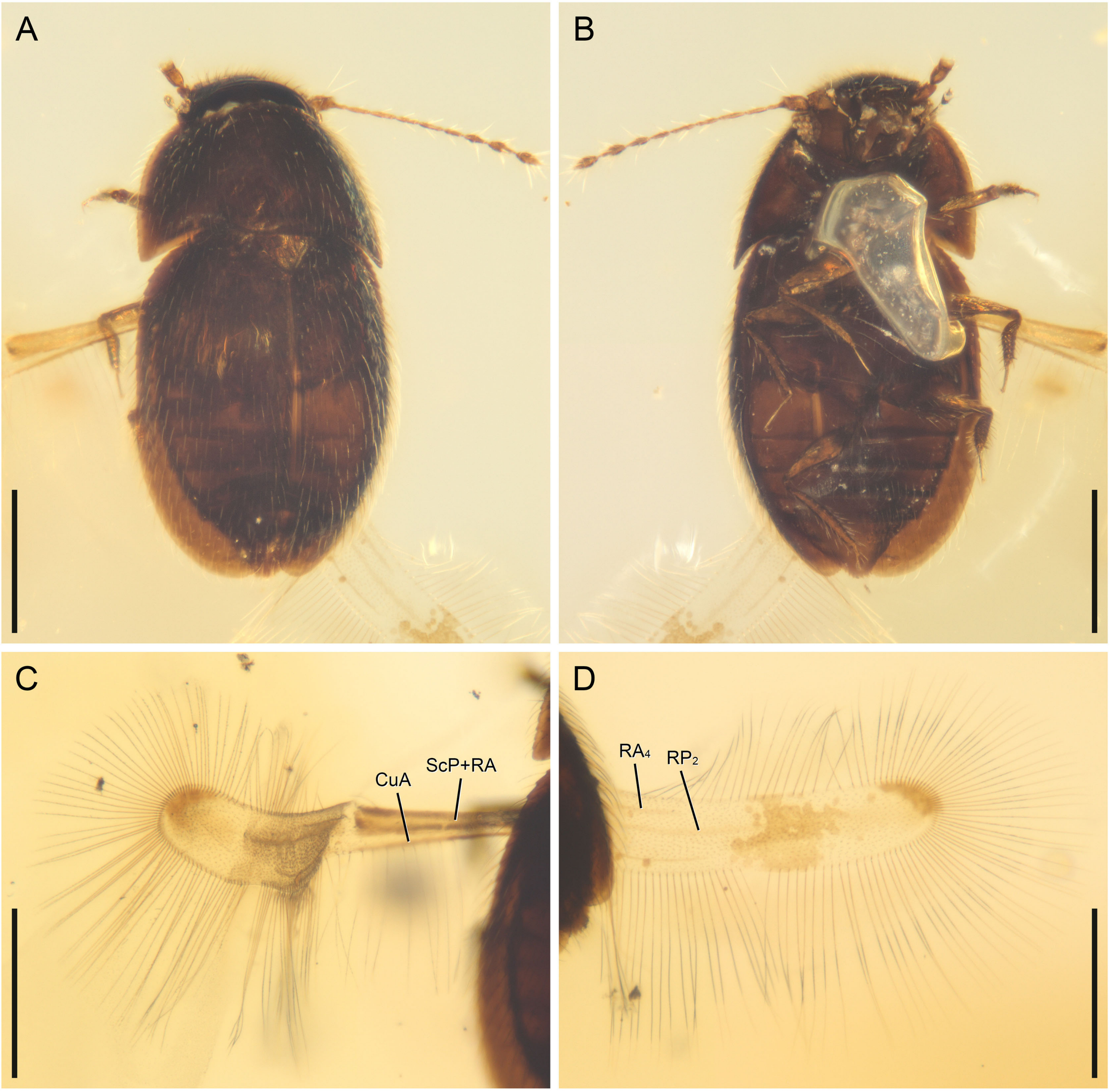

FIGURE 1 | *Crenossidium slipinskii* Li, Newton and Cai **gen. et sp. nov.**, holotype, NIGP180053, under incident or transmitted light. **(A)** Habitus, dorsal view. **(B)** Habitus, ventral view. **(C)** Left hind wing, dorsal view. **(D)** Right hind wing, dorsal view. Scale bars: 200 µm.

widest basally (**Figure 4A**). Prosternal process narrow; procoxae (almost) touching (**Figure 4B**). Pygidium apically multidentate (**Figure 3D**).

Crenossidium slipinskii Li, Newton and Cai sp. nov.

Material

Holotype, NIGP180053 (**Figures 1–4**), mid-Cretaceous (upper Albian to lower Cenomanian; Shi et al., 2012; Mao et al., 2018) from amber mine near Noije Bum Village, Tanai Township, Myitkyina District, Kachin State, Myanmar.

Etymology

The species is named after Dr. Stanisław Adam Ślipiński, an internationally recognized coleopterist.

Diagnosis

As for the genus.

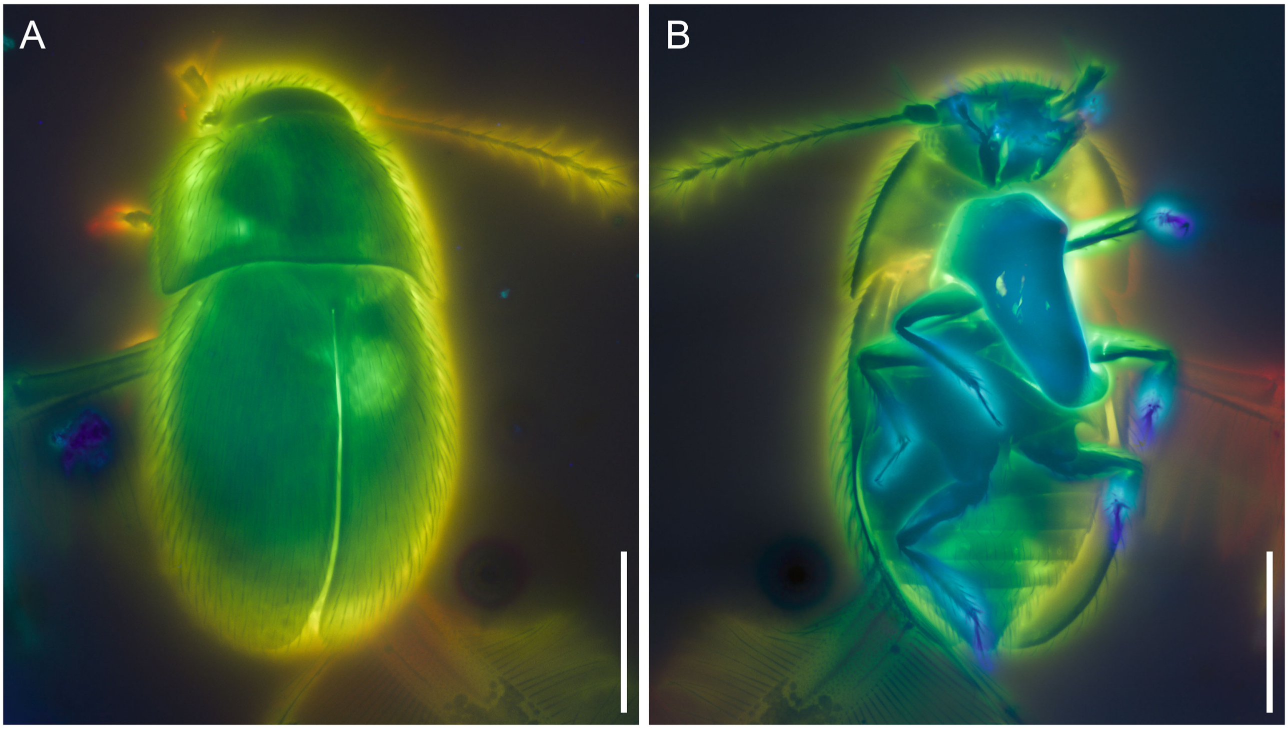

FIGURE 2 | *Crenossidium slipinskii* Li, Newton and Cai **gen. et sp. nov.**, holotype, NIGP180053, under confocal microscopy, with depth color coding. **(A)** Dorsal view. **(B)** Ventral view. Scale bars: 200 μm.

Description

Body small, about 0.69 mm long and 0.35 mm wide.

Head with vertex somewhat declined. Compound eyes well-developed. Antennal grooves absent. Antennae 11-segmented, generally filiform; antennomeres 1–2 moderately enlarged; antennomeres 3–8 slender and elongate, with similar width; antennomeres 9–11 forming a loose club; antennomere 9 about 1.5× as wide as 8; antennomeres 10–11 about twice as wide as 8. Mandibles distinctly retracted. Maxillary palps 4-segmented; palpomere 3 thicker than other segments, oval; palpomere 4 aciculate, more than half as wide at base as palpomere 3. Mentum rectangular, with subparallel sides.

Pronotal disk widest basally, gradually narrowed anteriorly; lateral edges convex, weakly serrate; posterior angles moderately produced posteriorly; surface smooth, without clear elevations or impressions. Prosternal process probably narrow. Procoxae touching apically.

Scutellar shield triangular. Elytra complete, apically rounded; lateral edges weakly serrate in anterior half; elytral epipleura present only in anterior half. Mesoventrite with a longitudinal keel medially. Metaventrite posteriorly with a bifurcate process between metacoxae. Metacoxae almost contiguous; plates developed proximally.

Legs short and slender. Femora not strongly flattened. Tibiae with relatively dense setae. Tarsi of typical ptiliid type, cylindrical, apparently 2-segmented. Pretarsal claws simple, equal in size.

Hind wings of typical nossidiine type (see Polilov et al., 2019a); wing blade comparatively wide; petiole with two veins (ScP+RA and CuA); wing margin with about 126 setae; anterior edge of petiole with a single seta; posterior edge of petiole with setae.

Abdomen with six ventrites (presumably sternites III–VIII). Hind margin of pygidium (presumably tergite X) with several clearly marked small teeth.

DISCUSSION

Crenossidium **gen. nov.** can be placed in Ptiliidae based on the following characters: antennomere 3 inserted in the apex of antennomere 2 and distinctly narrower than the latter (**Figure 3C**; Yavorskaya et al., 2017: Figure 4), antennal club 3-segmented, apical maxillary palpomere aciculate (**Figure 3C**; Yavorskaya et al., 2017: Figure 2C), and hind wings feather-like (wing blade narrower than the length of setae).

Based on the analysis of Polilov et al. (2019b), Ptiliidae can be divided into two subfamilies, Nossidiinae and Ptiliinae. Nossidiinae contains only four extant genera (Sörensson and Delgado, 2019), and is believed to have retained many "primitive" characters. The hind wing morphology of *Crenossidium* corresponds well with Nossidiinae. They share the presence of two veins in the petiole, edges of petiole with setae, and a comparatively wide wing blade (**Figures 1C,D**; Polilov et al., 2019a: Figures 1A,B, 2B) (petiole with a single vein, edges of

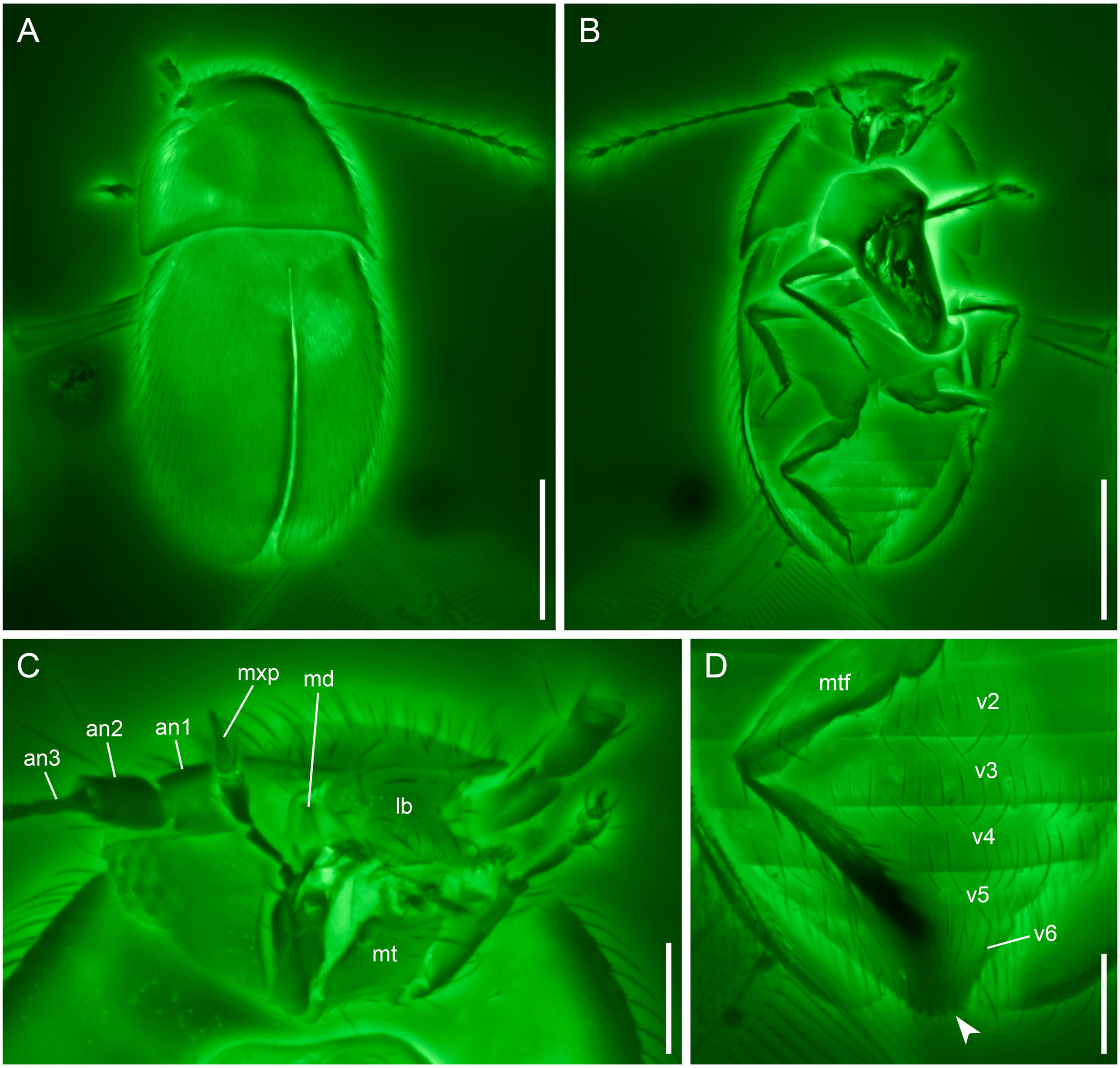

FIGURE 3 | *Crenossidium slipinskii* Li, Newton and Cai **gen. et sp. nov.**, holotype, NIGP180053, under confocal microscopy. **(A)** Habitus, dorsal view. **(B)** Habitus, ventral view. **(C)** Mouthparts, ventral view. **(D)** Abdomen, ventral view, showing the multidentate pygidium (arrowhead). an1–3, antennomeres 1–3; lb, labrum; md, mandible; mt, mentum; mtf, metafemur; mxp, maxillary palp; v1–6, ventrites 1–6. Scale bars: 200 µm in **(A,B)**, 50 µm in **(C,D)**.

petiole without setae, and wing blade narrower than half length of setae in Ptiliinae). The nossidiine affinity of *Crenossidium* is also confirmed through formal phylogenetic analyses (**Figure 5**, **Supplementary Figure 1**).

The accurate position of *Crenossidium* within Nossidiinae is not yet resolved, although it might be sister to all the remaining genera sampled, as suggested by the Bayesian analysis (**Figure 5**). There are fewer than 130 setae along the hind wing margin in *Crenossidium*. By contrast, according to Polilov et al. (2019b), the three extant nossidiine terminals sampled in the analysis have more than 200 setae along the wing margin (although in some species the setae may be somewhat fewer than 200; e.g., Darby, 2016: Figure 4E; Maté Nankervis, 2020: Figure 2F). The anterior margin of the petiole is free of setae in *Crenossidium* and *Sindosium* (actually, with a single seta), while setae are present on this portion in *Nossidium* and *Motschulskium* (Polilov et al., 2019a). *Crenossidium* shares a multidentate pygidium with *Nossidium* (**Figure 3D**; Darby, 2015: Figure 11), whereas the pygidium is bidentate in *Motschulskium* (Hall, 2000: Figure 53.17) and toothless in *Sindosium* and *Bicavella* Johnson (Johnson, 2007). *Crenossidium* differs from *Motschulskium* additionally in pronotum widest basally (widest in the middle

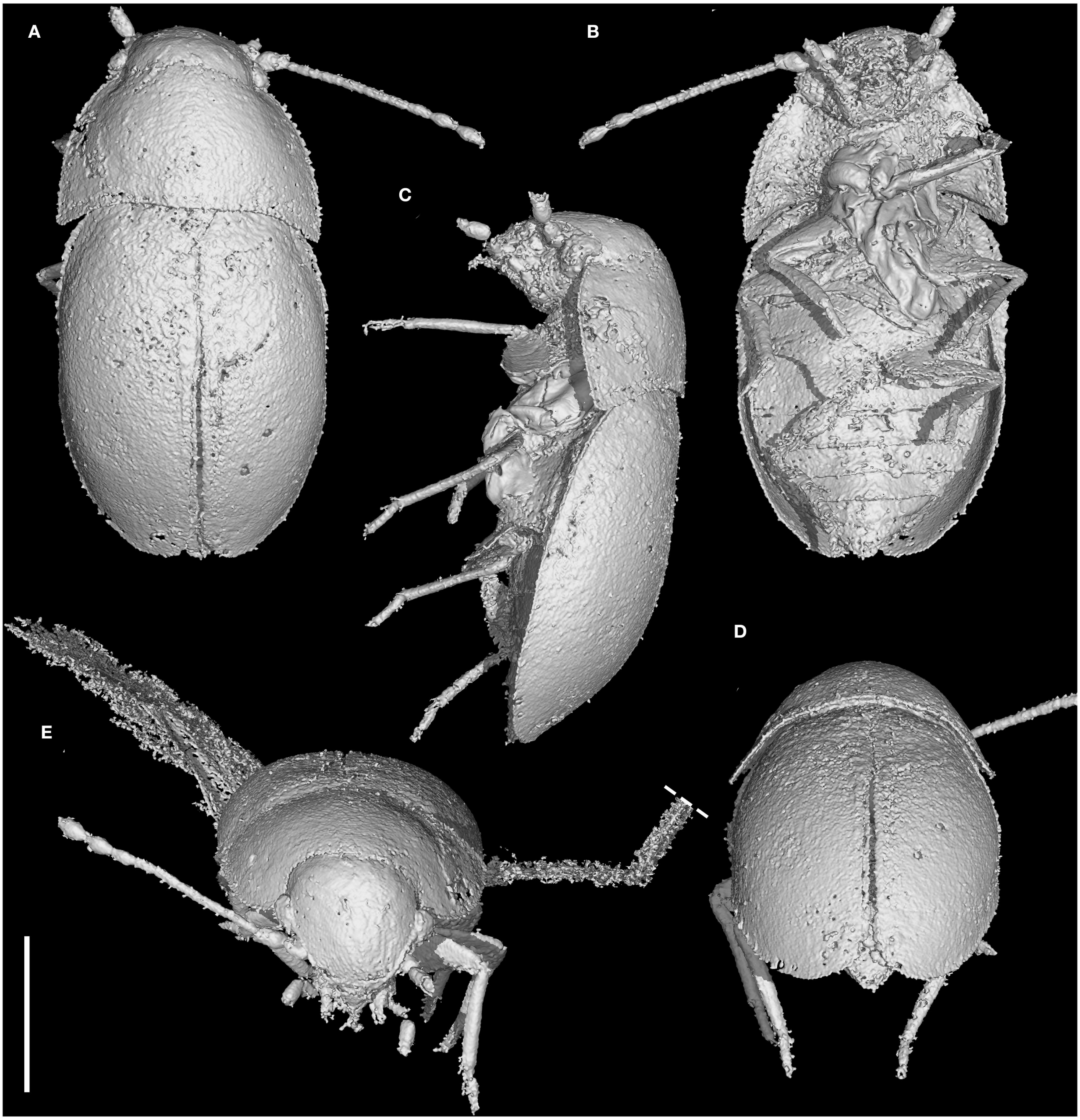

FIGURE 4 | X-ray microtomographic reconstruction of *Crenossidium slipinskii* Li, Newton and Cai **gen. et sp. nov.**, holotype, NIGP180053, with hind wings removed in **(A–D)**. **(A)** Dorsal view. **(B)** Ventral view. **(C)** Lateral view. **(D)** Posterodorsal view. **(E)** Anterodorsal view. Scale bar: 200 μm.

region in *Motschulskium*; Polilov et al., 2019b: Figure S1F). However, *Nossidium* has a moderately wide prosternal process, which clearly separates the procoxae (Polilov et al., 2019b: Figure S1D; though there might be some interspecific variation, A.F. Newton, personal observation), whereas the prosternal process is much narrower with procoxae (almost) touching in *Crenossidium* (**Figure 4B**), as well as in the other three extant genera (Johnson, 2007; Polilov et al., 2019b). *Crenossidium* is distinctive in Ptiliidae by its relatively wide apical maxillary palpomere, which is almost as wide at base as the penultimate one. In most of the modern nossidiines we examined, the palpomere 4 is at most one-third of the maximum width of palpomere 3, and to our knowledge, no modern member in the whole family has maxillary palpomere 4 distinctly wider than the half width of palpomere 3.

The divergence between Ptiliidae and Hydraenidae has been dated to the Early Jurassic, approximately 178–198 Ma (Cai et al., 2022). Therefore, it is reasonable to expect that Ptiliidae

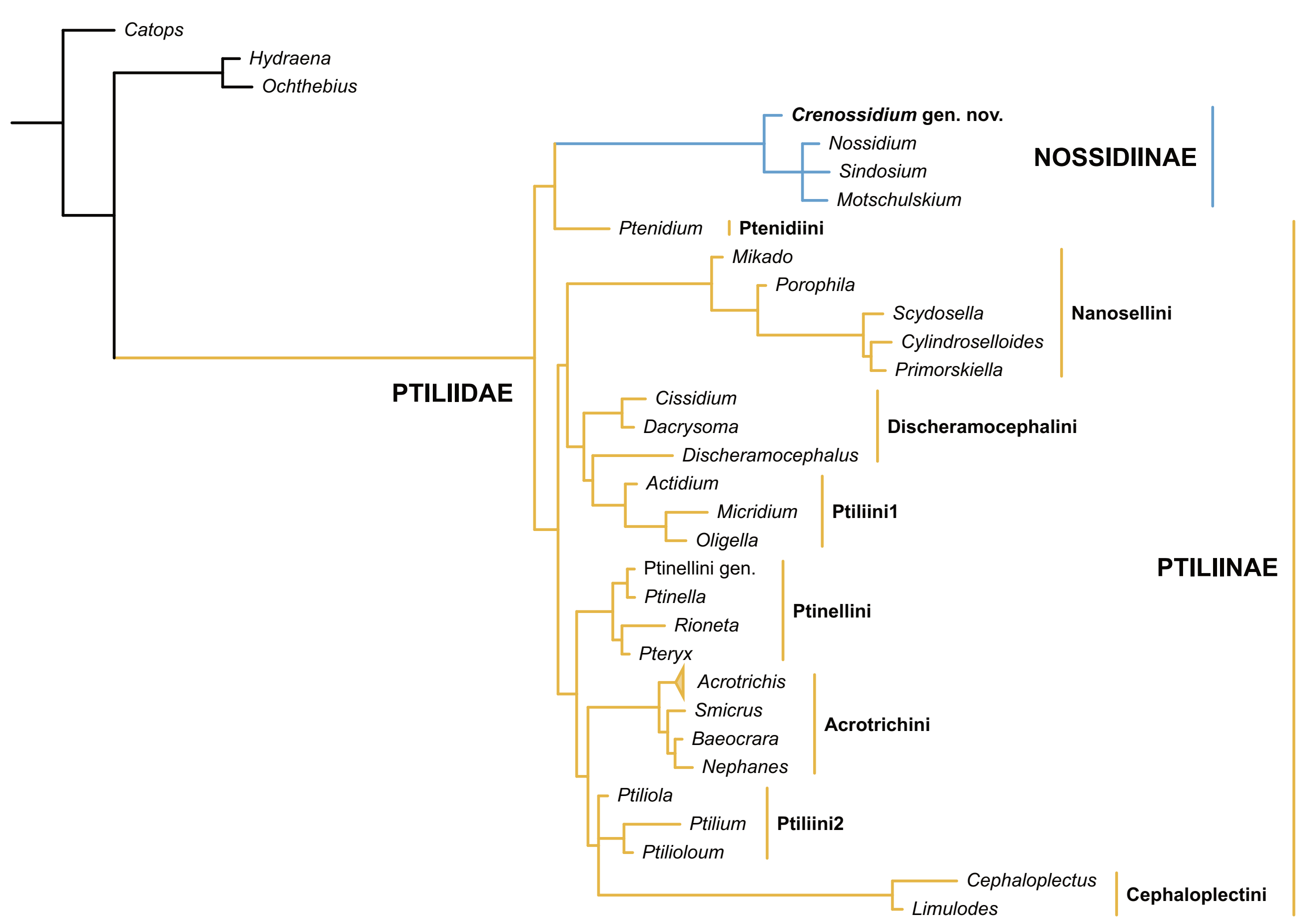

FIGURE 5 | Suggested placement of *Crenossidium slipinskii* Li, Newton and Cai **gen. et sp. nov.** within Ptiliidae. Tree resulting from the Bayesian analysis constrained by a molecular backbone tree.

might have already been highly diversified at least in the late Mesozoic. However, the Mesozoic fossil record of Ptiliidae is extremely scarce. Only one species has been described from Burmese amber before the current study (Yamamoto et al., 2018), with the addition of a few mentioned presences from Lebanese and Burmese ambers (Rasnitsyn and Ross, 2000; Grimaldi et al., 2002; Kirejtshuk and Azar, 2013; though the unproportionally high specimen number of Ptiliidae mentioned by Grimaldi et al., 2002 seems to be dubious). Indeed, miniaturized groups are often insufficiently documented in the fossil record (e.g., Cai et al., 2019). The minute size probably impeded their preservation as adpression fossils. Even if they have been successfully preserved as adpressions, most fossil collectors would not be able to notice them. Thus, it further emphasizes the importance of amber fossils in alleviating the bias against miniaturized taxa.

DATA AVAILABILITY STATEMENT

The original contributions presented in the study are included in the article/**Supplementary Material**. The original micro-CT and confocal data are available in Zenodo repository at https://doi.org/10.5281/zenodo.6527975. Further inquiries can be directed to the corresponding author/s.

AUTHOR CONTRIBUTIONS

C-YC and Y-DL conceived the study. C-YC and D-YH acquired and processed the specimen. Y-DL acquired and processed the photomicrographs, performed the analyses, and drafted the manuscript, to which AFN and C-YC contributed. All authors commented on the manuscript and gave final approval for publication.

FUNDING

Financial support was provided by the Strategic Priority Research Program of the Chinese Academy of Sciences (XDB26000000), the National Natural Science Foundation of China (42072022 and 41688103), and the Second Tibetan Plateau Scientific Expedition and Research project (2019QZKK0706).

ACKNOWLEDGMENTS

We are grateful to Su-Ping Wu for technical help in micro-CT reconstruction, and Rong Huang and Yan Fang for technical help with confocal imaging.

SUPPLEMENTARY MATERIAL

The Supplementary Material for this article can be found online at: https://www.frontiersin.org/articles/10.3389/fevo.2022.911512/full#supplementary-material

REFERENCES

Beutel, R. G., and Leschen, R. A. B. (2005). Phylogenetic analysis of Staphyliniformia (Coleoptera) based on characters of larvae and adults. *Syst. Entomol.* 30, 510–548. doi: 10.1111/j.1365-3113.2005.00293.x

Cai, C., Lawrence, J. F., Yamamoto, S., Leschen, R. A. B., Newton, A. F., Ślipiński, A., et al. (2019). Basal polyphagan beetles in mid-Cretaceous amber from Myanmar: biogeographic implications and long-term morphological stasis. *Proc. R. Soc. B.* 286, 20182175. doi: 10.1098/rspb.2018.2175

Cai, C., Tihelka, E., Giacomelli, M., Lawrence, J. F., Ślipiński, A., Kundrata, R., et al. (2022). Integrated phylogenomics and fossil data illuminate the evolution of beetles. *R. Soc. Open Sci.* 9, 211771. doi: 10.1098/rsos.211771

Darby, M. (2015). *Nossidium katyae*, a new species of Bolivian Ptiliidae (Coleoptera), was described and figured. *Zootaxa.* 4048, 436–440. doi: 10.11646/zootaxa.4048.3.8

Darby, M. (2016). New species and records of Costa Rican featherwing beetles (Coleoptera: Ptiliidae). *Zootaxa.* 4184, 41–51. doi: 10.11646/zootaxa.4184.1.2

Darby, M. (2020). A revision of *Cissidium* Motschulsky (Coleoptera: Ptiliidae) with seventy seven new species. *Eur. J. Taxon.* 622, 1–188. doi: 10.5852/ejt.2020.622

Farisenkov, S. E., Kolomenskiy, D., Petrov, P. N., Engels, T., Lapina, N. A., Lehmann, F. O., et al. (2022). Novel flight style and light wings boost flight performance of tiny beetles. *Nature.* 602, 96–100. doi: 10.1038/s41586-021-04303-7

Fikáček, M., Beutel, R. G., Cai, C., Lawrence, J. F., Newton, A. F., Solodovnikov, A., et al. (2020). Reliable placement of beetle fossils via phylogenetic analyses–Triassic *Leehermania* as a case study (Staphylinidae or Myxophaga?). *Syst. Entomol.* 45, 175–187. doi: 10.1111/syen.12386

Fu, Y.-Z., Li, Y.-D., Su, Y.-T., Cai, C.-Y., and Huang, D.-Y. (2021). Application of confocal laser scanning microscopy to the study of amber bioinclusions. *Palaeoentomology.* 4, 266–278. doi: 10.11646/palaeoentomology.4.3.14

Goloboff, P. A., Torres, A., and Arias, J. S. (2018). Weighted parsimony outperforms other methods of phylogenetic inference under models appropriate for morphology. *Cladistics.* 34, 407–437. doi: 10.1111/cla.12205

Grimaldi, D. A., Engel, M. S., and Nascimbene, P. C. (2002). Fossiliferous Cretaceous amber from Myanmar (Burma): its rediscovery, biotic diversity, and paleontological significance. *Am. Mus. Novit.* 3361, 1–71.

Hall, W. E. (2000). "Ptiliidae Erichson, 1845," in *American Beetles. Vol. 1. Archostemata, Myxophaga, Adephaga, Polyphaga: Staphyliniformia*, eds R. H. Arnett and M. C. Thomas (Boca Raton: CRC Press), 233–246.

Hall, W. E. (2016). "Ptiliidae Erichson, 1845," in *Handbook of Zoology, Arthropoda: Insecta, Coleoptera, beetles, Vol. 1: morphology and systematics (Archostemata, Adephaga, Myxophaga, Polyphaga partim). 2nd Edition*, eds R. G. Beutel and R. A. B. Leschen (Berlin: Walter de Gruyter), 345–356.

Johnson, C. (2007). Studies on Ptiliidae (Col.) from the Solomon Islands, 1. *Entomol. Mon. Mag.* 143, 213–227.

Kirejtshuk, A. G., and Azar, D. (2013). Current knowledge of Coleoptera (Insecta) from the Lower Cretaceous Lebanese amber and taxonomical notes for some Mesozoic groups. *Terr. Arthropod Rev.* 6, 103–134. doi: 10.1163/18749836-06021061

Lawrence, J. F., Ślipiński, A., Seago, A. E., Thayer, M. K., Newton, A. F., and Marvaldi, A. E. (2011). Phylogeny of the Coleoptera based on morphological characters of adults and larvae. *Ann. Zool.* 61, 1–217. doi: 10.3161/000345411X576725

Letunic, I., and Bork, P. (2021). Interactive Tree Of Life (iTOL) v5: an online tool for phylogenetic tree display and annotation. *Nucleic Acids Res.* 49, W293–W296. doi: 10.1093/nar/gkab301

Mao, Y., Liang, K., Su, Y., Li, J., Rao, X., Zhang, H., et al. (2018). Various amberground marine animals on Burmese amber with discussions on its age. *Palaeoentomology.* 1, 91–103. doi: 10.11646/palaeoentomology.1.1.11

Maté Nankervis, J. F. (2020). Description of two new species of *Sindosium* Johnson, 2007 from Australia (Coleoptera, Ptiliidae). *Zootaxa.* 4895, 528–540. doi: 10.11646/zootaxa.4895.4.4

Mckenna, D. D., Farrell, B. D., Caterino, M. S., Farnum, C. W., Hawks, D. C., Maddison, D. R., et al. (2015). Phylogeny and evolution of Staphyliniformia and Scarabaeiformia: forest litter as a stepping stone for diversification of nonphytophagous beetles. *Syst. Entomol.* 40, 35–60. doi: 10.1111/syen.12093

McKenna, D. D., Shin, S., Ahrens, D., Balke, M., Beza-Beza, C., Clarke, D. J., et al. (2019). The evolution and genomic basis of beetle diversity. *Proc. Natl. Acad. Sci. USA.* 116, 24729–24737. doi: 10.1073/pnas.1909655116

Newton, A. F. (2019). "StaphBase: Staphyliniformia world catalog database (version Nov 2018)," in *Catalogue of Life Checklist (Nov 2018)*, eds O. Bánki, Y. Roskov et al. Available online at: https://www.catalogueoflife.org/.

Petrov, P. N., Farisenkov, S. E., and Polilov, A. A. (2020). Miniaturization re-establishes symmetry in the wing folding patterns of featherwing beetles. *Sci. Rep.* 10, 16458. doi: 10.1038/s41598-020-73481-7

Poinar, G. (2019). Burmese amber: Evidence of Gondwanan origin and Cretaceous dispersion. *Hist. Biol.* 31, 1304–1309. doi: 10.1080/08912963.2018.1446531

Polilov, A. A. (2015). How small is the smallest? New record and remeasuring of *Scydosella musawasensis* Hall, 1999 (Coleoptera, Ptiliidae), the smallest known free-living insect. *ZooKeys.* 526, 61–64. doi: 10.3897/zookeys.526.6531

Polilov, A. A. (2016). "Structure of the principal groups of microinsects. III. Featherwing Beetles (Coleoptera: Ptiliidae)," *in At the Size Limit-Effects of Miniaturization in Insects* (Cham: Springer), 77–133. doi: 10.1007/978-3-319-39499-2_5

Polilov, A. A., and Perkovsky, E. E. (2004). New species of Late Eocene feather-winged beetles (Coleoptera, Ptiliidae) from the Rovno and Baltic amber. *Paleontol. J.* 38, 664–668.

Polilov, A. A., Reshetnikova, N. I., Petrov, P. N., and Farisenkov, S. E. (2019a). Wing morphology in featherwing beetles (Coleoptera: Ptiliidae): features associated with miniaturization and functional scaling analysis. *Arthropod Struct. Dev.* 48, 56–70. doi: 10.1016/j.asd.2019.01.003

Polilov, A. A., Ribera, I., Yavorskaya, M. I., Cardoso, A., Grebennikov, V. V., and Beutel, R. G. (2019b). The phylogeny of Ptiliidae (Coleoptera: Staphylinoidea)—the smallest beetles and their evolutionary transformations. *Arthropod Syst. Phylogeny.* 77, 433–455.

R Core Team (2021). R: A language and environment for statistical computing. R Foundation for Statistical Computing, Vienna, Austria. Available online at: https://www.R-project.org

Rasnitsyn, A. P., and Ross, A. J. (2000). A preliminary list of arthropod families present in the Burmese amber collection at The Natural History Museum, London. *Bull. Nat. Hist. Mus. Lond. (Geol.).* 56, 21–24.

Ronquist, F., Teslenko, M., Van Der Mark, P., Ayres, D. L., Darling, A., Höhna, S., et al. (2012). MrBayes 3.2: efficient Bayesian phylogenetic inference and model choice across a large model space. *Syst. Biol.* 61, 539–542. doi: 10.1093/sysbio/sys029

Shi, G., Grimaldi, D. A., Harlow, G. E., Wang, J., Wang, J., Yang, M., et al. (2012). Age constraint on Burmese amber based on U-Pb dating of zircons. *Cretac. Res.* 37, 155–163. doi: 10.1016/j.cretres.2012.03.014

Shockley, F. W., and Greenwalt, D. (2013). *Ptenidium kishenehnicum* (Coleoptera: Ptiliidae), a new fossil described from the Kishenehn oil shales, with a checklist of previously known fossil ptiliids. *Proc. Entomol. Soc. Wash.* 115, 173–181. doi: 10.4289/0013-8797.115.2.173

Smith, M. R. (2019). Bayesian and parsimony approaches reconstruct informative trees from simulated morphological datasets. *Biol. Lett.* 15, 20180632. doi: 10.1098/rsbl.2018.0632

Smith, M. R. (2021). TreeSearch: morphological phylogenetic analysis in R. *bioRxiv*. doi: 10.1101/2021.11.08.467735

Sörensson, M., and Delgado, J. A. (2019). Unveiling the smallest–systematics, classification and a new subfamily of featherwing beetles based on larval morphology (Coleoptera: Ptiliidae). *Invertebr. Syst*. 33, 757–806.

Westerweel, J., Roperch, P., Licht, A., Dupont-Nivet, G., Win, Z., Poblete, F., et al. (2019). Burma Terrane part of the Trans-Tethyan arc during collision with India according to palaeomagnetic data. *Nat. Geosci*. 12, 863–868. doi: 10.1038/s41561-019-0443-2

Yamamoto, S., Grebennikov, V. V., and Takahashi, Y. (2018). *Kekveus jason* gen. et sp. nov. from Cretaceous Burmese amber, the first extinct genus and the oldest named featherwing beetle (Coleoptera: Ptiliidae: Discheramocephalini). *Cretac. Res*. 90, 412–418. doi: 10.1016/j.cretres.2018.05.016

Yavorskaya, M., Beutel, R. G., and Polilov, A. (2017). Head morphology of the smallest beetles (Coleoptera: Ptiliidae) and the evolution of sporophagy within Staphyliniformia. *Arthropod Syst. Phylogeny*. 75, 417–434.

Zhang, S.-Q., Che, L.-H., Li, Y., Liang, D., Pang, H., Ślipiński, A., et al. (2018). Evolutionary history of Coleoptera revealed by extensive sampling of genes and species. *Nat. Commun*. 9, 205. doi: 10.1038/s41467-017-02644-4

Conflict of Interest: The authors declare that the research was conducted in the absence of any commercial or financial relationships that could be construed as a potential conflict of interest.

Publisher's Note: All claims expressed in this article are solely those of the authors and do not necessarily represent those of their affiliated organizations, or those of the publisher, the editors and the reviewers. Any product that may be evaluated in this article, or claim that may be made by its manufacturer, is not guaranteed or endorsed by the publisher.

frontiers | Frontiers in Ecology and Evolution

ORIGINAL RESEARCH
published: 18 July 2022
doi: 10.3389/fevo.2022.927537

The Oldest Fossils From China Provide the Most Direct Evidence for the Ancestral State of Fossula Spongiosa and Stridulitrum of Reduviidae

*Peipei Zhang[1], Yingqi Liu[2], Dong Ren[1] and Yunzhi Yao[1]**

[1] Key Lab of Insect Evolution and Environmental Changes, College of Life Sciences and Academy for Multidisciplinary Studies, Capital Normal University, Beijing, China, [2] Department of Entomology and MOA Key Lab of Pest Monitoring and Green Management, College of Plant Protection, China Agricultural University, Beijing, China

OPEN ACCESS

Edited by:
*Chenyang Cai,
Nanjing Institute of Geology and Paleontology (CAS), China*

Reviewed by:
*Dominik Chłond,
University of Silesia in Katowice, Poland
Andrei Legalov,
Institute of Systematics and Ecology of Animals (RAS), Russia*

***Correspondence:**
*Yunzhi Yao
yaoyz100@126.com*

Specialty section:
This article was submitted to Paleontology, a section of the journal Frontiers in Ecology and Evolution

Received: *24 April 2022*
Accepted: *24 May 2022*
Published: *18 July 2022*

Citation:
Zhang P, Liu Y, Ren D and Yao Y (2022) The Oldest Fossils From China Provide the Most Direct Evidence for the Ancestral State of Fossula Spongiosa and Stridulitrum of Reduviidae. Front. Ecol. Evol. 10:927537. doi: 10.3389/fevo.2022.927537

This study describes a new genus *Simplicivenius* gen. nov. of Reduviinae with two new species, *Simplicivenius tuberculosus* sp. nov. and *Simplicivenius rectidorsius* sp. nov. from the Yixian Formation in northeastern China. The diagnosis of the genus includes the width of the scutellum about 2/3 of the width of the pronotum and the absence of longitudinal veins around the exterior cell of the membrane. This is the oldest fossil record of Reduviinae and indeed Reduviidae at present, dating back to the Early Cretaceous. This implies that Reduviinae existed before the Late Cretaceous biological mass extinction, hinting that Reduviinae may be a basal taxon within the Higher Reduviidae. Moreover, the fossils prove the correctness of the previous speculations on the ancestral state of the stridulitrum and the fossula spongiosa of the assassin bugs. The fossula spongiosa on the mid leg and fore leg are subequal in size and both occupy 1/3 of the tibia is considered the primitive type of fossula spongiosa.

Keywords: Reduviinae, fossil, new genus, stridulitrum, fossula spongiosa, Early Cretaceous

INTRODUCTION

Reduviidae is the second-largest family within Heteroptera, including about 25 subfamilies and more than 7,000 described species at present (Weirauch et al., 2014). Among them, Reduviinae is a cosmopolitan group, which is most abundant in tropical and subtropical regions. It is the second-largest subfamily of Reduviidae, including 141 genera and more than 1,070 species (Shah et al., 2022). Species of this subfamily are predatory and prey on other animals for their food (Hwang and Weirauch, 2012). Most of them live under dead bark, sometimes near human dwellings, in bushes, and in arid environments such as deserts, where their habitats are more sophisticated and varied (Sahayaraj, 2007). The first extant species of this subfamily, *Reduvius personatus*, was described in 1758 by Linnaeus (Javahery, 2013).

There are only 33 genera and 51 species of fossils that have been described in Reduviidae, which is quite different from the present situation in that it is the second-largest family of Heteroptera. Among these 51 species, there are 18 species whose subfamilies are undetermined, and the remaining 33 species are classified into eight subfamilies: Reduviinae, Holoptilinae, Emesinae, Centrocnemidinae, Triatominae, Phymatinae, Harpactorinae, and Ectrichodiinae. Germar et al. (1856) found a fossil of assassin bugs in Eocene amber from the Baltic (Germar et al., 1856), which is the first report of Reduviidae fossils. A large number of Reduviidae fossils had been found and reported in the 20th century, but the geological age is still in Cenozoic. Poinar (2019) discovered a primitive Triatominae fossil in early Late Cretaceous amber from northern Myanmar, this is the earliest record of fossil specimens of Reduviidae and the first report of Mesozoic assassin bugs fossil (Bush, 2021). To sum up, the current fossil records of Reduviidae are mostly Cenozoic, only a few fossils have been reported in Mesozoic, and the geological period stays in the early Late Cretaceous.

A new genus and two new species of Reduviinae are described in this article, which can be traced back to the Early Cretaceous and is the earliest known fossil record of Reduviidae in the world. The discovery of these fossils will enrich the diversity of the fossil species of Reduviidae to a certain extent, and provide direct fossil evidence for the subsequent interpretation of the evolution and origin of Reduviidae.

MATERIALS AND METHODS

The research materials involved in this study are three impression fossils, all of which were excavated from the Yixian Formation of Liaoning Province, Northeast China. The geological period of the Yixian Formation is suggested to be Early Cretaceous Aptian-Barremian (Barrett, 2000; He et al., 2008; Chang et al., 2017). Two of them are fossil pairs of plates. All are preserved in the Fossil Herbarium, Key Lab of Insect Evolution and Environmental Changes, College of Life Sciences, Capital Normal University, Beijing, China (Curator: Yunzhi Yao). The morphological aspects were mainly observed under a Nikon SMZ25 microscope, which was connected in real-time to a Nikon DS-Ri2 digital photographic system. The morphological terminology used in this study is mainly referenced by Lent and Wygodzinsky (1979), Weirauch (2008), and Zhang and Weirauch (2011). All units of dimensions are in millimeters (mm).

RESULTS

Systematic Paleontology

Order Hemiptera Linnaeus, 1758

Suborder Heteroptera Latreille, 1810

Infraorder Cimicomorpha Leston, Pendergrast & Southwood, 1954

Family Reduviidae Latreille, 1807

Subfamily Reduviinae Amyot & Serville, 1843

Genus *Simplicivenius* Zhang, Liu, and Yao, gen. nov.

Type Species. *Simplicivenius tuberculosus* sp. nov. (**Figure 1**).

Etymology. The name of this new genus is a combination of "*Simpl-*" (meaning "simple") and "*Civenius*" (meaning "vein"). Gender masculine. The reason for this name is that the veins of this new genus are relatively simple, with only two large wing cells on the membrane and no small longitudinal veins protruding from the outer edge of the cell formed by the M and Cu veins.

Diagnosis. Medium-sized, with a long oval shape. Anteocular region slightly longer and wider than postocular region, postocular region with obvious lateral constriction; antennae divided into four segments, with scape thickest and pedicel longest, pedicel with no obvious pseudosegmentation; anterior lobe of pronotum obviously shorter than posterior lobe, margin of posterior lobe prominent or nearly straight, with spines at humeral angle and slightly variable in shape; scutellum triangular, width obviously larger than length, apical scutellar process upturned, width of scutellum about 2/3 of width of pronotum; apical portion of corium with the macula, membrane with two large parallel cells, exterior cell slightly wider than the inner cell, without longitudinal vein extending from the outer margin of the exterior cell.

Comparison. This new fossil genus shares the following characteristics with the Reduviinae of the type genus *Reduvius*: both fore leg and mid leg straight and hemelytron without discoidal cell. However, it can be distinguished from the latter genus by the following characteristics: anterior lobe of pronotum significantly shorter than the posterior lobe. Other than that, the two new fossil species appear at first glance to be very similar to *Acanthaspis quinquespinosa* Fabricius, 1781 in the genus *Acanthaspis*, both of which have the following features: scape thickest and pedicel longest; anterior lobe of pronotum shorter than posterior lobe; scutellum triangular; apical scutellar process upturned and macula at sub-apical part of the corium. Nevertheless, further observations revealed the following unique features of the new fossil genus: width of scutellum approximately 2/3 of width of pronotum; no longitudinal vein in exterior cell of membrane.

Simplicivenius tuberculosus sp. nov. (**Figure 1**).

Holotype. CNU-HET-LB2022001, adult male.

Etymology. The name of this species comes from the Latin word "*tuberculosus*" (meaning "tuberculate"), referring to the multiple tubercles on the side of the pronotum and the scutellum.

Locality and Horizon. Early Cretaceous, Aptian-Barremian, Yixian, Liaoning Province, Northeast China.

Diagnosis. Conspicuous tubercles distributed on collar; posterior lobe of pronotum twice as long as anterior lobe, anterior lobe of pronotum and lateral area of scutellum, posterior margin of pronotum convex; hemelytron with a large macula on sub-apical portion of corium, a small sub-triangular macula on apical portion, a small rectangular macula on clavus; two elongated large cells consisting of M, Cu and Pcu veins on membrane.

Description. Head medium-sized, 1/8 of body length, anteocular region about 1.32 times of postocular region, postocular region short and cylindrical; eye large, dorsal length of almost 1/3 of head, dorsal width of greater than 1/2 of interocular space; interocellar space greater than single ocellar width, interocular space about 3.4 times of interocellar space;

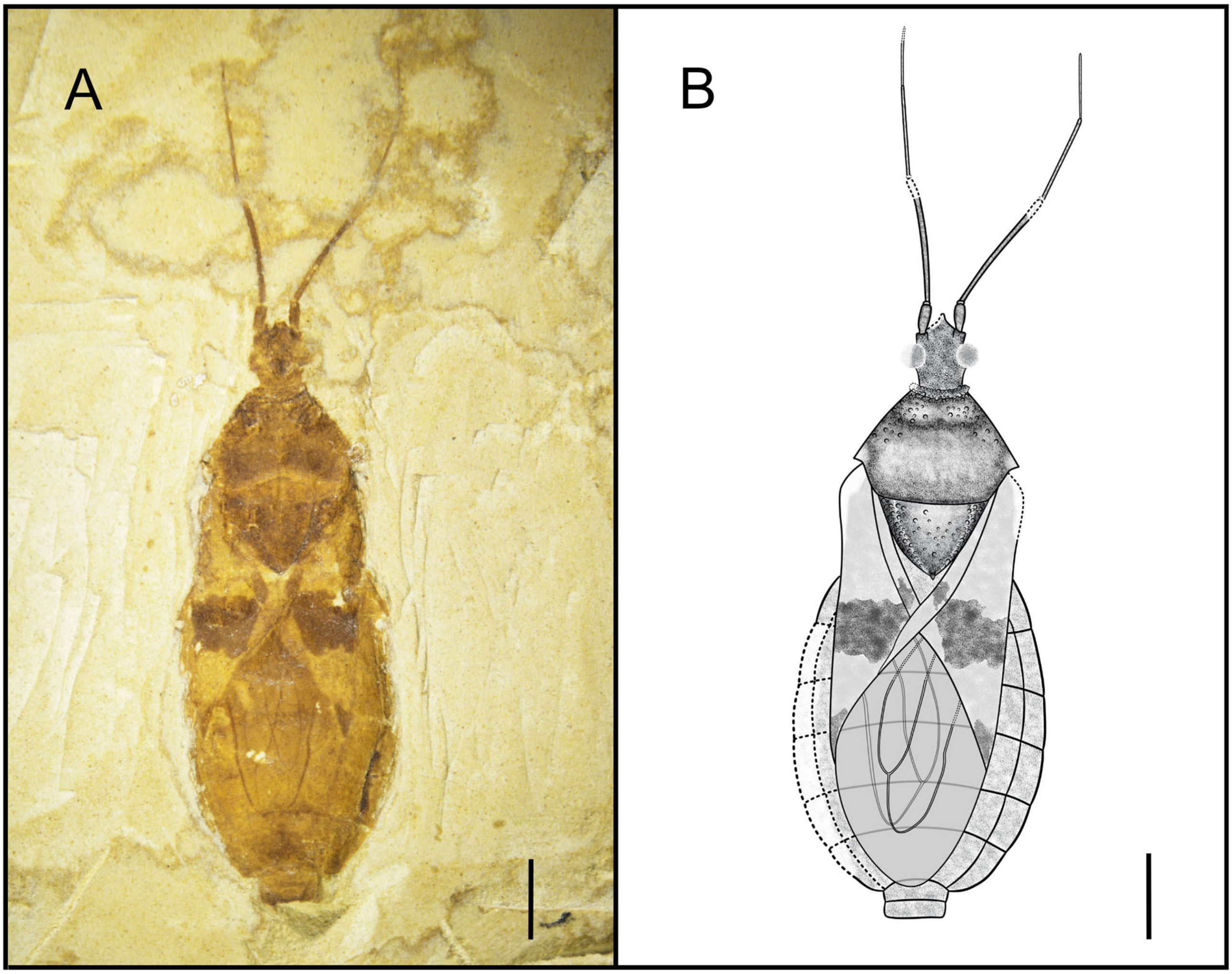

FIGURE 1 | Dorsal habitus of *Simplicivenius tuberculosus* gen. et sp. nov., holotype CNU-HET-LB2022001 **(A)** Photograph. **(B)** Line drawing. Scale bars = 2 mm.

antenna divided into four segments, width of four segments tapered, scape and pedicel rod-shaped, width of scape twice width of pedicel, basiflagellomere and distiflagellomere obviously slender, distiflagellomere thinnest, its width 1/5 of the width of scape, pedicel longest, its length about four times that of scape; labium not preserved.

Collar incompletely preserved, edges of collar have small tubercles of different sizes; anterior margin of anterior lobe of pronotum slightly concave inward, anterior lobe has small tubercles symmetrical from left to right, lateral part of subanterior margin of anterior lobe predominant, closer area to transverse sulcus of pronotum fewer tubercles, median longitudinal groove faint, pronotal transverse sulcus with a small number of small tubercles on sides, humeral angle with slightly shorter and thicker spine-like process, apex of process is slightly pendulous, lateral angle rounded and blunt, posterior margin convex; scutellum triangular, about 1.48 times as wide as long, width almost as long as distance between two humeral angles, length about 1/8 of body length, sides of scutellum with symmetrical and dense tubercles, tubercles on middle part relatively sparse.

Hemelytra large macula on corium, which contrasts with other colors around corium, its size about 1/3 of corium, whereas macula on middle of clavus and apex of corium much smaller; abdomen elliptical and basically well preserved, intersegmental sutures also well preserved.

Legs not preserved.

Although the key characteristics of male genitalia are not preserved, it can be seen that the apex of the abdomen is very flat. Female external genitalia are generally more pointed, so it is difficult to press into such a shape and then combined with its size, this specimen is more likely to be male.

Dimensions (mm). Body length: 14.22; maximum abdominal width: 6.07; head length: 1.80; length of anteocular region: 0.7; length of postocular region: 0.53; width of interocular space: 0.75; width of interocellar space: 0.22; antennal segment lengths I-IV:

0.72, 2.96, 2.14, 1.42; length of anterior lobe of pronotum: 0.78; length of posterior lobe of pronotum: 1.75; width of pronotum: 3.92; length of scutellum: 1.79; width of scutellum: 2.65.

Simplicivenius rectidorsius sp. nov. (**Figures 2**, **3**).

Holotype. CNU-HET-LB2022002, part, and counterpart, adult female.

Etymology. The species name is a combination of the Latin words "*rect-*" (meaning "straight") and "*dorsalis*" (meaning "dorsal"), referring to the nearly straight posterior margin of the pronotum.

Locality and Horizon. Early Cretaceous, Aptian-Barremian, Yixian, Liaoning Province, Northeast China.

Diagnosis. Collar well-developed, collar process slightly uplifted; ratio of length of anterior and posterior lobes of pronotum about 2:3, posterior margin of pronotum nearly straight with position of humeral angle about the same level; lateral part of scutellum with symmetrical tubercles; stridulitrum long and wide; sub-apical portion of corium with irregular small macula, membrane with two elongated large cell, exterior cell wider than inner cell; fossula spongiosa on fore leg and mid leg occupying about 1/3 of tibial ventral surface, tarsus of fore and mid legs three-segmented, hind coxae close together.

Description. Head medium-sized, 1/8 of body length, anteocular region measures 1.32 times that of postocular region, postocular region short and cylindrical; eye large, dorsal length almost 1/3 of head, dorsal width more than 1/2 of interocular space; interocellar space more than single ocellar width, interocular space is about 3.4 times that of interocellar space; antenna divided into four segments, width of four segments tapered, scape and pedicel rod-shaped, width of scape twice width of pedicel, basiflagellomere and distiflagellomere obviously slender, distiflagellomere thinnest, its width 1/5 of width of scape, pedicel longest, and its length about four times that of scape; labium is not preserved.

Collar well-developed, collar process slightly elevated; posterior lobe of pronotum approximately 1.62 times longer than anterior lobe, anterior margin of pronotum slightly depressed inward, median longitudinal groove faint, humeral angle on posterior lobe elongated spine, posterior margin of pronotum at same level as base of spines at humeral angle, nearly flat; scutellum triangular, 1/8 of body length and width, about 1.17 times its length, with small projections on lateral margins, a thicker base of apical portion of scutellum, tip of scutellar process sharp and upturned; stridulitrum incompletely preserved, but can be identified as long and wide under the microscope (**Figures 3A,B**). Middle of mesostethium and metastethium with a longitudinal ridge.

Femur and tibia of right fore leg well preserved, fossula spongiosa impressions on fore tibia, which well preserved, coxa and trochanter of left fore leg largely intact, fore coxae elongated, distance between fore coxae is greater than width of one coxa, fore femur robuster than fore tibia, femur elliptical columnar, middle wider than both ends, widest point 0.91 mm, tibia cylindrical, width basically equal everywhere, width about 0.32 mm, fossula spongiosa relatively large, occupying about 1/3 of whole tibia (**Figure 3C**), tarsus three-segmented, first segment shortest and third longest; right mid leg not preserved; outer edges of coxa and trochanter of left mid leg largely preserved, fossula spongiosa impression on mid tibia (**Figure 3D**) (preserved on the fossil is the ventral view of fossula spongiosa, probably caused by the turning of the tibial segment), and mid tarsus well preserved, mid coxae nearly triangular, fossula spongiosa also occupies about 1/3 of tibia, mid tarsus three-segmented, first and second segments basically equal in length, third segment longest; only coxae of hind leg is preserved, sub-circular hind coxae close to each other, distance between hind coxae smaller than width of one coxa.

Abdomen well preserved, elliptical, intersegmental sutures also basically well preserved. Connexivum well preserved, paranotum very broad. Female genitalia can be observed with valvifers and valvulae (**Figures 3E,F**).

Dimensions (mm). Body length: 14.92; maximum abdominal width: 6.72; head length: 2.25; length of anteocular region: 0.95; length of postocular region: 0.71; width of interocular space: 0.56; width of interocellar space: 0.25; antennal segment lengths I-IV: 0.91, 1.31, 1.16, 0.50; length of anterior lobe of pronotum: 0.74; length of posterior lobe of pronotum: 1.20; width of pronotum: 4.20; length of scutellum: 1.86; width of scutellum: 2.71; length of fore femur: 2.88; length of fore tibia: 3.33; length of fossula spongiosa of fore leg: 1.10; length of total fore tarsus: 0.94; length of mid tibia: 3.14; length of fossula spongiosa of mid leg: 1.10; length of total mid tarsus: 1.05.

Associated Specimen. In addition to the assassin bug, this fossil also has a rove beetle larva next to it, which belongs to Coleoptera, and although it is documented that the assassin bugs prey on Coleoptera as well (Youssef and Abd-Elgayed, 2015; Loko et al., 2022), there is no direct evidence that this assassin bug was preying on the rove beetle larva in this fossil, but the leg of the assassin bug was in contact with the carapace of the larva. Coincidentally, the assassin bug fossil documented by Swanson also shows Coleoptera (Swanson et al., 2021), and the leg of the assassin bug is also in contact with the body of the beetle.

DISCUSSION

The present fossil genus can be identified as Reduviidae on the basis of the following characteristics:membrane with two large cells, prosternal sulcus with stridulitrum present, head necklike behind eyes (Schuh and Weirauch, 2020). According to the zoogeographic classification of the world by Olson et al. (2001), the fossils of this study were recovered from northeastern China, which falls within the Palaearctic boundary that encompasses mainly the Eurasian and northern African regions. Within Reduviidae, Emesinae, Ectrichodiinae, Harpactorinae, Holoptilinae, Peiratinae, Stenopodainae, and Reduviinae are distributed in this lineage, so the fossils in this study are mainly compared to these seven subfamilies (Weirauch et al., 2014). Emesinae has a slender body which differs greatly from the oval body of the fossils in this study, and therefore, this subfamily is not considered in the first place (Wygodzinsky, 1966). The main difference between Ectrichodiinae and other subfamily assassin bugs is the presence

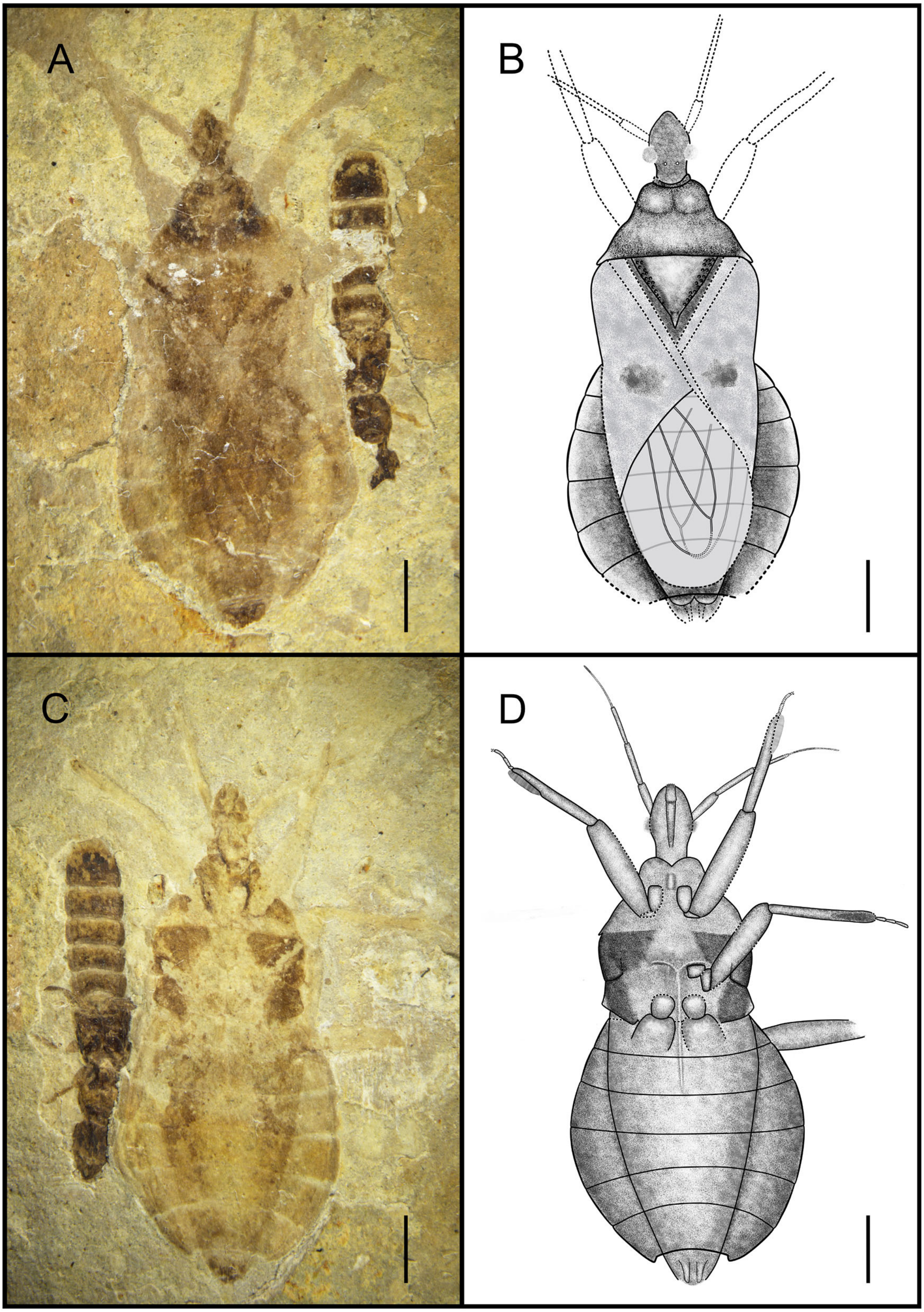

FIGURE 2 | Habitus of *Simplicivenius rectidorsius* gen. et sp. nov., holotype. CNU-HET-LB2022002 **(A)** Photograph in dorsal view. **(B)** Line drawing in dorsal view. **(C)** Photograph in ventral view. **(D)** Line drawing in ventral view. Scale bars = 2 mm.

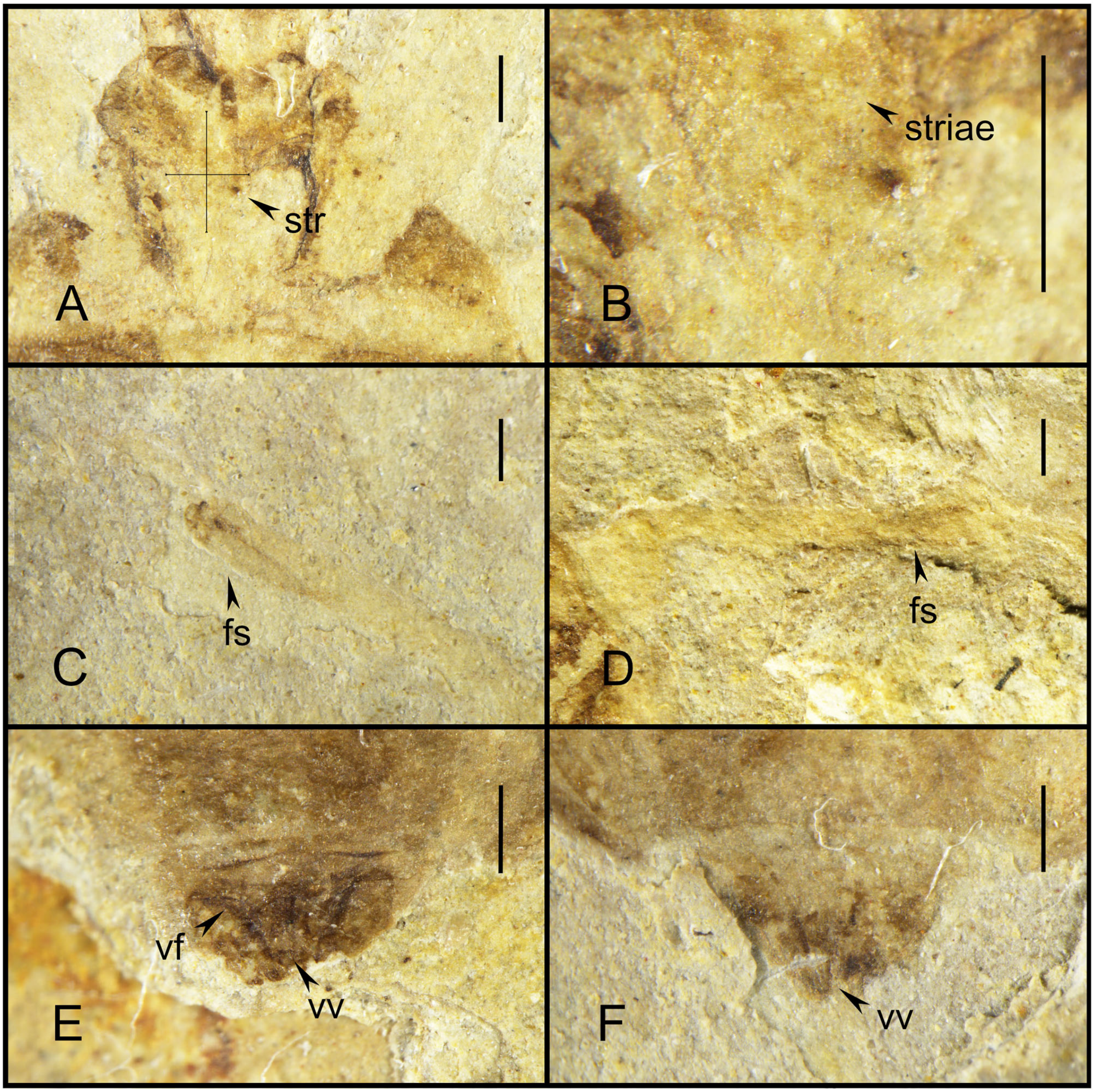

FIGURE 3 | *Simplicivenius rectidorsius* gen. et sp. nov. photographs with morphological details, holotype. CNU-HET-LB2022002. **(A)** Conservation range of stridulitrum. **(B)** Structures of striae. **(C)** Fossula spongiosa on fore tibia. **(D)** Fossula spongiosa on mid tibia. **(E)** Female genitalia in dorsal view. **(F)** Female genitalia in ventral view. Scale bars = 0.5 mm. str, stridulitrum; fs, fossula spongiosa; vf, valvifer; vv, valvula.

of at least two apical scutellar processes, unlike the present fossils where only one apical scutellar process is present (Forthman et al., 2016). The key identifying character of Peiratinae is that the anterior lobe of the pronotum is significantly longer than the posterior lobe, which is the opposite of all the fossils in this study (Liu et al., 2020). In addition, the fossils in this study are clearly observed two large parallel cells present only at the membrane of hemelytron, whereas Harpactorinae has a square cell at the corium and Stenopodainae has a pentagonal or hexagonal cell at the corium (Wygodzinsky and Giacchi, 1994; Forero et al., 2004; Chen et al., 2020), the fossils are fundamentally different from the distribution of cells in these two subfamilies. Holoptilinae is missing the fossula spongiosa on the tibiae and has long setae on the body and each leg (Malipatil, 1985); the fossils in this study do not reveal the preservation of a large number of setae, although it is not certain whether the taxa represented by the fossils did not have setae covering the whole body itself or whether the setal structure was not preserved because the fossils are too old, the fossula spongiosa can be clearly observed in *Simplicivenius rectidorsius* gen. et sp. nov. Reduviinae is identified by the presence of the ocellus, three-segmented tarsus, two closed cells on the membrane of the hemelytron, and the fossula spongiosa on the tibia of fore and mid legs. In addition, Reduviinae is usually identified by the lack of specific morphological features unique to other subfamilies (Weirauch, 2014). The fossils in this study are highly overlapping with Reduviinae in terms of identifying features. Therefore, after a comprehensive comparison, the two fossils were finally classified as Reduviinae.

Hwang and Weirauch (2012) estimated the divergence dating of key evolutionary nodes within Reduviidae based on BEAST analysis using a relaxed-clock model and 11 fossil calibrations points. It is shown that the diversification of Higher Reduviidae began at 97 Ma (81–113 Ma) in the Late Cretaceous, coinciding with two global changes in the timing of angiosperm and phytophagous insect radiation. The analysis also showed that all lineages of Reduviinae are located in the branches of Higher Reduviidae, and the same results were shown in the cladistic analysis of Reduviidae based on morphological characters (Weirauch, 2008), the molecular phylogeny within the assassin bugs obtained from mitochondrial and nuclear ribosomal genes (Weirauch and Munro, 2009), and in the phylogenetic analysis based on transcriptomic and ribosomal DNA data (Zhang et al., 2016). The fossils in this study are geologically dated to the Early Cretaceous, and there is ample evidence to support their classification as Reduviinae, which is the earliest known Reduviinae fossil in the world. This result suggests that the Reduviinae emerged well before the Late Cretaceous biological mass extinction (Newell, 1965) survived the Late Cretaceous biological mass extinction, and then gradually flourished with the radiation of angiosperms and phytophagous insects. Such an early geological age also allows the onset of diversification of the Higher Reduviidae from the Late Cretaceous at 97 Ma (81–113 Ma) to at least the Early Cretaceous, indicating that Reduviinae may have been a basal taxon within the Higher Reduviidae. Poinar (2019) suggested that the fossil species *Paleotriatoma metaxytaxa* Triatominae from the early Late Cretaceous (100 Ma) evolved from a clade of Reduviinae based on the presence of ocelli, three-segmented tarsi, two closed cells on the forewing membrane, slight bend in the labium and fossula spongiosa on the fore and mid tibias. This also seems to further imply that Reduviinae may be a basal taxon along with Peiratinae. But it is not sufficient to rely on the geological history period of fossil records to draw such a conclusion, so we will also discuss below from the perspective of morphological characters.

The oldest fossil of *Simplicivenius rectidorsius* gen. et sp. nov. also provides the most direct fossil evidence for previous studies on the stridulitrum and fossula spongiosa of Reduviidae. The evolution of the stridulitrum of Reduviid ae was investigated by Cai et al. (1994), which classified the stridulitrum of adult Reduviidae into nine terminal types and suggested that the subwide total-striate stridulitrum or wide total-striate stridulitrum probably represented the ancestral status of Reduviidae. However, this conclusion remains tentative, and direct evidence to support it is not available. The striae of the stridulitrum are preserved in the fossil species *Simplicivenius rectidorsius* gen. et sp. nov. Although the complete appearance of the stridulitrum is not preserved as the fossil is too old, it is not difficult to conclude that the stridulitrum of this fossil species is at least the subwide total-striate type, judging from the distribution range of the striae on the prosternum of the fossil. Besides, Zhang et al. (2016) reconstructed the ancestral state of the raptorial leg of the assassin bugs based on transcriptomic and ribosomal DNA data. The fossula spongiosa were present in the ancestors of assassin bugs, as reported by Zhang et al. (2016). And auspiciously, the fossula spongiosa is also clearly preserved in *Simplicivenius rectidorsius* gen. et sp. nov. The fossula spongiosa of the fore leg can be seen, and the horizontal plate impressions that evolved only within Reduviidae to separate the fossula spongiosa cavity from the medial of the tibia are also preserved in the mid leg, and the fossula spongiosa impressions of the fore leg and mid leg are preserved simultaneously and both occupy 1/3 of the tibia (Weirauch, 2007). Another fossil species of Triatominae *Paleotriatoma metaxytaxa* found in the early Late Cretaceous (100 Ma) also has fossula spongiosa on both the fore leg and mid leg that occupy 1/3 of the tibia (Poinar, 2019). The fossula spongiosa were found to be present in both fore and mid legs in most species, and the fossula spongiosa of fore leg were usually larger than the fossula spongiosa of mid leg, while only a few taxa have fossula spongiosa on the fore leg only (Weirauch, 2007). From the above, it can be seen that there are three types of the fossula spongiosa of mid leg: first, the fossula spongiosa on the fore leg and mid leg being subequal in size; second, the fossula spongiosa on the fore leg being significantly larger than that on the mid leg; third, the fossula spongiosa on the mid leg is absent. The type I is relatively more developed and emerged earlier than the other two types. The evolution of fossula spongiosa throughout the Reduviidae showing a degenerative trend as revealed from the study by Zhang et al. (2016). The law of irreversibility states that an organ that has degenerated or disappeared completely during the evolutionary process will never reappear in subsequent evolutionary processes. If an organ that has disappeared in response to environmental changes is needed again, the organism can only produce another organ to perform the role of the original organ (Gould, 1970). The developmental priority also assumes that the earlier features in individual development are plesiomorphic and the later features are apomorphic (Hennig, 1999). Therefore, the type I represented by *Simplicivenius rectidorsius* gen. et sp. nov and *Paleotriatoma metaxytaxa* are presumed to be the ancestral states in assassin bugs and the remaining two types emerged subsequently. This also implies that the lack of fossula spongiosa in most species of mid leg which play an auxiliary role in fixing the prey seems to be eliminated firstly during the degradation of the fossula spongiosa. This may be caused by changes in the predatory behavior of Reduviidae due to changes in the predator (Haridass and Ananthakrishnan, 1980; Weirauch and Cassis, 2006; Zhang and Weirauch, 2014; Wang and Liang, 2015; Castro-Huertas et al., 2019). The most primitive types of fossula spongiosa and stridulitrum in Reduviidae are found in the fossils of Reduviinae in this study, which further indicates that Reduviinae is probably the basal taxon in the Higher Reduviidae, rather than the branching taxon suggested in previous studies (Weirauch, 2008; Weirauch and Munro, 2009; Hwang and Weirauch, 2012; Zhang et al., 2016). The results of Weirauch (2008) based on morphological characters showed that Harpactorinae that lack fossula spongiosa in most species as a basal taxon within the Higher Reduviidae, which may need to be reconsidered.

DATA AVAILABILITY STATEMENT

The original contributions presented in the study are included in the article/supplementary material, further inquiries can be directed to the corresponding author.

AUTHOR CONTRIBUTIONS

Conceptualization, methodology, and formal analysis: PZ and YL. Validation: PZ, DR, and YY. Investigation and writing—original draft preparation: PZ. Resources, project administration, and funding acquisition: DR and YY. Data curation: YY. Writing—review and editing: YL, DR, and YY. Visualization and supervision: YL. All authors have read and agreed to the published version of the manuscript.

FUNDING

This project is supported by the National Natural Science Foundation of China [Nos. 31970436, 31730087, 42288201, and 32020103006] and the Beijing Municipal Natural Science Foundation and Beijing Municipal Education Commission [KZ201810028046].

ACKNOWLEDGMENTS

We are grateful to the editor and reviewers for constructive criticism and valuable comments on the manuscript.

REFERENCES

Barrett, P. M. (2000). Evolutionary consequences of dating the Yixian Formation. *Trends Ecol. Evol.* 15, 99–103. doi: 10.1016/S0169-5347(99)01782-6

Bush, T. N. (2021). *Systematics of Ectrichodiella Fracker and Bruner, 1924 with a description of the first fossil millipede assassin bug (Insecta: Heteroptera: Reduviidae: Ectrichodiinae)*. UC Riverside: University Honors. Available onlilne at: https://escholarship.org/uc/item/0zx7m0dj

Cai, W., Chou, Y., and Lu, J. (1994). The morphology, postembryonic development and evolution of stridulitra in Reduviidae with special reference to their taxonomic importance (Heteroptera: Reduvioidea). *Insect Sci*. 1, 1–16. doi: 10.1111/j.1744-7917.1994.tb00190.x

Castro-Huertas, V., Forero, D., and Grazia, J. (2019). Comparative morphology of the raptorial leg in thread-legged bugs of the tribe Metapterini Stål, 1859 (Hemiptera, Heteroptera, Reduviidae, Emesinae). *Zoomorpholog*. 138, 97–116. doi: 10.1007/s00435-019-00431-x

Chang, S. C., Gao, K. Q., Zhou, C. F., and Jourdan, F. (2017). New chronostratigraphic constraints on the Yixian Formation with implications for the Jehol Biota. *Palaeogeogr. Palaeoclimatol. Palaeoecol.* 487: 399–406. doi: 10.1016/j.palaeo.2017.09.026

Chen, Z., Liu, Y., and Cai, W. (2020). Notes on the genus *Enoplocephala* Miller (Hemiptera: Reduviidae: Stenopodainae), with the description of a new species from Borneo. *Raffles. B. Zool.* 68. doi: 10.1080/00379271.2020.1844048

Forero, D., Weirauch, C., and Baena, M. (2004). Synonymy of the reduviid (Hemiptera: Heteroptera) genus *Torrealbaia* (Triatominae) with *Amphibolus* (Harpactorinae), with notes on *Amphibolus venator* (Klug, 1830). *Zootaxa*. 670, 1–12. doi: 10.11646/zootaxa.670.1.1

Forthman, M., Chłond, D., and Weirauch, C. (2016). Taxonomic monograph of the endemic millipede assassin bug fauna of Madagascar (Hemiptera: Reduviidae: Ectrichodiinae). *Bull. Am. Mus. Nat. Hist.* 2016, 1–152. doi: 10.1206/amnb-928-00-01.1

Germar, D. F., Berendt, G. C., and Hagen, H. (1856). *Die im bernstein befindlichen Hemipteren und Orthopteren der Vorwelt*. Berlin: Nicolaische Buchhandlung.

Gould, S. J. (1970). Dollo on Dollo's law: Irreversibility and the status of evolutionary laws. *J. Hist. Biol.* 3, 189–212. doi: 10.1007/BF00137351

Haridass, E. T., and Ananthakrishnan, T. N. (1980). Functional morphology of the fossula spongiosa in some reduviids (Insecta-Heteroptera-Reduviidae). *Proceedings: Animal Sciences.* 89, 457–466. doi: 10.1007/BF03179132

He, H., Pan, Y., Tauxe, L., Qin, H., and Zhu, R. (2008). Toward age determination of the M0r (Barremian–Aptian boundary) of the Early Cretaceous. *Phys. Earth Planet*. 169, 41–48. doi: 10.1016/j.pepi.2008.07.014

Hennig, W. (1999). *Phylogenetic* systematics. USA: University of Illinois Press.

Hwang, W. S., and Weirauch, C. (2012). Evolutionary history of assassin bugs (Insecta: Hemiptera: Reduviidae): insights from divergence dating and ancestral state reconstruction. *PLoS ONE.* 7, e45523. doi: 10.1371/journal.pone.0045523

Javahery, M. (2013). Natural history of *Reduvius personatus* Linnaeus (Hemiptera: Heteroptera: Reduviidae) in North America. *Mun. Ent. Zool.* 8, 685–703.

Lent, H., and Wygodzinsky, P. (1979). Revision of the Triatominae (Hemiptera, Reduviidae), and their significance as vectors of Chagas' disease. *Bull. Am. Mus. Nat Hist.* 163, 123–520.

Liu, Y., Chen, Z., Webb, M. D., and Cai, W. (2020). *Oblongiala zimbabwensis*, a new assassin bug genus, and species from Zimbabwe, with a key to the Afrotropical genera of Peiratinae (Hemiptera: Heteroptera: Reduviidae). *Acta Ent. Mus. Nat. Pra.* 60, 659–665. doi: 10.37520/aemnp.2020.047

Loko, Y. L. E., Toffa, J., Gavoedo, D. M., Kitherian, S., Orobiyi, A., and Tam,ò, M. (2022). Effect of population density on oviposition, development, and survival of *Alloeocranum biannulipes* (Hemiptera: Reduviidae) preying on Dinoderus porcellus (Coleoptera: Bostrichidae). *JoBAZ.* 83, 1–8. doi: 10.1186/s41936-022-00267-w

Malipatil, M. B. (1985). Revision of Australian holoptilinae (Reduviidae: Heteroptera). *Aus. J. Zool.* 33, 283–299. doi: 10.1071/ZO9850283

Newell, N. D. (1965). Mass extinctions at the end of the Cretaceous period. *Science.* 149, 922–924. doi: 10.1126/science.149.3687.922

Olson, D. M., Dinerstein, E., Wikramanayake, E. D., Burgess, N. D., Powell, G. V., Underwood, E. C.,et al. (2001). Terrestrial ecoregions of the world: a new map of life on EarthA new global map of terrestrial ecoregions provides an innovative tool for conserving biodiversity. *BioScience.* 51, 933–938. doi: 10.1641/0006-3568(2001)051(0933:TEOTWA)2.0.CO;2

Poinar, G. (2019). A primitive triatomine bug, Paleotriatoma metaxytaxa gen. *et sp. nov*. (Hemiptera: Reduviidae: Triatominae), in mid-Cretaceous amber from northern Myanmar. *Cretac. Res.* 93: 90–97. doi: 10.1016/j.cretres.2018.09.004

Sahayaraj, K. (2007). Ecotypic variation in the biology of *Acanthaspis quinquespinosa* Fabricius 1781 (Hemiptera: Reduviidae: Reduviinae) from peninsular India. *Egypt. J. Biol.* 9.

Schuh, R. T., and Weirauch, C. (2020). *True bugs of the World (Hemiptera: Heteroptera) Classification and Natural history, 2nd ed.* Manchester, UK: Siri Scientific Press.

Shah, S. I. A., Ahmad, A., and Cai, W. (2022). Notes on *Acanthaspis quinquespinosa* Complex (Hemiptera: Reduviidae: Reduviinae) with Description of a New Species from Pakistan. *Pakistan J. Zool.* pp. 1–13. doi: 10.17582/journal.pjz/20210712100720

Swanson, D. R., Heads, S. W., Taylor, S. J., and Wang, Y. (2021). A new remarkably preserved fossil assassin bug (Insecta, Heteroptera, Reduviidae) from the Eocene Green River Formation of Colorado. *Pap. Palaeontol.* 7, 1459–1478. doi: 10.1002/spp2.1349

Wang, J., and Liang, A. P. (2015). Ultrastructure of the fossula spongiosa and pretarsus in Haematoloecha nigrorufa (Stål) (Hemiptera: Heteroptera: Reduviidae: Ectrichodinae). *Zootaxa.* 3963, 230. doi: 10.11646/zootaxa.3963.2.4

Weirauch, C. (2007). Hairy attachment structures in Reduviidae (Cimicomorpha, Heteroptera), with observations on the fossula spongiosa in some other Cimicomorpha. *Zool. Anz.* 246, 155–175. doi: 10.1016/j.jcz.2007.03.003

Weirauch, C. (2008). Cladistic analysis of Reduviidae (Heteroptera: Cimicomorpha) based on morphological characters. *Syst. Entomol.* 33, 229–274. doi: 10.1111/j.1365-3113.2007.00417.x

Weirauch, C., Bérenger, J. M., Berniker, L., Forero, D., Forthman, M., Frankenberg, S., et al. (2014). An illustrated identification key to assassin bug subfamilies and tribes (Hemiptera: Reduviidae). *Can. J. Arthropod Identif.* 26, 1–115.

Weirauch, C., and Cassis, G. (2006). Attracting ants: the trichome and novel glandular areas on the sternum of Ptilocnemus lemur (Heteroptera: Reduviidae: Holoptilinae). *Entomol. Am-ny.* 114, 28–37. doi: 10.1664/0028-7199(2006)114(28:AATTAN)2.0.CO;2

Weirauch, C., and Munro, J. B. (2009). Molecular phylogeny of the assassin bugs (Hemiptera: Reduviidae), based on mitochondrial and nuclear ribosomal genes. *Mol. Phylogenet. Evol.* 53, 287–299. doi: 10.1016/j.ympev.2009.05.039

Wygodzinsky, P., and Giacchi, J. C. (1994). Key to the genera of Stenopodainae of the new world (Insecta, Heteroptera, Reduviidae). *Physis.* 49: 5–9.

Wygodzinsky, P. W. (1966). A monograph of the Emesinae (Reduviidae, Hemiptera). *Bull. Am. Mus. Nat. Hist.* 133, 1–616.

Youssef, N. A., and Abd-Elgayed, A. A. (2015). Biological parameters of the predator, *Amphibolus venator* Klug (Hemiptera: Reduviidae) preying on larvae of Tribolium confusum Duv. (Coleoptera: Tenebrionidae). *Ann. Agric. Sci.* 60, 41–46. doi: 10.1016/j.aoas.2015.01.002

Zhang, G., and Weirauch, C. (2011). Matching dimorphic sexes and immature stages with adults: resolving the systematics of the *Bekilya* group of Malagasy assassin bugs (Hemiptera: Reduviidae: Peiratinae). *Syst. Entomol.* 36, 115–138. doi: 10.1111/j.1365-3113.2010.00551.x

Zhang, G., and Weirauch, C. (2014). Molecular phylogeny of Harpactorini (Insecta: Reduviidae): correlation of novel predation strategy with accelerated evolution of predatory leg morphology. *Cladistics.* 30, 339–351. doi: 10.1111/cla.12049

Zhang, J., Gordon, E. R., Forthman, M., Hwang, W. S., Walden, K., Swanson, D. R.,et al. (2016). Evolution of the assassin's arms: insights from a phylogeny of combined transcriptomic and ribosomal DNA data (Heteroptera: Reduvioidea). *Sci. Rep.* 6, 1–8. doi: 10.1038/srep22177

Conflict of Interest: The authors declare that the research was conducted in the absence of any commercial or financial relationships that could be construed as a potential conflict of interest.

Publisher's Note: All claims expressed in this article are solely those of the authors and do not necessarily represent those of their affiliated organizations, or those of the publisher, the editors and the reviewers. Any product that may be evaluated in this article, or claim that may be made by its manufacturer, is not guaranteed or endorsed by the publisher.

TYPE Original Research
PUBLISHED 03 November 2022
DOI 10.3389/fevo.2022.972343

OPEN ACCESS

EDITED BY
Tae-Yoon Park,
Korea Polar Research Institute,
South Korea

REVIEWED BY
Erik Tihelka,
University of Bristol, United Kingdom
Vitalii Igorevich Alekseev,
Immanuel Kant Baltic Federal
University, Russia

*CORRESPONDENCE
Chen-Yang Cai
cycai@nigpas.ac.cn

SPECIALTY SECTION
This article was submitted to
Paleontology,
a section of the journal
Frontiers in Ecology and Evolution

RECEIVED 18 June 2022
ACCEPTED 21 September 2022
PUBLISHED 03 November 2022

CITATION
Li Y-D, Leschen RAB, Liu Z-H, Huang D-Y and Cai C-Y (2022) An enigmatic beetle with affinity to Lamingtoniidae in mid-Cretaceous amber from northern Myanmar (Coleoptera: Cucujoidea). *Front. Ecol. Evol.* 10:972343. doi: 10.3389/fevo.2022.972343

An enigmatic beetle with affinity to Lamingtoniidae in mid-Cretaceous amber from northern Myanmar (Coleoptera: Cucujoidea)

Yan-Da Li[1,2,3], Richard A. B. Leschen[4], Zhen-Hua Liu[5], Di-Ying Huang[1,2] and Chen-Yang Cai[1,2,3]*

[1]State Key Laboratory of Palaeobiology and Stratigraphy, Nanjing Institute of Geology and Palaeontology, Chinese Academy of Sciences, Nanjing, China, [2]Center for Excellence in Life and Paleoenvironment, Nanjing Institute of Geology and Palaeontology, Chinese Academy of Sciences, Nanjing, China, [3]School of Earth Sciences, University of Bristol, Bristol, United Kingdom, [4]Manaaki Whenua Landcare Research, New Zealand Arthropod Collection, Auckland, New Zealand, [5]Guangdong Key Laboratory of Animal Conservation and Resource Utilization, Guangdong Public Laboratory of Wild Animal Conservation and Utilization, Institute of Zoology, Guangdong Academy of Sciences, Guangzhou, China

An enigmatic cucujiform beetle, *Alloterocucus atratus* Li, Leschen, Liu, and Cai **gen. et sp. nov.**, is reported from mid-Cretaceous Burmese amber. The character combination of the new fossil is not completely consistent with any of the known cucujoid or erotyloid families. Based on our phylogenetic analyses, *Alloterocucus* is assigned to Cucujoidea and may be allied to Lamingtoniidae, which contains a single Australasian genus in the extant fauna. *Alloterocucus* shares with Lamingtoniidae a similar habitus and a series of characters, including the absence of postocular constriction, 3-segmented antennal club, externally open procoxal cavities, laterally open mesocoxal cavities, exposed pro- and mesotrochantins, and the absence of epipleural fovea and pronotal setose cavities, but differs from extant Lamingtoniidae in its apically truncate terminal maxillary palpomeres, 5-5-4 tarsi in male and absence of distinct dorsal punctation.

Zoobank registration: [https://zoobank.org/], identifier [111CE15E-5B49-4154-9E4A-7B3A738C6D2A].

KEYWORDS

Cucujoidea, phylogeny, fossil, Burmese amber, Mesozoic

Introduction

The beetle superfamily Cucujoidea of the series Cucujiformia has a complex taxonomic history. Historically, it is essentially a group of families without clear diagnostic characteristics of other superfamilies (especially Tenebrionoidea; Crowson, 1955; Lawrence and Newton, 1982). The coccinelloid group, once regarded as the cerylonid series, was recognized based on multiple lines of morphological (Crowson, 1955; Ślipiński and Pakaluk, 1991) and molecular evidence (Hunt et al., 2007; Robertson et al., 2008, 2015; Bocak et al., 2014), and formally removed from Cucujoidea and elevated to its superfamilial status by Robertson et al. (2015). The phylogenetic relationships within the remaining Cucujoidea vary dramatically among various morphological and molecular studies (e.g., Leschen et al., 2005; Robertson et al., 2008, 2015; Lawrence et al., 2011; McElrath et al., 2015; Timmermans et al., 2016; Zhang et al., 2018; McKenna et al., 2019). Although some molecular analyses either based on a few gene markers (Robertson et al., 2015) or a larger dataset (95 nuclear protein-coding genes) (Zhang et al., 2018) under a site-homogeneous substitution model supported a monophyletic Cucujoidea *sensu* Robertson et al. (2015), recent studies using transcriptomic data (McKenna et al., 2019) or a better-fitting site-heterogeneous model (Cai et al., 2022) have consistently demonstrated the paraphyly of Cucujoidea *sensu* Robertson et al. (2015). In light of the more recent phylogenomic results, Cai et al. (2022) therefore formally divided Cucujoidea into three superfamilies, namely, Erotyloidea, Nitiduloidea, and Cucujoidea *sensu stricto*.

While some families can be characterized based on distinctive synapomorphies like Cyclaxyridae (Gimmel et al., 2019), parallelism and convergence of morphological characters in Cucujoidea *sensu lato* make it difficult to assign unusual beetles into an appropriate family, and this is no truer than amber fossils where the critical assessment of more subtle characters is required. Moreover, some of the more critical characters used for distinguishing Cucujoidea *sensu stricto* and Erotyloidea are internal genitalic characters (Cai et al., 2022; Gimmel and Leschen, 2022). For example, *Pleuroceratos* Poinar and Kirejtshuk from mid-Cretaceous Burmese amber was originally placed in Silvanidae, but this placement was later rejected by Liu et al. (2019) primarily based on its oblique procoxae with exposed protrochantins. Kirejtshuk et al. (2019) subsequently transferred *Pleuroceratos* to Sphindidae. However, Tihelka et al. (2020) suggested that *Pleuroceratos* is a member of Phloeostichidae based on a phylogenetic analysis of morphological characters.

Like the taxonomic case for the placement of *Pleuroceratos*, we have discovered an enigmatic Burmese amber fossil that requires a critical assessment of characters necessary for familial placement. This new taxon has a dorsal habitus similar to modern-day Erotylidae and Lamingtoniidae (**Figure 1**), though, unlike these families that have 5-5-5 tarsomeres in both sexes, this fossil has 5-5-4 tarsomeres, which is diagnostic for males of several families of Cucujoidea *sensu stricto* (Lawrence and Ślipiński, 2013). The position of the fossil is therefore subjected to phylogenetic analyses, and the results are discussed in the context of the current classification of Cucujoidea.

Materials and methods

Materials

The Burmese amber specimen studied herein (**Figures 1–3**) originated from amber mines near Noije Bum (26°20′ N, 96°36′ E), Hukawng Valley, Kachin State, northern Myanmar. The specimen is deposited in the Nanjing Institute of Geology and Palaeontology (NIGP), Chinese Academy of Sciences, Nanjing, China. The amber piece was trimmed with a small table saw, ground with emery papers of different grit sizes, and finally polished with polishing powder.

Fossil imaging

Brightfield images were taken using a Zeiss Discovery V20 stereo microscope. Confocal images were obtained with a Zeiss LSM710 confocal laser scanning microscope, using the 488 nm Argon laser excitation line (Fu et al., 2021). Brightfield images were stacked in Helicon Focus 7.0.2 and Adobe Photoshop CC. Confocal images were stacked with color coding for depth in ZEN 3.4 (Blue Edition), or semi-manually stacked in Helicon Focus 7.0.2 and Adobe Photoshop CC. Images were further processed in Adobe Photoshop CC to adjust brightness and contrast.

Morphological phylogenetic analysis

To evaluate the systematic placement of the new species within Cucujoidea, we conducted formal morphological phylogenetic analyses under weighted parsimony. The data matrix (**Supplementary Data 1, 2**) was mainly derived from the previously published dataset by Leschen et al. (2005), which has the advantage of having been developed for Cucujoidea *sensu lato* prior to the classification in Cai et al. (2022). Therefore, we can determine if the new species is a member of Cucujoidea *sensu stricto*, Erotyloidea, or Nitiduloidea with outgroups from Cleroidea and Derodontoidea. The full matrix includes 66 adult and 33 larval characters, among which we successfully coded 36 adult characters for the new fossil.

Both parsimony analyses were performed under implied weights with R 4.1.0 (R Core Team, 2021) and the R package TreeSearch 1.0.1 (Smith, 2021; **Supplementary Data 3**). Parsimony analyses achieve the highest accuracy under a moderate weighting scheme (i.e., when concavity constants, *K*, are between 5 and 20) (Goloboff et al., 2018; Smith, 2019). Therefore, the concavity constant was set to 12 here, as suggested by Goloboff et al. (2018). In the unconstrained analysis, the clade support was generated based on 1,000 jackknife pseudoreplicates.

FIGURE 1
General habitus of *Alloterocucus atratus* Li, Leschen Liu, and Cai gen. et sp. nov., holotype, NIGP180056, under incident light. **(A)** Dorsal view. **(B)** Ventral view. Scale bars: 500 μm.

Since the morphology-based phylogeny of Cucujoidea was largely discordant with the molecular phylogeny, a constrained analysis was conducted as well (e.g., Slater, 2013; Fikáček et al., 2020). The interrelationships among extant families were fixed according to the synthesized tree (their figure 2) by McKenna et al. (2019). The intrafamilial relationships within extant Phloeostichidae and Priasilphidae were somewhat arbitrarily decided (partly based on Leschen et al., 2005). The fossil was allowed to move freely across the reference tree. An exhaustive search was conducted to find the best placement for the new genus.

The trees were drawn with the online tool iTOL 6.5.2 (Letunic and Bork, 2021) and graphically edited with Adobe Illustrator CC 2017.

Systematic paleontology

Order Coleoptera Linnaeus, 1758
Suborder Polyphaga Emery, 1886
Series Cucujiformia Lameere, 1938
Superfamily Cucujoidea Latreille, 1802
Family *incertae sedis*

Genus *Alloterocucus* Li, Leschen, Liu, and Cai gen. nov.

Type species

Alloterocucus atratus sp. nov.

FIGURE 2
General habitus of *Alloterocucus atratus* Li, Leschen Liu, and Cai gen. et sp. nov., holotype, NIGP180056, under confocal microscopy. **(A)** Dorsal view. **(B)** Ventral view. Scale bars: 400 μm.

Etymology

The generic name is formed based on the Greek "*allótrios*," strange, and "cucujoid," referring to its unique character combination within the traditional Cucujoidea. The name is masculine in gender.

Diagnosis

Body elongate. Postocular constriction absent (Figures 3A,G). Antennal club 3-segmented (Figure 3B). Apical maxillary palpomere subcylindrical, apically truncate (Figure 3A). Genal projections acute (Figure 3B). Ventral surface of head smooth, without any grooves (Figure 3B). Procoxal cavities externally open (Figure 3C). Mesocoxal cavities laterally open (Figure 3D). Pro- and mesotrochantins exposed (Figures 3C,D). Mesoventrite distinctly longer than half-length of metaventrite. Metaventral discrimen absent (Figure 3E). Elytra without well-developed punctures (Figures 3H,I). Tarsi 5-5-4 (probably in male) (Figures 3C–E).

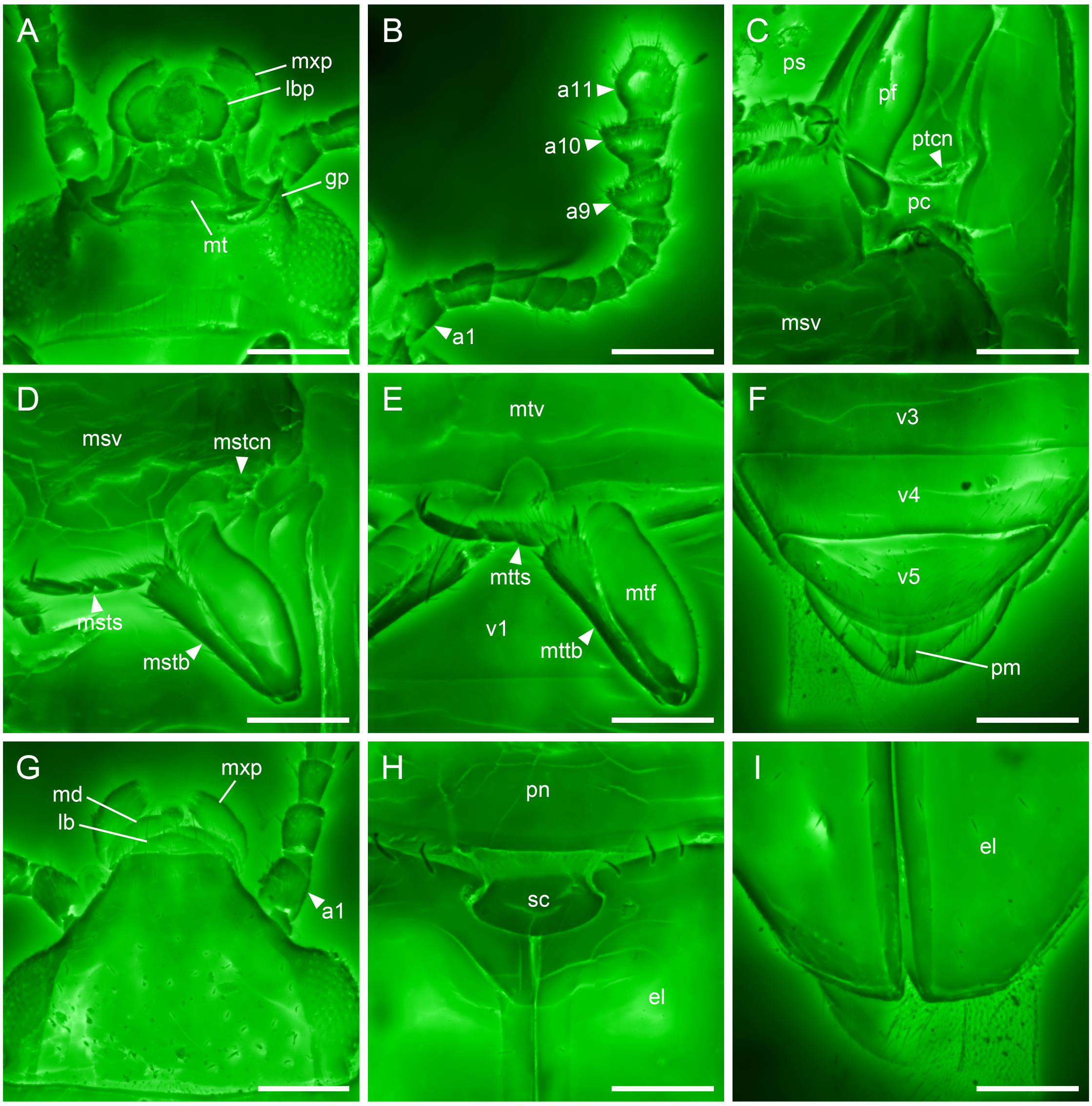

FIGURE 3
Details of *Alloterocucus atratus* Li, Leschen Liu, and Cai gen. et sp. nov., holotype, NIGP180056, under confocal microscopy. **(A)** Head, ventral view. **(B)** Antenna, ventral view. **(C)** Prothorax, ventral view. **(D)** Mid leg, ventral view. **(E)** Hind leg, ventral view. **(F)** Abdominal apex, ventral view. **(G)** Head, dorsal view. **(H)** Scutellum, dorsal view. **(I)** Elytral apex, dorsal view. a1–11, antennomeres 1–11; el, elytron; gp, genal projection; lb, labrum; lbp, labial palp; md, mandible; mstb, mesotibia; mstcn, mesotrochantin; msts, mesotarsus; msv, mesoventrite; mt, mentum; mtf, metafemur; mttb, metatibia; mtts, metatarsus; mtv, metaventrite; mxp, maxillary palp; pc, procoxa, pf, profemur; pm, paramere; pn, pronotum; ps, prosternum; ptcn, protrochantin; sc, scutellum; v1–5, ventrites 1–5. Scale bars: 100 µm.

Alloterocucus atratus Li, Leschen, Liu, and Cai sp. nov.

Material

Holotype, NIGP180056 (Figures 1–3), probably male (refer to Remarks), mid-Cretaceous (upper Albian to lower Cenomanian; Shi et al., 2012; Mao et al., 2018), from the amber mine near Noije Bum Village, Tanai Township, Myitkyina District, Kachin State, Myanmar.

Etymology

The specific name refers to the blackened (carbonized) appearance of the holotype.

Diagnosis

As for the genus.

Description

Body small, elongate, about 1.62 mm long, 0.56 mm wide.

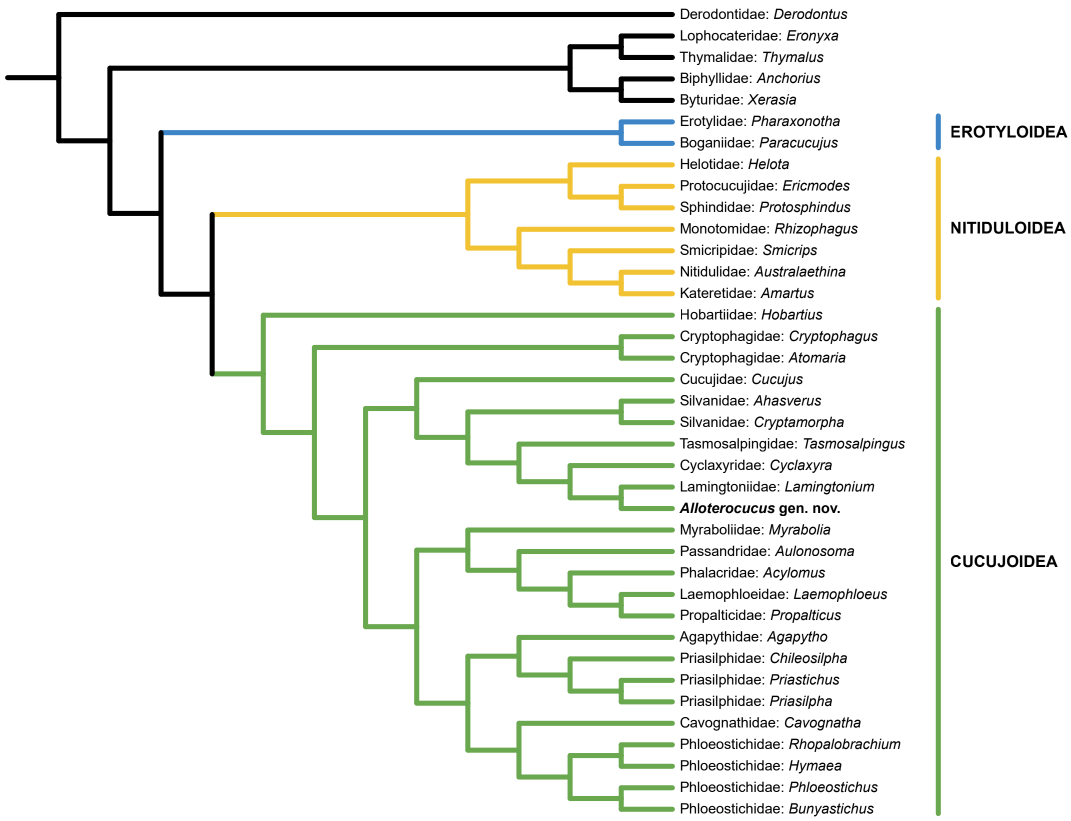

FIGURE 4
Placement of *Alloterocucus* Li, Leschen Liu, and Cai gen. nov. based on the single tree resulting from the constrained parsimony analysis.

Head prognathous, not constricted posteriorly, somewhat flattened; supra-antennal ridges or bead absent. Eyes moderately large, somewhat protuberant, entire, finely facetted, without interfacetal setae. Frontoclypeal suture absent; frontal carina on each side gradually narrowed anteriorly, almost reaching anterior end of clypeus; clypeus truncate anteriorly. Antennal insertions located laterally, hidden in dorsal view. Antennal grooves absent. Antennae 11-segmented, with distinct, 3-segmented club; antennomeres 9 and 10 transverse, slightly asymmetrical, with distinct rims. Labrum transverse, with broadly rounded apex. Maxillary palps with terminal palpomere relatively wide and somewhat cylindrical, not narrowed or dilated apically. Mentum basally with a transverse depression; deep or shallow lines extending backward from maxillary base absent. Genae produced anteriorly and acute. Ventral surface of head smooth, without any clear ridges or grooves.

Pronotum weakly transverse, about 1.4× as wide as long; lateral sides subparallel, with raised border; anterior angles slightly produced forward; posterior angles more or less right; posterior edge slightly bisinuate; disc lacking impressions. Prosternum in front of coxae longer than procoxal cavity; prosternal process relatively broad, laterally margined, with broadly rounded apex. Procoxal cavities transverse, without trochantinal notch, externally probably broadly open, with narrow lateral extensions. Procoxae not projecting. Protrochantins exposed.

Scutellar shield transverse, posteriorly broadly rounded. Elytra about 1.7 times as long as combined width and about 2.5 times as long as pronotum; width at base about as wide as width of pronotum; disc with scattered setae, without well-developed punctures; sutural striae present and complete from base to apex; epipleura gradually narrowed posteriorly, distinct toward apex; subapical gape absent. Mesoventrite relatively long and broad, about as long as half maximum width. Mesocoxal cavities moderately widely separated, open laterally, not closed by the meeting of mesoventrite and metaventrite. Mesotrochantins exposed. Mesometaventral junction slightly curved posteriorly, with metaventrite and mesoventrite coplanar. Metaventrite broad, without median discrimen. Metacoxae strongly transverse, narrowly separated; plates absent.

Legs relatively slender. Trochanterofemoral joints not strongly oblique, with femora not contacting coxae. Tibiae not parallel-sided and expanded toward apex with several stout setae along distal end; tibial spurs 2-2-2. Tarsi 5-5-4; tarsomeres not

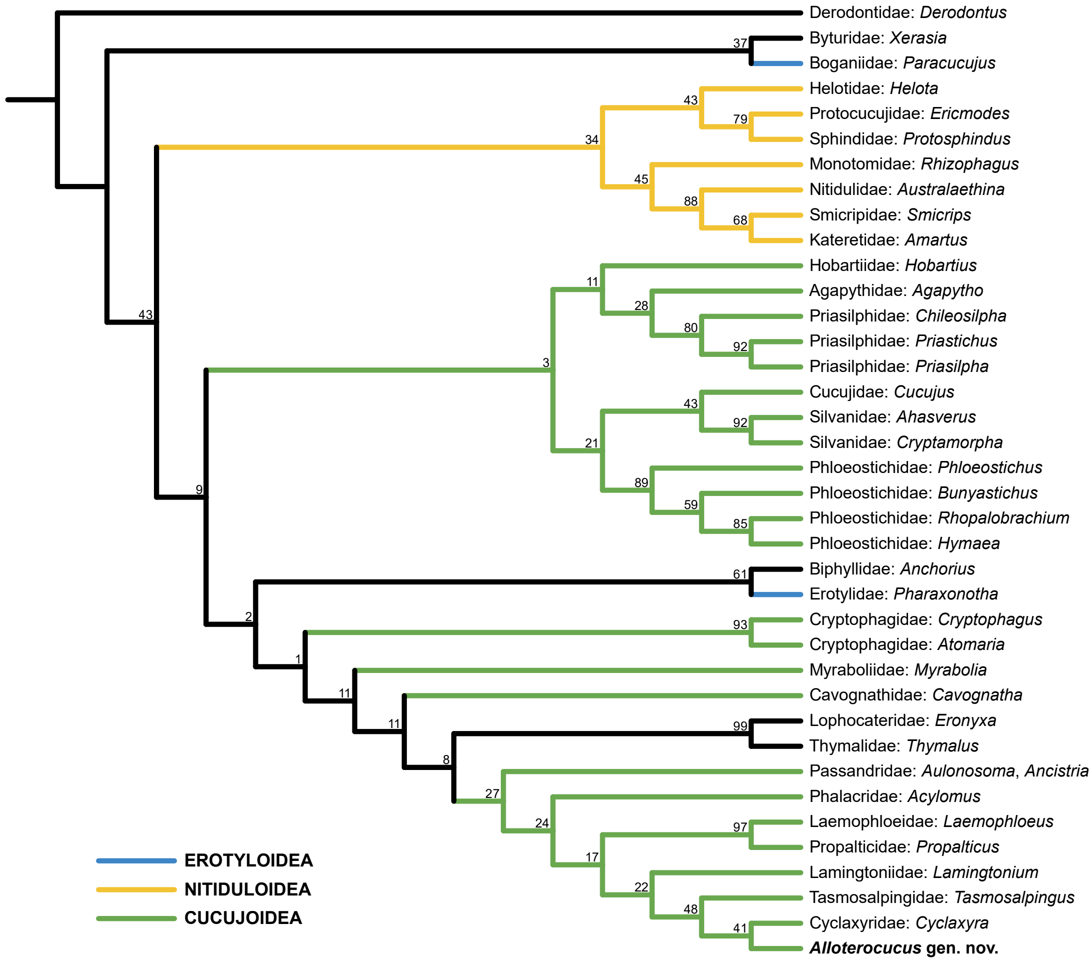

FIGURE 5
Placement of *Alloterocucus* Li, Leschen Liu, and Cai gen. nov. based on the single tree resulting from the unconstrained parsimony analysis.

lobed ventrally; basal tarsomeres short and subequal; apical tarsomere longer. Pretarsal claws simple.

Abdomen with five ventrites; ventrite 1 not much longer than 2; intercoxal process narrowly rounded apically.

Remarks

A pair of segments bearing setae protruding from the abdominal apex are visible in the holotype, which might be interpreted as the styli of the female ovipositor. However, the 5-5-4 tarsi in females rarely occur outside of Tenebrionoidea, and other characters of *Alloterocucus* do not fit well with Tenebrionoidea. For example, *Alloterocucus* does not have the heteromeroid type trochanterofemoral joint (not strongly oblique) nor does it have projecting procoxae, externally closed procoxal cavities, or well-exposed protrochantins present in some similar groups of tenebrionoids. Alternatively, the protruding segments may be interpreted as the elongate parameres of a male specimen, similar to what may be present in Erotylidae. Many Cucujoidea *sensu lato* have dimorphic tarsal formulae with males having 5-5-4 and females with 5-5-5, and it is plausible that our *Alloterocucus* specimen is a male.

Discussion

The character combination of *Alloterocucus* is not completely accordant with any present-day cucujoid or erotyloid families. Our constrained phylogenetic analysis (Figure 4) excludes *Alloterocucus* from Erotyloidea, despite having a similar habitus to some dacnine Erotylidae. Furthermore, we can exclude *Alloterocucus* from Erotyloidea by the presence of 5-5-4 tarsomeres, and lack of visible glandular ducts and open mesocoxal cavities, which exclude it from Erotylidae (see below), and the absence of the frontoclypeal suture, which excludes it from Boganiidae. It can also be excluded from Cryptophagidae by the open mesocoxal cavities, the subequal basal abdominal ventrites, and the elytra with complete (albeit narrow)

FIGURE 6
Extant representatives of Lamingtoniidae, Tasmosalpingidae, and Cyclaxyridae. **(A,B)** *Lamingtonium loebli* Lawrence and Leschen. **(C,D)** *Tasmosalpingus quadrispilotus* Lea. **(E,F)** *Cylaxyra politula* Broun. Scale bar: 500 µm.

epipluera and no subapical gape. *Alloterocucus* is placed within the Cucujoidea *sensu stricto* in a trio consisting of Tasmosalpingidae, Cyclaxyridae, and Lamingtoniidae, as sister to Lamingtoniidae.

In the unconstrained analysis (Figure 5), *Alloterocucus* was also grouped together with the same trio, but as sister to Cyclaxyridae. Therefore, we conclude that *Alloterocucus* is likely a member of Cucujoidea *sensu stricto* and related to these monogeneric Australasian families, which are absent from the fossil record, apart from Cyclaxyridae known from Burmese and Baltic ambers (Gimmel et al., 2019). *Alloterocucus* shares the following characters with these families: absence of postocular constriction, 3-segmented antennal club, externally open procoxal cavities, laterally open mesocoxal cavities, exposed pro- and mesotrochantins, and the absence of metaventral discrimen. Tasmosalpingidae and Cyclaxyridae additionally have 5-5-4 tarsi in males, and if we assume that the specimen of *Alloterocucus* is a male, this will support the classification of this genus in Cucujoidea *sensu stricto*.

Alloterocucus differs from Tasmosalpingidae, Cyclaxyridae, and Lamingtoniidae by having apically truncate terminal maxillary palpomeres, and the group bears different habitus and individual characters. Cyclaxyridae (Figures 6E,F) is characterized by an ovate and strongly convex body, well-developed antennal grooves, the absence of genal projections, and the presence of epipleural fovea (body elongate, antennal grooves absent, genal projections acute, and epipleural fovea absent in *Alloterocucus*). Tasmosalpingidae (**Figures 6C,D**) is somewhat sinuate in outline and is moderately convex. It also has characters including the antennal insertions exposed in dorsal view, clear antennal grooves, confused elytral punctation, and laterally opening setose cavities of the pronotum, which are all absent in *Alloterocucus*.

Alloterocucus most closely resembles members of Lamingtoniidae (**Figures 6A,B**), but lacks distinct dorsal punctation, and the pronotal width is equal to the combined widths of the elytra. If we make some assumptions on the character states of the mandible (i.e., lacking a tubercle, which can be inferred sometimes based on the shape of the clypeus), *Alloterocucus* can be keyed to couplet 26 in the family-group key provided by Leschen et al. (2005), and since it lacks the distinctive setose cavities on the prothorax of *Tasmosalpingus* Lea, *Alloterocucus* can be keyed further to couplet 27 containing Lamingtoniidae and Cucujidae. Apart from the raised supra-ocular carinae and the tarsal formula, which is 5-5-5 in extant Lamingtoniidae, it can be placed into this family and excluded from Cucujidae by having a well-defined antennal club. However, if we were able to see the internal structure of the meso-metaventral articulation, a key feature of this couplet, then we would be able to better place *Alloterocucus* in Cucujoidea *sensu stricto*.

Sen Gupta and Crowson (1969) excluded Lamingtoniidae from the cerylonid series (now Coccinelloidea) by the 5-5-5 tarsal formula, and from several families of the Cucujoidea *sensu lato* based on other characters, arguing that the family is related to Languriidae (now included in Erotylidae), as proposed by Kirejtshuk (2000) but rejected by Lawrence and Leschen (2003) based on larval and adult characters. The open mesocoxal cavities exclude *Alloterocucus* from Erotylidae, a character shared by most members of the family (but see Yoshida and Leschen, 2020) and support its affinity to Lamingtoniidae. *Alloterocucus* differs from members of *Lamingtonium* Sen Gupta and Crowson by several characters, including those mentioned above, but also the absence of curved longitudinal grooves extending backward from the maxillary base (present in *Lamingtonium binnaburrense* Sen Gupta and Crowson and *L. loebli* Lawrence and Leschen but absent in *L. thayerae* Lawrence and Leschen).

Two recent phylogenomic analyses recognized three separate lineages of Cucujoidea *sensu lato*. Thus, it was divided into three superfamilies by Cai et al. (2022): Erotyloidea, Nitiduloidea, and Cucujoidea *sensu stricto*. However, the relationships among the traditional cucujoid families are still far from being settled. Many small, rare families were not sampled in the analysis by Cai et al. (2022). McKenna et al. (2019) presented a synthesized tree in their figure 2, with all cucujoid families present, but some of the families (Smicripidae, Cyclaxyridae, Cavognathidae, Agapythidae, and Priasilphidae) were not included in their phylogenetic analysis and were manually inserted into the synthesized tree based on the results of McKenna et al. (2015). McKenna et al. (2015), however, though with a broader taxon sampling, used only eight genes, which may not be sufficient for inferring deeper interfamilial relationships as suggested by the discrepancies between their maximum likelihood and Bayesian inference analyses and low support. The topologies of many groups in McKenna et al. (2015) were largely inconsistent with the recent more comprehensive studies, especially for deeper nodes (McKenna et al., 2019; Cai et al., 2022). Thus, the positions of these families remain questionable until more genetic data are available.

Although Tasmosalpingidae and Lamingtoniidae were placed in the Cucujoidea-3 lineage (Cucujoidea *sensu stricto*; Cai et al., 2022) by McKenna et al. (2019), no molecular data exist for either family and their current placements are based on morphology. Moreover, the inconsistency between morphological (Leschen et al., 2005; Lawrence et al., 2011) and molecular (McKenna et al., 2019; Cai et al., 2022) phylogenies of Cucujoidea indicates that morphology-based studies may not be sufficient for properly resolving the systematic positions of cucujoid families due mainly to rampant convergences (McElrath et al., 2015). Thus, the superfamilial attribution of Tasmosalpingidae and Lamingtoniidae (as well as *Alloterocucus*) should still be viewed as contentious. The future inclusion of these families in a phylogenomic study will not only help better understand their phylogenetic relationships but also shed light on the position of the enigmatic fossil genus *Alloterocucus*.

Data availability statement

The original contributions presented in this study are included in the article/**Supplementary material**. The original confocal data are available in Zenodo repository (doi: 10.5281/zenodo.6717396). Further inquiries can be directed to the corresponding author.

Author contributions

C-YC and Y-DL conceived the study. C-YC and D-YH acquired and processed the specimen. Y-DL and Z-HL acquired and processed the photomicrographs. Y-DL performed the analyses. Y-DL and RABL drafted the manuscript, to which C-YC and Z-HL contributed. All authors commented on the manuscript and gave final approval for publication.

Funding

Financial support was provided by the Strategic Priority Research Program of the Chinese Academy of Sciences (XDB26000000), the National Natural Science Foundation of China (42222201 and 42288201), and the Second

Tibetan Plateau Scientific Expedition and Research project (2019QZKK0706). Y-DL was supported by a scholarship granted by the China Scholarship Council (202108320010). RABL was funded by Strategic Science Investment Funding for Crown Research Institutes from the Ministry of Business, Innovation, and Employment's Science and Innovation Group.

Acknowledgments

We are grateful to Rong Huang and Yan Fang for their technical help with confocal imaging. The editor and two reviewers provided helpful comments on the manuscript.

Conflict of interest

The authors declare that the research was conducted in the absence of any commercial or financial relationships that could be construed as a potential conflict of interest.

Publisher's note

All claims expressed in this article are solely those of the authors and do not necessarily represent those of their affiliated organizations, or those of the publisher, the editors and the reviewers. Any product that may be evaluated in this article, or claim that may be made by its manufacturer, is not guaranteed or endorsed by the publisher.

Supplementary material

The Supplementary Material for this article can be found online at: https://www.frontiersin.org/articles/10.3389/fevo.2022.972343/full#supplementary-material

References

Bocak, L., Barton, C., Crampton-Platt, A., Chesters, D., Ahrens, D., and Vogler, A. P. (2014). Building the Coleoptera tree-of-life for >8000 species: composition of public DNA data and fit with Linnaean classification. *Syst. Entomol.* 39, 97–110. doi: 10.1111/syen.12037

Cai, C., Tihelka, E., Giacomelli, M., Lawrence, J. F., Ślipiński, A., Kundrata, R., et al. (2022). Integrated phylogenomics and fossil data illuminate the evolution of beetles. *R. Soc. Open Sci.* 9:211771. doi: 10.1098/rsos.211771

Crowson, R. A. (1955). *The Natural Classification of the Families of Coleoptera*. London: Nathaniel Lloyd.

Fikáèek, M., Beutel, R. G., Cai, C., Lawrence, J. F., Newton, A. F., Solodovnikov, A., et al. (2020). Reliable placement of beetle fossils via phylogenetic analyses–Triassic *Leehermania* as a case study (Staphylinidae or Myxophaga?). *Syst. Entomol.* 45, 175–187. doi: 10.1111/syen.12386

Fu, Y.-Z., Li, Y.-D., Su, Y.-T., Cai, C.-Y., and Huang, D.-Y. (2021). Application of confocal laser scanning microscopy to the study of amber bioinclusions. *Palaeoentomology* 4, 266–278. doi: 10.11646/palaeoentomology.4.3.14

Gimmel, M. L., and Leschen, R. A. B. (2022). Revision of the genera of Picrotini (Coleoptera: Cryptophagidae: Cryptophaginae). *Acta Entomol. Mus. Natl. Pragae* 62, 61–109. doi: 10.37520/aemnp.2022.006

Gimmel, M. L., Szawaryn, K., Cai, C., and Leschen, R. A. B. (2019). Mesozoic sooty mould beetles as living relicts in New Zealand. *Proc. R. Soc. B* 286:20192176. doi: 10.1098/rspb.2019.2176

Goloboff, P. A., Torres, A., and Arias, J. S. (2018). Weighted parsimony outperforms other methods of phylogenetic inference under models appropriate for morphology. *Cladistics* 34, 407–437. doi: 10.1111/cla.12205

Hunt, T., Bergsten, J., Levkanicova, Z., Papadopoulou, A., John, O. S., Wild, R., et al. (2007). A comprehensive phylogeny of beetles reveals the evolutionary origins of a superradiation. *Science* 318, 1913–1916. doi: 10.1126/science.1146954

Kirejtshuk, A. G. (2000). On origin and early evolution of the superfamily Cucujoidea (Coleoptera, Polyphaga). Comments on the family Helotidae. *Kharkov Entomol. Soci. Gazette* 8, 8–38.

Kirejtshuk, A. G., Willig, C., and Chetverikov, P. E. (2019). Discovery of a new sphindid genus (Coleoptera, Sphindidae, Protosphindinae) in Cretaceous amber of Northern Myanmar and taxonomic notes. *Palaeoentomology* 2, 602–610. doi: 10.11646/palaeoentomology.2.6.11

Lawrence, J. F., and Leschen, R. A. B. (2003). "Review of Lamingtoniidae (Coleoptera: Cucujoidea) with descriptions of two new species," in *Systematics of Coleoptera: Papers Celebrating the Retirement of Ivan Löbl*, eds G. Cuccodoro and R. A. B. Leschen (Florida: International Associated Publishers), 905–919.

Lawrence, J. F., and Newton, A. F., Jr. (1982). Evolution and classification of beetles. *Ann. Rev. Ecol. Syst.* 13, 261–290. doi: 10.1146/annurev.es.13.110182.001401

Lawrence, J. F., and Ślipiński, A. (2013). *Australian Beetles. Volume 1: Morphology, Classification and Keys*. Clayton: CSIRO Publishing. doi: 10.1071/9780643097292

Lawrence, J. F., Ślipiński, A., Seago, A. E., Thayer, M. K., Newton, A. F., and Marvaldi, A. E. (2011). Phylogeny of the Coleoptera based on morphological characters of adults and larvae. *Ann. Zool.* 61, 1–217. doi: 10.3161/000345411X576725

Leschen, R. A. B., Lawrence, J. F., and Ślipiński, S. A. (2005). Classification of basal Cucujoidea (Coleoptera: Polyphaga): cladistic analysis, keys and review of new families. *Invert. Syst.* 19, 17–73. doi: 10.1071/IS04007

Letunic, I., and Bork, P. (2021). Interactive Tree Of Life (iTOL) v5: an online tool for phylogenetic tree display and annotation. *Nucleic Acids Res.* 49, W293–W296. doi: 10.1093/nar/gkab301

Liu, Z., Ślipiński, A., Wang, B., and Pang, H. (2019). The oldest Silvanid beetles from the Upper Cretaceous Burmese amber (Coleoptera, Silvanidae, Brontinae). *Cretac. Res.* 98, 1–8. doi: 10.1016/j.cretres.2019.02.002

Mao, Y., Liang, K., Su, Y., Li, J., Rao, X., Zhang, H., et al. (2018). Various amberground marine animals on Burmese amber with discussions on its age. *Palaeoentomology* 1, 91–103. doi: 10.11646/palaeoentomology.1.1.11

McElrath, T. C., Robertson, J. A., Thomas, M. C., Osborne, J., Miller, K. B., Mchugh, J. V., et al. (2015). A molecular phylogenetic study of Cucujidae s.l. (Coleoptera: Cucujoidea). *Syst. Entomol.* 40, 705–718. doi: 10.1111/syen.12133

McKenna, D. D., Wild, A. L., Kanda, K., Bellamy, C. L., Beutel, R. G., Caterino, M. S., et al. (2015). The beetle tree of life reveals that Coleoptera survived end-Permian mass extinction to diversify during the Cretaceous terrestrial revolution. *Syst. Entomol.* 40, 835–880. doi: 10.1111/syen.12132

McKenna, D. D., Shin, S., Ahrens, D., Balke, M., Beza-Beza, C., Clarke, D. J., et al. (2019). The evolution and genomic basis of beetle diversity. *Proc. Natl. Acad. Sci. U.S.A.* 116, 24729–24737. doi: 10.1073/pnas.1909655116

R Core Team (2021). *R: A Language and Environment for Statistical Computing*. Vienna: R Foundation for Statistical Computing.

Robertson, J. A., Ślipiński, A., Moulton, M., Shockley, F. W., Giorgi, A., Lord, N. P., et al. (2015). Phylogeny and classification of Cucujoidea and the recognition of a new superfamily Coccinelloidea (Coleoptera: Cucujiformia). *Syst. Entomol.* 40, 745–778. doi: 10.1111/syen.12138

Robertson, J. A., Whiting, M. F., and McHugh, J. V. (2008). Searching for natural lineages within the Cerylonid Series (Coleoptera: Cucujoidea). *Mol. Phylogenet. Evol.* 46, 193–205. doi: 10.1016/j.ympev.2007.09.017

Sen Gupta, T., and Crowson, R. A. (1969). On a new family of Clavicornia (Coleoptera) and a new genus of Languriidae. *Proc. R. Entomol. Soc. Lond. B* 38, 125–131. doi: 10.1111/j.1365-3113.1969.tb00245.x

Shi, G., Grimaldi, D. A., Harlow, G. E., Wang, J., Wang, J., Yang, M., et al. (2012). Age constraint on Burmese amber based on U-Pb dating of zircons. *Cretac. Res.* 37, 155–163. doi: 10.1016/j.cretres.2012.03.014

Slater, G. J. (2013). Phylogenetic evidence for a shift in the mode of mammalian body size evolution at the Cretaceous-Palaeogene boundary. *Methods Ecol. Evol.* 4, 734–744. doi: 10.1111/2041-210X.12084

Ślipiński, S. A., and Pakaluk, J. (1991). "Problems in the classification of the Cerylonid series of Cucujoidea (Coleoptera)," in *Advances in Coleopterology*, eds M. Zunino, X. Belles, and M. Blas (Barcelona: European Association of Coleopterology), 79–88.

Smith, M. R. (2019). Bayesian and parsimony approaches reconstruct informative trees from simulated morphological datasets. *Biol. Lett.* 15:20180632. doi: 10.1098/rsbl.2018.0632

Smith, M. R. (2021). TreeSearch: morphological phylogenetic analysis in R. *bioRxiv [Preprint]* doi: 10.1101/2021.11.08.467735

Tihelka, E., Huang, D., and Cai, C. (2020). Pleuroceratos jiewenae sp. nov.: A new Cretaceous phloeostichid beetle (Coleoptera: Cucujoidea: Phloeostichidae). *Palaeoentomology* 3, 248–259. doi: 10.11646/palaeoentomology.3.3.6

Timmermans, M. J. T. N., Barton, C., Haran, J., Ahrens, D., Culverwell, C. L., Ollikainen, A., et al. (2016). Family-level sampling of mitochondrial genomes in Coleoptera: compositional heterogeneity and phylogenetics. *Genome Biol. Evol.* 8, 161–175. doi: 10.1093/gbe/evv241

Yoshida, T., and Leschen, R. A. B. (2020). A new genus of Pharaxonothinae from Australia (Coleoptera: Erotylidae). *Zootaxa* 4838, 273–282. doi: 10.11646/zootaxa.4838.2.7

Zhang, S.-Q., Che, L.-H., Li, Y., Liang, D., Pang, H., Ślipiński, A., et al. (2018). Evolutionary history of Coleoptera revealed by extensive sampling of genes and species. *Nat. Commun.* 9:205. doi: 10.1038/s41467-017-02644-4

frontiers | Frontiers in Earth Science

TYPE Original Research
PUBLISHED 11 January 2023
DOI 10.3389/feart.2022.901573

OPEN ACCESS

EDITED BY
Peter David Roopnarine,
California Academy of Sciences,
United States

REVIEWED BY
Olev Vinn,
University of Tartu, Estonia
Tian Jiang,
China University of Geosciences, China

*CORRESPONDENCE
Chen-Yang Cai,
cycai@nigpas.ac.cn

SPECIALTY SECTION
This article was submitted to Paleontology, a section of the journal Frontiers in Earth Science

RECEIVED 22 March 2022
ACCEPTED 31 October 2022
PUBLISHED 11 January 2023

CITATION
Li Y-D, Ślipiński A, Huang D-Y and Cai C-Y (2023), New fossils of Sphaeriusidae from mid-Cretaceous Burmese amber revealed by confocal microscopy (Coleoptera: Myxophaga). *Front. Earth Sci.* 10:901573.
doi: 10.3389/feart.2022.901573

New fossils of Sphaeriusidae from mid-Cretaceous Burmese amber revealed by confocal microscopy (Coleoptera: Myxophaga)

Yan-Da Li[1,2], Adam Ślipiński[3], Di-Ying Huang[1] and Chen-Yang Cai[1,2]*

[1]State Key Laboratory of Palaeobiology and Stratigraphy, Nanjing Institute of Geology and Palaeontology, Chinese Academy of Sciences, Nanjing, China, [2]Bristol Palaeobiology Group, School of Earth Sciences, University of Bristol, Bristol, United Kingdom, [3]Australian National Insect Collection, CSIRO, Canberra, ACT, Australia

Sphaeriusidae is a small family of tiny aquatic beetles in the suborder Myxophaga. In this study we characterize two new sphaeriusid fossils from the mid-Cretaceous Burmese amber with the help of confocal laser scanning microscopy. *Sphaerius martini* Li & Cai **sp. nov.** displays similarities with both extant *Bezesporum* and *Sphaerius*, although it can be readily recognized based on the parallel-sided prosternum. *Crowsonaerius minutus* Li & Cai **gen. et sp. nov.** differs from other genera of Sphaeriusidae in having unreduced apical maxillary palpomeres, lowered mesoventrite, large metacoxal plates, separated mesotrochanter and mesofemur, and equal pretarsal claws. The present study demonstrates the efficacy of confocal microscopy in studying minute and dark bioinclusions in amber.

urn:lsid:zoobank.org:pub:6E6EDC20-744A-4A75-849A-4B6126628C15.

KEYWORDS
Sphaeriusidae, fossil, Burmese amber, confocal microscopy, Cretaceous

1 Introduction

The suborder Myxophaga is a comparatively small group of Coleoptera, with approximately 65 extant species (Mesaroš, 2013). Recent molecular phylogenies generally supported a sister-group relationship between Myxophaga and Archostemata (e.g., Mckenna et al., 2019; Cai et al., 2022). Although the earliest fossils of Myxophaga date back to the Late Triassic (Fikáček et al., 2020; Qvarnström et al., 2021), myxophagan fossils have only been very sparsely reported. Myxophaga currently comprises four extant families of minute aquatic or riparian beetles, i.e., Lepiceridae, Torridincolidae, Hydroscaphidae and Sphaeriusidae. However, the interrelationships among the four families remain unsettled, as morphology and molecular-based phylogenies have yielded inconsistent topologies (Beutel, 1999;

Lawrence et al., 2011; Mckenna et al., 2015, 2019; Yavorskaya et al., 2018; Jałoszyński et al., 2020).

Sphaeriusidae is a small but widespread family, with only two genera and about 25 species known in extant fauna (Lawrence & Ślipiński, 2013; Hall, 2019; Fikáček et al., 2022). The adults of Sphaeriusidae are easily characterized by the tiny and dorsally convex body, 11-segmented antennae, fused mesotrochanterofemora, large metacoxal plates, 3 (rarely 2)-segmented tarsi, and abdomen with only three ventrites of which the second is short (Reichardt, 1973; Löbl, 1995; Fikáček et al., 2022). As pointed out by Beutel & Raffaini (2003), due to the small size of sphaeriusids, detailed morphology for extant species can only be properly documented when SEM (scanning electronic microscopy) techniques are applied. However, only a few sphaeriusids have been imaged under SEM (e.g., Löbl, 1995; Liang & Jia, 2018; Yavorskaya et al., 2018; Fikáček et al., 2022), and some of them were not identified to species level (e.g., Beutel, 1999; Beutel & Raffaini, 2003; Kamezawa & Matsubara, 2012). As a result, the taxonomy of this group has been insufficiently studied and the its species-level diversity is likely strongly underestimated (Fikáček et al., 2022).

Due to their minute body size, sphaeriusids are rarely documented and often overlooked in the fossil record. The only two fossils known to date are *Burmasporum rossi* Kirejtshuk and *Bezesporum burmiticum* Fikáček et al., both from mid-Cretaceous Burmese amber (Kirejtshuk, 2009; Fikáček et al., 2022). However, some important characters were not observed for these two fossils, partly due to the usage of traditional brightfield imaging technique only. In this study we report two new species of Sphaeriusidae from the Burmese amber, and provide detailed photos obtained with confocal microscopy.

2 Materials and methods

2.1 Materials

The Burmese amber specimens studied herein originated from amber mines near Noije Bum (26°20′ N, 96°36’ E), Hukawng Valley, Kachin State, northern Myanmar. The amber specimens are deposited in the Nanjing Institute of Geology and Palaeontology (NIGP), Chinese Academy of Sciences, Nanjing, China. The amber pieces were trimmed with a small table saw, ground with emery paper of different grit sizes, and finally polished with polishing powder. The specimens of extant *Sphaerius* sp. for comparison were collected in Cabbage Tree Creek in New South Wales, Australia.

2.2 Imaging

Photographs under incident light were taken with a Zeiss Discovery V20 stereo microscope. Confocal images were obtained with a Zeiss LSM710 confocal laser scanning microscope, mainly using the 488 nm Argon laser excitation line. Additional excitation wavelengths were also tested for comparison. The extant *Sphaerius* specimens were sputter-coated with gold and photographed with a Hitachi SU 3500 scanning electron microscope. Images were stacked in Helicon Focus 7.0.2 and Adobe Photoshop CC. Images were further processed in Adobe Photoshop CC to adjust brightness and contrast.

2.3 Phylogenetic analyses

To evaluate the systematic placement of the two new fossils, a constrained morphology-based phylogenetic analyses was performed under Bayesian inference. The data matrix (Supplementary Data S1, S2) was mainly derived from a recently published dataset (Fikáček et al., 2022). The definitions of some characters were modified to fit the inclusion of the new fossils and additional outgroups. The constraining backbone tree was constructed based on the molecular results by Mckenna et al. (2019) and Fikáček et al. (2022). Only the fossil taxa were allowed to move freely across the backbone tree (e.g., Fikáček et al., 2020; Li et al., 2022).

The Bayesian analysis was performed using MrBayes 3.2.6 (Ronquist et al., 2012). Two MCMC analyses were run simultaneously, each with one cold chain and three heated chains. Trees were sampled every 1,000 generations. Analyses were stopped when the average standard deviation of split frequencies remained below 0.01. The first 25% of sampled trees were discarded as burn-in, and the remains were used to build a majority-rule consensus tree.

The tree was drawn with the online tool iTOL Version 6.6 (Letunic and Bork, 2021) and graphically edited with Adobe Illustrator CC 2017.

3 Systematic paleontology

Order Coleoptera Linnaeus, 1758.
Suborder Myxophaga Crowson, 1955.
Family Sphaeriusidae Erichson, 1845.

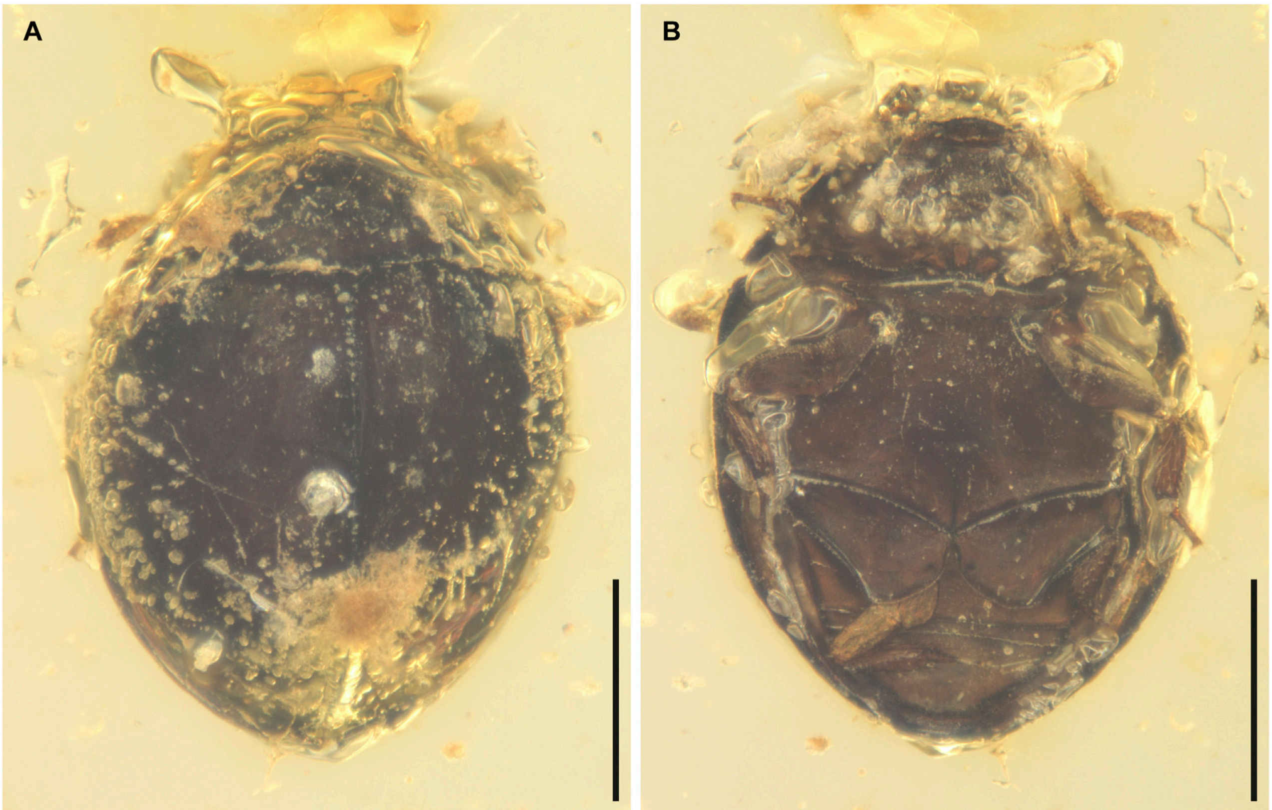

FIGURE 1
General habitus of *Sphaerius martini* Li and Cai sp. nov., holotype, NIGP178177, under incident light. **(A)** Dorsal view. **(B)** Ventral view. Scale bars: 200 μm.

3.1 *Sphaerius martini* Li & Cai sp. nov

3.1.1 Material

Holotype, NIGP178177 (Figures 1, 2), mid-Cretaceous (upper Albian to lower Cenomanian; Shi et al., 2012; Mao et al., 2018), from amber mine near Noije Bum Village, Tanai Township, Myitkyina District, Kachin State, Myanmar.

3.1.2 Etymology

The species is named after Dr. Martin Fikáček, an expert on aquatic beetles, who provided invaluable comments on the morphology of this fossil.

3.1.3 Diagnosis

Antennal club 4-segmented (Figure 2C). Prosternum parallel-sided (Figure 2C). Anterior margin of mesotrochanterofemur weakly sinuate (Figure 2B). Outer posterior edge of metacoxal plate slightly concave (Figure 2D). Metatarsus with very long setae (Figure 2D).

3.1.4 Description

Body broadly oval, strongly convex, about 0.60 mm long, 0.44 mm wide.

Head prognathous, short and broad. Antennal insertions exposed. Antennae 11-segmented with 4-segmented club; antennomeres 1 and 2 robust; antennomere 3 moderately elongated (about twice as long as 4); antennomeres 4–7 submoniliform; antennomeres 8–11 clubbed; antennomeres 9–11 with distinct setae. Mandibles flattened. Maxillary palps probably 4-segmented; apical palpomere distinctly shortened. Mentum subtrapezoidal, narrowing anteriad.

Pronotal disc convex, widest at hind angles. Scutellar shield small, triangular, posteriorly acute. Elytra complete, covering all abdominal segments. Prosternum parallel-sided. Mesoventrite relatively short, on the same plane with metaventrite, fused with the latter. Mesocoxae widely separated. Metaventrite broad, transverse. Metacoxae contiguous, extending laterally to elytra; metacoxal plates posteriorly not reaching abdominal ventrite 3, gradually narrowed laterally in outer half; outer posterior edge of metacoxal plate slightly concave. Legs short. Mesotrochanter fused with femur; anterior margin of mesotrochanterofemur

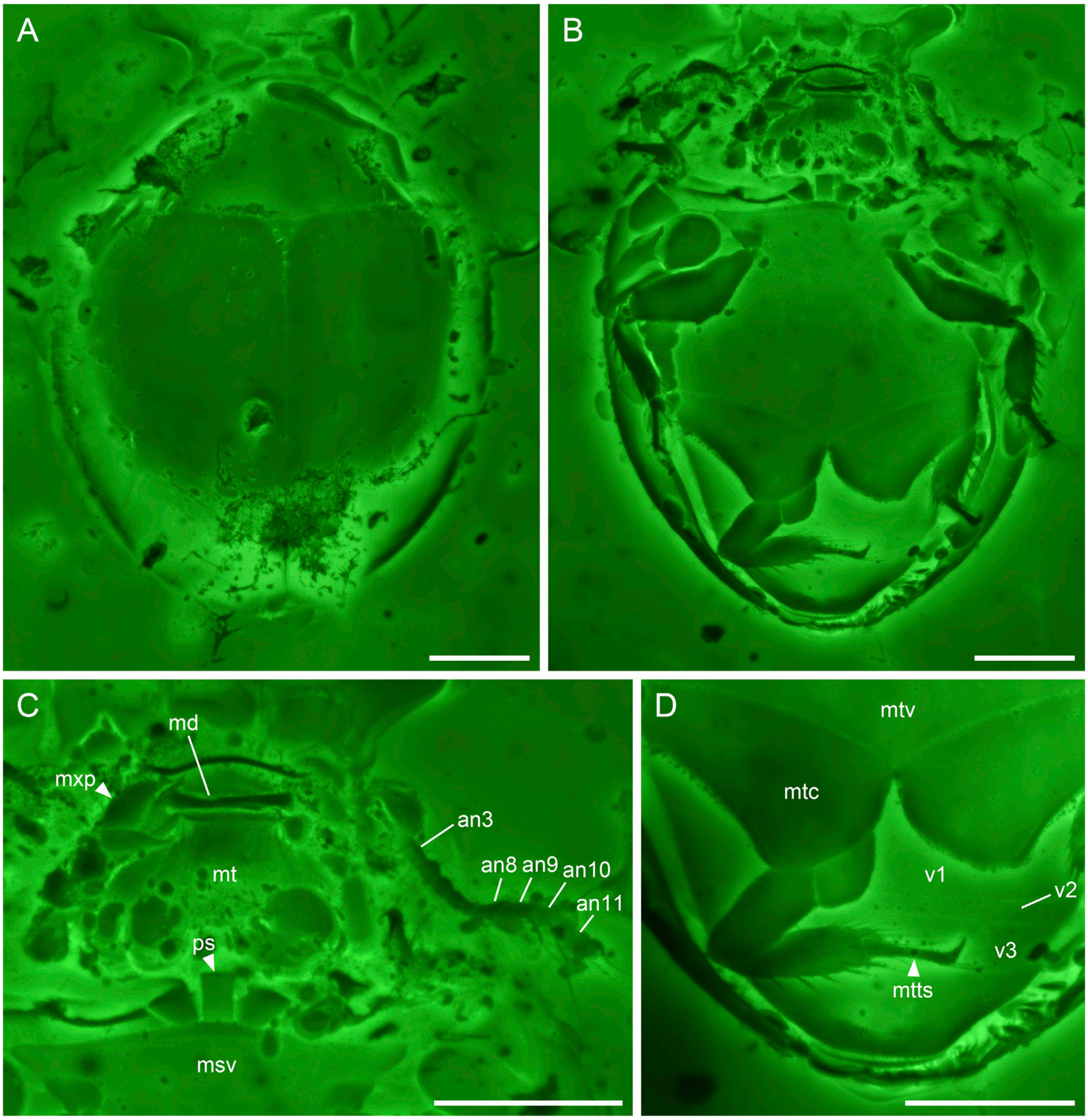

FIGURE 2
Sphaerius martini Li & Cai sp. nov., holotype, NIGP178177, under confocal microscopy. **(A)** Habitus, dorsal view. **(B)** Habitus, ventral view. **(C)** Head and prothorax, ventral view. **(D)** Hind leg and abdomen, ventral view. Abbreviations: an3–11, antennomeres 3–11; md, mandible; msv, mesoventrite; mt, mentum; mtc, metacoxa; mtts, metatarsus; mtv, metaventrite; mxp, maxillary palp; ps, prosternum; v1–3, ventrites 1–3. Scale bars: 100 μm.

weakly sinuate. Femora subglabrous. Tibiae and tarsi setose; metatarsus with very long setae. Pretarsal claws simple, unequal.

Abdomen with three ventrites; ventrite 2 distinctly shorter than ventrite 1 or 3.

3.1.5 Remarks

Sphaerius martini shares an overall similar morphology with extant Sphaeriusidae. It could be ruled out from the fossil genus *Burmasporum* Kirejtshuk based on the normal pronotal shape

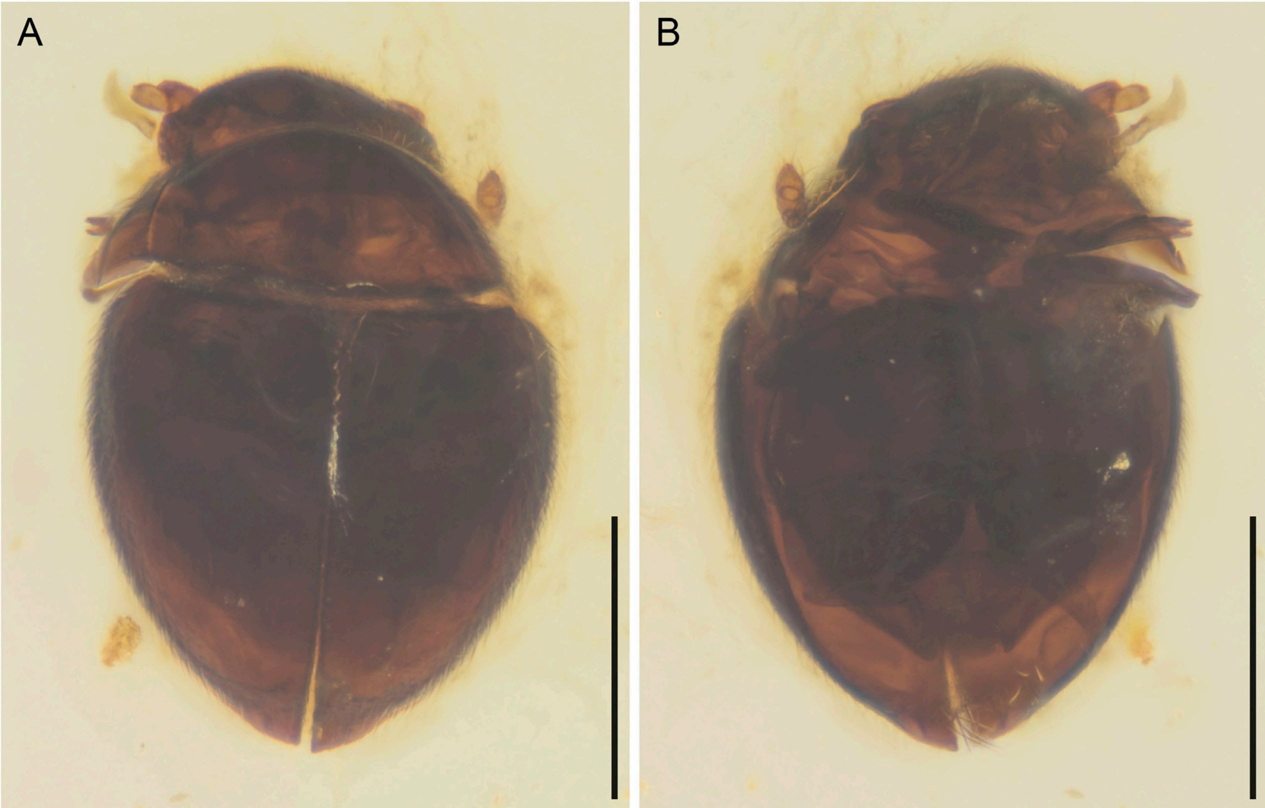

FIGURE 3
General habitus of *Crowsonaerius minutus* Li & Cai gen. et sp. nov., holotype, NIGP178178, under incident light. **(A)** Dorsal view. **(B)** Ventral view. Scale bars: 200 μm.

(Fikáček et al., 2022). Concerning the remaining two genera, the new species is tentatively assigned to *Sphaerius* Waltl, based on its subtrapezoidal mentum (Figure 2C), relatively short mesoventral plate (Figure 1B), and parallel-sided prosternum (Figure 2C) (mentum parallel-sided, mesoventral plate longer, and prosternum strongly T-shaped in *Bezesporum* Fikáček et al., 2022). Extant *Bezesporum* and aberrant *Sphaerius* (from Australia and South Africa) have strongly T-shaped (anteriorly expanded) prosternum. In other typical *Sphaerius* the prosternum is less T-shaped. The prosternum of *S. martini* is even narrower and parallel-sided, which is distinctive in Sphaeriusidae. *Sphaerius martini* differs from extant *Sphaerius* in having very long setae on metatarsus, and additionally from most *Sphaerius* species in having 4-segmented antennal club (see also Discussion). Some important characters were not possible to observe in the previously reported *Be. burmiticum*, which was also described from Burmese amber. Nevertheless, aside from the length of mesoventral plate, *S. martini* could also be differentiated from *Be. burmiticum* based on the shape of metacoxal plate. The outer posterior edge of metacoxal plate is slightly concave in *S. martini*, while that of *Be. burmiticum* is somewhat sinuate.

3.2 *Crowsonaerius minutus* Li & Cai gen. et sp. nov

3.2.1 Material

Holotype, NIGP178178 (Figures 3, 4), mid-Cretaceous (upper Albian to lower Cenomanian; Shi et al., 2012; Mao et al., 2018), from amber mine near Noije Bum Village, Tanai Township, Myitkyina District, Kachin State, Myanmar.

3.2.2 Etymology

The generic name (masculine in gender) is constructed based on the last name of Prof. Roy A. Crowson, in recognition of his great contribution to the systematics of Myxophaga, and the generic name *Sphaerius*, the type genus of Sphaeriusidae. The specific name refers to the minute size of the species.

3.2.3 Diagnosis

Antennae 11-segmented with 3(?)-segmented club (Figure 4C). Apical maxillary palpomere unreduced (compared to extant *Sphaerius*) (Figure 4C). Mesoventrite probably lower than metaventrite (Figure 4D). Metacoxal

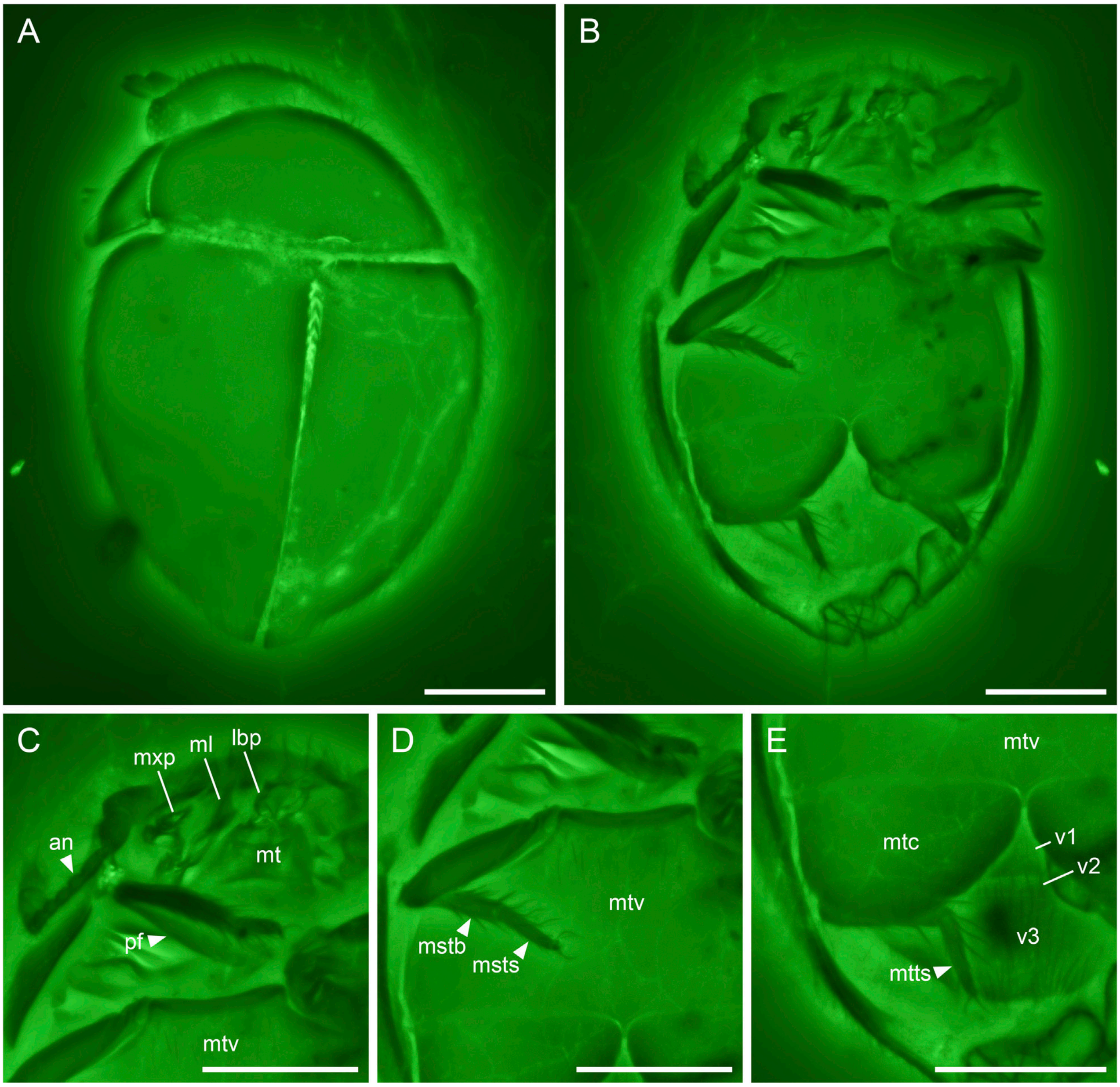

FIGURE 4
Crowsonaerius minutus Li & Cai gen. et sp. nov., holotype, NIGP178178, under confocal microscopy. **(A)** Habitus, dorsal view. **(B)** Habitus, ventral view. **(C)** Head and prothorax, ventral view. **(D)** Metathorax, ventral view. **(E)** Hind leg and abdomen, ventral view. Abbreviations: an, antenna; lbp, labial palp; mstb, mesotibia; msts, mesotarsus; ml, mala; mt, mentum; mtc, metacoxa; mtts, metatarsus; mtv, metaventrite; mxp, maxillary palp; pf, profemur; v1–3, ventrites 1–3. Scale bars: 100 μm.

plates nearly contiguous, not narrowed laterally (Figure 4E). Mesotrochanter not fused with femur (Figure 4D). Tarsi *Sphaerius*-like; metatarsus without very long setae. Pretarsal claws equal (Figures 4C–E). Abdomen with three ventrites of which the second is short (Figure 4E).

3.2.4 Description

Body broadly oval, strongly convex, about 0.49 mm long, 0.33 mm wide.

Head prognathous, short and broad. Antennal insertions exposed. Antennae 11-segmented with 3(?)-segmented club;

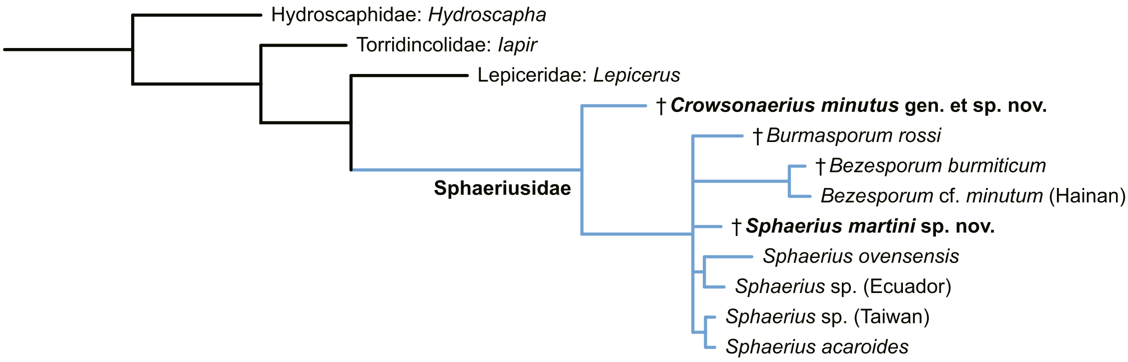

FIGURE 5
Suggested placement of *Sphaerius martini* and *Crowsonaerius minutus* within Sphaeriusidae. Tree resulting from the Bayesian analysis constrained by a molecular backbone tree.

antennomeres 1 and 2 robust; antennomere 3 moderately elongated (about twice as long as 4); antennomeres 9(?)–11 clubbed. Maxilla with undivided mala; maxillary palps 4-segmented; apical palpomere not distinctly shortened, seemingly apically pointed. Mentum subtrapezoidal, narrowing anteriad.

Pronotal disc convex, widest at hind angles. Scutellar shield small, triangular, posteriorly acute. Elytra complete, covering all abdominal segments. Mesoventrite not seen, probably lower than metaventrite. Mesocoxae widely separated. Metaventrite broad, transverse. Metacoxae nearly contiguous, extending laterally to elytra; metacoxal plates large, posteriorly reaching abdominal ventrite 3, gradually narrowed medially in medial half. Hind wing present; margin lined with setae. Legs short. Mesotrochanter not fused with femur. Femora glabrous. Tibiae and tarsi setose; metatarsus without very long setae. Pretarsal claws simple, equal.

Abdomen with three ventrites; ventrite 2 distinctly shorter than ventrite 1 or 3.

3.2.5 Remarks

The key character assigning *Crowsonaerius* to Sphaeriusidae is the abdomen with three ventrites of which the second is short (Figure 4E). Such an abdomen with three ventrites is unknown in any other beetle families (Lawrence et al., 2011). Additional characters excluding *Crowsonaerius* from other families in Myxophaga include the presence of antennal club (Figure 3B), elongated antennomere 3 (Figure 4C), and large and contiguous metacoxal plates (Figure 4E).

Crowsonaerius could be separated from all other sphaeriusid genera based on its equal pretarsal claws. In both *Sphaerius* and *Bezesporum*, as well as *Burmasporum*, one of the tarsal claws is strongly reduced in all three pairs of legs (Fikáček et al., 2022). *Crowsonaerius* also differs from other genera in the shape of metacoxal plate. *Sphaerius*, *Bezesporum* and *Burmasporum* have metacoxal plates gradually narrowed laterally, while in *Crowsonaerius* the edges of metacoxal plates are not laterally converged. The metacoxal plates of *Crowsonaerius* are also larger, reaching the posterior edge of ventrite 1. In addition, *Crowsonaerius* is distinctive in having a lowered mesoventrite (without clear mesoventral plate), and separated mesotrochanter and mesofemur. In extant *Sphaerius* and *Bezesporum*, the mesoventral plate is on the same plane with metaventrite and fused with the latter, and the mesotrochanter and mesofemur are fused together (Fikáček et al., 2022) (the states of these characters are unclear in *Burmasporum*). The apical maxillary palpomere of *Crowsonaerius* seems not to be distinctly reduced. Within Myxophaga, such a normal apical maxillary palpomere was previously only known in Lepiceridae, while in the other three families the apical maxillary palpomere is distinctly reduced.

The retention of equal pretarsal claws and separated mesotrochanter and mesofemur supports *Crowsonaerius* as the basalmost member within Sphaeriusidae (Figure 5).

4 Discussion

4.1 Morphological distinction between *Sphaerius* and *Bezesporum*

Extant sphaeriusids are generally highly uniform in external morphology, and has long been classified in a single genus. Only very recently, Fikáček et al. (2022) divided *Sphaerius* into two genera, *Sphaerius s.s.* (Figure 6) and *Bezesporum*, based on both morphological and molecular evidences. Extant *Bezesporum* differs from *Sphaerius s.s.* in a series of characters, including the 4-segmented antennal club, parallel-sided mentum, anteriorly converging clypeus, relatively long mesoventral plate, and metatarsus with very long setae. Typical *Sphaerius* also has a relatively narrow prosternum, whereas the prosternum of extant *Bezesporum* and a few aberrant *Sphaerius* is wider (Figure 6E). Fikáček et al. (2022) also reported the fossil *Be. burmiticum*, where the generic assignment was made based solely

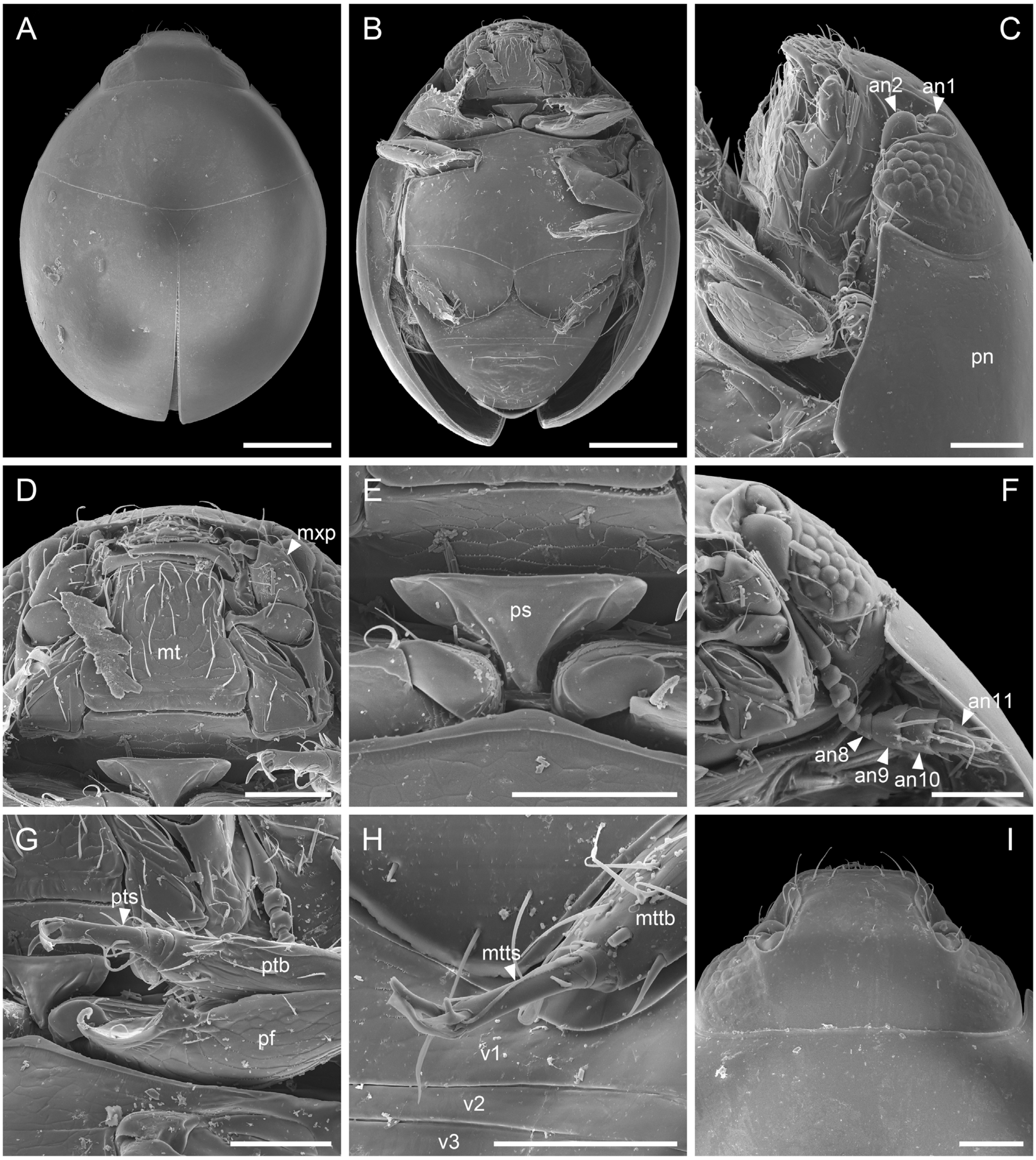

FIGURE 6
Extant *Sphaerius* sp. from Australia, under scanning electron microscopy. **(A)** Habitus, dorsal view. **(B)** Habitus, ventral view. **(C)** Head and prothorax, lateral view. **(D)** Mouthparts, ventral view. **(E)** Prosternum, ventral view. **(F)** Antenna. **(G)** Fore leg. **(H)** Metatarsus. **(I)** Head, dorsal view. Abbreviations: an1–11, antennomeres 1–11; mt, mentum; mttb, metatibia; mtts, metatarsus; mxp, maxillary palp; pf, profemur; pn, pronotum; ps, prosternum; ptb, protibia; pts, protarsus; v1–3, ventrites 1–3. Scale bars: 150 μm in **(A,B)**, 50 μm in **(C–I)**.

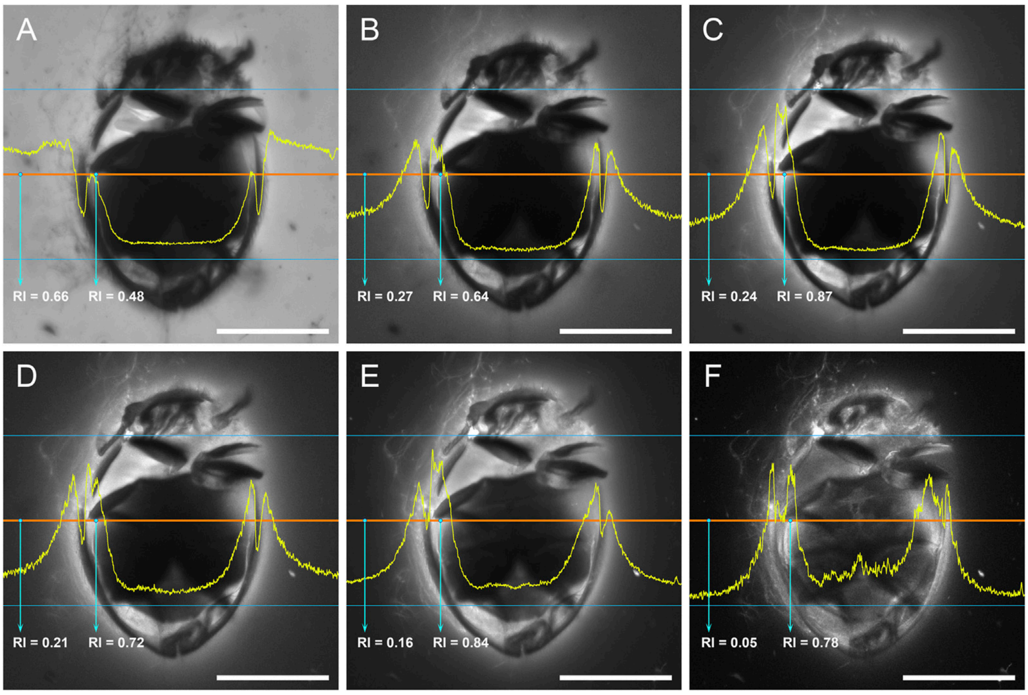

FIGURE 7
Crowsonaerius minutus in amber under confocal microscopy, excited with laser of different wavelengths. The yellow profile shows the relative intensity (RI) along the mid-section (red line). **(A)** 405 nm (Diode 450-30). **(B)** 458 nm (Argon). **(C)** 488 nm (Argon). **(D)** 514 nm (Argon). **(E)** 561 nm (DPSS 561-10). **(F)** 633 nm (HeNe633). Scale bars: 200 μm.

on the 4-segmented antennal club and the relatively long mesoventral plate. The states of other diagnostic characters mentioned above are unknown in *Be. burmiticum*.

The better preservation state and the usage of confocal microscopy enable us to extract more morphological information from the newly discovered *S. martini*. The new species generally shares more similar characters with extant *Sphaerius* (e.g., mentum, prosternum and mesoventrite). However, *S. martini* has very long setae on metatarsus and a somewhat sinuate anterior margin of mesotrochanterofemur, which are actually characteristic of *Bezesporum*, whereas such very long setae are absent and the anterior mesotrochanterofemoral margin is straight in extant *Sphaerius*. Generally *Sphaerius* should have 3-segmented antennal clubs (although some specimens from Japan or Taiwan have more or less 4-segmented antennal clubs; Kamezawa & Matsubara, 2012: figure 4A; Fikáček et al., 2022: figure 4C). The antennal club of *S. martini* is clearly 4-segmented, which has also been proposed as a diagnostic character of *Bezesporum*. As mentioned by Fikáček et al. (2022), the *Sphaerius* species from Australia and South Africa (aberrant *Sphaerius*) exhibit a somewhat intermediate morphology between *Bezesporum* and typical *Sphaerius*. The discovery of *S. martini* further highlights the morphological variability within the *Bezesporum* + *Sphaerius* group. As no molecular data are available for *S. martini* (also considering that few informative morphological characters are available for sphaeriusids), it would be hard to accurately determine its systematic position within this group. More comprehensive studies on the morphological and genetic diversity of extant Sphaeriusidae might be helpful to further justify (or reject) the separation of *Bezesporum* from *Sphaerius*.

4.2 Relationship between Sphaeriusidae and other myxophagan families

Regarding the position of Sphaeriusidae within Myxophaga, morphological phylogenetic studies have suggested a relationship of (Lepiceridae + (Torridincolidae + (Sphaeriusidae + Hydroscaphidae))) (Beutel, 1999; Lawrence et al., 2011; Yavorskaya et al., 2018; Jałoszyński et al., 2020). The monophyly of Myxophaga excluding Lepiceridae is partly supported by their distinctly reduced apical maxillary palpomere, while Lepiceridae has normal-sized apical maxillary palpomere and represents the basalmost lineage in Myxophaga. However, this morphology-based phylogeny was not supported by molecular studies, where Sphaeriusidae was sister to Lepiceridae, and Hydroscaphidae was the basalmost lineage in Myxophaga (Mckenna et al., 2015; Mckenna et al., 2019). The discovery of unreduced apical maxillary palpomere in *Crowsonaerius* seems to be in accordance with the molecular-based phylogeny. Under this scenario, the common ancestor of Lepiceridae and Sphaeriusidae might have a normal apical maxillary palpomere, and the palpomere was later reduced in crown-group Sphaeriusidae.

4.3 Confocal imaging for fossil insects in amber

Scanning electron microscope is an excellent tool for examining the surface morphology of extant insects. SEM can achieve a higher resolution than optical methods, and therefore can properly record fine microstructures (e.g., microsculptures, hairs or sensilla). SEM is helpful for the observation of macrostructure as well. Compared with ordinary optical images, the structural boundaries are generally more clearly outlined in SEM images, especially for dark specimens (e.g., Figure 6). For the study of fossil insects in amber, fluorescence microscopy can achieve a somewhat similar purpose, where fluorescence generated around the insect surface clearly outlines the structural boundaries (Fu et al., 2021). Compared with widefield fluorescence microscopy, confocal laser scanning microscopy could further achieve a higher signal to noise ratio due to the exclusion of out of focus lights. Many studies have shown that confocal microscopy is effective for imaging insects (and other arthopods) in amber (e.g., Yamamoto et al., 2016; Li et al., 2021a; Li et al., 2021b; Su et al., 2021; Vorontsov & Voronezhskaya, 2022).

In the present study, we further test the effect of using different excitation wavelengths when imaging amber fossils with confocal microscopy. When excited with light of short wavelength (e.g., 405 nm; Figure 7A), the amber matrix has strong emission, which is consistent with previous studies (without inclusions involved) (e.g., Zhang et al., 2020a; Zhang et al., 2020b). The strong emission from the amber matrix masks the useful signal from the boundary layer between the amber matrix and the fossil inclusion; thus it is not ideal for the imaging of the inclusion. When the excitation wavelength become longer, the emission from amber matrix become weaker, and the emission from the boundary layer become comparatively stronger, which clearly illustrates the surface structures of the inclusion (Figures 7B–E). At the longest excitation wavelength we tested (633 nm; Figure 7F), the emission from amber matrix is very low, leading to the highest contrast of targeted structures. The chemical compounds behind the amber fluorescence have been suggested as various aromatic hydrocarbons (e.g., Bellani et al., 2005; Chekryzhov et al., 2014; Bechtel et al., 2016), although it is difficult to accurately determine their specific composition. It appears that during the formation of amber, the inclusion might have been involved in some chemical reactions with the amber matrix, leading to a shift of boundary layer emission toward longer wavelength (e.g., aggregation of aromatics; Vogler, 2018).

Although the exact mechanism behind this phenomenon is not yet clear, our study nevertheless suggests that using excitation light of longer wavelengths may further improve the signal to noise ratio, especially for amber specimens with strong background fluorescence. However, the emission may be too weak at the red region (e.g., when excited at 633 nm), therefore requiring a time-consuming exposure. Based on our experience, an excitation wavelength of 488–561 nm could generally produce ideal confocal photos for most inclusions from Burmese amber.

Data availability statement

The original contributions presented in the study are included in the article/Supplementary Material. The original confocal data are available in Zenodo repository (doi: 10.5281/zenodo.7319965). Further inquiries can be directed to the corresponding author.

Author contributions

C-YC and Y-DL conceived the study. C-YC, D-YH, and AS acquired and processed the specimens. Y-DL acquired and processed the photomicrographs and performed the analysis. Y-DL drafted the manuscript, to which C-YC and AS contributed. All authors commented on the manuscript and gave final approval for publication.

Funding

Financial support was provided by the Second Tibetan Plateau Scientific Expedition and Research project (2019QZKK0706), the Strategic Priority Research Program of the Chinese Academy of Sciences (XDB26000000), and the National Natural Science Foundation of China (42222201 and 42288201). Y-DL is supported by a scholarship granted by the China Scholarship Council (202108320010).

Acknowledgments

We are grateful to Martin Fikáček for the detailed discussion. We thank Rong Huang and Yan Fang for technical help with confocal imaging, and Chun-Zhao Wang for technical help with SEM imaging. The editor and two reviewers provided helpful comments on the manuscript.

Conflict of interest

The authors declare that the research was conducted in the absence of any commercial or financial relationships that could be construed as a potential conflict of interest.

Publisher's note

All claims expressed in this article are solely those of the authors and do not necessarily represent those of their affiliated organizations, or those of the publisher, the editors and the reviewers. Any product that may be evaluated in this article, or claim that may be made by its manufacturer, is not guaranteed or endorsed by the publisher.

Supplementary material

The Supplementary Material for this article can be found online at: https://www.frontiersin.org/articles/10.3389/feart.2022.901573/full#supplementary-material

References

Bechtel, A., Chekryzhov, I. Y., Nechaev, V. P., and Kononov, V. V. (2016). Hydrocarbon composition of Russian amber from the Voznovo lignite deposit and Sakhalin Island. *Int. J. Coal Geol.* 167, 176–183. doi:10.1016/j.coal.2016.10.005

Bellani, V., Giulotto, E., Linati, L., and Sacchi, D. (2005). Origin of the blue fluorescence in Dominican amber. *J. Appl. Phys*. 97, 016101. doi:10.1063/1.1829395

Beutel, R. G. (1999). Phylogenetic analysis of Myxophaga (Coleoptera) with a redescription of *Lepicerus horni* (Lepiceridae). *Zool. Anz.* 237, 291–308.

Beutel, R. G., and Raffaini, G. B. (2003). First record of Sphaeriusidae for Argentina. *Koleopterol. Rundsch.* 73, 1–6.

Cai, C., Tihelka, E., Giacomelli, M., Lawrence, J. F., Slipinski, A., Kundrata, R., et al. (2022). Integrated phylogenomics and fossil data illuminate the evolution of beetles. *R. Soc. Open Sci.* 9, 211771. doi:10.1098/rsos.211771

Chekryzhov, I. Y., Nechaev, V. P., and Kononov, V. V. (2014). Blue-fluorescing amber from Cenozoic lignite, eastern Sikhote-Alin, Far East Russia: Preliminary results. *Int. J. Coal Geol.* 132, 6–12. doi:10.1016/j.coal.2014.07.013

Fikáček, M., Beutel, R. G., Cai, C., Lawrence, J. F., Newton, A. F., Solodovnikov, A., et al. (2020). Reliable placement of beetle fossils via phylogenetic analyses – Triassic *Leehermania* as a case study (Staphylinidae or Myxophaga?) *Syst. Entomol.* 45, 175–187. doi:10.1111/syen.12386

Fikáček, M., Yamamoto, S., Matsumoto, K., Beutel, R. G., and Maddison, D. R. (2022). Phylogeny and systematics of Sphaeriusidae (Coleoptera: Myxophaga): minute living fossils with underestimated past and present-day diversity. *Syst. Entomol.* doi:10.1111/syen.12571

Fu, Y.-Z., Li, Y.-D., Su, Y.-T., Cai, C.-Y., and Huang, D.-Y. (2021). Application of confocal laser scanning microscopy to the study of amber bioinclusions. *Palaeoentomology* 4, 266–278. doi:10.11646/palaeoentomology.4.3.14

Hall, W. E. (2019). "Sphaeriusidae Erichson, 1845," in *Australian beetles. Volume 2: Archostemata, Myxophaga, adephaga, polyphaga (part)*. Editors A. Ślipiski and J. F. Lawrence (Collingwood, Australia: CSIRO Publishing), 15–17.

Jałoszyński, P., Luo, X.-Z., Hammel, J. U., Yamamoto, S., and Beutel, R. G. (2020). The mid-Cretaceous †*Lepiceratus* gen. nov. and the evolution of the relict beetle family Lepiceridae (Insecta: Coleoptera: Myxophaga). *J. Syst. Palaeontol.* 18, 1127–1140. doi:10.1080/14772019.2020.1747561

Kamezawa, H., and Matsubara, Y. (2012). A faunistic note on a species of the genus *Sphaerius* Waltl, 1838 (Myxophaga, Sphaeriusidae) collected from Tamagawa river, Tokyo Metropolis, central Honshu. *Sayabane* (6), 25–27.

Kirejtshuk, A. G. (2009). A new genus and species of Sphaeriusidae (Coleoptera, Myxophaga) from Lower Cretaceous Burmese amber. *Denisia* 26, 99–102.

Lawrence, J. F., and Ślipiński, A. (2013). *Australian beetles. Volume 1: morphology, classification and keys*. Collingwood, Australia: CSIRO Publishing.

Lawrence, J. F., Ślipiński, A., Seago, A. E., Thayer, M. K., Newton, A. F., and Marvaldi, A. E. (2011). Phylogeny of the Coleoptera based on morphological characters of adults and larvae. *Ann. Zool.* 61, 1–217. doi:10.3161/000345411x576725

Letunic, I., and Bork, P. (2021). Interactive tree of life (iTOL) v5: An online tool for phylogenetic tree display and annotation. *Nucleic Acids Res.* 49, W293–W296. doi:10.1093/nar/gkab301

Li, Y.-D., Kundrata, R., Packova, G., Huang, D.-Y., and Cai, C.-Y. (2021b). An unusual elateroid lineage from mid-Cretaceous Burmese amber (Coleoptera: Elateroidea). *Sci. Rep.* 11, 21985. doi:10.1038/s41598-021-01398-w

Li, Y.-D., Newton, A. F., Huang, D.-Y., and Cai, C.-Y. (2022). The first fossil of Nossidiinae from mid-Cretaceous amber of northern Myanmar (Coleoptera: Ptiliidae). *Front. Ecol. Evol.* 10, 911512. doi:10.3389/fevo.2022.911512

Li, Y.-D., Tihelka, E., Leschen, R. A. B, Yu, Y., Ślipiński, A., Pang, H., Huang, D., et al. (2021a). An exquisitely preserved tiny bark-gnawing beetle (Coleoptera: Trogossitidae) from mid-Cretaceous Burmese amber and the phylogeny of Trogossitidae. *J. Zool. Syst. Evol. Res.* 59, 1939–1950. doi:10.1111/jzs.12515

Liang, Z.-L., and Jia, F. (2018). A new species of *Sphaerius* Waltl from China (Coleoptera, Myxophaga, Sphaeriusidae). *ZooKeys* 808, 115–121. doi:10.3897/zookeys.808.30600

Löbl, I. (1995). New species of terrestrial *Microsporus* from the Himalaya (Coleoptera: Microsporidae). *Entomol. Blätter* 91, 129–138.

Mao, Y., Liang, K., Su, Y., Li, J., Rao, X., Zhang, H., et al. (2018). Various amberground marine animals on Burmese amber with discussions on its age. *Palaeoentomology* 1, 91–103. doi:10.11646/palaeoentomology.1.1.11

McKenna, D. D., Shin, S., Ahrens, D., Balke, M., Beza-Beza, C., Clarke, D. J., et al. (2019). The evolution and genomic basis of beetle diversity. *Proc. Natl. Acad. Sci. U.S.A.* 116, 24729–24737. doi:10.1073/pnas.1909655116

McKenna, D. D., Wild, A. L., Kanda, K., Bellamy, C. L., Beutel, R. G., Caterino, M. S., et al. (2015). The beetle tree of life reveals that Coleoptera survived end-Permian mass extinction to diversify during the Cretaceous terrestrial revolution. *Syst. Entomol.* 40, 835–880. doi:10.1111/syen.12132

Mesaroš, G. (2013). Sphaeriusidae (Coleoptera, Myxophaga): A new beetle family to the fauna of Serbia. *Bull. Nat. Hist. Mus.* 6, 71–74. doi:10.5937/bnhmb1306071m

Qvarnström, M., Fikáček, M., Wernström, J. V., Huld, S., Beutel, R. G., Arriaga-Varela, E., et al. (2021). Exceptionally preserved beetles in a Triassic coprolite of putative dinosauriform origin. *Curr. Biol.* 31, 3374–3381. doi:10.1016/j.cub.2021.05.015

Reichardt, H. (1973). A critical study of the suborder Myxophaga, with a taxonomic revision of the Brazilian Torridincolidae and Hydroscaphidae (Coleoptera). *Arq. Zool.* 24, 73–162. doi:10.11606/issn.2176-7793.v24i2p73-162

Ronquist, F., Teslenko, M., Van Der Mark, P., Ayres, D. L., Darling, A., Höhna, S., et al. (2012). MrBayes 3.2: Efficient Bayesian phylogenetic inference and model choice across a large model space. *Syst. Biol.* 61, 539–542. doi:10.1093/sysbio/sys029

Shi, G., Grimaldi, D. A., Harlow, G. E., Wang, J., Wang, J., Yang, M., et al. (2012). Age constraint on Burmese amber based on U-Pb dating of zircons. *Cretac. Res.* 37, 155–163. doi:10.1016/j.cretres.2012.03.014

Su, Y.-T., Cai, C.-Y., and Huang, D.-Y. (2021). Morphological revision of *Siphonophora hui* (Myriapoda: Diplopoda: Siphonophoridae) from the mid-

Cretaceous Burmese amber. *Palaeoentomology* 4, 279–288. doi:10.11646/palaeoentomology.4.3.15

Vogler, A. (2018). Photoluminescence of Baltic amber. *Z. Naturforsch. B* 73, 673–675. doi:10.1515/znb-2018-0106

Vorontsov, D., and Voronezhskaya, E. E. (2022). Pushing the limits of optical resolution in the study of the tiniest fossil arthropods. *Hist. Biol.* 34, 2415–2423. doi:10.1080/08912963.2021.2017920

Yamamoto, S., Maruyama, M., and Parker, J. (2016). Evidence for social parasitism of early insect societies by Cretaceous rove beetles. *Nat. Commun.* 7, 13658. doi:10.1038/ncomms13658

Yavorskaya, M. I., Anton, E., Jałoszyński, P., Polilov, A., and Beutel, R. G. (2018). Cephalic anatomy of Sphaeriusidae and a morphology-based phylogeny of the suborder Myxophaga (Coleoptera). *Syst. Entomol.* 43, 777–797. doi:10.1111/syen.12304

Zhang, Z., Jiang, X., Wang, Y., Kong, F., and Shen, A. H. (2020b). Fluorescence characteristics of blue amber from the Dominican Republic, Mexico, and Myanmar. *Gems Gemol.* 56, 484–496. doi:10.5741/gems.56.4.484

Zhang, Z., Jiang, X., Wang, Y., Shen, A. H., and Kong, F. (2020a). Fluorescence spectral characteristic of amber from Baltic Sea region, Dominican republic, Mexico, Myanmar and China. *J. Gems Gemol.* 22, 1–11.

TYPE Original Research
PUBLISHED 22 August 2023
DOI 10.3389/fevo.2023.1015627

OPEN ACCESS

EDITED BY
Xing Xu,
Yunnan University, China

REVIEWED BY
Yongjie Wang,
Guangdong Academy of Sciences, China
Yanhong Pan,
Nanjing University, China

*CORRESPONDENCE
Chen-Yang Cai
cycai@nigpas.ac.cn

RECEIVED 09 August 2022
ACCEPTED 21 July 2023
PUBLISHED 22 August 2023

CITATION
Li Y-D, Tihelka E, Yamamoto S, Newton AF, Xia F-Y, Liu Y, Huang D-Y and Cai C-Y (2023) Mesozoic *Notocupes* revealed as the sister group of Cupedidae (Coleoptera: Archostemata). *Front. Ecol. Evol.* 11:1015627. doi: 10.3389/fevo.2023.1015627

Mesozoic *Notocupes* revealed as the sister group of Cupedidae (Coleoptera: Archostemata)

Yan-Da Li[1,2], Erik Tihelka[1,2], Shûhei Yamamoto[3], Alfred F. Newton[4], Fang-Yuan Xia[5], Ye Liu[6,7], Di-Ying Huang[1] and Chen-Yang Cai[1,2]*

[1]State Key Laboratory of Palaeobiology and Stratigraphy, Nanjing Institute of Geology and Palaeontology, Chinese Academy of Sciences, Nanjing, China, [2]Bristol Palaeobiology Group, School of Earth Sciences, University of Bristol, Bristol, United Kingdom, [3]Hokkaido University Museum, Hokkaido University, Sapporo, Japan, [4]Integrative Research Center, Field Museum of Natural History, Chicago, IL, United States, [5]Lingpoge Amber Museum, Shanghai, China, [6]Paleo-diary Museum of Natural History, Beijing, China, [7]Fujian Paleo-diary Bioresearch Centre, Fuzhou, China

Despite encompassing only about 50 extant species, beetles of the suborder Archostemata have a rich fossil history, being known from the Permian and dominating coleopteran assemblages in the Mesozoic before declining in richness towards the Late Cretaceous. Given the limited diversity of extant archostematans, fossils provide a valuable line of evidence for reconstructing the relationships among its constituent families. Here we re-evaluate the phylogenetic position of the Triassic–Cretaceous genus *Notocupes*, the most species-rich archostematan taxon in the fossil record. Exquisitely preserved fossils from the Middle Jurassic Haifanggou Formation (Daohugou; ~165 Ma) and mid-Cretaceous amber (~99 Ma) reveal critical differences from Ommatidae in the presence of separated procoxae and overlapping abdominal ventrites. Our analyses confirm that *Notocupes* is not a member of Ommatidae, but is closely related to Cupedidae. Our fossils reveal that *Notocupes* possessed unique adaptations for protecting their appendages, such as unusual dorsal pronotal grooves for the reception of antennae and epipleural grooves for the reception of legs, shedding light on ecological interactions in Mesozoic saproxylic habitats. The high similarity between Jurassic and Cretaceous *Notocupes* provides an exceptional example of long-term morphological stasis, suggesting a consistent microhabitat for the group.

KEYWORDS

Archostemata, *Notocupes*, Cupedidae, compression fossils, amber

1 Introduction

Archostemata is one of the four extant beetle suborders. While just around 50 extant archostematan species are known in 15 genera (Hörnschemeyer, 2016), the group was considerably diverse in the geological past. Archostematans dominated early Mesozoic fossil beetle assemblages and over 200 extinct species have been described across the world

(Ślipiński et al., 2011). In some analyses, Archostemata (*sensu stricto*, not including stem-group beetles such as Tshekardocoleidae and Permocupedidae) is recovered as the earliest-diverging clade within Coleoptera (Friedrich et al., 2009; Bocak et al., 2014), highlighting its importance for understanding the origin of the present-day diversity of beetles. Because they superficially resemble Permian stem-group beetles (Ponomarenko et al., 2014), archostematans have often been regarded as "living fossils" (Cai and Huang, 2017; Jarzembowski et al., 2020a). This is particularly the case for the families Cupedidae (reticulated beetles) and Ommatidae, which possess elytra with regularly arranged rows of window punctures resembling those found in early beetles from the Permian. Owing to their similar body plans, Cupedidae and Ommatidae have been at times regarded as a single family, Cupedidae *sensu lato* (Ponomarenko, 2000; Kirejtshuk, 2020). However, recent molecular phylogenetic studies indicate that Ommatidae is more closely related to Micromalthidae, rather than Cupedidae *sensu stricto*, and thus "Cupedidae *s.l.*" is not a monophyletic group (Mckenna et al., 2015; McKenna et al., 2019). Therefore, in this paper we treat Ommatidae and Cupedidae as separate families. The interrelationships of Cupedidae, Ommatidae, Micromalthidae and the two remaining archostematan families, Crowsoniellidae and the enigmatic Jurodidae, have been historically difficult to elucidate based on morphology, and no molecular data have been available for the latter two. Both Crowsoniellidae and Jurodidae are rare and species-poor in the recent fauna, with Crowsoniellidae known from only three specimens collected in 1973 in Italy (Pace, 1975; Kirejtshuk et al., 2010; Ge et al., 2011), and Jurodidae known from a single Recent specimen found in Far Eastern Russia and scarce Jurassic fossils (Lafer, 1996; Kirejtshuk, 1999; Yan et al., 2014). Since Jurodidae combines characters found in Adephaga, Archostemata and Polyphaga, some authors do not include it within Archostemata and treat it as a taxon of uncertain affinities (Lawrence, 2016).

Given the limited diversity of extant archostematan beetles, fossils provide crucial evidence for reconstructing the phylogeny of the group (Tan et al., 2012; Li et al., 2019). The fossil record of archostematans is also important for understanding biotic change in Mesozoic terrestrial ecosystems, namely the conversion from an archostematan-dominated beetle fauna to a polyphagan-dominated one in the late Mesozoic–early Cenozoic (Soriano and Delclòs, 2006; Friedrich et al., 2009).

Notocupes Ponomarenko is the most abundant genus of archostematans in Mesozoic deposits. With over 50 extinct species known from the Triassic–Cretaceous it is also one of the most species-rich insect genera in the fossil record (Strelnikova and Yan, 2023). Additional species are assigned to the form genus *Zygadenia* Handlirsch that is reserved for isolated elytra likely belonging to representatives of *Notocupes*. Since the first discovery of a *Zygadenia* elytron by Giebel (1856) from the Cretaceous Purbeck Limestone Group of southern England, the *Notocupes–Zygadenia* complex has been reported from Europe, Asia, South America, and Australia (Kirejtshuk, 2020). *Notocupes* has been historically placed into the family Ommatidae (or Ommatinae in Cupedidae *s.l.*), and into the tribe Notocupedini erected by Ponomarenko (Ponomarenko, 1966). Despite its wide distribution, the morphology of *Notocupes* remains insufficiently known. Most *Notocupes* specimens were described based on compressions from Mesozoic strata, and thus many morphological characters are difficult to interpret or not preserved at all. The morphology of the three *Notocupes* species reported from mid-Cretaceous Burmese amber (Tihelka et al., 2019; Jarzembowski et al., 2020b; Jiang et al., 2020) remains insufficiently described, owing to the challenging optical properties of the amber matrix. Here we report four exquisitely preserved *Notocupes* fossils from Middle–Late Jurassic Daohugou Biota and mid-Cretaceous Burmese amber. With the aid of a range of imaging techniques, including confocal laser scanning microscopy, scanning electron microscopy, and microtomography, we aim to clarify the external morphology of *Notocupes* and evaluate the systematic position of this genus within Archostemata.

2 Materials and methods

2.1 Fossils and imaging

The three compression fossils photographed herein (Figures 1A–F, 2) originated from Daohugou Village, Ningcheng County, Inner Mongolia, China (~165 Ma). An additional compression fossil (Supplementary Figure 2) originated from Huangbanjigou Village, Shangyuan Township, Beipiao City, Liaoning Province, China (~125 Ma). These specimens are deposited in the Nanjing Institute of Geology and Palaeontology (NIGP), Chinese Academy of Sciences, Nanjing, China. The Burmese amber specimen BA202101 (Figures 1G, H, 3) originated from amber mines near Noije Bum (26°20' N, 96°36' E), Hukawng Valley, Kachin State, northern Myanmar (~99 Ma), and is deposited in the Lingpoge Amber Museum, Shanghai, China.

Photographs under incident light were taken with a Zeiss Discovery V20 stereo microscope. Where necessary, compression fossils were moistened with 70% ethanol to improve contrast of morphological characters. Widefield fluorescence images were captured with a Zeiss Axio Imager 2 light microscope combined with a fluorescence imaging system. Confocal images were obtained with a Zeiss LSM710 confocal laser scanning microscope, using the 488 nm Argon laser excitation line (Fu et al., 2021). Images under incident light and widefield fluorescence were stacked in Helicon Focus 7.0.2 or Zerene Stacker 1.04. Confocal images were stacked with Helicon Focus 7.0.2. Scanning electron microscopic (SEM) images were obtained with a Hitachi SU 3500 scanning electron microscope, operating with an accelerating voltage of 18 kV and a pressure of 60 Pa. Microtomographic data for BA202101 were obtained with a Zeiss Xradia 520 Versa 3D X-ray microscope at the micro-CT laboratory of NIGP, and analyzed in VGStudio MAX 3.0. Scanning parameters were as follows: isotropic voxel size, 14.096 μm; power, 3 W; acceleration voltage, 40 kV; exposure time, 4 s; projections, 2001. Images were further processed in Adobe Photoshop CC to adjust brightness and contrast.

The full set of descriptions and figures, along with the new taxonomic acts, will be presented in a separate paper.

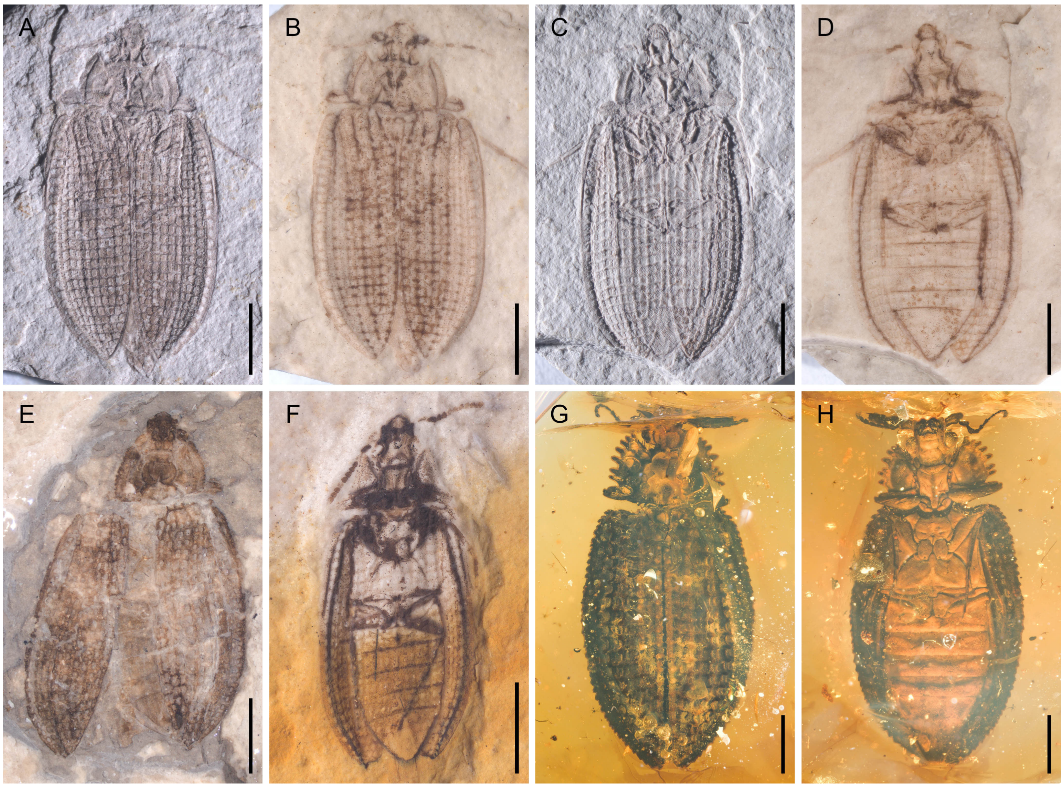

FIGURE 1
General habitus of *Notocupes* spp., under incident light, dry **(A, C)** or moistened with 70% ethanol **(B, D–F)**. **(A, B)** NIGP174673a. **(C, D)** NIGP174673b. **(E)** NIGP174674. **(F)** NIGP174675. **(G)** BA202101, dorsal view. **(H)** BA202101, ventral view. Scale bars: 5 mm in **(E)**, 3 mm in **(A–D)**, 2 mm in **(F–H)**.

2.2 Phylogenetic analysis

To evaluate the systematic placement of *Notocupes*, morphological phylogenetic analyses were performed. The data matrix (Supplementary Data 1, 2) was derived from a previously published dataset (Beutel et al., 2008). The original matrix consists of 90 morphological characters of recent and fossil beetles, including representatives of all archostematan families. Several changes to the scoring of the characters were made. Firstly, head protuberances are important for generic-level identification of Cupedidae (Hörnschemeyer, 2009). However, the definition of these protuberances is sometimes unclear for other archostematans. For example, the protuberances P3 were defined as "between P2, on both sides of the median line of the head" in (Hörnschemeyer et al., 2006), but in *Tetraphalerus* Waterhouse, the posterior protuberances are situated roughly posteriorly to P2 (Figure 10D in Beutel et al., 2008), making it difficult to determine if they should be coded as P3 or P4. Besides, there might be some miscoding for head protuberances in Beutel et al. (2008). For example, the protuberances P2 for *Omma* Newman were coded as strongly pronounced, but we failed to detect any strongly pronounced protuberances on the head of *Omma* (Figure 16 in Escalona et al., 2020). We therefore excluded characters 6–9 in Beutel et al. (2008) from our analysis. Secondly, Beutel et al. (2008) coded the propleuron as reaching the anterior margin of prothorax in *Tetraphalerus* and *Crowsoniella* Pace (their character 42). In fact, the propleuron of *Tetraphalerus* does not reach the anterior prothoracic margin (Friedrich et al., 2009; Li et al., 2021), and no separate propleuron is present in *Crowsoniella* at all (Figure 16 in Kirejtshuk et al., 2010); we adapted our character matrix accordingly. Lastly, character 31 in Beutel et al. (2008) was coded as (2) for *Crowsoniella*, which is a non-existent character state and was therefore corrected in our matrix. Thus, our decisive matrix included 86 characters in total.

The problematic family Jurodidae has been considered as a member of Adephaga, Archostemata, or Polyphaga (Ponomarenko, 1985; Lafer, 1996; Kirejtshuk, 1999; Beutel et al., 2008; Hörnschemeyer, 2009). Its puzzling combination of characters, seemingly combining states found in three coleopteran suborders, represents a potential source of incongruence in phylogenetic analyses. Hence, we prepared two matrices, one including Jurodidae (represented by the extant *Sikhotealinia* Lafer and the extinct *Jurodes* Ponomarenko), and one excluding the family.

Parsimony analyses were conducted in the program TNT 1.5 (Goloboff et al., 2008; Goloboff and Catalano, 2016). We experimented with the use of equal and implied weighting. Parsimony analyses have been shown to achieve higher accuracy under a moderate weighting scheme (e.g., when concavity constants, *K*, are between 5 and 20) (Goloboff et al., 2018; Smith, 2019). Therefore, we set the concavity constant to 12 in our analyses with implied weighting, as suggested by Goloboff et al. (2018). Most parameters were set as default in the "new technology search", while the value for "find min. length" was changed from 1 to 100. When multiple most parsimonious trees were obtained, a strict consensus tree was calculated, and a standard bootstrap analysis was implemented with 1,000 pseudoreplicates, where the support values were shown as frequency differences (Goloboff et al., 2003). Settings for the equal weighting approach were identical, employing default parameters. Character states were mapped onto the tree with WinClada 1.00.08. The tree was graphically edited with Adobe Illustrator CC 2017.

3 Systematic paleontology

Order Coleoptera Linnaeus, 1758
Suborder Archostemata Kolbe, 1908

3.1 Genus *Notocupes* Ponomarenko, 1964

3.1.1 Type species

Notocupes picturatus Ponomarenko, 1964

3.1.2 Revised diagnosis

Head (Figure 2E) prognathous, nearly as long as wide, narrowing behind eyes and forming distinct neck region. Compound eyes hemispherical, distinctly protruding. Antennae (Figure 2H) moderately long, slightly serrate, extending at most to posterior pronotal apices. Mandibles with horizontal cutting edge, lacking vertically arranged mandibular teeth (Figure 3E). Suture separating mentum and gulamentum present. Weakly impressed grooves on dorsal surface of pronotum for housing antennae at least sometimes present (Figures 2C, G). Pronotal disc broad, often with produced anterior angles, with lateral margins straight or jagged. Prosternum in front of coxae subquadrate, with tarsal grooves along pleurosternal sutures (Figures 2A, 3B, G). Prosternal process well-

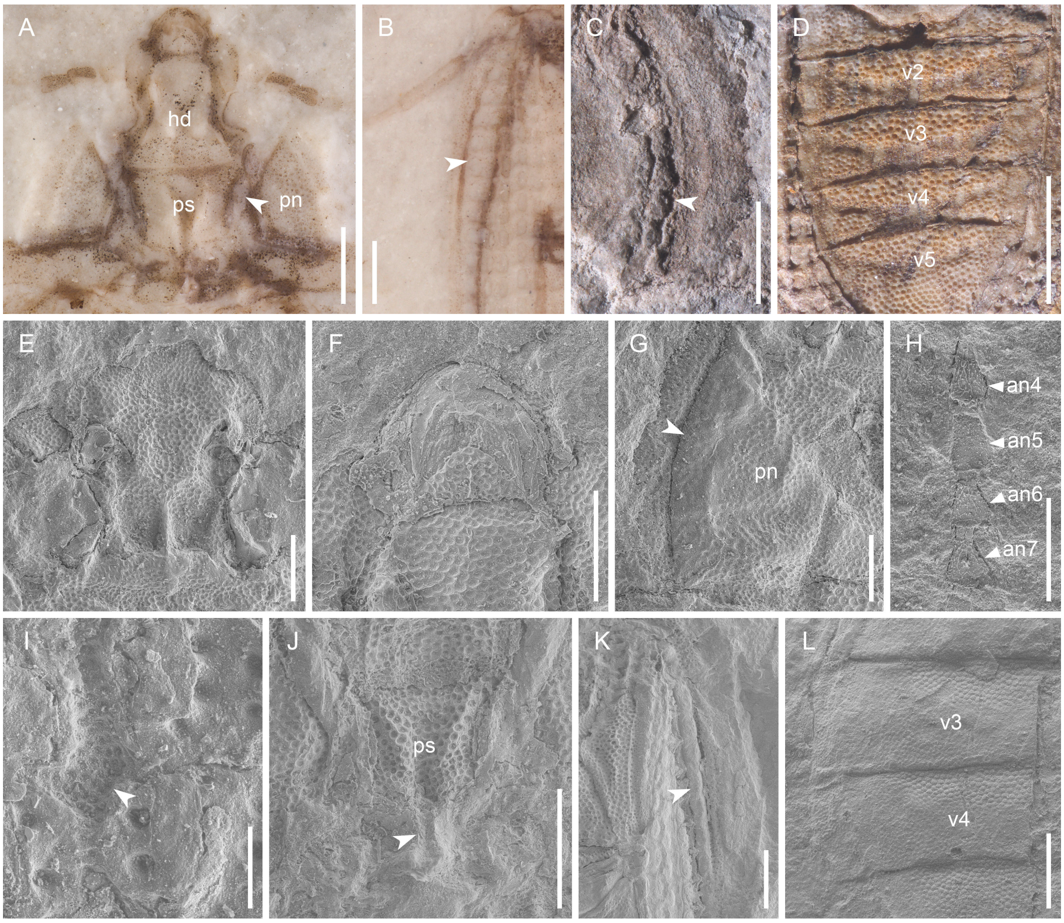

FIGURE 2
Details of *Notocupes* spp. from the Middle Jurassic Daohugou biota, under incident light **(A–D)** or scanning electron microscopy **(E–L)**. **(A)** NIGP174673a, head and prothorax, showing the protarsal groove along pleurosternal suture (arrowhead). **(B)** NIGP174673b, groove on the elytral epipleuron for housing mesotibia and -tarsus (arrowhead). **(C)** NIGP174674, antenna in the prothoracic antennal groove (arrowhead). **(D)** NIGP174675, abdomen with overlapping ventrites. **(E)** NIGP174673a, head. **(F)** NIGP174673b, mouthparts. **(G)** NIGP174673a, prothoracic antennal groove (arrowhead). **(H)** NIGP174673a, antenna. **(I)** NIGP174673a, scale-covered coniform protuberances on elytron (arrowhead). **(J)** NIGP174675, prosternum, showing the complete prosternal process (arrowhead). **(K)** NIGP174675, groove on the elytral epipleuron (arrowhead). **(L)** NIGP174674, abdomen with overlapping ventrites. an4–7, antennomeres 4–7; hd, head; pn, pronotum; ps, prosternum; v2–5, ventrites 2–5. Scale bars: 1 mm in **(A–D, L)**, 500 µm in **(E–H, J–K)**, 200 µm in **(I)**.

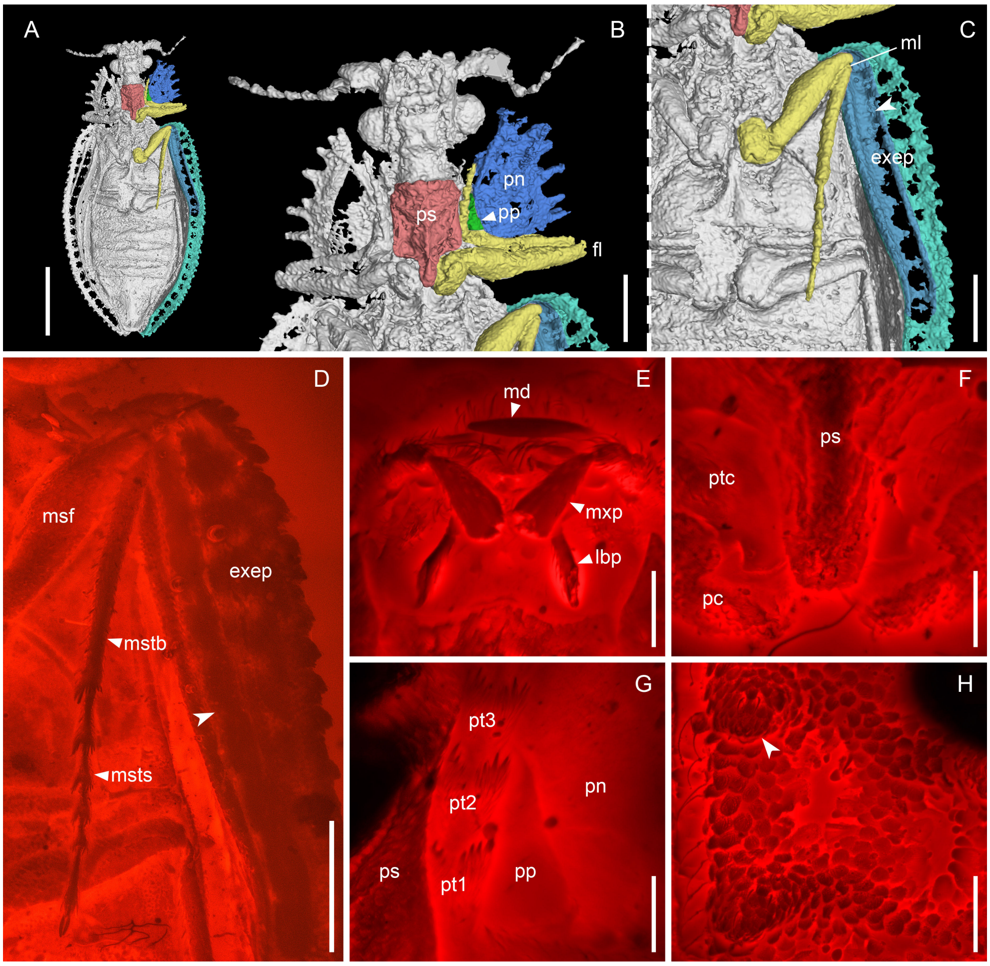

FIGURE 3
Notocupes sp., BA202101, in mid-Cretaceous amber from Myanmar. **(A–C)**, X-ray microtomographic reconstruction, ventral view, with groove on the elytral epipleuron for housing mesotibia and -tarsus highted in **(C)** (arrowhead). **(D)** Groove on the elytral epipleuron, ventral view, under widefield fluorescence. **(E–H)** Confocal images. **(E)** Mouthparts, ventral view. **(F)** Prothorax, ventral view. **(G)** Protarsus in the protarsal groove, ventral view. **(H)** Elytron, dorsal view, showing the scale-covered coniform protuberances (arrowhead). exep, explanate epipleuron; fl, fore leg; lbp, labial palp; md, mandible; ml, mid leg; msf, mesofemur; mstb, mesotibia; msts, mesotarsus; mxp, maxillary palp; pc, procoxa; pn, pronotum; pp, propleuron; ps, prosternum; pt1–3, protarsomeres 1–3; ptc, protrochanter. Scale bars: 3 mm in **(A)**, 1 mm in **(B–D)**, 200 µm in **(E–H)**.

developed, extending beyond middle of procoxae (Figures 2J, 3B, F). Procoxae narrowly separated by prosternal process. Elytra elongate, with ten longitudinal rows of window punctures on disc and one row of window punctures on explanate epipleuron, sometimes with raised veins with coniform protuberances (elytral spines; Figures 2I, 3H), veins A1 and CuA fused before elytral apex. Anterior portion of explanate elytral epipleura at least sometimes with grooves for housing mesotibiae and mesotarsi (Figures 2B, K, 3C, D). Tarsi 5-segmented, elongate; tarsomeres not emarginate or ventrally lobed (Figures 3D, G). Abdominal ventrites overlapping (Figures 1H, 2D, L).

3.1.3 Remarks

Notocupes has sometimes been treated as a junior synonym of *Zygadenia* (e.g., Ponomarenko, 2000; Kirejtshuk, 2020). The name *Zygadenia* Handlirsch was proposed based on an isolated elytron. As elytra with similar morphology may belong to different taxa (Strelnikova and Yan, 2021), we here reserve *Notocupes* for complete body fossils of unambiguous systematic assignment, following the practice of Ponomarenko and Ren (2010).

Notocupes differs from Ommatidae primarily by its horizontal cutting edge of mandibles, separated procoxae and overlapping abdominal ventrites, and differs from Cupedidae primarily by its relatively short prosternal process (not reaching posterior end of procoxae) and simple tarsomeres. *Notocupes* may deserve a new familial status. However, the morphology and phylogenetic placement of the genera historically associated with *Notocupes*, including *Notocupoides* Ponomarenko, *Rhabdocupes* Ponomarenko, and *Eurydicton* Ponomarenko, are not currently clear. Thus, *Notocupes*, along with these genera, is temporarily left in Archostemata, without a familial attribution.

4 Discussion

4.1 Exceptional fossils illuminate the morphology of *Notocupes*

4.1.1 Compression fossils and amber inclusions provide a complementary view of *Notocupes* morphology

Traditionally, *Notocupes* has been placed in the family Ommatidae (or Ommatinae in Cupedidae *s.l.*), primarily based on the length of its antennae and contiguous procoxae (Ponomarenko, 1964). However, our examination of exceptionally preserved *Notocupes* compressions from Daohugou and amber from northern Myanmar revealed a suite of morphological characters that are not diagnostic for Ommatidae, but correspond well to Cupedidae *s. s.*

Some beetles possess a transverse suture between the posterior tentorial pits, separating the submentum and gula, while in others (including all extant Ommatidae) this suture is reduced, and the submentum and gula are fused into a single gulamentum. Though this suture was not explicitly described, the line drawings by Ponomarenko (Ponomarenko, 1969) suggested the presence of a distinct suture separating the submentum and gula in *Notocupes* and closely related genera. Our observations, in contrast, showed no suture between the posterior tentorial pits, but a suture separating the mentum and gulamentum (Figure 1H).

The Ommatidae + Micromalthidae clade is characterized by vertically arranged mandibular teeth (Hörnschemeyer, 2009; Li et al., 2020b; Tihelka et al., 2020b), while in Cupedidae the mandibles have a horizontal cutting edge. Similar to cupedids, *Notocupes* also possesses a horizontal mandibular cutting edge (Figure 3E).

In Ommatidae, the procoxae are contiguous (except for the aberrant genus *Stegocoleus* Jarzembowski & Wang which gained this character independently; Jarzembowski and Wang, 2016; Li et al., 2020a; Tihelka et al., 2020a), and the prosternal process is reduced, not reaching the posterior half of the procoxae. In the *Notocupes* specimen from Burmese amber we examined, the prosternal process is relatively well-developed, extending beyond the middle of procoxae, though not reaching the posterior end of procoxae (Figures 2J, 3B, F). The procoxae are completely separated by the prosternal process, which are similar to Cupedidae and contradictory to previous descriptions of this genus based on compression fossils (Ponomarenko, 1964; Tan and Ren, 2009). We suppose that the contiguous procoxae reported by previous researchers could have been a taphonomic artefact caused by distortion during the fossilization processes. Indeed, the elongate prosternal process has also been inexplicitly noted by Ponomarenko (in Jarzembowski et al., 2015), and recently reported by Lee et al. (2022).

In most ommatids, the abdominal ventrites are coplanar and separated by wide grooves (Beutel et al., 2008) (Figure 4A in Yamamoto, 2017; Figures 71–74 in Escalona et al., 2020). In most cupedids, the abdominal ventrites are overlapping (Beutel et al., 2008; but see Kirejtshuk et al., 2016). *Notocupes* has overlapping abdominal ventrites (Figures 1H, 2D, L) which are discordant with a placement in Ommatidae (Ponomarenko, 1969; Ponomarenko, 2006; Ponomarenko and Ren, 2010; Tan et al., 2012; Strelnikova, 2019). Notably, Kirejtshuk (2020) transferred *Ovatocupes alienus* Tan & Ren, a species reported from the Yixian Formation, into *Notocupes*. However, it was originally placed in Cupedidae based on its separated procoxal cavities and overlapping abdominal ventrites (Tan and Ren, 2006).

4.1.2 New potential apomorphies of *Notocupes*

Curiously, *Notocupes* possesses a pair of weak grooves on the dorsal surface of the pronotum. In NIGP174674 and the holotype of *N. denticollis* (likely also in the holotype of *N. ohmkuhnlei*), the antennae are positioned within these grooves (Figure 2C). This character is unusual, as most beetles with antennal grooves have ventral ones, not dorsal ones (Lawrence and Ślipiński, 2013). This character represents a potential apomorphy of *Notocupes*, provided its presence can be confirmed in other early members of the genus.

There is a distinct groove along the propleurosternal suture in *Notocupes*, which functions for housing the protarsi, as clearly shown in the amber specimen BA202101 and other compression fossils (Figures 2A, 3B, G). This protarsal groove is also preserved in some previously noted amber and compression fossils of *Notocupes* (e.g., Plate II, Figure 2 in Tan et al., 2006; Figure 1 in Jarzembowski et al., 2020b). Grooves for housing the protarsi are also present in the majority of extant Cupedidae (except for *Priacma* LeConte and *Paracupes* Kolbe) and Crowsoniellidae. However, in Cupedidae, the protarsal groove runs along the notopleural and notosternal sutures; and in *Crowsoniella*, the propleuron is reduced or fused with other sclerites, and the protarsal groove runs along the apparent notosternal suture (Figure 16 in Kirejtshuk et al., 2010). Notably, such prothoracic grooves for housing tarsi are absent in Ommatidae (Lawrence, 1999).

A groove is also present in the anterior portion of the elytral epipleura of *Notocupes*, most clearly shown by the amber specimen BA202101 (Figures 3C, D). The position and length of this groove suggest that it housed the mesotibia and mesotarsus. Similar structures are also preserved in our newly discovered compression *Notocupes* fossils from Daohugou (Figures 2B, K). However, it would be hard to correctly interpret them without the aid of amber fossils. The groove for housing legs in elytral epipleura is, to our knowledge, reported in beetles for the first time, and may represent a further apomorphy of *Notocupes*.

4.2 Systematic placement of *Notocupes* and the evolution of Archostemata

4.2.1 Phylogeny of Archostemata

We integrated our updated understanding of *Notocupes* morphology into a formal phylogenetic analysis to evaluate the placement of the genus within Archostemata. The result was generally consistent with Beutel et al. (2008), except for the position of Ademosynidae and Schizophoridae. Our analyses have consistently recovered a monophyletic Archostemata, including the extinct family Catiniidae, albeit with low support (Figure 4). The monophyly of Archostemata including Catiniidae was unaffected by the exclusion of Jurodidae (Supplementary Figure 1). The relationships among archostematan families remained almost the same regardless of the analytical approach used or the dataset analyzed. Ommatidae appears to be the earliest-diverging archostematan family in the present analyses, though with extremely low support. Our analyses, regardless of the weighting used or the dataset analysed, supported three archostematan clades, (i) Ommatidae, (ii) Crowsoniellidae, Micromalthidae, and Catiniidae, and (ii) *Notocupes* and Cupedidae, although the support values were not high (bootstrap values = 23–52).

4.2.2 Systematic placement of *Notocupes*

Regardless of the analytical method used or the inclusion of Jurodidae, *Notocupes* was always recovered as sister to Cupedidae (bootstrap values = 34–52). Cupedidae excluding *Notocupes* was strongly supported as monophyletic (bootstrap values = 88–92). *Notocupes* shares with Cupedidae the apomorphic arrangement of the abdominal sterna with both taxa possessing overlapping ventrites (character 62: 1). Both taxa also share the presence of scale-like setae (3: 1). *Notocupes* differs from Cupedidae in possessing a distinctly developed mentum: (35: 0) and possessing prosternal grooves for tarsomeres (40: 1). Besides these characters, *Notocupes* differs from Cupedidae by its relatively short prosternal process not reaching posterior end of procoxae and simple tarsomeres.

Based on the previous discussions, we conclude that *Notocupes* differs substantially from Ommatidae in morphology. Since a potential inclusion of *Notocupes* in Cupedidae would necessitate a dramatic revision of the latter's diagnosis, we prefer to temporarily leave *Notocupes* without familial attribution, before more information is available for the possibly associated *Notocupoides*, *Rhabdocupes* and *Eurydicton*.

4.3 Paleobiology and evolutionary significance

Extant members of Cupedidae and Ommatidae are associated with decaying wood, although some adults have been reported to feed on pollen (Crowson, 1962; Atkins, 1963; Evans, 2014; Escalona et al., 2020). A saproxylic mode of life may also be expected in *Notocupes*. The relatively flattened habitus of *Notocupes* suggests that the beetles may have occupied narrow spaces such as crevices under bark, while the presence of sharp spines in some species suggest the beetles also occurred in open habitats, such as on tree trunks. Species from Burmese amber, fossils previously placed into the genus *Amblomma*, and NIGP174673, possessed dentate lateral edges of the prothorax or (and) sharp spines on elytra (Tan and Ren, 2009; Tihelka et al., 2019; Jiang et al., 2020) that may have fulfilled a defensive function or alternatively played a role in bark mimesis. Color patterns preserved in some Cretaceous *Notocupes*/

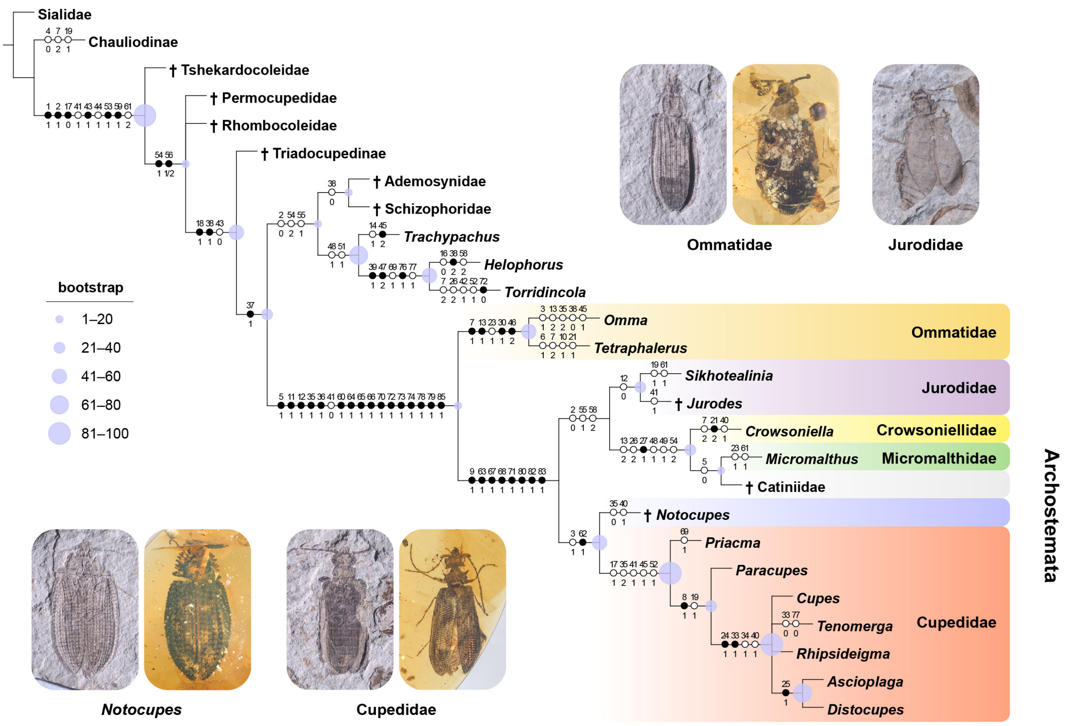

FIGURE 4
Strict consensus tree of three equally shortest trees from TNT implied weighting parsimony analysis, with all taxa included. The equal weighting analysis produced exactly the same topology. Black circles indicate nonhomoplasious changes; white circles indicate homoplasious characters; numbers above the branches of the strict consensus tree indicate character numbers. The insets show representatives of Archostemata from Daohugou and Burmese amber.

Zygadenia elytra (Jarzembowski et al., 2015; Strelnikova and Yan, 2021) (Supplementary Figure 2) may have served as disruptive camouflage, breaking up the beetle's outline and concealing them from visual predators. Grooves along the pleurosternal suture for housing the protarsi, grooves on the dorsal surface of the pronotum for housing the antennae, and epipleural grooves represent further morphological adaptations for life in confined space or may have served a protective function.

The more than 80 Myr range of the *Notocupes–Zygadenia* complex in the fossil record, from the Middle Triassic (Bathonian) to the Late Cretaceous (Coniacian), makes *Notocupes* a prime example of morphological, and probably also ecological, conservatism in Mesozoic archostematans. The morphology of Middle Jurassic *Notocupes* from Daohugou corresponds astonishingly well to that of the mid-Cretaceous one from Burmese amber. The prothoracic protarsal grooves and the epipleural mesotibial and -tarsal grooves remained almost unchanged for at least 66 Myr. Even some fine structures, such as the scale-covered coniform protuberances on elytra, persisted at least in some of the lineages. This high-level of morphological stability might suggest the group managed to track an almost consistent microhabitat (Marín et al., 2018; Cerca et al., 2020), in spite of the dramatic climatic changes over geological timescale. Nevertheless, some other pressures may have also played a role in conserving some characters.

Notocupes highlights ancestral character states with respect to Cupedidae, facilitating future comparative work on the latter family. Our study highlights the importance of examining fossils representing different types of preservation, such as compressions and amber inclusions, to shed light on controversial characters that may be distorted by taphonomic processes and build a more accurate evolutionary picture of extinct insect groups.

Data availability statement

The original contributions presented in the study are included in the article/Supplementary Material. Further inquiries can be directed to the corresponding author.

Author contributions

Y-DL and C-YC conceived the study. D-YH, C-YC, F-YX and YL acquired and processed the fossils. Y-DL acquired and processed the photomicrograph data. Y-DL, ET and C-YC drafted the manuscript, to which SY and AFN contributed. All authors commented on the manuscript and gave final approval for publication.

Funding

Financial support was provided by the Strategic Priority Research Program of the Chinese Academy of Sciences (XDB26000000 and XDB18000000), the National Natural Science Foundation of China (42222201 and 42288201), the Second Tibetan Plateau Scientific Expedition and Research project (2019QZKK0706), and Grant-in-Aid for JSPS Fellows (20J00159) from the Japan Society for the Promotion of Science.

Acknowledgments

We are grateful to Margaret K. Thayer for helpful discussion, Su-Ping Wu for technical help in micro-CT reconstruction, Yan Fang for technical help in confocal imaging, and Chun-Zhao Wang for technical help in SEM imaging.

Conflict of interest

The authors declare that the research was conducted in the absence of any commercial or financial relationships that could be construed as a potential conflict of interest.

Publisher's note

Supplementary material

The Supplementary Material for this article can be found online at: https://www.frontiersin.org/articles/10.3389/fevo.2023.1015627/full#supplementary-material

References

Atkins, M. (1963). The Cupedidae of the world. *Can. Entomol.* 95 (2), 140–162. doi: 10.4039/Ent95140-2

Beutel, R. G., Ge, S.-Q., and Hörnschemeyer, T. (2008). On the head morphology of *Tetraphalerus*, the phylogeny of Archostemata and the basal branching events in Coleoptera. *Cladistics* 24 (3), 270–298. doi: 10.1111/j.1096-0031.2007.00186.x

Bocak, L., Barton, C., Crampton-Platt, A., Chesters, D., Ahrens, D., and Vogler, A. P. (2014). Building the Coleoptera tree-of-life for >8000 species: composition of public DNA data and fit with Linnaean classification. *Syst. Entomol.* 39 (1), 97–110. doi: 10.1111/syen.12037

Cai, C., and Huang, D. (2017). *Omma daxishanense* sp. nov., a fossil representative of an extant Australian endemic genus recorded from the Late Jurassic of China (Coleoptera: Ommatidae). *Alcheringa* 41 (2), 277–283. doi: 10.1080/03115518.2016.1225251

Cerca, J., Meyer, C., Stateczny, D., Siemon, D., Wegbrod, J., Purschke, G., et al. (2020). Deceleration of morphological evolution in a cryptic species complex and its link to paleontological stasis. *Evolution* 74 (1), 116–131. doi: 10.1111/evo.13884

Crowson, R. (1962). Observations on the beetle family Cupedidae, with descriptions of two new fossil forms and a key to the recent genera. *Ann. Mag. Nat. Hist.* 5 (51), 147–157. doi: 10.1080/00222936208651227

Escalona, H. E., Lawrence, J. F., and Ślipiński, A. (2020). The extant species of the genus *Omma* Newman and description of *Beutelius* gen. nov. (Coleoptera: Archostemata: Ommatidae: Ommatinae). *Zootaxa* 4728 (4), 547–574. doi: 10.11646/zootaxa.4728.4.11

Evans, A. V. (2014). "Reticulated beetles (Cupedidae)," in *Beetles of Eastern North America* (Princeton, NJ: Princeton University Press), 60.

Friedrich, F., Farrell, B. D., and Beutel, R. G. (2009). The thoracic morphology of Archostemata and the relationships of the extant suborders of Coleoptera (Hexapoda). *Cladistics* 25 (1), 1–37. doi: 10.1111/j.1096-0031.2008.00233.x

Fu, Y.-Z., Li, Y.-D., Su, Y.-T., Cai, C.-Y., and Huang, D.-Y. (2021). Application of confocal laser scanning microscopy to the study of amber bioinclusions. *Palaeoentomology* 4 (3), 266–278. doi: 10.11646/palaeoentomology.4.3.14

Ge, S.-Q., Hörnschemeyer, T., Friedrich, F., and Beutel, R. G. (2011). Is *Crowsoniella relicta* really a cucujiform beetle? *Syst. Entomol.* 36 (1), 175–179. doi: 10.1111/j.1365-3113.2010.00552.x

Giebel, C. (1856). Die Insecten und Spinnen der Vorwelt mit steter Berücksichtigung der lebenden Insekten und Spinnen. *Die Fauna der Vorwelt* 2, 1–511.

Goloboff, P. A., and Catalano, S. A. (2016). TNT version 1.5, including a full implementation of phylogenetic morphometrics. *Cladistics* 32 (3), 221–238. doi: 10.1111/cla.12160

Goloboff, P. A., Farris, J. S., Källersjö, M., Oxelman, B., Ramírez, M. J., and Szumik, C. A. (2003). Improvements to resampling measures of group support. *Cladistics* 19 (4), 324–332. doi: 10.1111/j.1096-0031.2003.tb00376.x

Goloboff, P. A., Farris, J. S., and Nixon, K. C. (2008). TNT, a free program for phylogenetic analysis. *Cladistics* 24 (5), 774–786. doi: 10.1111/j.1096-0031.2008.00217.x

Goloboff, P. A., Torres, A., and Arias, J. S. (2018). Weighted parsimony outperforms other methods of phylogenetic inference under models appropriate for morphology. *Cladistics* 34 (4), 407–437. doi: 10.1111/cla.12205

Hörnschemeyer, T. (2009). The species-level phylogeny of archostematan beetles—where do *Micromalthus debilis* and *Crowsoniella relicta* belong? *Syst. Entomol.* 34 (3), 533–558. doi: 10.1111/j.1365-3113.2009.00476.x

Hörnschemeyer, T. (2016). "Introduction and phylogeny. Archostemata Kolbe, 1908," in *Handbook of Zoology, Arthropoda: Insecta, Coleoptera, beetles, Vol. 1: morphology and systematics (Archostemata, Adephaga, Myxophaga, Polyphaga partim), 2nd Edition*. Eds. R. G. Beutel and R. A. Leschen (Berlin: Walter de Gruyter), 41–43.

Hörnschemeyer, T., Goebbels, J., Weidemann, G., Faber, C., and Haase, A. (2006). The head morphology of *Ascioplaga mimeta* (Coleoptera: Archostemata) and the phylogeny of Archostemata. *Eur. J. Entomol.* 103 (2), 409. doi: 10.14411/eje.2006.055

Jarzembowski, E. A., and Wang, B. (2016). An unusual basal beetle from Myanmar (Coleoptera: Archostemata). *Alcheringa* 40 (2), 297–302. doi: 10.1080/03115518.2016.1132493

Jarzembowski, E. A., Wang, B., Zhang, H., and Fang, Y. (2015). Boring beetles are not necessarily dull: new notocupedins (Insecta: Coleoptera) from the Mesozoic of Eurasia and East Gondwana. *Cretac. Res.* 52, 431–439. doi: 10.1016/j.cretres.2014.03.006

Jarzembowski, E. A., Wang, B., and Zheng, D. (2020a). An archaic-beetle 'Jaws' from mid-Cretaceous Burmese amber (Coleoptera: Archostemata). *Proc. Geo. Assoc.* 131 (2), 155–159. doi: 10.1016/j.pgeola.2020.02.003

Jarzembowski, E. A., Wang, B., and Zheng, D. (2020b). The first notocupedin beetle in mid-Cretaceous amber of northern Myanmar (Insecta: Coleoptera: Archostemata). *Cretac. Res.* 106, 104225. doi: 10.1016/j.cretres.2019.104225

Jiang, Z., Li, Y., Song, C., Shi, H., Liu, Y., Chen, R., et al. (2020). A new species of the genus *Notocupes* from mid-Cretaceous Burmese amber (Coleoptera: Archostemata: Ommatidae). *Cretac. Res.* 108, 104335. doi: 10.1016/j.cretres.2019.104335

Kirejtshuk, A. G. (1999). *Sikhotealinia zhiltzovae* (Lafer 1996)–Recent representative of the Jurassic coleopterous fauna (Coleoptera, Archostemata, Jurodidae). *Proc. Zool. Inst. Russ. Acad. Sci.* 281, 21–26.

Kirejtshuk, A. G. (2020). Taxonomic review of fossil coleopterous families (Insecta, Coleoptera). Suborder Archostemata: superfamilies Coleopseoidea and Cupedoidea. *Geosciences* 10 (2), 73. doi: 10.3390/geosciences10020073

Kirejtshuk, A. G., Nel, A., and Collomb, F.-M. (2010). New Archostemata (Insecta: Coleoptera) from the French Paleocene and Early Eocene, with a note on the composition of the suborder. *Ann. Soc. Entomol. Fr.* 46 (1-2), 216–227. doi: 10.1080/00379271.2010.10697661

Kirejtshuk, A., Nel, A., and Kirejtshuk, P. (2016). Taxonomy of the reticulate beetles of the subfamily Cupedinae (Coleoptera: Archostemata), with a review of the historical development. *Invertebr. Zool.* 13 (2), 61–190. doi: 10.15298/invertzool.13.2.01

Lafer, G. S. (1996). "Fam. Sikhotealiniidae Lafer," in *Key to the Insects of the Russian Far East*, vol. 3, part 3. Ed. P. Lafer (Vladivostok: Dal'nauka), 298–302.

Lawrence, J. F., and Ślipiński, A. (2013). *Australian Beetles. Volume 1: Morphology, Classification and Keys* (Clayton: CSIRO Publishing).

Lawrence, J. F. (1999). The Australian Ommatidae (Coleoptera: Archostemata): new species, larva and discussion of relationships. *Invertebr. Syst.* 13 (3), 369–390. doi: 10.1071/IT99008

Lawrence, J. F. (2016). "Classification (families & subfamilies)," in *Handbook of Zoology, Arthropoda: Insecta, Coleoptera, beetles, Vol. 1: morphology and systematics (Archostemata, Adephaga, Myxophaga, Polyphaga partim), 2nd Edition*. Eds. R. G. Beutel and R. A. Leschen (Berlin: Walter de Gruyter), 13–22.

Lee, S. B., Nam, G. S., and Li, Y.-D. (2022). A new species of *Notocupes* (Coleoptera: Archostemata) from the Lower Cretaceous (Albian) Jinju Formation in South Korea. *Cretac. Res.* 140, 105357. doi: 10.1016/j.cretres.2022.105357

Li, Y.-D., Huang, D.-Y., and Cai, C.-Y. (2021). Revisiting the morphology and systematic placement of the enigmatic Cretaceous ommatid beetle *Bukhkalius lindae* (Coleoptera: Archostemata: Ommatidae). *Pap. Avulsos Zool.* 61, e20206063. doi: 10.11606/1807-0205/2021.61.28

Li, Y.-D., Liu, Z.-H., Jarzembowski, E. A., Yin, Z.-W., Huang, D.-Y., and Cai, C.-Y. (2019). Early evolution of Cupedidae revealed by a mid-Cretaceous reticulated beetle from Myanmar (Coleoptera: Archostemata). *Syst. Entomol.* 44 (4), 777–786. doi: 10.1111/syen.12355

Li, Y.-D., Tihelka, E., Yamamoto, S., Huang, D.-Y., and Cai, C.-Y. (2020a). A close affinity of the enigmatic genus *Stegocoleus* with *Lepidomma* revealed by new fossil evidence (Coleoptera: Archostemata: Ommatidae). *Palaeoentomology* 3 (6), 632–640. doi: 10.11646/palaeoentomology.3.6.15

Li, Y.-D., Yamamoto, S., Huang, D.-Y., and Cai, C.-Y. (2020b). A miniaturized ommatid beetle in mid-Cretaceous Burmese amber (Coleoptera: Archostemata: Ommatidae). *Pap. Avulsos Zool.* 60, e20206063. doi: 10.11606/1807-0205/2020.60.63

Marín, A. G., Olave, M., Avila, L. J., Sites, J. W.Jr., and Morando, M. (2018). Evidence of body size and shape stasis driven by selection in Patagonian lizards of the *Phymaturus patagonicus* clade (Squamata: Liolaemini). *Mol. Phylogenet. Evol.* 129, 226–241. doi: 10.1016/j.ympev.2018.08.019

McKenna, D. D., Shin, S., Ahrens, D., Balke, M., Beza-Beza, C., Clarke, D. J., et al. (2019). The evolution and genomic basis of beetle diversity. *Proc. Natl. Acad. Sci.* 116 (49), 24729–24737. doi: 10.1073/pnas.1909655116

Mckenna, D. D., Wild, A. L., Kanda, K., Bellamy, C. L., Beutel, R. G., Caterino, M. S., et al. (2015). The beetle tree of life reveals that Coleoptera survived end-Permian mass extinction to diversify during the Cretaceous terrestrial revolution. *Syst. Entomol.* 40 (4), 835–880. doi: 10.1111/syen.12132

Pace, R. (1975). An exceptional endogeous beetle: *Crowsoniella relicta* n. gen. n. sp. of Archostemata Tetraphaleridae from Central Italy. *Boll. Mus. civ. stor. nat. Verona* 2, 445–458.

Ponomarenko, A. (1964). New beetles of of the family Cupedidae from the Jurassic of Karatau. *Paleontol. Zh.* 2, 49–62.

Ponomarenko, A. (1966). Beetles of the family Cupedidae, Lower Triassic of Soviet. *Paleontol. Zh.* 4, 47–68.

Ponomarenko, A. (1969). Historical development of archostomatan beetles. *Trudy Paleontologicheskogo Instituta Akademii Nauk SSSR* 125, 1–240.

Ponomarenko, A. (1985). "Coleoptera," in *Jurassic Insects of Siberia and Mongolia. Trudy Paleontologicheskogo Instituta Akademii Nauk SSSR*. Ed. A. Rasnitsyn (Moscow: Nauka), 47–87.

Ponomarenko, A. (2000). Beetles of the family Cupedidae from the Lower Cretaceous locality of Semen, Transbaikalia. *Paleontol. J.* 34 (SUPP/3), S317–S322.

Ponomarenko, A. (2006). On the types of Mesozoic archostematan beetles (Insecta, Coleoptera, Archostemata) in the Natural History Museum, London. *Paleontol. J.* 40 (1), 90–99. doi: 10.1134/S0031030106010102

Ponomarenko, A., and Ren, D. (2010). First record of *Notocupes* (Coleoptera: Cupedidae) in locality Daohugou, Middle Jurassic of Inner Mongolia, China. *Ann. Zool.* 60 (2), 169–171. doi: 10.3161/000345410X516812

Ponomarenko, A., Yan, E., and Huang, D.-Y. (2014). New beetles (Coleoptera) from the terminal Middle Permian of China. *Paleontol. J.* 48 (2), 191–200. doi: 10.1134/S0031030114010109

Ślipiński, S. A., Leschen, R. A. B., and Lawrence, J. F. (2011). Order Coleoptera Linnaeus, 1758. In: Zhang, Z.-Q. (Ed.) Animal biodiversity: An outline of higher-level classification and survey of taxonomic richness. *Zootaxa* 3148 (1), 203–208. doi: 10.11646/zootaxa.3148.1.39

Smith, M. R. (2019). Bayesian and parsimony approaches reconstruct informative trees from simulated morphological datasets. *Biol. Lett.* 15 (2), 20180632. doi: 10.1098/rsbl.2018.0632

Soriano, C., and Delclòs, X. (2006). New cupedid beetles from the Lower Cretaceous of Spain and the palaeogeography of the family. *Acta Palaeontol. Pol.* 51, 185–200.

Strelnikova, O. D. (2019). New Cupedidae (Insecta: Coleoptera, Cupedidae) from the Lower Cretaceous of Buryatia. *Paleontol. J.* 53 (3), 292–299. doi: 10.1134/S0031030119030146

Strelnikova, O. D., and Yan, E. V. (2021). Redescriptions of beetles of the *Notocupes* generic complex (Coleoptera: Archostemata: Ommatidae) from the Lower Cretaceous of Buryatia. *Palaeoentomology* 4 (5), 499–514. doi: 10.11646/palaeoentomology.4.5.15

Strelnikova, O. D., and Yan, E. V. (2023). Redescriptions of the Triassic *Notocupes* beetles (Archostemata: Ommatidae) from Kyrgyzstan and South Kazakhstan. *Palaeoentomology* 6 (25), 174–190. doi: 10.11646/palaeoentomology.6.2.9

Tan, J.-J., and Ren, D. (2006). *Ovatocupes*: a new cupedid genus (Coleoptera: Archostemata: Cupedidae) from the Jehol Biota (Late Jurassic) of western Liaoning, China. *Entomol. News* 117 (2), 223–232. doi: 10.3157/0013-872X(2006)117[223:OANCGC]2.0.CO;2

Tan, J., and Ren, D. (2009). *Mesozoic Archostematan Fauna from China* (Beijing: Science Press).

Tan, J., Ren, D., Shih, C., and Ge, S. (2006). New fossil beetles of the family Ommatidae (Coleoptera: Archostemata) from the Jehol Biota of China. *Acta Geol. Sin.* 80 (4), 474–485. doi: 10.1111/j.1755-6724.2006.tb00266.x

Tan, J., Wang, Y., Ren, D., and Yang, X. (2012). New fossil species of ommatids (Coleoptera: Archostemata) from the Middle Mesozoic of China illuminating the phylogeny of Ommatidae. *BMC Evol. Biol.* 12 (1), 113. doi: 10.1186/1471-2148-12-113

Tihelka, E., Huang, D., and Cai, C. (2019). New notocupedin beetle in Cretaceous Burmese amber (Coleoptera: Archostemata: Ommatidae). *Palaeoentomology* 2 (6), 570–575. doi: 10.11646/palaeoentomology.2.6.5

Tihelka, E., Huang, D., and Cai, C. (2020a). New data on Ommatidae (Coleoptera) from mid-Cretaceous Burmese amber. *Cretac. Res.* 106, 104253. doi: 10.1016/j.cretres.2019.104253

Tihelka, E., Huang, D., and Cai, C. (2020b). A new genus and species of Micromalthidae from Burmese amber (Coleoptera: Archostemata). *Earth Environ. Sci. Trans. R. Soc. Edinb.* 111 (1), 39–46. doi: 10.1017/S1755691019000185

Yamamoto, S. (2017). A new genus of Brochocoleini beetle in Upper Cretaceous Burmese amber (Coleoptera: Archostemata: Ommatidae). *Cretac. Res.* 76, 34–39. doi: 10.1016/j.cretres.2017.04.008

Yan, E. V., Wang, B., Ponomarenko, A. G., and Zhang, H. (2014). The most mysterious beetles: Jurassic Jurodidae (Insecta: Coleoptera) from China. *Gondwana Res.* 25 (1), 214–225. doi: 10.1016/j.gr.2013.04.002

Frontiers in
Ecology and Evolution

Ecological and evolutionary research into our natural and anthropogenic world

This multidisciplinary journal covers the spectrum of ecological and evolutionary inquiry. It provides insights into our natural and anthropogenic world, and how it can best be managed.

Discover the latest Research Topics

See more →

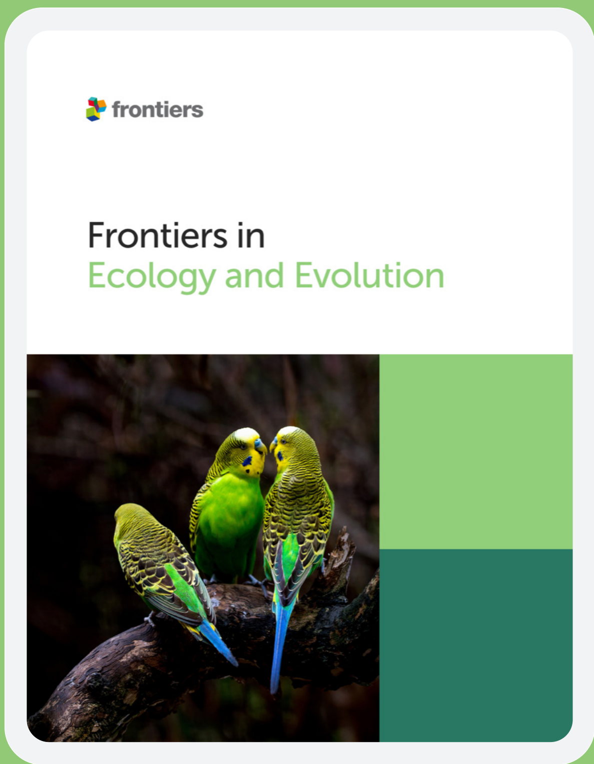

Frontiers

Avenue du Tribunal-Fédéral 34
1005 Lausanne, Switzerland
frontiersin.org

Contact us

+41 (0)21 510 17 00
frontiersin.org/about/contact